1wf

CR 114372
AVAILABLE TO THE PUBLIC

HSER—5195

Development of Atmospheric Gust Criteria for Supersonic Inlet Design

By Frank W. Barry

DECEMBER 1968

A Final Report for Contract NAS 2-4515 by

HAMILTON STANDARD
Division of United Aircraft Corporation
Windsor Locks, Connecticut

for

AMES RESEARCH CENTER
National Aeronautics and Space Administration

Hamilton Standard
DIVISION OF UNITED AIRCRAFT CORPORATION
WINDSOR LOCKS, CONNECTICUT • U.S.A.

NASA CR-

DEVELOPMENT OF ATMOSPHERIC GUST CRITERIA FOR SUPERSONIC INLET DESIGN

By Frank W. Barry

December 1968

Issued by Originator as HSER 5195

Prepared under Contract No. NAS2-4515 by

HAMILTON STANDARD
Division of United Aircraft Corporation
Windsor Locks, Connecticut

for

AMES RESEARCH CENTER

NATIONAL AERONAUTICS AND SPACE ADMINISTRATION

ABSTRACT

A method is developed for relating transient tolerances in inlet throat Mach number and shock position to the frequency of unstarts of a supersonic inlet due to atmospheric disturbances. Data on high-altitude atmospheric turbulence is collected and evaluated. A general linear analytical model is developed to compute changes in inlet throat Mach number and shock position. The relation of inlet transient tolerances to propulsion system performance is presented. A stepwise procedure for relating frequency of inlet unstarts to transient tolerances is presented and applied to a representative example.

CONTENTS

Page

DEVELOPMENT OF ATMOSPHERIC GUST CRITERIA

FOR SUPERSONIC INLET DESIGN

by Frank W. Barry
Hamilton Standard

SUMMARY

A theoretical method is presented for relating the frequency of unstarts of a supersonic inlet, due to atmospheric gusts, to transient tolerances in inlet throat Mach number and normal shock position. The purpose of this study was to develop a method for relating frequency of inlet unstarts to propulsion-system performance losses for aircraft flying at high Mach numbers where inlets with internal contraction are used. Published test data on atmospheric turbulence at altitudes over 30 000 ft are collected and evaluated, general linearized analytical models for changes in throat Mach number and shock position are developed, a new method for relating propulsion system performance to inlet tolerances is presented, and a stepwise procedure for relating frequency of inlet unstarts to transient performance penalties is presented and applied to a representative example. The most significant conclusions are that flight data are not adequate yet to provide a reliable statistical model of turbulence at altitudes above about 60 000 ft, that ambient temperature changes which occur over short distances are as significant in causing an inlet unstart as atmospheric turbulence, and that significant performance penalties may be required to keep the frequency of inlet unstarts to an acceptable level.

INTRODUCTION

The role of atmospheric gust criteria in the design of aircraft structures has been recognized for many years. Procedures have been established in design specifications which use experience and measurements to specify maximum single atmospheric gust and cyclic (fatigue) gust environments. Recently (e.g., see ref. 1) similar procedures were applied to supersonic inlets. It was shown that atmospheric gusts could cause undesirable unstarts of internal-contraction inlets operating at supersonic speeds. The frequency of unstarts was related to the propulsion system performance.

Hamilton Standard contracted with the Ames Research Center of the National Aeronautics and Space Administration to develop atmospheric gust criteria for supersonic inlet design, that is, to develop a method for relating frequency of inlet unstarts due to atmospheric turbulence to transient tolerances in inlet throat Mach number and shock position. With this method the designer can select the transient inlet control tolerances required for a preselected interval between inlet unstarts. Reference 2 is the final report on the classified task of the contract. Theoretical predictions of the analytical inlet models developed in this report are compared in ref. 2 to experimental data supplied by NASA. The experimental data include steady-state and transient changes in shock position due to exit airflow disturbances and to upstream disturbances induced by an airfoil ahead of the inlet.

This report is the final report on the unclassified tasks of the contract. The primary objective of the study was to develop a procedure for relating the frequency of inlet unstarts, due to atmospheric turbulence (gusts), to transient tolerances in inlet throat Mach number and normal shock position. The procedure for estimating frequency of unstarts is summarized in ten steps. Secondary tasks necessary to complete development of the procedure included compilation and discussion of data on high-altitude atmospheric turbulence; development of several general models for changes in inlet throat Mach number and shock position due to changes in flight and ambient atmospheric conditions, inlet geometry, and exit corrected airflow; development of relations between changes in propulsion system performance and changes in inlet and engine operating conditions; writing of several digital computer programs; and demonstration of the developed procedure by applying it to a representative inlet.

Readers who are interested only in predicting the frequency of inlet unstarts may turn directly to the section STEPWISE PROCEDURE FOR CALCULATING FREQUENCY OF INLET UNSTARTS.

SYMBOLS

A	duct cross-sectional area, ft^2
A	ratio of rms amplitude of output disturbance to rms amplitude of free-stream disturbance (see equation (54))
a	speed of sound, ft/sec
b	rms amplitude of turbulence
b_1, b_2, b_3	rms amplitude of primary, secondary, and tertiary turbulence (see Table III and figs. 12 and 13)
C	constant in case 6 spectra (see Table II)
C	constant
C	mean wing chord in equation (1), ft
C_D	drag coefficient
C_d, C_d'	duct pressure loss coefficients (see equations (44) and (45))
C_{ij}	functions of M_1 in Table IV, i = 1 to 7, j = 4 to 6
D	drag, lb
e	2.718 .., base of natural logarithms
F	thrust, lb
F_n	engine net thrust, lb
f	frequency, Hertz, $\omega/2\pi$
f_{th}	function of M_{th} (see fig. 20)
G	number of times disturbance crosses 0 while increasing per unit distance
g	standard acceleration of gravity, ft/sec^2
H	transfer function, frequency-response function

i	$\sqrt{-1}$
K_{A_1}, K_{M_i}, K_{M_1}, K_{M_2}, $K_{w_{ci}}$	coefficients defined by equations (A6), (B20), (A5), (A3), and (A4) respectively
K_u, K_v, K_w	coefficients in equation (13)(see fig. 19)
K_1 to K_{11}	coefficients defined by equations (D16) to (D26), also K_1 and K_2 are coefficients in fig 39.
L	duct length (see fig. 23), ft
L	scale of turbulence, ft
ℓ	length of Helmholtz volume (see fig. 23), ft
M	Mach number
m	mass stored in volume (see fig. 23), lb
N	number of times disturbance amplitude X is exceeded per unit time
N_s, N_{th}, N_0	number of times disturbance crosses 0 while increasing per unit time, GV
n	parameter in Taylor-Bullen spectra (see Table II)
P	absolute pressure, psf
P	probability of atmospheric turbulence (see Table I and fig. 1)
P_1, P_2, P_3	probability of primary, secondary, and tertiary turbulence (see Table III and figs. 10 and 11)
P_R	total pressure recovery factor
$p(\sigma)$	probability density of σ
R	gas constant, ft-lb/lb-°R
S	Laplace variable, /sec
s	specific entropy, ft-lb/lb-°R

T	absolute temperature, °R
TSFC	thrust specific fuel consumption, w_f/F, /hr
t	time, sec
U	longitudinal velocity, positive downstream, fps
U_{DE}	derived equivalent vertical gust velocity in equation (1), fps
U_s	shock velocity, positive downstream, fps
u, v, w	longitudinal, lateral, and vertical components of free-stream gust, true airspeed, fps
V	flight velocity, fps
V	volume of duct downstream of shock (see fig. 23), ft^3
W_R	relative airflow, ratio of airflow rate to airflow rate through reference area, e.g. A_ℓ, at flight velocity and free-stream density, $w/A_\ell V \rho_0$
w	airflow rate, lb/sec
w_c	corrected airflow rate, lb/sec
w_f	engine fuel flow rate, lb/hr
X	amplitude of disturbance
X	distance along duct, positive downstream, ft
X	distance from beginning of gust in equation (1), ft
X_s	normal shock station, positive downstream, ft
α	angle of attack, deg
α	parameter in equations (5) to (9)
β	angle of sideslip, deg
Δ	change in quantity

δ	angle between lower surface of wing and free stream in fig. 19, deg
δ	ramp or cone half angle, deg
ϵ	parameter defined by equation (7)
θ_{ℓ}	lip angle, rad
θ_w	shock-wave angle, rad
λ	wavelength, ft.
ρ	density, lb/ft^3
σ	complete rms amplitude
σ_1	truncated rms amplitude
τ_{A_1}, τ_{M_1}, τ_s, τ_V, $\tau_{w_{ci}}$	time constants defined by equations (B16), (B15), (A1), (B19), and (B14), sec
τ_d	duct dead time, sec
τ_{Pt}	time constant defined by equation (B13) or (D32), sec
τ_{Tt}	time constant defined by equation (C13) or (D33), sec
τ_1 to τ_9	coefficients defined in Appendices B, C and D
ϕ	power spectral density
Ω	spatial frequency, rad/ft
Ω_c	cutoff spatial frequency, rad/ft
ω	frequency, rad/sec, $2\pi f$
ω_c	cutoff frequency, rad/sec

Subscripts

BL	bleed spillage
BY	bypass spillage

D	derived from acceleration measurements, also drag in C_D
DE	derived from acceleration measurements, equivalent airspeed
d	duct volume (see fig. 23), also see C_d and C_d' on page 3
EXT	external spillage
e	engine face
H	Helmholtz volume (see fig. 23)
IN	installed
i	diffuser exit (see fig. 23)
L	local conditions ahead of inlet
ℓ	inlet lip
s	shock
t	total or stagnation
th	throat
UN	uninstalled
u, v, w	longitudinal, lateral and vertical components
z	downstream end of Helmholtz volume (see fig. 23)
0	atmospheric ambient, flight
1	fixed station just upstream of normal shock (see fig. 23)
2	fixed station just downstream of normal shock (see fig. 23)
1 to 11	subscripts denoting different members of a group, otherwise no specific significance
27	static pressure at exit (see fig. 24)

ATMOSPHERIC TURBULENCE DATA

The objectives of this section are to summarize and evaluate available data on high-altitude atmospheric turbulence. Over 280 references were located with the help of Scientific and Technical Aerospace Reports, International Aerospace Abstracts, Technical Abstract Bulletin Indexes, U. S. Government Research and Development Reports Indexes and refs. 3, 4, 5, and 6. These references exclude those concerned primarily with meteorological aspects of turbulence. For the purposes of this study, only atmospheric turbulence data for altitudes above 30 000 ft (9.14 km) will be reported. The NASA VGH program, initiated in the early 1930's to collect operational experiences of commercial transport aircraft, has accumulated data from nearly 150 million flight miles, of which only 2.5 million were recorded on turbojet transports mostly at the higher altitudes. In more recent years the USAF has conducted a similar program. These data have served as a basis for determining aircraft gust and maneuver loading requirements.

References 7 to 11 are proceedings of five recent conferences on atmospheric turbulence.

Probability Of Atmospheric Turbulence

VGH data records, which are time traces of aircraft velocity, V, vertical acceleration, G, and altitude, H, have been analysed by several organizations to determine the portion of the flight distance (or time) that the aircraft encounters turbulence. Data from refs. 12 to 23 are shown in figure 1 and/or Table I. The following factors should be considered in assessing these data:

1. Size of sample (see Table I). For example, data from ref. 13 should be more reliable than that from ref. 12 because the sample includes nearly three times the flight distance.

2. Turbulence avoidance procedures employed. The probability from ref. 15 is high because the flights were made near thunderstorms. The probabilities from refs. 14 and 18 are high because the HICAT U-2 aircraft deliberately flew into areas of expected turbulence. For ferry flights the probability is about 0.02. Generally, standard commercial procedures of turbulence avoidance provide the more realistic probabilities.

3. Aircraft speed and size. VGH data from a large high-speed aircraft, such as the B-70 (ref. 17), in long wavelength turbulence would be classified as turbulence whereas that from a small slow aircraft, such as the U-2, could be classified as pilot maneuver. Moreover, Steiner in ref. 11 suggests that some of the B-70 data classified as due to turbulence may be due to other sources,

such as the inlets. These conditions will result in the B-70 data showing a higher probability of turbulence than the U-2 data.

4. Acceleration threshold (minimum acceleration level at which turbulence is recorded). The Russian balloon radiosonde data (ref. 22 in figure 1) shows a high probability because of the relatively low threshold used compared to airplane data from other references. Reference 20 shows a low probability because of the relatively large (0.2g) threshold used.

5. Terrain. Probabilities obtained over rough terrain, e.g. Japan (see refs. 12 and 13) and the western United States (ref. 17), are expected to be high compared to probabilities over plains or oceans. Since the probabilities listed in Table I are for flights over various types of terrain, they would generally be higher than would be experienced for flights over oceans only. Variation of probability with location and season over the United States is shown in ref. 21.

Based on the data presented in figure 1 and Table I, the probability of atmospheric turbulence varies from roughly 0.01 to 0.15 above 30 000 ft. That the range is quite large at any altitude suggests the difficulty of obtaining meaningful statistical data. However, even the lowest (0.01) probability of encountering turbulence is significant and warrants development of an atmospheric gust criteria for supersonic inlet design.

Discrete Gust Model

The amplitude of the turbulence is as important as the probability of turbulence for selecting the design operating condition of the inlet. An increased amplitude requires that the inlet performance be reduced by increasing the design transient tolerance in order to prevent an unstart. Relations between gust probability and amplitude have been derived from measured VGH data. The gust amplitude is derived from acceleration measurements by assuming that each acceleration peak is produced by a discrete gust of known shape.

The magnitudes of the discrete acceleration peaks from the VGH records may be counted. The results are plotted typically as the logarithm of the cumulative frequency per flight mile against incremental vertical acceleration (e.g., see ref. 19). These acceleration peaks are related linearly to a derived equivalent gust velocity U_{DE} by an equation which includes as parameters the slope of the lift curve, aircraft equivalent airspeed, wing loading and a gust factor which depends on the airplane mass ratio. The equation was derived in ref. 24 by assuming that the acceleration peak is produced by a single vertical discrete gust defined by the equation

$$w_{DE} = \frac{U_{DE}}{2} \left(1 - \cos \frac{2\pi X}{25C}\right) \tag{1}$$

where X is the distance from the beginning of the gust ($0 \le X \le 25$ C) and C is the mean aircraft wing chord. This gust shape is shown in the top of figure 2. The number of times per flight mile that a given value of vertical acceleration is exceeded is read from VGH records. The value of U_{DE} corresponding to this acceleration is computed and the frequency (times per mile) is plotted against U_{DE}. Some high-altitude data from ref. 13 are shown in figure 3. In this figure the derived equivalent gust velocity U_{DE} normally used as the abscissa has been converted to a derived true gust velocity and then to a derived gust Mach number by dividing by the standard altitude speed of sound. This data, like most published data, is concave to the right. Because of the assumptions inherent in the use of a single discrete gust of arbitrary shape, values of derived gust velocity have little relation to the maximum true velocity producing the acceleration peak. For example, the maximum derived gust velocity recorded during the National Severe Storms Project in 1960 was 50 fps but the maximum true vertical gust was 208 fps. The reason for the discrepancy is that the wavelength of the actual gust was larger than 25 chords and therefore it produced a relatively small acceleration. The amplitude of the true gust will differ from that of a derived gust because the wavelength and aircraft response used for the derived gust calculation are not correct.

In spite of the shortcomings of the concept of derived gust velocity, it is still being used for structural design purposes. Specifications for the military (ref. 25), the American SST (ref. 26) and the Anglo-French SST (ref. 27) at cruise speed were converted into terms of derived gust Mach number and are plotted in figure 4. In America, for subsonic aircraft the specification derived equivalent gust velocity at a speed for maximum gust loads is 66 fps up to an altitude of 20 000 ft and decreases linearly with altitude above 20 000 ft to 38 fps at 50 000 ft altitude. For supersonic cruise speeds (ref. 26), the specification derived true gust velocity is 82.2 fps above 20 000 ft. Inlet upstarts can occur only at high Mach numbers which are achieved at altitudes above about 50 000 ft. NASA has obtained nearly 10 million miles of VGH data from turbojet- and turboprop-powered commercial aircraft. From this large sample they estimate that a U_{DE} of 66 fps would be exceeded once in 2.78 million nautical miles if normal storm avoidance procedures are employed. This distance reduces to only 1820 miles if all the flying is in thunderstorms.

Power Spectral Density

The derived gust velocity data obtained with the discrete gust model discussed above has several disadvantages. First, atmospheric turbulence does not consist of discrete gusts but of a continuous variation as shown in the center of figure 2. Second, gusts do not have a single wavelength dependent on the aircraft size but actually are a continuous velocity variation which may be represented as the sum of many components each with a different wavelength, as suggested at the bottom of figure 2. Third, the derived gust velocity bears little relation to the true gust velocity, as mentioned above.

Fourth, only vertical and lateral gusts are considered and longitudinal gusts are not considered. Fifth, as pointed out in ref. 13, the relatively high speed and large size of an SST causes it to respond to disturbances with a longer wavelength than those affecting the high-altitude gust data now available. Last, for an analysis of an inlet with an inlet control, it is necessary to have data relating the gust amplitude to gust wavelength in order to assess the capability of the inlet control to reduce the probability of an unstart. For long wavelengths, and therefore low disturbance rates, the inlet control can reduce the transient disturbances in the inlet significantly, whereas for short wavelengths a practicable inlet control cannot respond, and therefore cannot reduce the transient disturbances in the inlet.

Because of these disadvantages of the discrete gust model, it is desirable to have data which relate true amplitude of the vertical, lateral, and longitudinal gust components to wavelength. Such data have been obtained with a few specially-instrumented aircraft (e.g., see refs. 18 and 28) for wavelengths in the range 0.1 to 40 000 ft. The short wavelength limit is determined by instrument response limitations and the long wavelength limit is determined by instrument drift limitations and the size of the patch of turbulence. The data are reduced digitally and presented in the form of power spectral density distributions, such as figure 5. The ratio of the square of the gust amplitude to the spatial frequency bandwidth is plotted against spatial frequency, which is related to wavelength as shown. For a given flight velocity the spatial frequency is also proportional to the frequency ω. The values of σ_1 indicate the severity of the turbulence. The slope of the spectra at short wavelengths ranges from -1.2 to -3. (ref. 29). The theoretical slope is -5/3. It is believed that inherent inadequacies in the data reduction procedures used are responsible for the large variations of the slope obtained.

Several assumptions are usually made in deriving analytical equations for power spectra. One is the assumption of homogeneity, that is, that the statistical properties of the turbulence do not change with translation of the coordinate axes on which measurement is based. This assumption is limited to small translations since a typical patch of turbulent air is a few thousand feet thick and about 10 miles across. The assumption of isotropy requires that the statistical properties be invariant with rotation of the axes. This assumption is good at short wavelengths but may not be good at long wavelengths such as occur in mountain waves, for example. Equations for five families of power spectra which satisfy these two assumptions are presented in Table II. The variables are the complete rms amplitude σ_u or σ_w, the scale of turbulence L, and the spatial frequency Ω. Useful relationships between the various parameters are indicated in the notes under Table II. The Von Karman and Dryden spectra represent special cases of the Taylor-Bullen spectra. The Von Karman spectra have the advantage of having the theoretical slope at large frequency and the Dryden spectra have the advantage of a simpler mathematical form. Both spectra are commonly used. The case 6 spectra represent a modification of the Dryden spectra which have a finite value of G_0 (see page 12).

The case 2 spectra have a less sharp knee than the others. The latter two spectra have not been used except in reference 30. Normalized spectra for the last four families are plotted in figures 6 and 7. The normalized spectra have a corner at a referred frequency of 0.5 for the longitudinal component and of 1.0 for the vertical and lateral components. Other equations for vertical spectra which are contained in the literature do not satisfy the assumptions of homogeneity and isotropy.

Two integrals of the spectra are of interest (e.g., see ref. 31). The complete rms amplitude is defined by the integral

$$\sigma = \sqrt{\int_0^{\infty} \Phi(\Omega)\, d\Omega} = \sqrt{\int_0^{\infty} \Phi(\omega)\, d\omega} \tag{2}$$

A truncated rms amplitude, defined by

$$\sigma_1 = \sqrt{\int_0^{\Omega_c} \Phi(\Omega)\, d\Omega}$$

indicates the contribution to σ up to a finite cutoff spatial frequency Ω_c. The quantity $1 - (\sigma_1/\sigma)$ is plotted in figures 8 and 9 by lines sloping down to the right. As the plots indicate, the truncated rms amplitude σ_1 will equal 99% of the complete rms amplitude σ for all referred frequencies of 100 radians or more.

The number of times that the increasing gust velocity crosses zero per unit flight distance is

$$G_0 = \frac{\sqrt{\int_0^{\infty} \Omega^2 \Phi(\Omega)\, d\Omega}}{2\pi\sqrt{\int_0^{\infty} \Phi(\Omega)\, d\Omega}} \tag{3}$$

As with σ, truncated values of G_0 may be obtained by integrating from 0 to Ω_c rather than from 0 to ∞ in equation (3). Values of the truncated G_0 are plotted in figures 8 and 9 by lines sloping up to the right. Examination of equation (3) shows that G_0 approaches infinity as Ω_c increases unless the slope of Φ is greater than -2 as Ω becomes large. Of the spectral families shown in Table II, only the Taylor-Bullen family with $n > 1/2$ or the case 6 family have the large slope and, therefore, a finite value of G_0. For the longitudinal case 6 spectra,

$$G_0 L = \frac{N_0 L}{V} \leq \frac{(1 + C^2)\sqrt{2C - 1}}{2\pi C^2}$$

and for the vertical and lateral spectra,

$$G_0 L = \frac{N_0 L}{V} \leq \frac{(1 + C^2)\sqrt{4C-2}}{2\pi C^2}$$

With C = 50, as suggested in ref. 30, these maximum values of G_0L are 1.584 and 2.240, respectively. Usually the problem of an infinite value of G_0 with the other spectra is resolved by reducing the upper limit of the integrals in equation (3). Certainly the integration should not be carried to wavelengths less than some significant dimension such as the wing chord or the inlet diameter. For aircraft structural calculations the upper frequency limit used is about 10 Hz (cps). Dr. Houbolt has suggested that the upper frequency limit be that for which the truncated σ_1 is 95% of σ .

Several reports use the concept of power spectral density to relate aircraft vertical acceleration to a vertical gust environment. These reports present exceedance models of the atmospheric turbulence environment which fit the observed aircraft loads experience. That is, the models predict the frequency at which an aircraft load, or any similar parameter, is exceeded. The model is expressed in terms of 1, 2 or 3 probabilities of encountering turbulence P and the corresponding rms amplitudes b. Thus, statistically, aircraft loads experience is considered to be the sum of up to four patches. The first patch has insignificant turbulence. In the second patch, representing P_1 of the flight distance, the aircraft encounters turbulence with an rms amplitude of b_1. In the third patch, representing a smaller portion P_2 of the flight distance, the aircraft encounters more severe turbulence with an rms amplitude of b_2. For this model the number of times a disturbance amplitude X is exceeded per unit time is given by the equation

$$N = N_0 \left(P_1 e^{-\frac{X}{b_1 A}} + P_2 e^{-\frac{X}{b_2 A}} + P_3 e^{-\frac{X}{b_3 A}} \right) \tag{4}$$

where N_0 and A are computed by integrating the power spectral density of the output disturbance (see page 42). The values of the P's and b's are determined by curve fitting plots of cumulative frequency of gust velocity (e.g., see ref. 24). In the earlier literature, e.g. ref. 32, the terms "clear-air" and "storm" are used to designate the patches associated with P_1 and P_2. In order to avoid any implication of the absence or presence of clouds, the terms "primary", "secondary", and "tertiary" are employed here to designate the three terms used to fit loads experience data. Values for the P's and b's from 13 references are collected in Table III and figures 10 to 13. In figures 12 and 13 the b's are expressed in units of Mach number obtained by dividing the b's in Table III by the standard atmosphere speed of sound a_0 shown at the bottom of Table III.

Examination of Table III shows that most of the references were written in a 2 1/2-year period. Since little new high-altitude loads data became available during this period, differences between the models are due mainly to the individual author's interpretation of the available data and approach to fitting the data. For example, Firebaugh (ref. 43) keeps b_1 constant and uses a large variation in the scale of turbulence L to fit the data. Dr. Houbolt (ref. 42) uses a single probability which is greater for day than night, lets the rms amplitude b depend on L, and uses different exceedance models than the other authors (see page 15). Austin in ref. 41 repeats the values from ref. 35 except at low altitudes. Each model is associated with a specific power spectral density family. Based largely on a discussion with Dr. Houbolt the following comments are made:

1. Values of P in the models of atmospheric turbulence are quite accurate. Dr. Houbolt, in ref. 42, shows that errors in P have little effect on the frequency of load exceedance. Therefore, by analogy, the small errors in P have a small effect on the computed frequency of inlet unstarts.

2. Values of b in the models of atmospheric turbulence are inaccurate. Dr. Houbolt, in ref. 42, shows that errors in b have a large effect on the frequency of load exceedance. Therefore, the errors in b have a large effect on the computed frequency of inlet unstarts.

3. The Von Karman family (see Table II) is the best spectral family to use. At long wavelengths, in what is called the inertial subrange, the slope of the Von Karman spectra is the theoretical slope of -5/3. This range of wavelengths is of most interest in a study of the frequency of inlet unstarts. At very short wavelengths, less than about 1 cm, ϕ should vary as Ω^{-7} because of viscous effects. However these extreme wavelengths are too small to be of interest. At the other extreme of very large wavelengths, in the buoyant subrange, the Von Karman spectra are nearly constant whereas theoretical slopes of -11/5 and -3 have been proposed. However, extremely long wavelengths are not of concern because of the finite size of turbulence patches and because disturbances with a long wavelength present no real problem to an inlet control.

4. The value of b should vary as the cube root of L.

5. The numerical filtering procedure used to compute the power spectral density, and the length of the turbulence patch, affect the computed value of the scale of turbulence L. Dr. Houbolt recommends L = 1000 to 2000 ft.

6. Considering ref. 42, for high altitudes Dr. Houbolt prefers case "j" with α =8 to 9. A second choice is case "m" with $\alpha = 0.002$ to 0.005 and a third choice is case "k" with $\alpha = 0.0005$.

For his case "j",

$$N = PN_0 \, e^{-\sqrt{1+\epsilon}\,X/bA} \qquad X \leq \alpha bA/\sqrt{1+\epsilon} \tag{5}$$

or

$$N = PN_0 \left(\frac{\alpha \; b \; A}{e\sqrt{1+\epsilon X}} \right)^{\alpha} \, , \qquad X \geq \gamma bA/\sqrt{1+\epsilon} \tag{6}$$

where

$$\epsilon = \frac{\alpha + 2}{\alpha - 2} \; e^{-\alpha} \tag{7}$$

For his case "m",

$$N = PN_0 \left[(1-\alpha) \, e^{-\frac{X}{bA}} + \frac{\alpha bA}{3.17X} \left(e^{-\frac{0.289X}{b\,A}} - e^{-\frac{3.46\,X}{b\,A}} \right) \right] \tag{8}$$

For his case "k",

$$N = PN_0 \left[(1-\alpha) \, e^{-\frac{\sqrt{1+5.25\,\alpha}\,X}{b\,A}} + \alpha e^{-\frac{0.4\sqrt{1+5.25\alpha}\,X}{bA}} \right] \tag{9}$$

The four exceedance models are shown in figure 14. Curvature in the straight line for case "a" can be introduced by including secondary and tertiary turbulence in equation (4).

7. The best model of high-altitude atmospheric turbulence probably is provided by refs. 35 and 41, although it is believed to be conservative by AFFDL personnel.

Atmospheric Temperature Gradients

Changes in ambient temperature as well as gusts present a disturbance to a supersonic aircraft, as shown by equation (12) developed on page 20. Although an examination of temperature transients is not included in the work statement of the contract under which this report was prepared, some data has been collected and is presented here.

Equation (12) shows that the change in flight Mach number is proportional to the product of flight Mach number and ambient temperature change. Therefore, ambient temperature changes produce a larger effect on a high-speed aircraft, such as an SST, than on subsonic aircraft. Analysis of data from thirteen cases from references 18 and 44 showed that the Mach number change resulted from the addition of temperature and longitudinal gust effects in nine cases and the difference in four cases. The case sample size is too small to predict the percentage of time the temperature change would produce a significant change in flight Mach number. It is interesting to note that for a flight Mach number of 2.7 the effect of temperature change on flight Mach number exceeded that of the longitudinal gust in several cases.

The severity of the flight Mach number change due to an ambient temperature change depends on both the magnitude of the temperature change and the distance along the flight path in which the temperature change occurs. A large temperature change over a short distance will increase the requirements of the inlet control. Some available data on the relationship between horizontal distance and ambient temperature change are shown in figure 15. The circles show data obtained over storms at 45 000 ft altitude by the National Severe Storms Laboratory. The squares show data presented by the Canadian National Aeronautical Establishment for a flight at 39 000 ft altitude in a mountain wave over the Sierras. Data from several flights of the HICAT aircraft showing large temperature changes are shown by triangles. The two diamonds represent data from a British research aircraft in standing-wave conditions over the Sierra Nevadas. The quarter-circle symbols come from B-70 data and the half-circle symbols from U-2 data, both at 60 000 ft. The line comes from the airworthiness standards for the Concorde and represents the best advice available at the time it was prepared. To illustrate the importance of the temperature changes shown, a change in ambient temperature of 12° F will change the Mach number of a Mach 2.7 aircraft by 0.075 units. The same Mach number change requires a gust of 73 fps true air speed. This is a severe gust which is encountered very infrequently.

HICAT Program

Table I shows that all the atmospheric turbulence data for altitudes over 45 000 ft were obtained by U-2 and B-70 aircraft. By far the largest sample was obtained by NASA U-2 aircraft with a VGH recorder or by a WU-2 aircraft for the HICAT program supported by the AFFDL. The latter aircraft was extensively instrumented to measure total temperature, airspeed, true gust velocities and altitude (see refs. 14, 18 and 28). The HICAT flight program terminated in Feb. 1968 and a final report is scheduled to be published.

The objective of the HICAT program "is to determine the statistical characteristics of high altitude CAT so as to improve structural design criteria." Because of the purpose and because of instrumentation limitations, the reported HICAT data has several shortcomings when application to predicting inlet unstarts is considered.

Two Lockheed vane sensors with a high natural frequency were used to sense vertical and lateral components of gusts relative to the aircraft. The longitudinal component was sensed by a dynamic pressure transducer connected to the nose pitot-static boom. Absolute gust velocities were determined by adding the absolute aircraft velocities provided by an inertial platform to the relative velocities. The maximum wavelength at which power spectra can be presented is limited to roughly 40 000 ft by drift of the platform with time and by the size of the turbulence patches. The minimum wavelength of roughly 200 ft is limited by the response of the instrumentation and by a cutoff frequency of 1 to 5 hertz used to process the raw data. An examination of the published instrumentation characteristics showed that the response of the total temperature sensor may be unsatisfactory. According to ref. 18, the total temperature probe "has a frequency response which is flat within 1 percent to about 5.7 Hz". But in ref. 49, the authors state that "it does not adequately follow changes of temperature whose frequencies are greater than one cycle/sec." Reference 51 presents data on time constants for the sensor. The longer time constant, associated with the support structure, is about 2.5 sec and the shorter time constant, associated with the sensing element, is about 0.03 sec. Therefore, significant errors occur at frequencies over 0.06 Hz. Mr. Boone, of AFFDL, was contacted regarding this discrepancy but he was unable to resolve the problem at the time this report was written. However, it is believed that the response of the total temperature sensor may be inadequate to permit the cross-correlation function between ambient static temperature and longitudinal gust velocity being calculated with meaningful precision. Also, the accuracy of some of the temperature gradient data presented in figure 15 is suspect over short distances.

Because the atmospheric turbulence data required to predict loads or inlet unstart experience is statistical rather than deterministic, many flight hours are required to obtain significant results. The HICAT program did not reach a significant level of flight hours and is especially deficient in presenting the effects of terrain on turbulence. Effects of terrain on P and b can be found in ref. 49.

Summary

The available data on the random vertical turbulence environment at high altitudes is very limited. Because it uses the Von Karman power spectrum and because it is the result of the most comprehensive analysis of the data, the definition of this environment in ref. 35 is believed to be the best available. The assumption of isotropy is required to obtain comparable definitions for longitudinal and lateral turbulence. Longitudinal temperature gradients have been measured and can contribute significantly to changes in flight Mach number.

Several references present specifications for disturbances applicable to a supersonic aircraft. From four of these references the rate of change of flight Mach number and the amplitude of the Mach number change were computed and are plotted in figure 16. The relation between these two parameters for longitudinal gusts with a Von Karman spectrum, L = 2500 ft, a band width of 1 Hz, and $\sigma_u = 48$ fps, is shown by the dashed curve. The larger rates of change shown are generally associated with smaller changes in flight Mach number. Therefore the envelope of the disturbances shown represents roughly a constant transient error. Vertical gusts are considered in figure 17 for changes in angle of attack. The word "draught" is used in ref. 49 to refer to a quasi-steady vertical wind shear with a true velocity of up to ±200 fps and a width of 1000 to 20 000 ft. The disturbances in the Boeing AIC specification (ref. 53) appear to be conservative with the exception of an ambient temperature change shown in figure 16.

ANALYTICAL INLET MODEL

An analytical inlet model is required to relate changes in the inlet performance to the imposed upstream atmospheric disturbances. This model must give the time-dependent change in throat Mach number and in shock position due to changes in free-stream conditions (flight velocity, angles of attack and sideslip, ambient pressure and temperature), inlet geometry (spike position, throat area), and diffuser exit flow (bypass and engine corrected airflows). Existing inlet models (e.g., ref. 54) are not complete enough to be used here. Among the omissions are no model of change in flow conditions ahead of inlet due to changes in free-stream conditions, no linear model of change in inlet throat flow conditions due to changes in flow conditions ahead of inlet and in inlet geometry, and model not linearized. Therefore, the necessary analytical inlet models are developed in this section. An overall schematic of the inlet model is presented in figure 18. The blocks shown for the throat Mach number and shock position controls include the signal gain and pneumatic transmission line dynamics as well as the control gains and dynamics.

For convenience, the model is divided into three groups:

1. A model which relates changes in local flow conditions ahead of the inlet to changes in free-stream conditions (three components of a gust, ambient temperature and pressure).

2. A model which relates changes in inlet throat flow conditions to changes in local flow conditions and inlet geometry.

3. Four models, of varying complexity, which relate transient and steady-state changes in normal shock position to transient and steady-state changes in throat flow, throat area and exit corrected airflow.

These three groups are represented by the three large blocks in figure 18 and are discussed in the following three subsections. The third subsection includes a comparison of four models of normal shock position with each other and with digital method-of-characteristics calculations for a representative inlet configuration. A fourth subsection presents a discussion of the affects of changes in throat Mach number and shock position on the installed performance of a propulsion system.

The following assumptions are made:

1. Air is a perfect gas with a ratio of specific heats equal to 1.4.

2. Small disturbances from an average steady-state condition occur. Therefore, the flow equations may be linearized.

3. The effects of viscosity are not included explicitly. Therefore, the normal shock inside the diffuser has zero thickness and there is no steady-state loss in total pressure downstream of the normal shock.

4. The flow at each station inside the inlet is uniform across the inlet flow area and is a function of time only.

5. Internal bleed flows near the normal shock are not included explicitly in the models for the normal shock position, although only a simple modification would be required to include the effects of bleed.

Analytical Model of Local Conditions Ahead of Inlet

The purpose of this section is to derive and present equations for changes in the local flow upstream of the inlet due to changes in ambient atmospheric conditions. The changes in local flow conditions (ΔP_{tL}, ΔT_{tL}, ΔM_L, and flow angle) are used as disturbances for the analytical model of the flow at the inlet throat, page 21. The changes in ambient conditions are temperature ΔT_0, pressure ΔP_0, and the three gust components u, v, and w.

Changes in the local flow total pressure and temperature are given by the following two equations:

$$\frac{\Delta P_{tL}}{P_{tL}} = \frac{\Delta P_0}{P_0} + \frac{\Delta P_{R_L}}{P_{R_L}} + \frac{1.4\ M_0}{1 + 0.2M_0^2}\ \Delta M_0 \tag{10}$$

$$\frac{\Delta T_{tL}}{T_{tL}} = \frac{\Delta T_0}{T_0} + \frac{0.4\ M_0}{1 + 0.2M_0^2}\ \Delta M_0 \tag{11}$$

The $\Delta P_{RL}/P_{RL}$ term allows for any change in total pressure recovery between the free stream and the local flow ahead of the inlet due to shock waves from the fuselage, for example. The assumption is made that the aircraft absolute flight velocity is constant for the short time intervals of interest. Therefore, the aircraft relative Mach number changes are due to changes in ambient speed of sound (temperature) and in relative velocity due to a longitudinal gust (u). Thus,

$$\Delta M_0 = \frac{u}{a_0} - \frac{M_0}{2} \frac{\Delta T_0}{T_0} \tag{12}$$

where a positive longitudinal gust is rearwards.

An analytical model for the change in local Mach number is dependent on the aircraft configuration. The input disturbances are ΔM_0 from equation (12), the vertical gust component w and the lateral gust component v. The following equation defines the three coefficients K_u, K_v and K_w:

$$\Delta M_L = K_u \Delta M_0 + K_v \frac{v}{a_0} + K_w \frac{w}{a_0} \tag{13}$$

A vertical gust velocity w changes M_L by the same amount as an increase in aircraft angle of attack of $\frac{w}{M_0 a_0}$. Likewise, a lateral gust produces an angle of sideslip of $\frac{v}{M_0 a_0}$. Therefore, the three coefficients K_u, K_v and K_w may be calculated by determining the effects on M_L of changes in flight Mach number, angle of sideslip and angle of attack, respectively. The values of these coefficients are dependent on the aircraft configuration. If the inlet is underneath an unswept wing whose lower surface is flat, the equations for oblique shock waves in ref. 55 may be used to calculate K_u and K_w. A graphical approach to determine the change in Mach number behind an oblique shock wave due to a change in upstream Mach number and in shock deflection angle may be used to calculate K_u and K_w respectively. Alternatively, the theory and equations in ref. 56 may be adapted. The latter approach was used to calculate the values of K_u and K_w plotted in figure 19. The value of δ is the angle between the lower surface of the wing and the free stream. For other aircraft geometries, with the inlet not in the shadow of an unswept wing, the values of K_u and K_w will vary from those shown in figure 19. However, it is expected that K_u will remain near unity. In general, it is expected that K_v is small.

As discussed on page 11, atmospheric turbulence is generally considered to be isotropic. That is, the rms amplitudes of the three components (σ_u, σ_v and σ_w) are equal Also, all directions for the gust have equal probability. For this case, considering only gusts and not temperature changes, the rms amplitude of the change in local Mach number is

$$\Delta M_L = \sqrt{\frac{K_u^2 + K_v^2 + K_w^2}{3}} \left(\frac{b_o}{b_o}\right) \tag{14}$$

where b_0 is the rms amplitude of the gusts. The above equation (14) applies to a time average whereas equations (10) to (13) apply at any instant of time. The rms vertical gust components b reported in the literature (see Table III) equal $b_0/\sqrt{3}$.

No attempt is made to derive a general model for the change in local flow angle because any model is very dependent on the aircraft geometry.

Analytical Model of Flow at Inlet Throat

The purpose of this section is to derive equations for changes in the flow conditions at the inlet throat due to changes in local flow upstream of the inlet. The changes in inlet throat flow (ΔP_{tth}, ΔT_{tth}, and ΔM_{th}) of interest are the upstream disturbances for the analytical models of normal shock position presented on page 24. The input disturbances of ΔP_{tL}, ΔT_{tL}, ΔM_L and local flow angle ahead of the inlet are presented in the preceding section.

The fact that the flow from upstream of the inlet to the throat is supersonic justifies exclusion of any internal dynamic effects in the analysis. Any dead time would be very small and would only be considered if the inlet control senses local flow conditions. The assumption that dynamic effects may be neglected permits using the steady-state flow equation. Therefore,

$$P_{t1} = P_{tth} = P_{R_{th}} P_{tL} = P_{R_{th}} P_{R_L} P_{t0} \tag{15}$$

and

$$T_{t1} = T_{tth} = T_{tL} \tag{16}$$

where the factor $P_{R_{th}}$ accounts for losses in total pressure from ahead of the inlet to the throat. Locations of P_{t1} and T_{t1} are presented in figure 23.

The steady-state continuity equation between the local and throat flows is

$$W_R A_L \frac{M_L}{(1 + 0.2 M_L^2)^3} \frac{P_{th}}{\sqrt{T_{t_L}}} = A_{th} \frac{M_{th}}{(1 + 0.2 M_{th}^2)^3} \frac{P_{t_{th}}}{\sqrt{T_{t_{th}}}} \tag{17}$$

The following equation for the change in throat Mach number is obtained by differentiating equation (17) and substituting equations (15) and (16):

$$\Delta M_{th} = f_{th}\left[\frac{\Delta A_L}{A_L} + \left(\frac{A_{th}\ \partial W_R}{W_R\ \partial A_{th}} - \frac{A_{th}\partial\ P_{Rth}}{P_{Rth}\partial\ A_{th}} - 1\right)\frac{\Delta A_{th}}{A_{th}} + \left(\frac{1-M_L^2}{M_L\ (1+0.2M_L^2)} + \frac{\partial\ W_R}{W_R\,\partial\ M_L} - \frac{\partial\ P_{Rth}}{P_{Rth}\,\partial\ M_L}\right)\Delta M_L\right] \tag{18}$$

$$\text{where}\quad f_{th} = \frac{M_{th}\ (1 + 0.2\ M_{th}^2)}{1 - M_{th}^2} \tag{19}$$

The $\Delta A_L/A_L$ term allows for a change in the geometric inlet lip area; for most inlets this term is zero. The next term allows for changes in relative airflow due to changes in external geometry associated with a change in throat area, such as for a translating-spike inlet. The two terms with partial derivatives of P_{Rth} are generally small compared to the other terms in the brackets. The factor f_{th} is plotted in figure 20. It becomes large and varies rapidly as M_{th} approaches unity. An equation for the average value of f_{th} between $M_{th} = M$ and $M_{th} = M_{th}$ is obtained by integrating equation (19):

$$\bar{f}_{th} = \frac{M_{th} - M}{\ln\left(\dfrac{M_{th}\ (1 + 0.2\ M^2)^3}{M\ (1 + 0.2\ M_{th}^2)^3}\right)} \tag{20}$$

Average values of f_{th} for $M = 1.0$ and 1.3 are shown by dashed lines in figure 20. Use of an average f_{th} usually will provide acceptable accuracy.

The $\partial W_R/W_R\ \partial M_L$ term allows for the change in supercritical relative airflow with local Mach number for a fixed inlet geometry. For a two-dimensional wedge inlet an exact analytical solution may be obtained. Consideration of the inlet geometry leads to the following equation for relative airflow

$$W_R = \frac{W_R\ A_\ell}{A_\ell} = \frac{\cot\theta_\ell - \cot\delta}{\cot\ \theta_w - \cot\delta} \tag{21}$$

where the terms are defined in the following sketch.

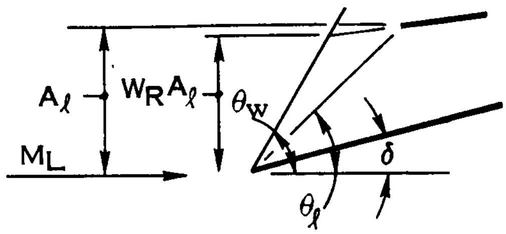

Upon differentiation, with constant δ and θ_ℓ

$$\frac{\partial W_R}{W_R \partial \theta_w} = \cot \theta_w - \cot (\theta_w - \delta) \qquad (22)$$

An equation for $\partial\theta_w/\partial M_L$ was obtained from ref. 56 and, therefore,

$$\frac{\partial W_R}{W_R\ \partial M_L} = \frac{4 \tan\delta\ (\cot\theta_w + \tan\delta)}{M_L \sin 2\theta_w\ \ (M_L^2 (\cos 2\theta_w + \tan\delta\ \sin 2\theta_w) + \csc^2\theta_w)\ (\tan\theta_w - \tan\delta)} \qquad (23)$$

This equation has been evaluated numerically for several wedge angles and the results are shown in the lower part of figure 21. One should note that the lip angle θ_ℓ is not involved. For an axially-symmetric conical inlet an analytical solution is not available. Hartsell presents the following equation in ref. 57 which he states is valid

$$W_R = \frac{\cot^2\theta_\ell - \cot^2\delta}{\cot^2\theta_w - \cot^2\delta} \qquad (24)$$

for $\delta \geq 10°$ and $M_L \geq 1.5$. Upon differentiation, one obtains

$$\frac{\partial W_R}{W_R\ \partial M_L} = \frac{-2\cos\theta_w}{\sin^3\theta_w\ (\cot^2\delta - \cot^2\theta_w)}\ \frac{\partial\theta_w}{\partial M_L} \qquad (25)$$

Several approximate equations for θ_w were found in the literature. However, the best results are obtained by using tabulated values of θ_w and $\partial\theta_w/\partial M_L$ in refs. 58 and 59. These values were used to compute the results plotted in the upper part of figure 21. Also, the relative airflow was plotted against M_L from computations described in ref. 60 and the slope determined. Somewhat different values of $\partial W_R/W_R\ \partial M_L$ were obtained which, unlike those shown in figure 21, depend on the lip angle θ_ℓ. However the curves in figure 21 should be adequate. More precise values of $\partial W_R/W_R\ \partial M_L$ may be obtained for a given geometry by plotting theoretical values of W_R from refs. 60 and 61.

The effect of local or free-stream flow direction on the throat Mach number is not as amenable to a theoretical analysis because internal flow distortion is so significant a factor. Therefore experimental data on axially-symmetric inlets with internal compression are used from refs. 62 to 68. In these references, the inlet unstart spike position is plotted against Mach number at zero angle of attack and against angle of attack at several local Mach numbers. Data at $M_L = 2.0$, 2.5 and 3.0 were selected for use in this report.

From these data the inlet unstart events are plotted as functions of local Mach number and angle of attack in figure 22 for different spike positions. Symbols corresponding to different spike positions for one M_L and one reference are joined. For each spike position, either increasing the inlet angle of attack to the abscissa value or reducing the local Mach number to the ordinate value will cause an unstart. Thus, these two changes, one in local flow direction and one in local Mach number, produce the same decrease in throat Mach number. This decrease in throat Mach number is related to the decrease in local Mach number by equation (18). With the aid of figure 22, therefore, it is possible to relate the decrease in throat Mach number due to local flow angle. For example, at $M_L = 3.0$, let $\Delta M_{th} = 1.8\ \Delta M_L$ according to equation (18). From figure 22, with $M_L = 3.0$, the average slope of the lines is roughly $-0.08\ \Delta M_L/$ deg. Therefore, $\Delta M_{th} = 1.8\ (-0.08)\ \Delta\alpha = -0.14\ \Delta\alpha$ or, in words, a one-degree increase in local flow angle reduces the minimum throat Mach by 0.14 units. Inspection of figure 22 shows that the slope of the lines increases with local Mach numbers. Therefore, the change of throat Mach number with flow angle increases with local Mach number.

The change in Mach number ahead of the shock ΔM_1 required in the next section may be obtained from equation (18) by simply replacing the subscript "th" by "1". Thus, in equation (19) M_1 is used in place of M_{th}.

Analytical Models of Normal Shock Position

The third group of models is one which predicts the change in normal shock position due to various upstream disturbances at the inlet throat or downstream disturbances at the exit. The upstream disturbances considered are changes in total pressure, total temperature, duct area (due to action of an inlet control), and Mach number. The downstream disturbances are changes in either exit Mach number or corrected airflow. Corrected airflow is a function of Mach number for a given area. If this functional relation

$$w_c = 85.384 \frac{AM}{(1 + 0.2M^2)^3}$$

is differentiated, the following relation between these two downstream disturbances is obtained:

$$\Delta M_i = \frac{M_i\ (1 + 0.2\ M_i^2)}{1 - M_i^2} \quad \frac{\Delta w_{c_i}}{w_{c_i}} \tag{26}$$

The substitution implied by this equation may be made into the equations (32), (33), (34), (35) and (D14) for the four models of normal shock position.

The first task is to derive equations for the change in selected flow parameters at a fixed station downstream of the shock (subscript "2") caused by changes in flow parameters at a fixed station upstream of the shock (subscript "1"), a displacement of the shock, or change in shock velocity. For convenience, the two fixed stations are considered to be separated by an insignificant distance. The two stations are fixed relative to the inlet, not the normal shock. If the shock is displaced downstream of station "2" the actual flow there changes from subsonic to supersonic. The properties of a fictitious subsonic flow at station "2" are obtained by using the theoretical stream-tube-area relations in ref. 55 and the flow properties at any station behind the shock. This fictitious subsonic flow at station "2" is consistent with that existing downstream of the shock if the shock were not present between the two stations.

Equations for the change in downstream flow parameters due to a change in upstream Mach number M_1 are obtained by differentiating the relations for a normal shock with respect to M_1. Thus, for M_2, $M_2^2 = (M_1^2 + 5)/(7M_1^2 - 1)$ and

$$\Delta M_2 = \frac{\partial M_2}{\partial M_1}\ \Delta M_1 = -\frac{36\ M_1}{\sqrt{M_1^2 + 5}\ \ (7M_1^2 - 1\ )^{1.5}}\ \ \Delta M_1$$

The other flow parameters are treated similarly. The coefficients, which are functions of M_1, are shown in column (j = 4) of Table IV. The coefficients for the other three upstream parameters (P_{t1}, T_{t1} and A_1) are shown in columns j = 1, 2 and 3.

Equations for the change in downstream flow parameters due to a change in shock position are derived in the following manner. Differentiating the stream-tube-area relations in ref. 55 produces the following equation relating Mach number gradient to duct area gradient:

$$\frac{dM}{dX} = \frac{M\ (1 + 0.2\ M^2)}{1 - M^2} \quad \frac{dA}{AdX} \tag{27}$$

This equation, with $M = M_1$, is used to determine the change in the Mach number upstream of the shock due to the shock displacement ΔX_s. The changes in downstream flow parameters behind the shock because of the change in upstream Mach number are computed by the procedure described in the preceding paragraph. The change in static pressure P_2 and Mach number M_2 at the fixed station are computed by theoretical extrapolation forward using $M = M_2$ in equation (27). The resulting terms are shown in one column ($j = 5$) of Table IV.

Equations for the change in downstream flow parameters due to shock velocity are derived in ref. 69 by differentiating the normal shock relations in terms of an upstream relative Mach number. This Mach number is the difference between the absolute upstream Mach number M_1 and a dimensionless shock velocity U_s/a_1. By an appropriate change of coordinates between a system moving with the shock and a fixed system (e.g., see refs. 54 and 69) the terms in column ($j = 6$) of Table IV are obtained.

A matrix of equations for the changes in seven downstream flow parameters is presented in Table IV. The downstream flow parameters are listed in the first column and the terms associated with the six quantities which may change are listed in the next six columns. As an example, consider changes in downstream corrected airflow. This is the fifth downstream flow parameter and the equation is on the line labeled i=5. It may be written as

$$\frac{\Delta w_{c2}}{w_{c2}} = \frac{\Delta A_1}{A_1} - \frac{30\,(M_1^2 - 1)}{M_1\,(7M_1^2 - 1)\,(M_1^2 + 5)}\,\Delta M_1 + \frac{7\,(M_1^2 - 1)}{7M_1^2 - 1}\,\frac{dA}{AdX}\,\Delta X_s + \frac{(M_1^2 - 1)\,(7M_1^2 + 5)}{M_1\,(7M_1^2 - 1)\sqrt{1 + 0.2M_1^2}}\,\frac{U_s}{a_t} \qquad (28)$$

Downstream corrected airflow is independent of upstream P_{t1} and T_{t1} (as shown by the coefficient "0.0" in Table IV) and increases with increasing duct area A_1, decreasing upstream Mach number M_1, downstream shock displacement ΔX_s (if $dA/AdX > 0$) and downstream shock velocity U_s. For convenience, the Mach number functions in Table IV are denoted by C_{ij}, where i and j represent the line and column in Table IV. Thus, equation (28) may be written as

$$\frac{\Delta w_{c2}}{w_{c2}} = \frac{\Delta A_1}{A_1} - C_{54}\,\Delta M_1 + C_{55}\,\frac{dA}{AdX}\,\Delta X_s + C_{56}\,\frac{U_s}{a_t} \qquad (29)$$

With the exception of C_{14} for $M_1 < 1.484$, all C_{ij} are positive functions of M_1.

A useful result which can be obtained easily from the equations in Table IV is a set of equations for the steady-state displacement of the normal shock due to several disturbances. As an example, consider that the upstream Mach number M_1 and duct area A_1 are constant, i.e., $\Delta M_1 = \Delta A_1 = 0$. For steady-state disturbances $U_s = 0$. Therefore, by rearranging equation (28), the following equation for the steady-state shock displacement due to a change in downstream corrected airflow is obtained:

$$\Delta X_s = \frac{7M_1^2 - 1}{7\,(M_1^2 - 1)} \; \frac{AdX}{dA} \; \frac{\Delta w_{c2}}{w_{c2}}$$

One may note that $\Delta w_{ci}/w_{ci} = \Delta w_{c2}/w_{c2}$. This equation and five others are collected in Table V. The first three equations apply to changes in three downstream flow parameters with constant upstream conditions, and the last three equations apply to changes in upstream conditions with constant downstream corrected airflow. For coordinated changes in duct area and upstream Mach number at constant airflow which would be produced by a throat Mach number control, the bottom equation shows that the normal shock remains at a constant duct area.

The second task is to derive four equations, representing four models, for the transient displacement of the normal shock due to transient changes in diffuser exit corrected airflow or Mach number, upstream total pressure or temperature, upstream Mach number and duct area near the shock. The nomenclature used for these four analytical models of normal shock position is illustrated in figure 23. Many of the quantities shown are not required for the simpler models. The discussion of the models is arranged in order to the complexity of the model, starting with the simplest. Detailed derivations of these four models are contained in Appendices A through D. Equations for the time-dependent change in shock position are expressed in Laplace notation. Readers who are not familiar with the Laplace operator S may think of it as the operator for the time derivative. Thus, the shock velocity U_s may be written as $S\Delta X_s$. The steady-state shock displacement is obtained by setting $S = 0$.

First analytical model of shock position. - It is shown in ref. 70 that a first-order lag relation for shock position results from the assumption that the disturbance is a linear function of shock position and of shock velocity. This assumption is made in the analysis leading to the equations shown in Tables IV and V. Therefore, these equations are used to derive a first-order lag relation for shock position in Appendix A.

If a step change in a downstream flow parameter is imposed, a step change in shock velocity must occur to balance the disturbance. This shock velocity can be predicted by using the coefficient shown in the right-hand column (j = 6) of Table IV on the appropriate line, depending on the flow parameter disturbed. At a much later time, the shock reaches an equilibrium stationary position, and the steady-state displacement can be predicted by using the preceding coefficient (j = 5) on the same line of Table IV or by using the appropriate equation in Table V. For any time, the shock displacement can be represented by a first-order lag relationship involving a gain (steady-state displacement) and a shock time constant. This time constant is the ratio of the last two coefficients in the equation shown in Table IV. For example, for a disturbance in either downstream corrected airflow (i = 5) or Mach number (i = 6) the time constant is

$$\tau_s = \frac{C_{56}}{C_{55}} \frac{AdX}{dA} \frac{1}{a_t} = \frac{C_{66}}{C_{65}} \frac{AdX}{dA} \frac{1}{a_t}$$

or

$$\tau_s = \frac{7 M_1^2 + 5}{7M_1 \sqrt{1 + 0.2 M_1^2}} \frac{AdX}{dA} \frac{1}{a_t} \tag{31}$$

The steady-state displacements are given by the equations in Table V. The following equation for the shock displacement is derived in Appendix A:

$$\Delta X_s = \frac{K_{wc_i} e^{-\tau_d S} \frac{\Delta w_{c_i}}{w_{c_i}} + K_{M_1} \Delta M_1 + K_{A_1} \frac{\Delta A_1}{A_1}}{1 + \tau_s S} \tag{32}$$

where τ_s is given by equation (31), τ_d is a dead time introduced to account for the time required for a sound wave to move upstream against the flow from the exit to the shock wave, and the gains K are defined in Appendix A in terms of the Mach number M_1 and the duct area gradient at the shock dA/AdX. Equation (32) represents the first analytical model for shock position.

Second analytical model of shock position. - The first analytical model, expressed by equation (32), is especially applicable to short inlets. For inlets with a long diffuser, however, allowance should be made for the effect of changes in the mass of air stored in the volume between the normal shock and the diffuser exit on the shock dynamics. The change of this mass stored in the volume is proportional to the diffuser volume and to changes in the stagnation density and average Mach number M_d in the volume (see figure 23). The details of the analysis, which is based on that in ref. 69, are presented in Appendix B. The following equation represents the second analytical model of shock position:

$$\Delta X_s = \frac{K_{wc_i} (1 + \tau_{wc_i} S) e^{-\tau_d S} \frac{\Delta w_{c_i}}{w_{c_i}} + K_{M_1} (1 + \tau_{M_1} S) \Delta M_1 + K_{A_1} (1 + \tau_{A_1} S) \frac{\Delta A_1}{A_1} + \tau_{P_t} S \left(\frac{\Delta P_{t_1}}{P_{t_1}} - \frac{\Delta T_{t_1}}{T_{t_1}} \right)}{1 + \tau_1 S + \tau_2 S^2} \tag{33}$$

It differs from equation (32) of the first model by having a quadratic lag, by having lead time constants in the Δw_{ci}, ΔM_1 and ΔA_1 terms, and by including a term proportional to the rate of change of upstream total pressure and temperature. These changes result from including a volume behind the shock. Equations for the coefficients are contained in Appendix B.

Third analytical model of shock position. - Several analyses of supersonic inlets have included the pressure differential required to accelerate the mass in the Helmholtz volume (see fig. 23) behind the shock. Appendix C presents an analysis which introduces the Helmholtz mass into the second model. The following equation for the resulting third analytical model of shock position is derived:

$$\Delta X_s = \frac{K_{w_{ci}}(1 + \tau_{w_{ci}}S)e^{-\tau_d S}\frac{\Delta w_{ci}}{w_{ci}} + K_{M_1}(1 + \tau_1 S + \tau_2 S^2)\Delta M_1 + K_{A_1}(1 + \tau_{A_1}S)\frac{\Delta A_1}{A_1} + \tau_{P_t} S\frac{\Delta P_{t1}}{P_{t1}} + \tau_{T_t}S(1 + \tau_3 S)\frac{\Delta T_{t1}}{T_{t1}}}{1 + \tau_4 S + \tau_5 S^2 + \tau_6 S^3} \tag{34}$$

It differs from equation (33) of the second model by having a first-order plus a quadratic lag, a quadratic lead in the ΔM_1 term and a lead in the ΔT_{t1} term. These changes result from including the inertia of the air in a Helmholtz volume behind the shock. Equations for the coefficients are contained in Appendix C.

Fourth analytical model of shock position.—A nonlinear representation of a supersonic inlet is presented by North American Aviation in ref. 54. Both storage volume and Helmholtz mass effects are included. An analytical model is derived in Appendix D by linearizing the equations in ref. 54 for started inlet operation. This fourth analytical model of shock position is expressed by the equation

$$\Delta X_s = \frac{K_{w_{ci}}(1 + \tau_V S)e^{-\tau_d S}\frac{\Delta w_{ci}}{w_{ci}} + K_{M_1}(1 + \tau_1 S + \tau_2 S^2)\Delta M_1 + K_{A_1}(1 + \tau_3 S + \tau_4 S^2)\frac{\Delta A_1}{A_1} + \tau_{P_t}(1 + \tau_V S)S\frac{\Delta P_{t1}}{P_{t1}} + \tau_{T_t}(1 + \tau_5 S)S\frac{\Delta T_{t1}}{T_{t1}}}{1 + \tau_6 S + \tau_7 S^2 + \tau_8 S^3 + \tau_9 S^4} \tag{35}$$

It differs from equation (34) of the third model by having two quadratic lags, a quadratic lead in the ΔA_1 term and a lead in the ΔP_{t1} term. Equations for the coefficients are contained in Appendix D. If one desires to evaluate changes in other aerodynamic parameters, such as a pressure in the diffuser, equation (35) must be replaced by a set of equations such as (D3), (D13), (D14) and (D15) in Appendix D.

Comparison of analytical models of shock position. - This subsection has three objectives:

1. to illustrate the response of the shock wave to various sinusoidal disturbances.

2. to compare the predictions of the four analytical models of shock position with each other.

3. to compare these predictions with calculations made by a method-of-characteristics procedure.

The area distribution of the inlet configuration selected for the purpose of achieving these objectives is presented in figure 24. The following values for the required parameters are used (in this section the dimensions of some parameters are not consistent with those shown in the section SYMBOLS because distance along the duct is measured in inches rather than feet):

$$
\begin{aligned}
X_s &= 1.5 \text{ in.} \\
M_1 &= 1.32 \\
a_{t1} &= 14\ 200 \text{ in./sec} \\
\frac{dA}{AdX} &= 0.008/\text{in.} \\
\ell &= 4 \text{ in.} \\
A_z &= 0.634 \text{ ft}^2 \\
M_z &= 0.644 \\
V &= 36 \text{ ft}^2\text{-in.} \\
L &= 35 \text{ in.} \\
M_d &= 0.334 \\
M_i &= 0.25 \\
\text{and } \tau_d &= 0.004 \text{ sec}
\end{aligned}
$$

For the first analytical model of shock position, equation (32) becomes

$$
\Delta X_s = \frac{269.3e^{-0.004S} \dfrac{\Delta w_{ci}}{w_{ci}} + 60.19\ \Delta M_1 - 269.3\ \dfrac{\Delta A_1}{A_1}}{1 + 0.01411S} \tag{36}
$$

The product 269.3 $\Delta w_{ci}/w_{ci}$ may be replaced by 997.1 ΔM_i as per equation (26) in this and the following three equations. The shock time constant is 0.01411 sec.

For the second analytical model, which includes the volume effect, equation (33) becomes

$$\Delta X_s = \frac{269.3(1-0.000469S)e^{-0.004S}\dfrac{\Delta w_{ci}}{w_{ci}} + 60.19\,(1-0.00599S)\,\Delta M_1 - 269.3(1+0.000469S)\dfrac{\Delta A_1}{A_1} + 2.009S\left(\dfrac{\Delta P_{t1}}{P_{t1}} - \dfrac{\Delta T_{t1}}{T_{t1}}\right)}{1 + 0.01393S + 0.0000319S^2} \tag{37}$$

For the third analytical model, which includes the Helmholtz mass effect, equation (34) becomes

$$\Delta X_s = \frac{269.3(1-0.000469S)e^{-0.004S}\dfrac{\Delta w_{ci}}{w_{ci}} + 60.19\,(1-0.00518S + 0.0000061S^2)\Delta M_1 - 269.3(1+0.000469S)\dfrac{\Delta A_1}{A_1} + 2.009S\dfrac{\Delta P_{t1}}{P_{t1}} - 2.053\,S\,(1+0.000159S)\dfrac{\Delta T_{t1}}{T_{t1}}}{1 + 0.01475S + 0.0000490S^2 + 0.000000082S^3} \tag{38}$$

For the fourth analytical model, which is a linearized version of the North American analysis, equation (35) becomes

$$\Delta X_s = \frac{269.3(1+0.00746S)e^{-0.004S}\dfrac{\Delta w_{ci}}{w_{ci}} + 60.19(1+0.00194S-0.0000412S^2)\Delta M_1 - 269.3(1+0.008397S+0.00000699S^2)\dfrac{\Delta A_1}{A_1} + 2.009(1+0.00746S)\dfrac{\Delta P_{t1}}{P_{t1}} - 1.505S\,(1+0.00185S)\dfrac{\Delta T_{t1}}{T_{t1}}}{1 + 0.02640S + 0.0002126S^2 + 0.000000415S^3 + 0.00000000023S^4} \tag{39}$$

Gains and phase lags were computed from the preceding four equations for sinusoidal disturbances in

1. Diffuser-exit Mach number, ΔM_i
2. Upstream Mach number, ΔM_1
3. Upstream duct area, ΔA_1
4. Upstream total pressure, ΔP_{t1}
5. Upstream total temperature, ΔT_{t1}

Bode plots showing the computed results are shown in figures 25 through 29 for frequencies between 1 and 1000 rad/sec. The results for the four analytical models are shown by the four sets of lines. In addition, calculations of shock position for four frequencies from 5 to 30 Hz were made using a digital program (number H200) developed by Hamilton Standard. This program uses a method-of-characteristics method at the nine stations downstream of the shock shown by circles in figure 24. The results from this program are shown by the circles in figures 25 through 30 and are believed to be the most accurate theoretical results available. Therefore, results from the four models will be compared to the method-of-characteristics results.

For disturbances in diffuser exit Mach number (or corrected airflow) shown in figure 25 the gain is nearly constant below 10 Hz. At higher frequencies the four models give similar decreasing gains but the fourth ("linearized NAA") model agrees best with the circles. The two lines of phase angle for the "linearized NAA" model indicate that a dead time should be included, contrary to the recommendation of ref. 54. The results for disturbances in upstream Mach number shown in figure 26 are similar. The fourth model, shown by the solid lines, shows best agreement with the circles. Results for a disturbance in area at the shock (or throat) are presented in figure 27. Again the gain decreases with increasing frequency but the phase lag at low frequencies is 180° rather than 0. No method-of-characteristics calculations for this disturbance are available for comparison because the digital program used did not allow for changes in duct areas with time. The gain for a disturbance in upstream total pressure shown in figure 28 reaches a maximum at about 20 Hz. At low frequencies the phase lag is larger than at high frequencies, that is, about 270°, or about 90° lead. An upstream disturbance in entropy was used for the method-of-characteristics solutions and was converted to an equivalent total pressure or total temperature disturbance using the relation

$$\frac{\Delta s_1}{R} = - \frac{\Delta P_{t1}}{P_{t1}} + 3.5 \frac{\Delta T_{t1}}{T_{t1}}$$

Again, agreement with the fourth model (solid lines) is best. Results for an upstream disturbance in total temperature are shown in figure 29. The largest gains are obtained from the method-of-characteristics solution and the smallest gain is obtained from the fourth model. At low frequencies the phase shift is 90°. Best agreement with phase shift is provided by the fourth model. It should be noted that the first model does not include disturbances in either upstream total pressure or temperature and, therefore, results are not shown in figures 28 and 29. Inspection of figures 25 to 29 leads to the following conclusions:

1. All four models predict nearly the same gains and phase shifts at low frequencies but the scatter of the predictions increases with frequency.

2. With one exception, best agreement with a method-of-characteristics solution is provided by the fourth model (solid line).

3. An increase in the gain for an upstream total temperature change would improve agreement for the fourth model.

4. A dead time should be included for an airflow disturbance at the diffuser exit.

5. The first model does not allow for upstream total pressure and temperature disturbances.

The change in diffuser exit static pressure also was computed using the four models and the method-of-characteristics program for a disturbance in diffuser exit Mach number. The change in this static pressure is

$$\frac{\Delta P_{27}}{P_{27}} = \frac{\Delta P_{td}}{P_{td}} + \frac{\partial (P_{27}/P_{td})}{P_{27}/P_{td}\ \partial M_i} \Delta M_i \tag{40}$$

For the first two models $\Delta P_{td}/P_{td} = \Delta P_{t2}/P_{t2}$ and, using the equation in Table IV for $\Delta P_{t2}/P_{t2}$ $(i = 2)$,

$$\frac{\Delta P_{27}}{P_{27}} = -\,0.003813\ \Delta X_s - 0.000024S\ \Delta X_s - 0.345\ \Delta M_i \tag{41}$$

For the third model $\Delta P_{td}/P_{td}$ is computed from equation (C9) and, therefore,

$$\frac{\Delta P_{27}}{P_{27}} = -\,0.003813\Delta X_s - 0.000027S\Delta X_s - 0.000000004S^2\Delta X_s - 0.345\Delta M_i \tag{42}$$

For the fourth model, equation (40) is used and equation (39) is replaced by the following equivalent four equations (see (D3), (D13), (D14) and (D15)):

$$\frac{\Delta w_2}{w_2} + 0.00000402S\Delta X_s = 0 \tag{43a}$$

$$(1+0.00746S)\frac{\Delta T_{td}}{T_{td}} - 0.0000175S\Delta X_s = 0 \tag{43b}$$

$$S(0.0000211 + 0.000000022S)\Delta X_s + (1 + 0.000937S)\frac{\Delta w_2}{w_2} + (0.5 + 0.00793S)$$

$$\frac{\Delta T_{td}}{T_{td}} - (1+0.00746S)\frac{\Delta P_{td}}{P_{td}} = 3.704\Delta M_i \tag{43c}$$

$$(245\ 940 + 1400S + S^2)\Delta X_s - 16\ 493\ 000\frac{\Delta T_{td}}{T_{td}} + 66\ 236\ 000\frac{\Delta P_{td}}{P_{td}} = 0 \tag{43d}$$

The results are presented in figure 30. As in the previous four figures, the best agreement with the method-of-characteristics program is provided by the fourth model.

It was anticipated that the third and fourth models of shock position would give the best results because they both include volume and Helmholtz mass effects. This expectation is confirmed by the results. However, the fourth model is generally better than the third model. Therefore, the fourth analytical model of shock position is recommended.

The predictions of the four analytical models of shock position are compared in ref. 2 to test data. In order to allow for the effects of internal bleed near the throat, the area-gradient factor dA/AdX in the analytical models is adjusted to match steady-state data for the variation of shock position with diffuser-exit static and total pressures. For a sinusoidal variation in diffuser-exit Mach number, close agreement between the four models and test data is demonstrated. For a variation in upstream flow conditions, agreement is poor because the actual test conditions are poorly defined.

Analytical Model of Propulsion System Performance

The performance characteristics of a mixed-compression supersonic inlet are generally expressed in terms of four parameters: engine-face pressure recovery, relative airflow, spillage drag coefficient, and engine-face flow distortion. A typical relationship between the first three of these parameters for an inlet with bleed near the throat is shown in figure 31. The maximum pressure recovery usually is obtained with the minimum throat area which permits supersonic flow past the throat and with the minimum bypass area which permits the normal shock to be just downstream of the throat. A slight reduction in throat area or bypass area will cause an inlet unstart with a sudden large decrease in pressure recovery and thrust, and possibly unstable airflow which causes vibrational problems throughout the propulsion system. In practice, both the throat area and bypass area are increased from the minimum values by steady-state and transient tolerances to establish the mean operating areas. The steady-state tolerances allow for inlet control tolerances, scheduling compromises and inlet fabrication tolerances. The transient tolerances depend on the inlet and control dynamics and the disturbance rates.

A line of constant engine corrected airflow is shown in the upper part of figure 31. If, with a closed bypass, the throat area is increased from the minimum area to the operating area, the inlet operating condition changes from that indicated by the circle to that indicated by the triangle. The engine-face pressure recovery drops and the inlet drag increases. Both these changes reduce the propulsion system performance. In addition, because the shock moves forward in the throat, the shock-position tolerance is reduced. An acceptable shock-position tolerance is obtained by opening the bypass so that the inlet operates at the condition indicated by the diamond. The pressure recovery and bleed drag decrease but the bypass drag increases. The net change in drag is shown as a decrease. Depending on the relative magnitudes of the changes in pressure recovery and net drag, the thrust specific fuel consumption decreases or increases.

The turbojet manufacturer specifies the uninstalled engine performance for a standard inlet pressure recovery, $P_{R_{UN}}$, with no inlet drag. A deviation from this standard inlet pressure recovery to a value of P_{R_e} produces a change in the uninstalled thrust and engine fuel flow w_f. Duct loss coefficients C_d and C_d' are presented in engine specifications to permit calculation of these changes from the following two equations:

$$\frac{F_{UN}-F_n}{F_n} = (1 + C_d)\,\frac{P_{R_e} - P_{R_{UN}}}{P_{R_{UN}}} \tag{44}$$

and $$\frac{w_{f_{UN}} - w_f}{w_f} = (1 + C_d') \frac{P_{R_e} - P_{R_{UN}}}{P_{R_{UN}}} \tag{45}$$

Values of C_d are usually between 0.2 and 1.0 and values of C_d' are usually zero, so that the change in uninstalled thrust specific fuel consumption is:

$$\frac{\Delta TSFC_{UN}}{TSFC_{UN}} = -C_d \frac{P_{R_e} - P_{R_{UN}}}{P_{R_{UN}}} \tag{46}$$

If the inlet pressure recovery is greater than the standard value, the specific fuel consumption is reduced and the thrust is increased, the effect on the thrust being several times greater than that on the specific fuel consumption. The thrust is increased both by increased airflow and by increased efficiency. The installed thrust is computed by subtracting the external spillage drag, the throat bleed drag, and the bypass bleed drag from the uninstalled thrust corrected for pressure recovery by equation (44).

$$F_{IN} = F_{UN} - D_{EXT} - D_{BL} - D_{BY} \tag{47}$$

The installed thrust specific fuel consumption is computed from

$$TSFC_{IN} = \frac{w_{f\,UN}}{F_{IN}} \tag{48}$$

where $w_{f_{UN}}$ is evaluated from equation (45).

Several reports (e.g., refs. 1, 71 and 72) which present studies of the effects of inlet operating conditions on propulsion system performance have been published. For the purposes of this report, the inlet and engine sizes are constant and only inlet geometry (e.g. A_{th}), bypass area and engine throttle position are variable. The results of a representative study of the effects of control tolerances on performance with fixed power lever position are presented in ref. 1. For some applications it is desirable to keep a fixed flight altitude. Consequently, the installed thrust must not be altered by changes in inlet geometry. Changes in the three drag terms in equation (47) must be offset by a corresponding change in the uninstalled thrust caused by a change in throttle position. Figure 32 presents uninstalled performance data for a typical turbojet at fixed altitude, flight Mach number, and pressure recovery. A change in the engine net thrust is accompanied by a change in engine fuel flow and, at low thrusts, by a change in engine corrected airflow. Assume that the performance has been corrected for installation effects at a particular operating condition. Then, for constant installed thrust, the change in engine fuel flow is:

$$\Delta w_f = \frac{dw_f}{dF_n} \left(\Delta D_{EXT} + \Delta D_{BL} + \Delta D_{BY} - (1 + C_d) F_n \frac{\Delta P_R}{P_R}\right) + w_f \, (1 + C_d{}') \frac{\Delta P_R}{P_R} \tag{49}$$

and the change is thrust specific fuel consumption is:

$$\frac{\Delta TSFC}{TSFC} = \frac{\Delta w_f}{w_f} \tag{50}$$

In these two equations the changes are from the initial corrected performance and are due to changes in inlet geometry and bypass area, for example.

An example will illustrate the concepts discussed above. The inlet performance characteristics are shown in figure 31. The following assumptions are made:

$$
\begin{aligned}
F_n &= 2370 \text{ lb} \\
w_f &= 3560 \text{ lb/hr} \\
C_d &= 0.3 \\
C_d{}' &= 0.0 \\
wc_e &= \text{constant} \\
dw_f/dF_n &= 2.3 \text{ lb/hr/lb} \\
D &= 2410\ C_D \text{ lb} \\
dC_{D_{BL}}/dW_{R_{BL}} &= 1.6 \\
dC_{D_{BY}}/dW_{R_{BY}} &= 1.0 \\
C_{D_{EXT}} &= 0.0055
\end{aligned}
$$

Then, using equations (44), (45), (47) and (48), the installed thrust specific fuel consumption was calculated for several points on the minimum A_{th} inlet characteristic with D_{BY} = zero. The point for minimum $TSFC_{IN}$ is taken as the reference condition from which the transient tolerances apply. Five cases are discussed.

For the first case the throat area is increased so that the inlet pressure recovery curve is displaced downward, in a similar manner to that shown in figure 31. Because the bypass is assumed to remain closed, the inlet relative airflow decreases and the terminal normal shock moves upstream. Thus, for example, the operating point changes from the circle to the triangle in figure 31. The decreases in installed thrust F_{IN} and in pressure recovery P_R and the increase in $TSFC_{IN}$ are shown as a function of the throat Mach number tolerance by solid lines in figure 33. Thus, increasing the throat Mach number by 0.103 to 1.303 reduces P_R by 0.27%, reduces F_{IN} by 0.75% and increases $TSFC_{IN}$ by 0.48%.

Unfortunately, for case 1 the shock position tolerance decreases as the throat Mach number tolerance increases. For case 2, the bypass opens as the throat Mach number increases in order to maintain a fixed inlet relative airflow. Thereby the shock position tolerance remains nearly constant. Opening the bypass moves the operating point from the triangle to near the diamond in figure 31. The changes in performance are shown by short-dashed lines in figure 33. The performance losses for case 2 are significantly larger than those for case 1.

Case 3 demonstrates the results of increasing the engine thrust by advancing the engine power lever in order to maintain the reference installed thrust. For this case there is no loss in F_{IN} and the pressure recovery loss is the same as that for case 2. However, because of the increased fuel flow required, the increase in $TSFC_{IN}$ is much greater than that for case 2, as shown by the long-dashed line in figure 33.

Case 4 in fig. 34 shows the effects of increasing the bypass area in order to increase the shock-position tolerance, i. e., to move the shock back from the throat. In figure 31, for example, the operating condition is changed from the circle to the square. The decreases in pressure recovery and in installed thrust and the increase in $TSFC_{IN}$ are shown by the solid lines in figure 34 as a function of shock position tolerance, which is expressed as a percent of corrected airflow.

The fifth case, like case 3, assumes that the engine power lever is advanced to maintain a constant installed thrust. The loss in pressure is the same as for case 4 but the increase in $TSFC_{IN}$ is nearly double, as shown by the dashed line in figure 34.

The following table lists a representative set of parameters computed for each of the five cases discussed above. For each case, several such sets were computed in order to produce the curves in figures 33 and 34.

Case	Reference	1	2	3	4	5
M_{th}	1.200	1.303	1.300	1.300	1.200	1.200
P_{Re}	0.8765	0.8741	0.8646	0.8646	0.8600	0.8600
W_{Ri}	0.9200	0.9175	0.9200	0.9200	0.9210	0.9210
D_{EXT}, lb	13.2	13.2	13.2	13.2	13.2	13.2
D_{BL}, lb	3.8	13.5	3.8	3.8	0.0	0.0
D_{BY}, lb	0.0	0.0	30.0	30.0	44.2	44.2
F_{IN}, lb	2449.0	2430.7	2376.1	2449.0	2348.9	2449.0
$w_{f_{IN}}$, lb/hr	3671.0	3661.0	3621.3	3789.0	3601.9	3832.1
$TSFC_{IN}$, lb/hr/lb	1.499	1.506	1.524	1.547	1.533	1.565
w_{c_i}, %	100.00	100.00	101.37	101.37	102.03	102.03

The values of the performance losses computed from equations (44) to (50) depend on the throat Mach number and shock position tolerances used. In addition, the losses depend on the inlet and engine performance characteristics used. For this reason, the losses shown in figure 4 of ref. 1 differ from the losses shown in figures 33 and 34 of this report. However, given the inlet and engine performance characteristics, such as shown in figures 31 and 32, the performance losses can be calculated from the equations in this section. The performance losses depend on the ground rules assumed, for example on whether the inlet size or the power lever position may be varied or are fixed. These ground rules are likely to change as the aircraft design progresses from the preliminary design phase to the flight operational phase.

FREQUENCY OF INLET UNSTARTS

Previous sections present data on the atmospheric turbulence environment and on a linearized model of a supersonic inlet. This section develops a procedure for estimating the frequency of inlet unstarts. This is done by deriving an equation for the frequency of a given change in throat Mach number or shock position. These given changes, the transient control tolerances, are assumed to be just enough to cause an inlet unstart due to choking the throat or the shock moving upstream of the throat, respectively. Transient disturbances in the other direction are presumed to cause no harm. Plots of flight miles between unstarts against the transient control tolerances, which are related to performance penalties, are the final result. Similar plots are shown in ref. 1.

Power Spectrum of Output Disturbances

The inlet model shown in figure 18 is simplified to produce the schematic in figure 35. Only longitudinal gusts are considered at this point. Here the C's are constants and the H's are functions of frequency ω which, with the exception of H_1, are unity at zero frequency. Values for the six constants and equations for the seven frequency-response functions H are determined by the inlet model, such as that developed in a preceding section, and the characteristics of the throat Mach control and shock position control. The equations in figure 35 relating the changes in throat Mach number and shock position to the change in flight Mach number are functions of frequency because of the "H" terms. Both ΔM_{th} and ΔX_s are linear functions of the upstream disturbances.

The power spectrum ϕ_0 of ΔM_0 is selected. The Von Karman spectrum (see Table II) is recommended. It can be shown (e.g., see refs. 31 and 42) that the power spectra of ΔM_{th} and ΔX_s are given by the equation

$$\phi(\omega) = \left|H(\omega)\right|^2 \phi_0(\omega) \qquad (51)$$

where the appropriate subscript "th" or "s" is appended to $\phi(\omega)$ on the left and $H(\omega)$ is the appropriate linear frequency-response function. For example, $H(\omega)$ is a coefficient of ΔM_0 on the right of one of the equations in figure 35. Usually, the frequency-response functions are available as functions of the Laplace variable S rather than frequency ω. Therefore, it is necessary to convert an equation for H(S) to an equation for $\left|H(\omega)\right|^2$. This may be done by using the following equation.

$$\left|H(\omega)\right|^2 = H(i\omega)\,H(-i\omega) = H(S)H(-S) \qquad (52)$$

That is, H(S) is multiplied by H(-S) and then S is replaced by $i\omega$ to obtain the desired equation, which must have only real terms. For example, if $H(S) = 1 + \tau S$,

$$\begin{aligned}\left|H(\omega)\right|^2 &= (1+\tau S)(1-\tau S) = 1-\tau^2S^2 \\ &= 1-\tau^2(i\omega)^2 = 1+\tau^2\omega^2\end{aligned}$$

While the algebraic processes performed above are straightforward, the actual execution for more complicated functions H(S) can be very difficult because several hundred terms may occur. Consequently, a digital program was written to read an equation for the frequency-response function H(S) and to derive and print the equation for the amplitude of the square of the frequency-response function $\left|H(\omega)\right|^2$. This program is described in Appendix E. The complete frequency-response function may be considered to be the product of a number of functions in the numerator and in the denominator, each of which may be considered separately and the final equations combined.

Thus from figure 35,

$$\Delta M_{th} = \frac{C_1 \; H_2}{-f_{th} \; C_2 + H_2} \; \Delta M_0$$

and from equation (51) with $H(\omega)$ replace by the factor of ΔM above:

$$\phi_{M_{th}}(\omega) = \frac{C_1^2 \; \left| H_2(\omega) \right|^2}{\left| -f_{th} \; C_2 + H_2(\omega) \right|^2} \; \phi_{M_0}(\omega) \tag{53}$$

That is, the terms C_1, H_2, and $-f_{th} \; C_2 + H_2$ are converted separately to equations for the square of the frequency response and then combined in equation (53). Several simple functions of S appear frequently in H(S). Some of these are shown in Table VI alongside the corresponding equation for $\left| H(\omega) \right|^2$. Table VI and the program described in Appendix E may be used to develop an equation for the square of the frequency-response function in equation (51).

Several representative examples for the square of the frequency-response function have been worked out. The results are shown in figures 36, 37 and 38. Figure 36 is drawn for a simple throat Mach control consisting of an ideal integrator. Curves are drawn for loop velocity constants ($-f_{th} \; C_2$) of 0 (no control), 5, 10, 20, and 40/sec. At low frequencies ω, the throat Mach number power spectral density is significantly reduced by the control. In practice, H_2 should be a more complicated function of S in order to account for the dynamics of pneumatic transmission lines, a sensor, and a servo valve. Figure 37 is drawn for a representative function H_2 (S). Compared to figure 36, a resonance peak is introduced near 25 rad/sec. Three curves are drawn for a loop velocity constant of 20/sec. The dashed curve, when compared to the solid curve, shows the result of changed dynamic characteristics caused by lowering the pressure level (increasing altitude). The resonant peak is accentuated and moves to a lower frequency. The dash-dot curve shows that adding a lead term reduces the resonant peak and moves it to a higher frequency. Figure 38 is drawn for the power spectrum of the shock position. The ratio is nearly constant at about 300 if neither the throat Mach number nor the shock position controls operate. If just the throat Mach control operates, ϕ_S is increased by about a factor of 3 at low frequencies and dips sharply near 45 rad/sec. With the shock-position control also operating, ϕ_S is reduced at low frequencies and peaks about 15 rad/sec. The parameters in the block diagram in figure 35 are:

$C_1 = 1.85$	$H_1 = 0.34S$
$f_{th} = -2.23$	$C_2 = 8.9686$
$C_3 = -40.842$	$C_4 = 9.3062$

$$H_2 = (1 + 0.015S + 0.0001S^2)\,(1 + 0.002S)\,(1 + 0.01S)S$$
$$H_3 = 1 + 0.0009367S$$
$$H_4 = 1 - 0.0045075S + 0.000013281S^2$$
$$H_5 = 1 + 0.01899S + 0.000105S^2 + 0.00000027S^3$$

The dash and dash-dot lines show the effects of adding one and two lead terms, respectively, to the shock-position control simulation in order to minimize the resonant peak.

Two parameters A and N are used in the following subsection to compute exceedance statistics. They may be computed by integrating the power spectrum of the change in throat Mach number or shock position. The first parameter is the ratio of the rms amplitude of the output disturbance to the rms amplitude of the free-stream disturbance:

$$A = \sqrt{\frac{\int_0^\infty \phi \; d\omega}{\int_0^\infty \phi_0 \; d\omega}} = \frac{\sqrt{\int_0^\infty \phi \, d\omega}}{\sigma_0} = \frac{\sigma}{\sigma_0} \tag{54}$$

where the appropriate subscript, "th" or "s", should be appended to A and to ϕ and σ in the numerator. The digital program described in Appendix F was written to compute ϕ as a function of frequency and to perform the integration in equation (54). Actually, the upper limit of the integration in this program is a variable rather than infinity. However, as discussed in connection with equation (2), the contribution to the integral above some cutoff frequency ω_c is small and may be neglected.

The second parameter is the number of times the disturbance crosses zero with positive slope per unit time. This parameter, called N_{th} for throat Mach number, is computed from the equation

$$N_{th} = \frac{\sqrt{\int_0^\infty \omega^2 \phi_{th} \; d\omega}}{2\pi \sqrt{\int_0^\infty \phi_{th} \, d\omega}} = VG_{th} \tag{55}$$

Likewise, N_s for the shock position is:

$$N_s = \frac{\sqrt{\int_0^\infty \omega^2 \, \phi_s \, d\omega}}{2\pi \sqrt{\int_0^\infty \phi_s \, d\omega}} = VG_s \tag{56}$$

This parameter is also computed by the program described in Appendix F as a function of the upper limit of the integration. For most spectra this parameter becomes infinite if the upper limit is infinite. This effect is discussed in connection with equation (3). A solution to this problem which results in a finite value is described there and is recommended. As noted in refs. 42 and 73, the validity of equations (55) and (56) depends on the assumption that the probability distribution of σ is locally Gaussian. That is, that

$$p(\sigma) = \sqrt{\frac{2}{\pi}} \, \frac{1}{b} \, e^{-\sigma^2/2b^2} \tag{57}$$

where

$$\int_0^\infty p(\sigma) d\sigma = 1$$

Available data (e.g., see ref. 73) indicate that this assumption is not satisfied. However, since no better assumption is known, since the resulting error in equations (55) and (56) is not known but should be small, and since these equations are universally used in loads calculations, equations (55) and (56) will be considered valid.

Values for A_{th}, A_s, N_{th}, and N_s depend only on the shape of the power spectra ϕ_{th} and ϕ_s and on the cutoff frequency ω_c. To illustrate representative results, the program described in Appendix F was used for the inlet models of figures 37 and 38. A Von Karman longitudinal spectra with L = 2500 ft and V = 2613.82 fps was used for ϕ_{M_L}.

The results are presented in the following two tabulations for a cutoff frequency of 102.4 rad/sec.

Case, figure 37	$-f_{th} C_2$	A_{th}	N_{th}, /hr	G_{th}, /mile
	0	1.85000	6 982	4.508
	10	0.85277	16 444	10.618
	20	0.82379	19 153	12.368
low pressure	20	1.12642	14 185	9.160
with lead	20	0.69159	22 681	14.645
	30	0.91657	20 446	13.202

Case, figure 38	C_5	A_s, ft	N_s, /hr	G_s, /mile
	5	17.18305	8 135	5.253
	10	15.54177	9 954	6.427
one lead	10	13.66904	10 664	6.886
two leads	10	11.23797	12 004	7.751
	15	16.14338	11 130	7.187

It is apparent that changes in the shape of the power spectral density curve change the values of A, N and G. Generally an increase in A is associated with a decrease in N and G. As will be shown in the following subsection, low values for both A and G are desirable.

Exceedance Statistics

In this section there is derived an equation for the frequency of inlet unstarts. In order to simplify the discussion, only unstarts due to a decrease in throat Mach number will be considered. However, the discussion is also valid for an unstart due to an upstream shock displacement. The problem, then, is to determine the frequency (per flight mile or hour) that a level of ΔM_{th} is exceeded. This level is the throat Mach number transient tolerance; that is, the amount that the throat Mach number is increased above the minimum value for started operation in order to reduce the frequency of inlet unstarts due to transient disturbances such as atmospheric gusts. The procedure used is the same as that for calculating aircraft load exceedance curves (e.g., see refs. 31, 32, 35 and 42). Several assumptions are made:

1. The transfer function between a free-steam disturbance and ΔM_{th} is linear.

2. The shape of the power spectrum ϕ_{th} is fixed, although the level depends on σ_{th}.

3. Values of A_{th} and N_{th} are computed by equations (54) and (55).

4. A statistical description of atmospheric turbulence is available in terms of P and b.

5. The probability density distribution of the rms amplitude of the atmospheric turbulence in the many patches encountered is p (σ_0).

The frequency of crossings of a level ΔM_{th} with positive slope is (e.g., see refs. 31, 42, and 73):

$$N = PN_{th} \int_0^{\infty} p(\sigma_0) e^{-\frac{\Delta M_{th}}{2A_{th}\sigma_0}} d\sigma_0 \tag{58}$$

Usually, $p(\sigma_0)$ is assumed to be Gaussian with a variance of b^2, so that

$$p(\sigma_0) = \sqrt{\frac{2}{\pi}} \frac{1}{b} e^{-\sigma^2/2b^2} \tag{59}$$

For this probability density distribution, the integration in equation (58) can be performed analytically with the simple result

$$N = PN_{th} e^{-\Delta M_{th}/A_{th}b} \tag{60}$$

This equation, case "a" of ref. 42, results in a straight line on a semilog plot like figure 14. Experience, however, shows that the line should be curved. Usually this curvature is introduced by summing two or three terms to produce the following equation

$$N = N_{th} \left(P_1 e^{-\frac{\Delta M_{th}}{A_{th}b_1}} + P_2 e^{-\frac{\Delta M_{th}}{A_{th}b_2}} + P_3 e^{-\frac{\Delta M_{th}}{A_{th}b_3}}\right) \tag{61}$$

Values of P_1, P_2 and P_3 may be found in Table III and figures 10 and 11.

Values of b_1, b_2 and b_3 may be found in Table III and figures 12 and 13.

Generally, $P_1 > P_2 > P_3$ and $b_1 < b_2 < b_3$. Equations (60) and (61) determine the frequency (e.g., times per hour) that the throat Mach number decreases (or increases) by at least ΔM_{th} units or, in other words, the frequency that a tolerance ΔM_{th} is exceeded. In equation (60) the frequency is proportional to PN_{th} and, for a given frequency, ΔM_{th} is proportional to $A_{th}b$. Therefore, it is desirable that N_{th} and A_{th} be small. Dr. Houbolt (see ref. 42) investigated several probability density functions in place of that in equation (59), and obtained equations (5) to (9) in place of equation (60). The curvature of the exceedance curve provided by these equations depends on one parameter, α. The curvature required to fit some particular data is provided either by using two or three terms in equation (61); or by using equations (5-7), (8), or (9) with an appropriate value of α. At high exceedance probabilities (large N, low ΔM_{th}), all exceedance curves from these equations can coincide. Only at small exceedance probabilities (large ΔM_{th}) do they differ, as shown in figure 14. However, it is in this area that the available data on which the exceedance curves are based are most limited. Thus, to estimate the inlet transient tolerance which is exceeded once in 10 million miles is risky, because, as earlier discussion and Table I show, available experience barely extends to 1 million miles. An extrapolation to large distances between unstarts is very questionable.

STEPWISE PROCEDURE FOR CALCULATING FREQUENCY OF INLET UNSTARTS

The procedure for computing an exceedance curve of N, frequency of crossings, versus ΔM_{th} may be outlined in the following steps:

1. Select an analytical model of the inlet which expresses changes in ΔM_{th} as a linear function of the upstream disturbances u, v and w. These functions may be in terms of the Laplace variable S which must be converted into functions of ω. Suggested models are described in the section ANALYTICAL INLET MODEL.

2. Compute the PSD ratios ϕ_{th}/ϕ_u, ϕ_{th}/ϕ_v and ϕ_{th}/ϕ_w as functions of frequency ω from the functions in step 1. Preferably, these three ratios are analytical functions obtained by using Table VI and the digital program described in Appendix E.

3. Select an atmospheric turbulence model and corresponding power spectral density family from Table III. A model associated with the Von Karman family is preferable. Select the appropriate scale length L from Table III. The atmospheric turbulence model from refs. 35 and 41 is recommended.

4. Determine coefficients in equations for $\phi_u(\omega)/\sigma_u^2$ and $\phi_w(\omega)/\sigma_w^2$ (see Table II) which depend on L and flight velocity V.

5. Compute ϕ_{th}/σ_u^2, A_{th_u}, and G_{th_u} with the digital program described in Appendix F. The function PSD required by the digital program uses the equations for ϕ_{th}/ϕ_u from step 2 and for $\phi_u(\omega)/\sigma_u^2$ from step 4. A_{th_u} is the bottom number in the ninth column (headed "SIGMA UNITS") of the program output. The value of the G_{th_u} is read from column 10 on the line in which the number in the ninth column is 95 percent of A_{th_u}. Interpolation between lines may be employed.

6. Compute ϕ_{th}/σ_v^2, A_{th_v}, and G_{th_v} as in step 5 using ϕ_{th}/ϕ_v and $\phi_w(\omega)/\sigma_w^2$.

7. Compute ϕ_{th}/σ_w^2, A_{th_w}, and G_{th_w} as in step 5 using ϕ_{th}/ϕ_w and $\phi_w(\omega)/\sigma_w^2$.

8. Compute A_{th} from the equation

$$A_{th} = \sqrt{A_{th_u}^2 + A_{th_w}^2 + A_{th_v}^2} \tag{62}$$

For G_{th}, an average seems reasonable

$$G_{th} = (G_{th_u} + G_{th_w} + G_{th_v})/3 \tag{63}$$

9. For the atmospheric turbulence model selected in step 3, determine the parameters P and b for the given altitude from Table III or figures 10 to 13.

10. Compute the exceedance curve for ΔM_{th} by using the digital program described in Appendix G. Use exceedance model based on equation (4). If the atmospheric turbulence model is from ref. 42 use the exceedance model based on equations (5), (6) and (7) with $\alpha = 8$ to 9. Input parameters include A_{th} and G_{th} from step 8 and P_1, P_2, b_1 and b_2 from step 9. The amplitude $X = \Delta M_{th}$ may be plotted against either the number of nautical miles between exceedances (unstarts) or the number of hours between unstarts.

In addition, the performance penalties resulting from the transient tolerances in throat Mach number (ΔM_{th}) may be obtained by using the procedure already described in the Analytical Model of Propulsion System Performance section.

A similar analysis to that outlined above may be performed for the change in shock position ΔX_s. The results of the two analyses are expressed in two curves of miles (or hours) between unstarts against performance penalties, such as range. The two results, one for unstarts due to choking the throat and one for unstarts due to the shock moving upstream past the throat, may be combined if the throat Mach number and shock position transient tolerances are selected to give equal frequency of unstarts due to the two causes. For a given number of miles between inlet unstarts, the performance penalty associated with throat Mach number and the performance penalty associated with shock position are read from the two curves. The sum of these two penalties, or the total performance penalty, may be plotted against the given number of miles between inlet unstarts. This plot shows the relation between frequency of inlet unstarts at a given flight speed and altitude to the performance penalty required. With this relation available, it will be possible to select the required transient control tolerances based upon a particular mission profile and a preselected interval between inlet unstarts. The interval may be selected based upon a qualitative and quantitative assessment of the consequences of an inlet unstart to aircraft safety and passenger comfort.

The procedure presented above calculates the frequency of inlet unstarts for a selected altitude and flight speed. Actually, each flight will include a range of altitudes and flight speeds at which inlet unstarts are undesirable. Therefore, calculations should be performed for several sets of altitudes and flight speeds and the results combined by using weighting factors proportional to the flight time at each set of conditions. The result could be a plot of the number of trips between unstarts against some performance penalty, such as dollars per trip. It must be emphasized that this plot, like figures 42 to 46 of this report, is based on statistical theory. Thus, although the theory might predict one unstart in 1000 flights, several unstarts could occur in one flight through a large patch of severe turbulence.

If the performance penalties are too severe, several possible solutions may be investigated:

1. Change geometry of airplane and inlet to reduce sensitivity of throat Mach number and shock position to atmospheric turbulence.

2. Change inlet geometry to reduce performance penalties resulting from inlet transient tolerances.

3. Increase speed of response of inlet controls.

4. Use two levels of transient tolerances: one for normal operation, and a larger level when turbulence is expected. At present, a practical means for detecting turbulence far enough ahead of the aircraft to avoid it or to reset the transient tolerances is not available (see ref. 10).

APPLICATION OF PROCEDURE TO REPRESENTATIVE INLET

The procedure for relating the interval between unstarts to performance penalties will be illustrated by applying it to a representative inlet. The characteristics of this inlet were supplied by the Boeing Company and are shown in figure 39. The inlet representation is the result of independent studies by Boeing and does not reflect the model developed in this report. This block diagram contains some significant differences from that in figure 35 which complicate the analysis. First, on the left, terms involving the absolute value of a disturbance ($|\Delta\alpha|$and $|\Delta\beta|$) rather than the signed value of the disturbance are used. Second, in a block associated with shock position, $K_1 = 45$ and $K_2 = 0$ so that the gain depends on the sign of ΔX_s. Because of the limited time available for this part of the contract the following approach was used to resolve these two problems. The inlet and control shown schematically in figure 39, with $K_1 = 45$ and $K_2 = 0$, was simulated by a MIMIC digital program. Sinusoidal changes in M_0 were input at frequencies of 1, 10, and 100 rad/sec. In addition, the frequency response was calculated by a frequency-response program with several values of $K_1 = K_2$. The amplitude of ΔM_{th}, which is independent of K_1 and K_2, agreed exactly with the amplitude computed by the frequency-response program. Satisfactory agreement for the amplitude of ΔX_s was obtained with $K_1 = K_2 = 22.5$. Therefore, the gain calculations for ΔX_s with $K_1 = K_2 = 22.5$ are used. A sinusoidal change in α was input to the MIMIC program at a frequency of 10 rad/sec. Reasonable agreement for the gains of ΔM_{th} and ΔX_s computed by the MIMIC program was obtained from the frequency-response program with the $|\Delta\alpha|$ input term omitted. Therefore, only the $\Delta\alpha$ and not the $|\Delta\alpha|$input is used for the frequency-response function. A sinusoidal change in β was input to the MIMIC program at a frequency of 10 rad/sec. Reasonable agreement for the gains of ΔM_{th} and ΔX_s was obtained from the frequency-response program for half the input amplitude and twice the frequency. Therefore, the frequency-response functions for $\Delta\beta$ were obtained by halving the gain evaluated at twice the frequency.

The normalized longitudinal Von Karman spectrum with L = 2500 ft is shown in figure 40. The normalized spectrum of the throat Mach number change due to longitudinal gusts also is plotted in figure 40. Because the throat Mach number control cannot reduce throat Mach number disturbances at frequencies over roughly 20 rad/sec, the two spectra are parallel at high frequencies and have a ratio of 4.997^2. Figure 41 shows the corresponding spectrum for shock position. The shock-position spectrum has maxima at 4 and 90 rad/sec and a minimum near 38 rad/sec. It is apparent by comparing this spectrum with that of free-stream longitudinal turbulence in figure 40 that the shock-position transfer function has maxima near 10 and over 100 rad/sec and a minimum near 38 rad/sec.

The exceedance curves for an unstart due to choking the throat because of a longitudinal gust are shown in figure 42. This figure is for the representative inlet at a flight Mach number of 2.7 and an altitude of 60 000 ft. The parameters used to compute these curves are presented in the following tabulation:

Ref.	A_{th}	ω_c, rad/sec	G_{th}, /n. mi.	P_1	P_2	b_1	b_2	α
33	2.87	62.	7.1	0.019	0.000075	0.00276	0.0134	
34	2.87	62.	7.1	0.0021	0.000135	0.0037	0.00595	
35&41	2.36	82.	9.352	0.0012	0.000062	0.00382	0.00594	
36	2.14	62.	6.7	0.008	0.000027	0.00243	0.00806	
37	2.36	82.	9.352	0.008		0.0031		6.74
39	2.87	62.	7.1	0.008	0.000027	0.00243	0.00806	
42, a	2.36	82.	9.352	0.002946		0.00561		
42, k	2.36	82.	9.352	0.002945	0.0000015	0.00560	0.01400	0.0005
42, j	2.36	82.	9.352	0.002946		0.00561		8.0
42, m	2.36	82.	9.352	0.002946		0.00561		0.003

The value of G_{th} was evaluated at a frequency ω_c at which the truncated value of σ_{th_1} was 95 percent of the largest σ_{th} computed (at ω_c = 655 rad/sec). The value of A_{th} corresponds to ω_c = 655 rad/sec. The exceedance curve for ref. 33 shows that a large tolerance is required because a relatively large value for b_2 is involved. The remaining exceedance curves fall in a group with considerable scatter. Figure 43 presents curves for an unstart due to displacement of the shock upstream. The curves shown represent approximately the same extent of scatter illustrated in figure 42.

Figures 42 and 43 are for longitudinal gust disturbances only. Two exceedance models, those in ref. 35 and 42 (case "j", α = 8) were selected for an analysis which includes all three components of a gust; namely: longitudinal, vertical (resulting in a change in angle of attack), and lateral (resulting in a change in angle of sideslip). The Von Karman family with L=2500 ft is used for the free-stream turbulence spectra. Calculations of the output power spectral densities ϕ_{th} and ϕ_s are based on the assumptions described previously and the stepwise procedure presented in the preceding section. Some intermediate numerical results are presented in the following table:

Disturbance	A_{th}	G_{th}	A_s	G_s
Longitudinal	2.36	9.35	3.31	3.18
Vertical	1.44	11.0	1.97	3.20
Lateral	0.71	6.5	0.75	1.50
Combined	2.854	8.95	3.924	2.63

The combined values for A and G are computed from equations (62) and (63) respectively. The exceedance curves for combined gusts are presented in figures 44 and 45. Because vertical and lateral gusts are included, the curves in figures 44 and 45 lie to the right of the corresponding curves in figures 42 and 43, respectively. In other words, inclusion of three gust components rather than just the longitudinal gust component increases the transient tolerance required for a given number of nautical miles between unstarts.

Linear relations between range penalty and transient tolerances in throat Mach number and in shock position, provided by the Boeing Company, were used to plot the horizontal scales of range penalty at the bottom of figures 42 through 45. It should be pointed out that these relations need not be linear. The range penalties are used to combine the throat Mach number and shock position tolerances. The final combined result is presented in figure 46. A comparison of figures 44 and 45 shows that the range penalty due to the shock position tolerance is roughly one-quarter of that due to the throat Mach number tolerance. Boundary layer bleed near the inlet throat can enhance the stability of the normal shock and thereby reduce its displacement due to atmospheric turbulence. However, little can be done to diminish the change in throat Mach number. Therefore, the throat Mach number transient tolerances required to reduce the frequency of inlet unstarts are the major contributors to the overall range penalty shown in figure 46.

Reference 53 specifies certain discrete gusts as disturbances. Two disturbances are defined by the equations:

$$\Delta M_0 = -0.04275 \ (1-\cos 16.45t)$$

$$\Delta \alpha = 0.908 \ (1-\cos 16.45t)$$

By analogy, the following equation for a disturbance in angle of sideslip is used:

$$\Delta \beta = 0.908 \ (1-\cos 16.45t)$$

These three disturbances were used separately as inputs to the MIMIC simulation described previously and the maximum decrease in M_{th} and upstream displacement of the shock were determined. These amplitudes are shown by the vertical lines in figures 44 and 45. The combined range penalty is shown in figure 46. The angle of sideslip disturbance is the least severe and the flight Mach number disturbance is the most severe. The flight Mach number disturbance requires a range penalty about equal to that for 100 million miles between unstarts according to the model of ref. 42, but exceeds that according to the model of refs. 35 and 41.

The analysis of the representative inlet presented above uses assumed values for the cutoff frequency ω_c and the scale of turbulence. The effects of these assumptions are discussed briefly in the rest of this section. The discussion is limited to the effects of longitudinal gusts on throat Mach number. First, the effect of varying cutoff frequency ω_c is discussed. A Von Karman spectrum with L = 2500 ft is used. The results are expressed in the following tabulation:

ω_c rad/sec	A_{th}	G_{th}	ΔM_{th}
10.24	1.371	2.327	0.0613
40.96	2.097	6.367	0.1051
86.00	2.240	9.600	0.1173
163.84	2.292	13.842	0.1248
655.36	2.358	32.770	0.1398

As would be expected, both A_{th} and G_{th} increase with increasing ω_c. However, A_{th} is approaching a finite limit while G_{th} is increasing without a limit. The right-hand column lists the throat Mach number tolerance for 10 million miles between inlet unstarts, based on the atmospheric turbulence model in ref. 35. The exceedance curves presented in figures 42 to 46 are calculated from the largest value of A (2.358 in tabulation above) and from a value of G corresponding to an A equal to 95 percent of the maximum A(G = 9.6 in tabulation above). For this set of A_{th} and G_{th}, ΔM_{th} is 0.1235. It is apparent that G, and perhaps A, must be based on a truncated integration to a frequency ω_c. Selection of G based on a 95 percent factor for A is recommended, but A may be either the full or truncated (95 percent) value.

Secondly, the effect of varying the scale of turbulence, L, is considered. Both A_{th} and G_{th} are based on a truncated ω_c. The results are presented in the following tabulation:

L, ft	ω_c, rad/sec	A_{th}	G_{th}	ΔM_{th}
1000	240	3.06	17.9	0.262
2000	95	2.40	10.2	0.191
2500	86	2.24	9.6	0.177
3500	83	2.01	9.4	0.158
5000	92	1.79	9.8	0.142

The right-hand column is the throat Mach number tolerance for 10 million miles between inlet unstarts, based on the case "j" exceedance model in ref. 42 with b = 0.005597. Increasing the scale of turbulence, for a fixed value of b, decreases the transient tolerance. However, Dr. Houbolt (ref. 42) recommends that b vary as the cube root of L. The results in the following tabulation are obtained with this variation of b.

L, ft	b	ΔM_{th}
1000	0.004124	0.193
2000	0.005196	0.178
2500	0.005597	0.177
3500	0.006262	0.178
5000	0.007052	0.179

Use of a value of b which depends on L reduces the variation of ΔM_{th} considerably.

Thirdly, the effect of changing from the Von Karman spectrum to the Dryden spectrum is shown in the following tabulation:

L, ft	ω_c, rad/sec	A_{th}	G_{th}	b	ΔM_{th}
1000	52	2.72	6.6	0.004124	0.151
2000	42	2.03	5.7	0.005196	0.140

Compared to the quantities listed in the two preceding tabulations, ω_c, A_{th}, G_{th}, and ΔM_{th} are all reduced significantly by using the Dryden spectrum. A conclusion from these studies is that the proper power spectral density family and scale of turbulence, as shown in Table III, must be used in connection with the atmospheric turbulence model selected. The proper family and scale are those used to derive the model from measured loads data.

CONCLUDING REMARKS

A method is developed for relating transient tolerances in inlet throat Mach number and shock position to the frequency of unstarts of a supersonic inlet due to atmospheric turbulence. This method is an adaptation of standard statistical methods used to predict aircraft structural fatigue loads with a power spectral density analysis. The investigation included the collection and evaluation of data on high-altitude atmospheric turbulence; development of a general linearized analytical inlet model for changes in throat Mach number and shock position due to changes in flight conditions, inlet geometry, and exit corrected airflow; development of a method for relating propulsion system performance to inlet transient tolerances; and writing of three digital computer programs to facilitate required algebraic and numerical procedures. One large computer program reads an equation for a frequency-response function in terms of the Laplace variable and derives and prints the corresponding equation for the amplitude of the square of the frequency-response function in terms of the frequency (rad/sec). A stepwise procedure for relating frequency of inlet unstarts to transient tolerances is described and applied to an inlet configuration representative of that on an SST.

The investigation has led to the following conclusions:

1. The aircraft loads experience data collected at high altitudes (about 60 000 ft) is not adequate yet to provide a reliable statistical model of turbulence at these altitudes. At present, there is no firm program to collect more flight data.

2 θ

2. Atmospheric turbulence models based on continuous turbulence provide a better description of atmospheric turbulence for studies of the frequency of inlet unstarts than models based on discrete gusts.

3. Each atmospheric turbulence model is derived from loads data by assuming a specific power spectral density family and scale of turbulence. Therefore, the family and scale used to develop the model selected should be used to compute frequency of inlet unstarts.

4. The atmospheric turbulence model in refs. 35 and 41 is the most suitable for computing frequency of inlet unstarts.

5. Changes in atmospheric temperature which occur over short distances are as significant in causing an inlet unstart as atmospheric turbulence.

6. The four linear analytical models of shock position developed agree with each other at low disturbance frequencies, but differ at high frequencies. The predicted amplitude and phase shift based on these models, especially the model based on ref. 54,show good agreement with method-of-characteristics solutions and with test data.

7. Performance penalties depend on the assumptions made. The predicted penalty in thrust specific fuel consumption due to inlet transient tolerances increases if it is assumed that the installed thrust is maintained constant by moving the engine throttle.

8. Combining longitudinal, vertical, and lateral components of atmospheric turbulence appreciably increases the predicted frequency of inlet unstarts compared to a prediction based on only the longitudinal component.

9. For the representative inlet studied, significant penalties in range are required to keep the frequency of inlet unstarts to small values.

The work described in this report leads to the recommendation that further investigations be undertaken in the following areas:

1. Study effects of atmospheric turbulence combined with rapid ambient temperature changes on supersonic inlets. The problem is largely that of establishing a statistical model of ambient temperature changes and of combining this model with one for longitudinal turbulence. A comprehensive analysis of flight data, such as that obtained during the HICAT program, is required to establish correlations between ambient temperature changes and gusts.

2. Investigate methods and effects of introducing inlet and control nonlinearities into the linear frequency-response function required by a power spectral density analysis.

3. Compare the theoretical predictions of the generalized inlet model developed in this report with experimental data obtained recently at the Ames and Lewis Research Centers. In addition, the analytical inlet model recently developed at the Lewis Research Center should be evaluated.

4. It has been assumed that the diffuser-exit Mach number, or corrected airflow, is constant for the calculations with the four upstream disturbances presented in figures 26 to 29. This assumption is valid for tests with a choked throttle downstream of the inlet. However, the corrected airflow of a turbojet engine will vary due to rapid changes in engine-face total temperature. These temperature changes will occur due to changes in upstream total temperature, shock motion, and compression of the air in the diffuser volume and are predicted by the shock-position models. Therefore, the change in engine corrected airflow due to these temperature changes should be evaluated and the effects of this change introduced into the calculations leading to figures 26 to 29.

APPENDIX A

FIRST ANALYTICAL MODEL OF SHOCK POSITION

The first analytical model of shock position uses the concept of a first-order lag relation suggested in ref. 70. As discussed on page 28 of this report, for a disturbance in downstream corrected airflow or Mach number the first-order lag relation involves a gain and shock time constant computed from

$$\tau_s = \frac{7M_1^2 + 5}{7M_1\sqrt{1 + 0.2M_1^2}} \quad \frac{AdX}{dA} \quad \frac{1}{a_t} \tag{A1}$$

The parameter M_1 is the Mach number at a fixed station immediately upstream of the shock (see figure 23). It is noted in ref. 70 that this time constant is larger than the time constant for a downstream static pressure disturbance which can be derived from the first equation of Table IV (i = 1) as:

$$\tau_s = \frac{12M_1\sqrt{1 + 0.2\,M_1^2}}{1 + 7.4\,M_1^2} \quad \frac{AdX}{dA} \quad \frac{1}{a_t} \tag{A2}$$

The steady-state gains are given by the equations in Table V. Thus, for a disturbance in Mach number downstream of the shock:

$$K_{M_2} = \frac{(7M_1^2 - 1)^{1.5}}{8.4M_1\sqrt{5 + M_1^2}} \quad \frac{AdX}{dA} \tag{A3}$$

for a disturbance in corrected airflow downstream of the shock:

$$K_{W_{ci}} = \frac{7M_1^2 - 1}{7\,(M_1^2 - 1)} \quad \frac{AdX}{dA} \tag{A4}$$

for a disturbance in Mach number upstream of the shock:

$$K_{M_1} = \frac{30}{7M_1\,(M_1^2 + 5)} \quad \frac{AdX}{dA} \tag{A5}$$

and, for a disturbance in duct area at the shock:

$$K_{A_1} = - \frac{7M_1^2 - 1}{7(M_1^2 - 1)} \frac{AdX}{dA} = -K_{w_{ci}} \tag{A6}$$

For a disturbance originating at the diffuser exit, a dead time τ_d is introduced to account for the time required for a sound wave to move upstream against the flow from the exit to the shock wave.

The first-order lag relationship for normal shock position is given by the following equation, in Laplace notation:

$$\Delta X_s = \frac{K_{w_{ci}} e^{-\tau_d S} \frac{\Delta w_{ci}}{w_{ci}} + K_{M_1} \Delta M_1 + K_{A_1} \frac{\Delta A_1}{A_1}}{1 + \tau_s S} \tag{A7}$$

The first term, $K_{w_{c_i}} e^{-\tau_d S} \frac{\Delta w_{c_i}}{w_{c_i}}$, may be replaced by $K_{M_2} \Delta M_2$ for a disturbance in Mach number just downstream of the shock. For given time-dependent disturbances Δw_{c_i}, ΔM_1 and ΔA_1, singly or combined, equation (A7) gives the time-dependent shock displacement ΔX_s. The shock time constant τ_s is computed from equation (A1).

APPENDIX B

SECOND ANALYTICAL MODEL OF SHOCK POSITION

For inlets with a long diffuser, allowance should be made for changes in the mass of air stored in the volume between the normal shock and the diffuser exit. The derivation herein of an analytical model which allows for this volume follows the analysis in ref. 69 except that the derivatives are replaced by functions of Mach number and the duct area gradient at the shock. A linearized, lumped-constant analysis is used.

The flow conditions in the fixed volume between a fixed station downstream of the shock (subscript "2", see figure 23) and the diffuser exit are represented by the flow conditions at an intermediate station (subscript "d"). Note that for this model the Helmholtz volume shown in figure 23 is not included and therefore $\ell = 0$. Although the selection of the intermediate station is arbitrary, the following equation for the area is used:

$$A_d = V/L \tag{B1}$$

The difference between the mass flow rate entering the volume and leaving the volume is proportional to the rate of change of mass stored in the volume. The mass stored is proportional to the air density at the intermediate station. Therefore, in Laplace notation,

$$\Delta w_2 - \Delta w_i = VS\Delta\rho_d \tag{B2}$$

The change in the flow rate entering the volume is given by the fourth equation in Table IV (i=4), which may be written in the form

$$\frac{\Delta w_2}{w_2} = \frac{\Delta P_{t1}}{P_{t1}} - \frac{1}{2}\,\frac{\Delta T_{t1}}{T_{t1}} + \frac{\Delta A_1}{A_1} - C_{44}\,\Delta M_1 - \frac{C_{46}}{a_t}\,S\Delta X_s \tag{B3}$$

The change in the flow rate leaving the volume at the exit is given by the equation

$$\frac{\Delta w_i}{w_i} = \frac{\Delta w_{ci}}{w_{ci}} + \frac{\Delta P_{ti}}{P_{ti}} - \frac{1}{2}\,\frac{\Delta T_{ti}}{T_{ti}} \tag{B4}$$

or, alternatively, by

$$\frac{\Delta w_i}{w_i} = \frac{1-M_i^2}{M_i\,(1+0.2M_i^2)}\,\Delta M_i + \frac{\Delta P_{ti}}{P_{ti}} - \frac{1}{2}\,\frac{\Delta T_{ti}}{T_{ti}}$$

The change in the average density in the volume is

$$\frac{\Delta \rho_d}{\rho_d} = -\,\frac{M_d}{1+0.2M_d^2}\,\Delta M_d + \frac{\Delta P_{td}}{P_{td}} - \frac{\Delta T_{td}}{T_{td}} \tag{B5}$$

The change in the Mach number M_d is assumed to the determined by

$$\Delta w_{cd} = \frac{1}{2}\,(\Delta w_{c2} + \Delta w_{ci})$$

or $$\Delta M_d = \frac{1}{2}\cdot\frac{w_{cd}\,\partial M_d}{\partial w_{cd}}\left(\frac{\Delta w_{c2}}{w_{c2}} + \frac{\Delta w_{ci}}{w_{ci}}\right) \tag{B6}$$

Furthermore,

$$\frac{w_{cd}\,\partial M_d}{\partial w_{cd}} = \frac{M_d\,(1+0.2M_d^2)}{1 - M_d^2} \tag{B7}$$

$$\frac{\Delta P_{ti}}{P_{ti}} = \frac{\Delta P_{td}}{P_{td}} = \frac{\Delta P_{t1}}{P_{t1}} - C_{24}\Delta M_1 - C_{25}\,\frac{dA}{AdX}\,\Delta X_s - \frac{C_{26}}{a_t}\,S\Delta X_s \tag{B8}$$

$$\frac{\Delta T_{ti}}{T_{ti}} = \frac{\Delta T_{td}}{T_{td}} = \frac{\Delta T_{t1}}{T_{t1}} - \frac{C_{36}}{a_t}\,S\Delta X_s \tag{B9}$$

$$\frac{\Delta w_{c2}}{w_{c2}} = \frac{\Delta A_1}{A_1} - C_{54}\Delta M_1 + C_{55}\,\frac{dA}{AdX}\,\Delta X_s + \frac{C_{56}}{a_t}\,S\,\Delta X_s \tag{B10}$$

$$w_2 = w_i = w_d = \frac{\rho_d M_d a_t A_d}{\sqrt{1 + 0.2M_d^2}} \tag{B11}$$

An equation for the second analytical model of shock position is obtained by combining equations (B1) through (B11), and is

$$\Delta X_s = \frac{K_{w_{ci}} (1 + \tau_{w_{ci}} S) e^{-\tau_d S} \frac{\Delta w_{ci}}{w_{ci}} + K_{M_1}(1 + \tau_{M_1} S) \Delta M_1 + K_{A_1} (1 + \tau_{A_1} S) \frac{\Delta A_1}{A_1} + \tau_{P_t} S \left(\frac{\Delta P_{t1}}{P_{t1}} - \frac{\Delta T_{t1}}{T_{t1}}\right)}{1 + \tau_1 S + \tau_2 S^2} \qquad \text{(B12)}$$

where $K_{w_{ci}}$, K_{M1}, and K_{A_1} are given by equations (A4) to (A6).

$$\tau_{P_t} = \tau_V \frac{AdX}{dA} \frac{7 M_1^2 - 1}{7 (M_1^2 - 1)} \qquad \text{(B13)}$$

$$\tau_{w_{ci}} = - \tau_V \frac{M_d^2}{2 - 2 M_d^2} \qquad \text{(B14)}$$

$$\tau_{M_1} = \tau_V \left(\frac{M_d^2}{2 - 2 M_d^2} - \frac{7}{6} (M_1^2 - 1)\right) \qquad \text{(B15)}$$

$$\tau_{A_1} = - \tau_{w_{ci}} \qquad \text{(B16)}$$

$$\tau_1 = \frac{AdX}{dA} \frac{1}{a_t} \frac{M_1 + 6}{7 M_1 \sqrt{1+0.2 M_1^2}} + \tau_V \frac{2 - M_d^2}{2 - 2M_d^2} \qquad \text{(B17)}$$

$$\tau_2 = \frac{\tau_V}{a_t} \frac{AdX}{dA} \frac{1}{14 M_1 \sqrt{1 + 0.2 M_1^2}} \left(\frac{37-7M_1^2}{3} + \frac{M_d^2}{1-M_d^2} (7M_1^2+5)\right) \qquad \text{(B18)}$$

$$\tau_V = \frac{V}{A_d U_d} = \frac{L \sqrt{1 + 0.2 M_d^2}}{a_t M_d} \qquad \text{(B19)}$$

This is a quadratic relation in which the term τ_2 may be thought of as the reciprocal of the square of a natural frequency and the term τ_1 as twice the ratio of the damping constant to the natural frequency. The steady-state shock displacement is obtained by setting the Laplace operator S = 0 in equation (B12).

Equation (B12) for the shock displacement represents the second analytical model. The Δw_{ci}, ΔM_1 and $\Delta A1$ terms each contain lead time constants. The shock displacement is proportional to the rate of change of upstream total pressure and temperature. The effects of bleed near the shock may be introduced, if desired, by including a negative term $-C_{45}\ \Delta X_s$ on the right of equation (B3), where C45 depends on the bleed geometry. This change would alter the time constants τ_1, τ_2 and τ_{P_t} and the gains $K_{w\,ci}$, K_{M_1} and K_{A_1}. However, nearly the same effect can be obtained by adjusting the area gradient dA/AdX.

The product $K_{wci}\ \Delta\ w_{ci}/w_{ci}$ in equation (B12) may be replaced by either K_{wci} $\Delta w_{c2}/w_{c2}$ or $K_{M_i}\ \Delta M_i$, where

$$K_{M_i} = K_{wci} \frac{1 - M_i^2}{M_i\ (1 + 0.2\ M_i^2)} \tag{B20}$$

as desired.

APPENDIX C

THIRD ANALYTICAL MODEL OF SHOCK POSITION

Several analyses of supersonic inlets have considered the pressure differential required to change the average velocity of the mass of air behind the shock. This inertia effect is introduced into the model developed in Appendix B to obtain the third analytical model. The mass contained in a Helmholtz volume of length ℓ (see figure 23) is considered to be the mass whose inertia is included. Equations (B1) to (B7) and (B9) to (B11) are used for this model.

From Newton's law,

$$(\Delta P_2 - \Delta P_z)A_1 = \frac{m_H}{g} S\Delta U_2 = \frac{\rho_2 A_1 \ell}{g} S\Delta U_2 \tag{C1}$$

The pressure change providing the accelerative force is

$$\Delta P_2 - \Delta P_z = \frac{1}{\left(1+0.2M_2^2\right)^{3.5}} \left(\Delta P_{t2} - \Delta P_{tz}\right) \tag{C2}$$

Also,

$$\Delta P_{tz} = \Delta P_{td} = \Delta P_{ti} \tag{C3}$$

$$\rho_2 = \frac{P_{t2}}{RT_{t2}\left(1+0.2M_2^2\right)^{2.5}} \tag{C4}$$

$$\Delta U_2 = \frac{a_t}{\sqrt{1+0.2M_2^2}} \left(\frac{M_2}{2} \frac{\Delta T_{t2}}{T_{t2}} + \frac{\Delta M_2}{1+0.2M_2^2}\right) \tag{C5}$$

$$\frac{\Delta P_{t2}}{P_{t2}} = \frac{\Delta P_{t1}}{P_{t1}} - C_{24}\Delta M_1 - C_{25}\frac{dA}{AdX}\Delta X_s - \frac{C_{26}}{a_t} S\Delta X_s \tag{C6}$$

$$\Delta M_2 = -C_{64}\Delta M_1 + C_{65}\frac{dA}{AdX}\Delta X_s + \frac{C_{66}}{a_t} S\Delta X_s \tag{C7}$$

$$M_2^2 = \frac{M_1^2+5}{7M_1^2-1} \tag{C8}$$

Equations (C1) to (C5) may be combined to produce the equation

$$\frac{\Delta P_{td}}{P_{td}} = \frac{\Delta P_{t2}}{P_{t2}} - \frac{1.4\,\ell}{a_t}\left(\frac{\sqrt{1.8}\,M_1\sqrt{M_1^2+5}}{7M_1^2-1}\,S\,\frac{\Delta T_{t2}}{T_{t2}} + \sqrt{\frac{7M_1^2-1}{7.2\,M_1^2}}\,S\Delta M_2\right) \tag{C9}$$

Equations (C6), (C7) and (C9) replace equation (B8) of the second model. The second term on the right of equation (C9), which is proportional to the length ℓ, accounts for the Helmholtz mass.

By combining the three equations above and the ten equations from Appendix B, following equation for the third analytical model of shock position is obtained:

$$\Delta X_s = \frac{K_{w_{ci}}(1+\tau_{w_{ci}}S)\,e^{-\tau_d S}\,\frac{\Delta w_{ci}}{w_{ci}} + K_{M1}(1+\tau_1 S+\tau_2 S^2)\,\Delta M_1 + K_{A1}(1+\tau_{A_1}S)\,\frac{\Delta A_1}{A_1} + \tau_{P_t}S\,\frac{\Delta P_{t1}}{P_{t1}} + \tau_{T_t}S(1+\tau_3 S)\,\frac{\Delta T_{t1}}{T_{t1}}}{1+\tau_4 S+\tau_5 S^2+\tau_6 S^3} \tag{C10}$$

where $K_{w_{ci}}$, K_{M_1}, K_{A_1}, τ_{M_1}, τ_{A_1}, $\tau_{w_{ci}}$, τ_{P_t}, and τ_V are expressed by equations (A4), (A5), (A6), (B15), (B16), (B14), (B13), and (B19), respectively, and

$$\tau_1 = \tau_{M_1} + \frac{\tau_2}{\tau_V} \tag{C11}$$

$$\tau_2 = \tau_V\,\frac{1.68\,\ell\,M_1\sqrt{M_1^2+5}}{\sqrt{7.2}\,a_t\,(M_1^2-1)} \tag{C12}$$

$$\tau_{T_t} = -\,\tau_{P_t} - \frac{0.6\;M_1\ell\sqrt{1+0.2\,M_1^2}}{a_t\,(M_1^2-1)}\;\frac{AdX}{dA} \tag{C13}$$

$$\tau_3 = - \tau_V \frac{0.6\ell\, T_1 \sqrt{1 + 0.2\, M_1^2}}{a_t\,(M_1^2 - 1)\ \tau_{T_t}} \frac{AdX}{dA} \tag{C14}$$

$$\tau_4 = \frac{M_1 + 6}{7\, a_t\, M_1 \sqrt{1 + 0.2\, M_1^2}} \frac{AdX}{dA} + \tau_V \frac{2-M_d^2}{2-2M_d^2} + \frac{\tau_2}{\tau_V} \tag{C15}$$

$$\tau_5 = \frac{\tau_V}{a_t} \frac{1}{14\, M_1 \sqrt{1 + 0.2\, M_1^2}} \left(\frac{37 - 7M_1^2}{3} + \frac{M_d^2}{1-M_d^2} (7M_1^2 + 5) \right)$$

$$\frac{AdX}{dA} + \tau_2 + \frac{\tau_6}{\tau_V} \tag{C16}$$

$$\tau_6 = \frac{1.2\ell\, \tau_V}{a_t^2} \frac{M_1^2 + 1}{M_1^2 - 1} \frac{AdX}{dA} \tag{C17}$$

If $\ell = 0$, the transfer function represented by equation (C10) is identical to the function represented by equation (B12).

APPENDIX D

FOURTH ANALYTICAL MODEL OF SHOCK POSITION

A propulsion system dynamic simulation, which includes both volume and Helmholtz mass effects, is developed in ref. 54. The simulation is designed for calculations in timewise steps on a digital computer and includes five phases of inlet operation. Equations for the fourth analytical model of shock position are derived herein by linearizing the equations in ref. 54 for the started phase. Thus, as in the other three models, small disturbances about an average condition are assumed. Internal bleeds and total pressure losses considered in the simulation are neglected. The nomenclature, which is illustrated in figure 23, closely follows that in ref. 54. In order to aid the reader who wishes to compare this analysis with that in ref. 54, the initial set of equations used (D1 to D12) are related to the figures in ref. 54 from which they are derived.

From figure 13 of ref. 54, the conditions behind the normal shock are given by (see Table IV).

$$\frac{\Delta P_{t2}}{P_{t2}} = \frac{\Delta P_{t1}}{P_{t1}} - C_{24}\,\Delta M_1 - C_{25}\,\frac{dA}{Adx}\Delta X_s - \frac{C_{26}}{a_t}\,S\,\Delta X_s \qquad \text{(D1)}$$

$$\frac{\Delta T_{t_2}}{T_{t_2}} = \frac{\Delta T_{t1}}{T_{t_1}} - \frac{C_{36}}{a_t}\,S\,\Delta X_s \qquad \text{(D2)}$$

$$\frac{\Delta w_2}{w_2} = \frac{\Delta P_{t1}}{P_{t1}} - \frac{1}{2}\,\frac{\Delta T_{t1}}{T_{t1}} + \frac{\Delta A_1}{A_1} - C_{44}\Delta M_1 - \frac{C_{46}}{a_t}S\,\Delta X_s \qquad \text{(D3)}$$

From figure 19, the change in the mass in the duct volume is

$$\frac{\Delta m_d}{w_1} = \frac{1}{S}\left(\frac{\Delta w_2}{w_2} - \frac{\Delta w_i}{w_i} - \frac{1}{U_z}\,S\Delta X_s\right) \qquad \text{(D4)}$$

From figure 20, the change in the volume total temperature is:

$$\frac{\Delta T_{td}}{T_{td}} = \frac{\Delta T_{ti}}{T_{ti}} = \left(\frac{\Delta T_{t2}}{T_{t2}} + \frac{T_z}{T_t}\,\frac{1}{3.5U_z}\,S\Delta X_s\right) \Big/ \left(\frac{m_d}{w_1}\,S + 1\right) \tag{D5}$$

From figure 21, the change in the volume total pressure is:

$$\frac{\Delta P_{td}}{P_{td}} = \frac{\Delta P_{ti}}{P_{ti}} = \frac{\Delta m_d}{m_d} + \frac{\Delta T_{td}}{T_{td}} + \frac{M_d}{1+0.2M_d^2}\Delta M_d + \frac{A_z}{V}\,\Delta X_s \tag{D6}$$

$$\text{where } \Delta M_d = \frac{M_d\,(1+0.2M_d^2)}{1 - M_d^2}\left(\frac{\Delta w_2}{w_2} + \frac{1}{2}\,\frac{\Delta T_{td}}{T_{td}} - \frac{\Delta P_{t2}}{P_{t2}}\right) \tag{D7}$$

Also, the change in the static pressure downstream of station "z" is:

$$\frac{\Delta P_{zd}}{P_z} = \frac{1 + 0.4M_z^2}{1-M_z^2}\,\frac{\Delta P_{td}}{P_{td}} + \frac{1.4M_z^2}{1-M_z^2}\left(-\frac{\Delta w_2}{w_2} - \frac{1}{2}\,\frac{\Delta T_{td}}{T_{td}} + \frac{\Delta A_z}{A_z}\right) \tag{D8}$$

In place of the relations shown in figure 23, the following equations for the change in exit airflow are used:

$$\frac{\Delta w_i}{w_i} = \frac{\Delta w_{ci}}{w_{ci}} + \frac{\Delta P_{ti}}{P_{ti}} - \frac{1}{2}\,\frac{\Delta T_{ti}}{T_{ti}} \tag{D9}$$

$$\frac{\Delta w_i}{w_i} = \frac{1 - M_i^2}{M_i\,(1+0.2M_i^2)}\,\Delta M_i + \frac{\Delta P_{ti}}{P_{ti}} - \frac{1}{2}\,\frac{\Delta T_{ti}}{T_{ti}} \tag{D10}$$

From figure 24, the change in the static pressure upstream of station "z" is:

$$\frac{\Delta P_{zH}}{P_z} = \frac{1 + 0.4\,M_z^2}{1 - M_z^2}\,\frac{\Delta P_{t2}}{P_{t2}} + \frac{1.4\,M_z^2}{1 - M_z^2}\left(-\frac{\Delta w_2}{w_2} - \frac{1}{2}\,\frac{\Delta T_{t2}}{T_{t2}} + \frac{\Delta A_z}{A_z}\right) \tag{D11}$$

Finally, from figure 25, the Helmholtz volume acceleration is:

$$S^2 \Delta X_s = \frac{gA_z \rho_z}{m_H} \left(\frac{\Delta P_{zH}}{P_z} - \frac{\Delta P_{zd}}{P_z} \right) \tag{D12}$$

The preceding twelve equations may be combined algebraically to produce the following four equations which must be used if changes in flow conditions within the diffuser are desired.

$$\frac{\Delta w_2}{w_2} = \frac{\Delta P_{t1}}{P_{t1}} - \frac{1}{2} \frac{\Delta T_{t1}}{T_{t1}} + \frac{\Delta A_1}{A_1} - C_{44} \Delta M_1 - \frac{C_{46}}{a_t} S\Delta X_s \tag{D3}$$

$$(1 + \tau_V S) \frac{\Delta T_{td}}{T_{td}} + K_1 S\Delta X_s = \frac{\Delta T_{t1}}{T_{t1}} \tag{D13}$$

$$(K_2 + K_3 S)S\Delta X_s + (1 + K_4 S) \frac{\Delta w_2}{w_2} + (0.5 + K_5 S) \frac{\Delta T_{td}}{T_{td}} - (1 + \tau_V S) \frac{\Delta P_{td}}{P_{td}} = K_4 S \frac{\Delta P_{t1}}{P_{t1}} + K_6 S\Delta M_1 + \frac{\Delta w_{ci}}{w_{ci}} \tag{D14}$$

$$(K_7 + K_8 S + S^2) \Delta X_s + K_9 \frac{\Delta T_{td}}{T_{td}} + K_{10} \frac{\Delta P_{td}}{P_{td}} = K_9 \frac{\Delta T_{t1}}{T_{t1}} + K_{10} \frac{\Delta P_{t1}}{P_{t1}} + K_{11} \Delta M_1 \tag{D15}$$

where C_{ij} are positive functions of M_1 shown in Table IV, τ_V is given by equation (B19), and

$$K_1 = \frac{1}{a_t} \left(\frac{M_1^2 - 1}{3M_1 \sqrt{1 + 0.2M_1^2}} - \frac{1}{3.5M_z \sqrt{1 + 0.2M_z^2}} \right) \tag{D16}$$

$$K_2 = \tau_V \left(\frac{7M_d^2}{1-M_d^2} \; \frac{M_1^2-1}{7M_1^2-1} \; \frac{dA}{AdX} + \frac{A_z}{V} \right) \frac{\sqrt{1+0.2M_z^2}}{a_t\, M_z} \tag{D17}$$

$$K_3 = \frac{35\tau_V M_d^2 \,(M_1^2-1)\, \sqrt{1+0.2M_1^2}}{6\, a_t\, (1-M_d^2)\; M_1\; (7M_1^2-1)} \tag{D18}$$

$$K_4 = \tau_V \; \frac{M_d^2}{1-M_d^2} \tag{D19}$$

$$K_5 = \tau_V \; \frac{2-M_d^2}{2-2M_d^2} \tag{D20}$$

$$K_6 = -\,K_4\, C_{24} \tag{D21}$$

$$K_7 = \frac{a_t^2\,(M_1^2-1)}{0.2\ell\,(7M_1^2-1)} \; \frac{1+0.4\,M_z^2}{(1-M_z^2)\;(1+0.2M_z^2)} \; \frac{dA}{AdX} \tag{D22}$$

$$K_8 = \frac{a_t\,(M_1^2-1)}{4.2\,\ell\, M_1\sqrt{(1+0.2M_1^2)}\,(1-M_z^2)\,(1+0.2M_z^2)} \left(\frac{35(1+0.2M_1^2)(1+0.4M_z^2)}{2\,(7M_1^2-1)} - 0.7\,M_z^2 \right) \tag{D23}$$

$$K_9 = -\,\frac{a_t^2\, M_z^2}{2\ell\,(1-M_z^2)(1+0.2M_z^2)} \tag{D24}$$

$$K_{10} = \frac{a_t^2\,(1+0.4\,M_z^2)}{1.4\,\ell\,(1+0.2M_z^2)(1-M_z^2)} \tag{D25}$$

$$K_{11} = -K_{10}C_{24} \tag{D26}$$

The four equations (D3) and (D13) to (D15) may be combined into the following single equation:

$$\Delta X_s = \frac{K_{w_{ci}}(1+\tau_V S)\, e^{-\tau_d S}\, \frac{\Delta w_{ci}}{w_{ci}} + K_{M_1}(1+\tau_1 S+\tau_2 S^2)\,\Delta M_1 + K_{A_1}(1+\tau_3 S+\tau_4 S^2)\,\frac{\Delta A_1}{A_1} + \tau_{P_t} S(1+\tau_V S)\,\frac{\Delta P_{t1}}{P_{t1}} + \tau_{T_t} S(1+\tau_5 S)\,\frac{\Delta T_{t1}}{T_{t1}}}{1+\tau_6 S+\tau_7 S^2+\tau_8 S^3+\tau_9 S^4} \tag{D27}$$

where $K_{w_{ci}}$, K_{M_1}, K_{A_1} and τ_V are given by equations (A4) to (A6) and (B19), the K's are given by equations (D16) - (D25), and

$$\tau_1 = \tau_V \frac{7M_1^2-1}{6(1-M_d^2)}\left[1+\frac{7(M_1^2-1)}{(7M_1^2-1)}(M_d^2-2)\right] \tag{D28}$$

$$\tau_2 = \tau_V^2 \frac{(7M_1^2-1)}{6(1-M_d^2)}\left(M_d^2 - \frac{7(M_1^2-1)}{(7M_1^2-1)}\right) \tag{D29}$$

$$\tau_3 = \frac{\tau_V}{1-M_d^2} \tag{D30}$$

$$\tau_4 = \frac{\tau_V^2 M_d^2}{1-M_d^2} \tag{D31}$$

$$\tau_{P_t} = \tau_V K_{w_{ci}} \tag{D32}$$

$$\tau_{T_t} = -\tau_V \left(0.5 + \frac{0.7M_z^2}{1 + 0.4M_z^2}\right) K_{w_{ci}} \tag{D33}$$

$$\tau_5 = -\tau_V \left(\frac{M_d^2}{1 - M_d^2} - \frac{1.4\,M_z^2}{1 + 0.4M_z^2}\right) \frac{1 + 0.4\,M_z^2}{1 - M_z^2} \tag{D34}$$

$$\tau_6 = K_{w_{ci}} \left(K_2 - \frac{C_{46}}{a_t} - \frac{K_1}{2} + \frac{K_8 + 2\tau_V K_7 - K_1 K_9}{K_{10}}\right) \tag{D35}$$

$$\tau_7 = K_{w_{ci}} \left(K_3 + \tau_V K_2 - K_1 K_5 - \frac{C_{46}\tau_V}{a_t(1-M_d^2)} + \frac{\tau_V\,(\tau_V K_7 + 2K_8 + K_1 K_9) + 1}{K_{10}}\right) \tag{D36}$$

$$\tau_8 = K_{w_{ci}}\,\tau_V \left(K_3 - \frac{C_{46}K_4}{a_t} + \frac{\tau_V K_8 + 2}{K_{10}}\right) \tag{D37}$$

$$\tau_9 = \frac{\tau_V^2}{K_7} \tag{D38}$$

APPENDIX E

DIGITAL PROGRAM TO DERIVE EQUATION FOR SQUARE OF FREQUENCY - RESPONSE FUNCTION

This appendix describes a digital algebraic program which derives the equation for the amplitude of the square of a frequency-response function, expressed in terms of the frequency ω, from an equation for the frequency response function H(S). The program was written by the United Aircraft Corporation Research Laboratories in the AED-0 (see ref. 74) language for the UAC UNIVAC 1108 computer. The derived equation relates the power spectral density of an output parameter, such as throat Mach number, to the power spectral density of an input parameter, such as a disturbance in flight Mach number. The derived equation may be used in the subroutine required by the program described in Appendix F.

Description of the Program

The program does the following:

1) It accepts a symbolic expression called H(S), where S is a Laplace operator, and prints it. H(S) is a frequency-response function.

2) It forms the expression $H(i\omega) \cdot H(-i\omega)$, expands it algebraically, and prints it. Here $i = \sqrt{-1}$, and ω is in frequency of rad/sec. Note that the printer writes "ω" as "W". This is the expression for the amplitude of the square of the frequency-response function.

3) It substitutes arbitrary numerical values for any of the variables (except ω) in $H(i\omega) \cdot H(-i\omega)$ and prints the result as a function of the remaining variables and ω. By convention $H(i\omega) \cdot H(-i\omega)$ will be referred to as $H(\omega) \cdot H(\omega)$.

The permissible expressions for H(S) are given by the following rules:

1) The following symbols are permissible: S; T1, T2, ... T10; C1, C2, ... C10; W1, W2, ... W10; Z1W, Z2W, ... Z9W, and any real constant k where $10^{-38} < |k| < 10^{38}$.

2) H(S) is formed by combining the sumbols in 1) by the "+" and "·" operators.

3) The exponential term $e^{-Q \cdot S}$ is permissible, where Q is a dead-time constant. However, in any one H(S), only one Q may be used. Q may be any of the symbols in 1).

Some examples of H(S) are:

1) $T1 \cdot S + 1$

2) S

3) $((((T1 \cdot S + ((C1))))))$

4) $(T1 \cdot S + 1) \cdot (T2 \cdot S + 3.5) \cdot ((S)) + C1$

5) $T1 \cdot S + 1 + C1 \cdot e^{-T2 \cdot S}$

6) $S \cdot (1 + S \cdot (C1 + S \cdot (C2 + (-4.0))))$

7) $(T1 \cdot S + (-1) \cdot C1) + C2 \cdot e^{-T5 \cdot S}$

Although subtraction is not a permissible operation, 6) and 7) show how it can be achieved, albeit awkwardly. The maximum size of H(S) is limited only by core storage in the UNIVAC 1108, and the amount of computer time the user wishes to expend.

The program is written in the AED-0 (Algol Extended for Design, or Automated Engineering Design) language. Because it permits easy manipulation of pointers and, consequently, internal tree structures, AED-0 is especially convenient for this problem. The program is divided into ten decks, namely MAIN, RDCARD, PARSE, ALGEB, COLECT, GPOL, PRNT, SUBST, DOUBML, and STAKS. Each of these will now be discussed in detail.

MAIN - This deck controls the calling of the other subroutines. It also computes the time in seconds taken by each of the subroutines, plus the total time for the problem.

RDCARD - In order to read input from cards, the card must be read one column at a time. Since AED-0 has no FORTRAN-type implied do-loop for input statements, it is necessary to write a lengthy input statement. RDCARD was written to avoid writing the input statement out several times. What is more important, it also saves several hundred locations of core storage. When RDCARD reads a card with a "$" punch in col. 1, it terminates the run. RDCARD also looks for comment cards ("C" in column 1), and prints them.

PARSE - This routine takes the input expression H(S), checks it for obvious errors, and then constructs the internal binary tree structure which represents H(S).

The meaning of the last third of the above sentence can be best explained by an example. Let H(S) be the expression $(T1 \cdot S+1) \cdot (T2 \cdot S+C1) \cdot (T3 \cdot S \cdot S+S+1) + C2$.

Then the binary tree structure which represents H(S) is:

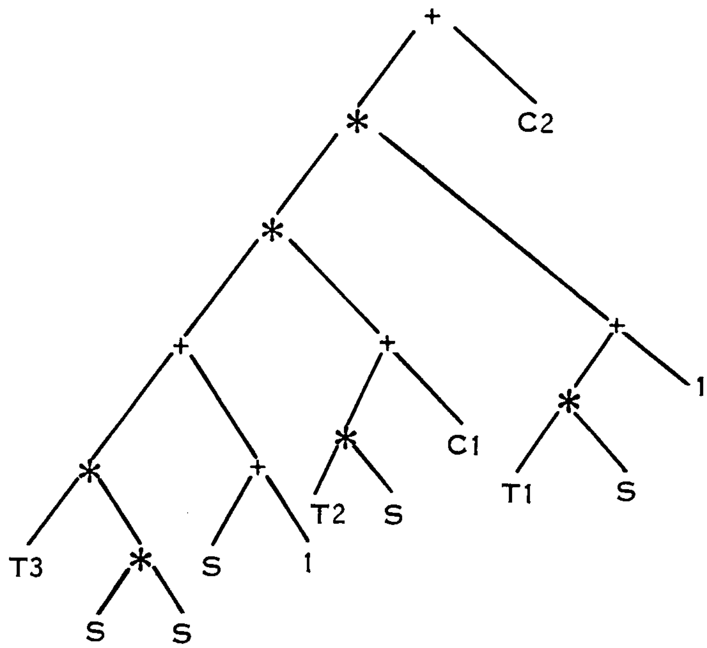

For a detailed discussion of how PARSE builds the tree structure from the card input, the AED-0 source language listing of PARSE should be consulted, but the following is a generalized description.

All items in H(S) are classified and put into a list type structure which contains a pointer to the item, rather than the item itself. The list structure here is similar to a FORTRAN array, the main difference being that each item in the list has associated with it a pointer to the next item in the list. List structures are especially convenient when deletions or insertions are made. The classification assigns a "1" to operators (·, +, and exponentiation), a "2" to symbols belonging to Q and pointers and a "3" to left and right parentheses. The termination symbol "$" is arbitrarily assigned a "1".

The list is scanned from left to right for occurrences of "(" and the pointers to this symbol are placed on a push-down stack as they are encountered. The "(" symbol is then removed from the list. Now the push-down stack is popped so the first pointer from the stack gives the beginning of the innermost parenthesized expression. This expression is scanned until the first ")" symbol for occurrences of pl op p2 where pl and p2 are pointers and op is one of the operators (·, +, and exp). Occurrences of pl op p2 are replaced by a pointer to a structure which represents pl op p2. The expression is scanned twice - first for op = "·", then for op = "+". These are both binary operators: since "exp" is a unary operator, it is handled in a special way. The ")" is then removed from the list.

This whole process is repeated for all pointers on the push-down stack. When the stack is empty, we will have a pointer to the top of the internal binary tree structure which represents H(S).

ALGEB - This routine first takes the internal tree structure for H(S) and constructs another tree representing H(-S), by replacing each occurrence of "S" by "-S". It then joins these two trees with a "·" operator, giving the tree for H(S) · H(-S). Next, occurrences of $e^{Q \cdot S}$ are replaced by $\cos(Q \cdot \omega) + i \sin(Q \cdot \omega)$. The substitution of $i \cdot \omega$ for occurrences of S outside the "exp" operator is postponed until the COLECT routine where it is more conveniently handled.

ALGEB then takes the tree and expands it algebraically. An algebraic expansion may be thought of as a process which transforms products of sums into sums of products. For example, the algebraic expansion of $(a + b) \cdot (c + d)$ is $a \cdot c + a \cdot d + b \cdot c + b \cdot d$. ALGEB does this by repeated applications of the distributive law of multiplication and addition. The law is applied by having the program look for the following pattern and transforming it as indicated.

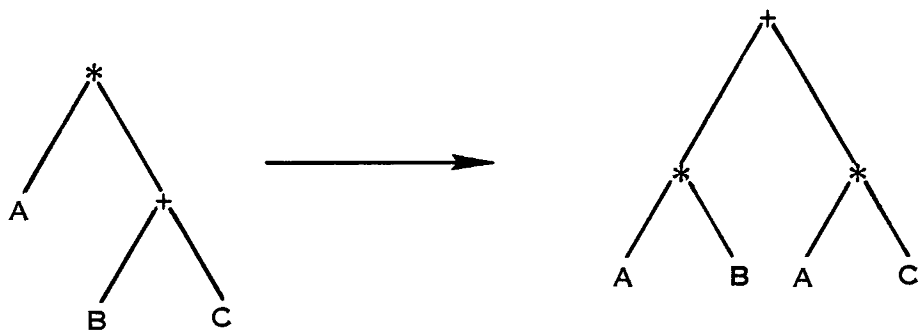

The transformation is applied repeatedly until the expression represented by the tree is completely expanded.

COLECT - When the binary tree has been expanded into sums of products, this routine will go through the tree and collect like terms. Each symbol used in H(S) is assigned a unique prime integer (see Operating Instructions, card input (3)). COLECT then scans the expanded binary tree. When it encounters a term (defined here as a symbol, or a set of symbols connected by · operators; e.g., S · T1 · S · T2 and S are each terms, while T1 + 1 is not a term), COLECT does three things. First, each occurrence of "S" is replaced by "$i \cdot \omega$". Second, if the term contains i to an odd power, COLECT rejects the term and continues on because the answer must be real. Third, a Goedel number is computed for the term. The Goedel number is computed by multiplying together the primes associated with each of the symbols in the term. A numerical coefficient is also computed by multiplying together all real numerics in the term. For example, let the set of symbols in H(S) be S, T1, and T2. The primes assigned to these symbols would be 2, 7, and 11. Suppose the term being considered is $S \cdot 3 \cdot T1 \cdot S \cdot 2 \cdot T2 \cdot T1$. The Goedel number for this term is $2 \cdot 7 \cdot 2 \cdot 11 \cdot 7 = 2156$, while the numerical coefficient is $3 \cdot 2 = 6$. By the unique factorization theorem, any other term which has a Goedel number of 2156 is identical to the given term even though the order of the factors is different. Conversely, any term with a Goedel number different from 2156 is different from the given term.

It now becomes a simple matter to collect like terms. For each term a Goedel number and numerical coefficient is computed. A table of previously encountered Goedel numbers and coefficients is searched. If a match is found between Goedel numbers, the two numerical coefficients are added. If no match is found, the Goedel number is appended to the table. Since sin and cos always refer to the same angle, they are treated as symbols, and always assigned the primes 3 and 5. The detection of the following situation then is quite easy:

$$f \cdot \sin^2 \theta + f \cdot \cos^2 \theta$$

If the quotients left by dividing each of the Goedel numbers first by 9 and 25, then by 25 and 9 are identical, the expression is reduced to "f".

The only difficulty with this method of collecting terms occurs when a Goedel number exceeds $2^{35} - 1$. When this happens, two or more storage locations must be used to hold the Goedel number. To compare Goedel numbers which occupy more than one location, we call subroutine GPOL.

GPOL - This subroutine writes the Goedel number as the coefficients of a polynomial in powers of 2^{35}. Since the polynomial is unique, we can then compare all pairs of Goedel numbers, no matter how large.

PRNT - After all like terms have been collected, this routine decomposes each Goedel number in the table, in turn, and prints the string of symbols associated with the Goedel number, preceded by the numerical coefficient. This is the final answer, $H(\omega) \cdot H(\omega)$.

SUBST - This routine reads one or more sets of cards, each set consisting of a list of numerical values of any or all of the variables in H(S). The substitution of the numerical value for the variable in $H(\omega) \cdot H(\omega)$ is done in the following way.

The prime associated with the variable is trial-divided into each of the Goedel numbers in the table computed by COLECT. If the division leaves a remainder, no change is made. If the division leaves no remainder, the Goedel number is replaced by the quotient, and the numerical coefficient of the Goedel number is multiplied by the indicated numerical value of the variable. When all substitutions have been made, an attempt is made to collect like terms on the new Goedel number table, and then PRNT is called.

STAKS - This is a routine which permits the use of push-down stacks in the PARSE, ALGEB, and COLECT subroutines.

DOUBML - This routine is written in UNIVAC 1108 machine language. It is called from GPOL and is used to perform a double-precision (70 bit) integer multiplication.

Figure 47 is a listing of the source program for a UNIVAC 1108.

Operating Instructions

The card input to the program consists of the following:

(1) Comment Cards

Use as many comment cards as desired (including none). Each must have a "C" punch in column 1. All information punched in columns 2-72 will print out before any other information from the problem.

(2) The Expression H(S)

With one minor exception, this is punched in standard FORTRAN format. As with all card input to the program, columns 1-72 are used, with columns 73-80 reserved for user identification information. As in FORTRAN, blanks are ignored. The exponential, $e^{-T1 \cdot S}$, should be punched as E(-T1*S). Up to four cards can be used for H(S), which must be terminated by a "$" punch. If H(S) uses more than one card, do not use the FORTRAN continuation card punch in column 6; just continue to the next card as shown in figure 48. Use decimal points where needed; they are optional for integers. However, the appearance of the answer will probably be enhanced if decimal points are omitted from integers. An integer (0 to 9) must precede any decimal point. Redundant parentheses cause no problem; e.g., (((T1) + ((1)))) is as good as T1 + 1. "S" must appear at least once in H(S). A minus sign must be preceded by a left parentheses and followed by a number, not by a variable or parenthesis.

(3) A List of the Variables Used in H(S)

These are strung out on the card with any number of blanks separating each variable. The list should be in the order of frequency of appearance in H(S) with the most frequently used symbol occurring first, so that "S" will probably be the first variable on the card. This is not an essential requirement, but the program may operate more efficiently if the requirement is met. Up to four cards may be used to list the variables. A "$" punch terminates the list. The list is limited to 35 variables.

(4) The Number of Independent Sets of Numerical Substitutions

This will be an integer punched in columns 1-3 of the card, right-justified. If there are no numerical substitutions, punch a "0" in column 3 (or use a blank card). Then skip to the next H(S) or to the termination card. The remainder of the card may be used for comments.

(5) The Number of Variables Which Receive Numerical Values

This card is needed for each independent set of numerical substitutions. It has the same format as card (4).

(6) The Numerical Values of the Variables

These are punched one to a card in columns 1-72. They are of the form "T1 = 0.6187", "Z1W = - 1.983", etc. Blanks are ignored, so the substitutions may appear anywhere on the card between columns 1 and 72. As with card (2), decimal points are used where needed, and must be preceded by an integer (0 to 9). The absolute numerical value must lie between 10^{-38} and 10^{+38}. Do not use floating point notation. No "$" punch is necessary to end the statement.

(7) Termination Card

This is the last card of the input deck and will terminate the run. It appears after the last set of input cards. It will have a "$" punch in column 1, plus any other information desired by the user.

Sample Cases

A listing of the input cards for four sample cases is presented in figure 48. The output for these sample cases is presented in figure 49. The output from the program is self-explanatory. The expression H(S) is printed, followed by the formula for $H(\omega)^*H(\omega)$. If there are any numerical substitutions to be made, the variables which are to be assigned numerical values are printed together with their assigned values. The numerical values are printed to five decimal places if their absolute value lies between 10^{4} and 10^{-4}; otherwise they are printed in floating point format to five significant figures. The expression for $H(\omega)^*(\omega)$ after the substitution is then printed.

After H(S) and all numerical substitutions have been processed, the time taken by each of the subroutines and the total time is printed (maximum error about one second). The four sample cases serve to illustrate the time required by a UNIVAC 1108. If less than two sets of substitutions are made, it may require less machine time to run two cases with the substitutions made in the original equations, as in the last example. Another version of the first case, with two more variables and without simplification of the equation, required nearly twice as much machine time.

Diagnostics

The program will print diagnostics if it runs into difficulty during execution. The diagnostics are as follows:

PARSE routine:

a) If the left and right parentheses in H(S) do not balance, an error message to this effect will print.

b) Certain meaningless adjacent combinations of symbols in H(S) such as ") (", "+ * ", etc., will give an error message.

c) An illegal character in H(S); i.e., one that does not belong to the set of permissible symbols (see Description of the Program), will give an error message.

d) An error in free storage will give an error message. This is a serious error and is probably caused by machine error, or by an H(S) too big for machine storage.

COLECT routine:

a) An illegal character in the list of variables used in H(S) will give an error message.

b) If there is a variable in H(S) which is not contained in the list of variables (see card input (2)), the message "Symbol missing from admissible symbol set" will print.

c) Depending on the complexity of H(S), the program will handle an $H(\omega) \cdot H(\omega)$ of about 700 terms, after simplification. If the error message "Goedel number table overflows" prints, then $H(\omega) \cdot H(\omega)$ has exceeded capacity. A remedy which may work is to recompile the following decks with the dimension of GOEDEL (integer array) and REALL (real array) both increased to a number higher than the present value of 1500. The decks are: PARSE, ALGEB, COLECT, PRNT, and SUBST.

SUBST routine:

a) If a variable of substitution does not appear in H(S), an error message will be printed.

b) If the numerical value of a variable of substitution contains an illegal character; i.e., anything other than the digits 0 to 9, an error message will be printed.

Machine-Dependent Instructions

The program will run on any UNIVAC 1108. Since AED compilers do exist for the IBM 7090 and 7094, the IBM 360 (most models) as well as the UNIVAC 1108, it should be possible to run the program on these computers without too many headaches*. The program was written to run successfully on the UAC UNIVAC 1108. Therefore, there are some instructions which depend on the internal representation of alphabetic characters in the 1108 or on the 1108's 36-bit word length. A list of these instructions and the subroutines in which they occur follows:

MAIN: DOITF is an instruction peculiar to UNIVAC 1108 AED. Its only function here is to permit calls to the FORTRAN time routine, so it is not needed for the success of the program.

PARSE:

(1) In the code between the comment "anything else must be S, T1, T2,.... " and the label D10, the symbol is assembled from the individual alphanumeric characters in the array IN. The program assembles the symbol by masking and shifting.

(2) About halfway between labels D6 and D7, the program places OP(Q) in its position in the word by shifting.

ALGEB: About ten lines after label A1, HOL(P) is compared with the internal UNIVAC representation for "S". This is, of course, machine dependent.

*The Computer Aided Design Group at United Aircraft Research Laboratories should be consulted first.

COLECT:

(1) In the code between labels C12 and C0, the program assembles a symbol by masking and shifting the individual alphanumeric characters in the array J.

(2) Just after label C15, HOL(P) is compared with the internal UNIVAC representation for "S".

(3) Starting at label C8, the 0's in the SYM array are changed to blanks, and the "S" symbol is changed to "W" in UNIVAC internal representation.

PRNT: Just after the comment "First replace S in angle by W and replace 0 by blank in other symbols", the program does just that in UNIVAC internal representation.

SUBST: In the code between labels E0 and E1, the program assembles a symbol by masking and shifting the individual alphanumeric characters in the array J.

DOUBML: This is an assembly-language program which takes two 35 bit integers and outputs the 70 bit product.

In addition to the above, the program assumes that the computer has a word length of 36 bits. Since the IBM 360 series has a word length of 32 bits, packed components will almost certainly have to be redefined. There will also be some changes to the free storage cells, if the number of words used in a bead must be changed.

APPENDIX F

DIGITAL PROGRAM TO EVALUATE POWER SPECTRAL DENSITY PARAMETERS

A digital program which evaluates several power spectral density parameters was written in FORTRAN IV language and is described in this appendix. In order to run, it requires that a function PSD(W,J) which evaluates the power spectral density as a function of frequency W (rad/sec) be available to the program. The integer J is 1 for the first case run, 2 for the second case, 3 for the third case, etc.

A listing of the program written for an IBM 1130 computer is presented in figure 50. It should be noted that the values of the integer constants IR and IP can be changed to fit the installation.

Program Input

The first card read for each case executed may have any legal Hollerith punches in its 80 columns. If the card is blank the subroutine START completes execution of the job by returning control to the system monitor. If the card is not blank it is printed with a 1 eject to the top of the page. The user may need to supply a START subroutine appropriate to his own installation. The second card contains the following input data in a (4F10.5, I10) format:

1. VF - the flight velocity in ft/sec. If this is zero it is computed from VK.

2. VK - the flight velocity in knots. This is computed from VF unless VF is zero. Thus, either VF or VK may be input and if VF is not zero the value of VK loaded is replaced by one computed from VF.

3. DW - the initial frequency ω, rad/sec.

4. WM - the program will proceed, doubling the frequency ω at each step, until $\omega \geq$ WM.

5. I - An integer which is the number of cards read next. At least one card will be read. The contents of each card are printed. Normally, the first column is not printed and should be blank.

Program Output

The initial card is printed at the top of a page by the START subroutine. The next line contains the flight velocity. The next I lines reproduce the I cards read. These cards may contain comments, the equation for the power spectral density, or any other material the user desires to print. Column headings are printed next. The contents of each column of numbers printed next are, starting at the left:

Column No.

1. Wavelength λ in feet

2. Wavelength λ in meters

3. Spatial frequency Ω in rad/ft

4. Power spectral density, ϕ (Ω)

5. Frequency f in Hz

6. Frequency ω in rad/sec

7. Power spectral density, ϕ (ω), evaluated by PSD(W, J)

8. $\sqrt{\omega\phi(\omega)}$

9. $\sqrt{\int_0^\omega \phi(\omega)\, d\omega}$

10. Number of zero crossings in positive direction per nautical mile G evaluated by integrating ϕ from 0 to frequency ω.

11. Number of zero crossings in positive direction per hour N_0 evaluated by integrating ϕ from 0 to frequency ω.

A five-point Gauss integration procedure is used to compute the last three columns.

The integration used to obtain the truncated rms amplitude in column 9 may be extended from the last frequency ω_c printed to infinity analytically if $\phi(\omega)$ varies as ω^{-n} at high frequencies. Typically $n = 5/3$ or 2. Let $\phi(\omega) = C\omega^{-n}$ where C may be evaluated from the last printed line using columns 6 and 7. Then,

$\sqrt{C/(n-1)\ \omega_c^{\,n-1}} = \sqrt{\omega_c\, \phi(\omega_c)/(n-1)}$ should be added to the last value in column 9. However, if the value of WM selected is large enough this correction is small and may be neglected.

Column 9 provides a value of "A" and column 10 of "G" for use in the program described in Appendix G.

Sample Cases

A listing of the function PSD, the input cards, and the output of two sample cases run on an IBM 1130 are presented in figures 51 and 52.

APPENDIX G

DIGITAL PROGRAM TO EVALUATE EXCEEDANCE PARAMETERS

A digital program which evaluates exceedance parameters was written in FORTRAN IV language and is described in this appendix. A listing of the program written for an IBM 1130 computer is presented in figure 53. It should be noted that the values of the integer constants IR and IP can be changed to fit the installation.

Program Input

Three cards are read for each case executed. The first card may have any legal Hollerith punches in its 80 columns. If the card is blank the subroutine START completes execution of the job by returning control to the system monitor. If the card is not blank it is printed with a 1 eject to the top of a page. The user may need to supply a START subroutine appropriate to his own installation. The second card contains the following input data in a (I 10, 7F10.5) format:

1. L - an integer which controls equation used for calculating exceedances, if $L = 0$ equation (4) is used, if $L < 0$ equation (8) is used and if $L > 0$ equations (5, 6 & 7) are used. These equations appear in the body of this report.

2. QG - number of zero crossings of output in positive direction per nautical mile, G_{th} or G_s.

3. A - rms amplitude of output/rms amplitude of input.

4. VF - the flight velocity in ft/sec. If this is zero it is computed from VK.

5. VK - the flight velocity in knots. This is computed from VF unless VF is zero. Thus, either VF or VK may be input and if VF is not zero the value of VK loaded is replaced by one computed from VF.

6. DI - maximum initial output disturbance.

7. DX - interval in output disturbance amplitude.

8. DM - program continues, increasing output disturbance by DX each cycle, until output disturbance exceeds DM.

The third card contains the following input data in a (8F10.5) format:

9. QNI - maximum initial nautical miles/exceedance.

10. QNM - program continues until computed miles/exceedance is greater than QNM.

11. P_1 - fraction of flight distance in primary turbulence, see figure 10.

12. P_2 - fraction of flight distance in secondary turbulence, see figure 11. Not required if $L \neq 0$.

13. P_3 - fraction of flight distance in tertiary turbulence, see figure 11. Not required if $L \neq 0$.

14. B_1 - rms amplitude of input primary turbulence, see figure 12.

15. B_2 - rms amplitude of input secondary turbulence, see figure 13, if L=0. Parameter α if $L \neq 0$.

16. B_3 - rms amplitude of input tertiary turbulence, see figure 13, if L=0. Not required if $L \neq 0$.

Program Output

For each case the initial card is printed at the top of a page by the START subroutine. The next three or four lines print the equation for G used and pertinent input data. If L=0 up to three case "a" of ref. 42 are summed, using equation (4). By appropriate choice of input parameters case "k" (equation (9)) may be solved. If L>0 case "j" of ref. 42 is solved, using equations (5), (6) and (7). If L<0 case "m" of ref. 42 is solved, using equation (8). Column headings are printed next. The columns contain, in groups of three, numerical values of:

1. Amplitude X of output disturbance, may be ΔM_{th} or ΔX_s.

2. Number of flight nautical miles between exceedances of X, 1/G.

3. Flight hours between exceedances of X.

Sample Cases

Listings of the input cards and the output of four sample cases run on an IBM 1130 are presented in figures 54 and 55 respectively. The sample cases represent, in order, cases "a", "k", "j", and "m" of ref. 42. In the second sample case a value of VK is loaded which does not match the value of VF loaded (see figure 54) but the program replaces the wrong value with one matching VF (see figure 55).

REFERENCES

1. Barry, F. W.: Effects of Atmospheric Gust Criteria on Supersonic Inlet Performance. Paper no. 66-367, AMS/AIAA, Mar. 1966.
2. Barry, F. W.: Development of Atmospheric Gust Criteria for Supersonic Inlet Design - Comparison of Analytical Inlet Models with Experiment. HSER 5196 (NASA CR-   ), Hamilton Standard, Dec. 1968, Confidential.
3. Peckham, C. G.: Flight-Measured Turbulence in the NATO Countries. AGARD Rept. 555, Feb. 1967.
4. Anon.: Clear Air Turbulence. NASA Literature Search no. 5180, Oct. 1967.
5. Anon.: Aircraft Gust Loads. NASA Literature Search no. 5588, Jan. 1968.
6. Bulford, D. E.: Clear Air Turbulence: A Bibliography 1950 - 1967. FAA National Aviation Facilities Experimental Center, Rept. NA-68-17, Mar. 1968.
7. Clear Air Turbulence Meeting. USAF (AD668080), Apr. 26-27, 1965.
8. Transactions of International Colloqium on Atmospheric Turbulence and Radio-Wave Propagation. Moscow, June 15-22, 1965.
9. National Air Meeting on Clear Air Turbulence. SAE, Feb. 23-24, 1966.
10. Symposium on Clear Air Turbulence And Its Detection. Boeing Scientific Research Laboratories, Document D1-82-0740, Aug. 14-16, 1968.
11. Meeting on Aircraft Response to Turbulence. NASA, Langley, Sept. 24-25, 1968.
12. Coleman, T. L.; and Steiner, R.: Atmospheric Turbulence Measurements Obtained from Airplane Operations at Altitudes between 20,000 and 75,000 Feet for Several Areas in the Northern Hemisphere. NASA TN D-548, Oct. 1960.
13. Steiner, R.: A Review of NASA High-Altitude Clear Air Turbulence Sampling Programs. J. of Aircraft, vol. 3, no. 1, Jan.-Feb. 1966, pp. 48-52 (Paper no. 65-13, AIAA, Jan. 1965).
14. Crooks, W.: High Altitude Clear Air Turbulence. AFFDL-TR-144, Sept. 1965.
15. Burnham, J.; and Spavins, C. S.: Some Results of a Study of Atmospheric Turbulence in Clear Air Above Thunderstorms and of its Relationship to Weather Radar Pictures. National Severe Storms Laboratory, Technical Memorandum no. 30, Dec. 1966, pp. 1-9.
16. Coy, R. G.: Atmospheric Turbulence Spectra From B-52 Flight Loads Data. AFFDL-TR-67-13, Apr. 1967.
17. Kordes, E. E.; and Love, B. J.: Preliminary Evaluation of XB-70 Airplane Encounters with High-Altitude Turbulence. NASA TN D-4209, Oct. 1967.
18. Crooks, W. M.; Hoblit, F. M.; Prophet, D. T.; et al: Project HICAT An Investigation of High Altitude Clear Air Turbulence. Rept. no. LR 20771 (AFFDL-TR-67-123), Lockheed-California Co., Nov. 1967.
19. Hunter, P. A.: An Analysis of VGH Data from One Type of Four-Engine Turbojet Transport Airplane During Commercial Operations. NASA TN D-4330, Feb. 1968.

20. Hunter, P. A.; and Brazziel, M. E.: Summary of VGH Data Collected on One Type of Twin-Engine Jet Airplane during Airline Operations. NASA TN D-4529, May 1968.
21. Endlich, R. M.; and Mancuso, R. L.: The Turbulence Climatology of the United States Between 20,000 and 45,000 Feet Estimated From Aircraft Reports and Meteorological Data. AFCRL-68-0337, June 1968.
22. Belyayev, V. P., et al: Some Results of the Experimental Investigations of the Atmospheric Turbulence Using Radiosondes. In Pinus, N.Z.: Atmospheric Turbulence. NASA TT F-246, Sept. 1965, pp. 1-65.
23. Vinnichenko, N. K.; Pinus, N. Z.; and Shur, G. N.: Some Data on Turbulence in the Upper Troposphere and Stratosphere Causing Airplane Buffeting. (Meteorology and Hydrology, no. 11, Nov. 1966) JPRS-39987, Feb. 21, 1967, pp. 35-47.
24. Pratt, K. G.; and Walker, W. G.: A Revised Gust-Load Formula and a Re-Evaluation of V-G Data taken on Civil Transport Airplanes From 1933 to 1950. NACA Rept. 1206, 1954.
25. Anon.: Military Specification Airplane Strength and Rigidity Flight Loads. MIL-A-8861, May 1960.
26. Anon.: Tentative Airworthiness Standards for Supersonic Transports. (rev. 1, Feb. 1966), Federal Aviation Agency, Flight Standards Service, Nov. 1, 1965.
27. Anon.: Supersonic Transport Aircraft Structures. TSS-Standard no. 8, issue 2, May 1, 1966.
28. Boone, J. P.: High Altitude Critical Atmospheric Turbulence Data System. AFFDL-TR-67-1, May 1967.
29. Pinus, N. Z.; Reiter, E. R.: Shur, G. N.; and Vinnichenko, N. K.: Power Spectra of Turbulence in the Free Atmosphere. Tellus, vol. XIX, no. 2, 1967, pp. 206-213.
30. Diederich, F. W.; and Drischler, J. A.: Effect of Spanwise Variations in Gust Intensity on the Lift Due to Atmospheric Turbulence. NACA TN 3920, Apr. 1957.
31. Houbolt, J. C.; Steiner, R.; and Pratt, K. G.: Dynamic Response of Airplanes to Atmospheric Turbulence Including Flight Data on Input and Response. NASA TR R-199, June 1964.
32. Press, H.; and Steiner, R.: An Approach to the Problem of Estimating Severe and Repeated Gust Loads for Missile Operations. NACA TN 4332, Sept. 1958.
33. Anon.: Military Specification Airplane Strength and Rigidity Reliability Requirements, Repeated Loads, and Fatigue. MIL-A-8866, May 1960.
34. Neuls, G. S.; Maier, H. G.; Lerwick, T. R.; Robb, E. A.; and Webster, I. J.: Optimum Fatigue Spectra. ASD-TR-61-235, Apr. 1962.
35. Hoblit, F. M.; Paul, N.; Shelton, J. D.; and Ashford, F. E.: Development of a Power-Spectral Gust Design Procedure for Civil Aircraft. Rept. no. 18253, rev. 2 (FAA-ADS-53, Jan. 1966), Lockheed-California Co., July 1965.

36. Pritchard, F. E.; Easterbrook, C. C.; and McVehil, G. E.: Spectral and Exceedance Probability Models of Atmospheric Turbulence for Use in Aircraft Design and Operation. AFFDL-TR-65-122, Nov. 1965.
37. Houbolt, J. C.: Preliminary Development of Gust Design Procedures Based on Power Spectral Techniques. Volume I. Theoretical and General Considerations. Rept. No. 83, vol. 1 (AFFDL-TR-66-58, vol. I), Aeronautical Research Associates of Princeton, Inc., July 1966.
38. Austin, W. H., Jr.: A Summary of Some Recent Developments in the Description of Atmospheric Turbulence Used for Aircraft Structural Design. Technical Report SEG-TR-66-45, Aug. 1966.
39. Pritchard, F. E.: A Statistical Model of Atmospheric Turbulence and a Review of the Assumptions Necessary for Its Use. Presented at the AGARD Specialists' Meeting on Stability and Control (Cambridge, England), Sept. 20-23, 1966.
40. Dempster, J. B.; and Roger, K. L.: Evaluation of B-52 Structural Response to Random Turbulence with Stability Augmentation Systems. J. of Aircraft, vol. 4, no. 6, Nov.-Dec. 1967, pp. 507-512 (paper 66-998, AIAA, Dec. 1966).
41. Austin, W. H., Jr.: Development of Improved Gust Load Criteria for United States Air Force Aircraft. Technical Rept. SEG-TR-67-28, (Preprint 670617, SAE, July 1967), Sept. 1967.
42. Houbolt, J. C.: Gust Design Procedures Based on Power Spectral Techniques. Rept. No. 106 (AFFDL-TR-67-74), Aeronautical Research Associates of Princeton, Inc., Aug. 1967.
43. Firebaugh, J. M.: Evaluations of a Spectral Gust Model Using VGH and V-G Flight Data. J. of Aircraft, vol. 4, no. 6, Nov.-Dec. 1967, pp. 518-525.
44. Mather, G. K.: Some Measurements of Mountain Waves and Mountain Wave Turbulence Made Using the NAE T-33 Turbulence Research Aircraft. Canadian National Research Council, Quarterly Bulletin, issue no. 2, 1967, pp. 1-27.
45. Burns, A.; and Harrold, T. W.: An Atmospheric Disturbance Encountered by a Canberra Over Storms at Oklahoma on May 27, 1965. National Severe Storms Laboratory, Technical Memorandum no. 30, Dec. 1966, pp. 11-20.
46. Black, H. C.: The Airworthiness of Supersonic Aircraft. The Aeronautical Journal of the Royal Aeronautical Society, vol. 72, Feb. 1968, pp. 115-122 (Also AIAA Preprint no. 67-751, Oct. 1967).
47. Ehernberger, L. J.: Meteorological Aspects of High-Altitude Turbulence Encountered by the XB-70 Airplane. A.M.S., Proc. of the 3rd National Conference on Aerospace Meteorology (New Orleans), May 1968, pp. 515-522.
48. Helvey, R. A.: Observations of Stratospheric Clear-Air Turbulence and Mountain Waves Over the Sierra Nevada Mountains - An Analysis of the U-2 Flights of 13-14 May, 1964. AFCRL-68-0001, Dec. 1967.
49. Ashburn, E. V.; Prophet, W. T.; and Waco, D. E.: High Altitude Clear Air Turbulence Models For Aircraft Design and Operation. Rept. no. LR 21501 (AFFDL-TR-68-79), Lockheed-California Co., July 1968.
50. Anon.: Supersonic Transport Aircraft -- Atmospheric Conditions. TSS-Standard no. 6, issue 1, Mar. 9, 1966.

51. Anon.: Total Temperature Sensors. Bulletin 7637, Rev. B, Rosemount Engineering Co., 1963.
52. Chun, K. S.; and Swanson, D. B.: Dynamic Simulation of Supersonic Inlet and Engine. Paper no. 64-598, AIAA, Aug. 1964.
53. Anon.: Boeing Model 2707 Air Induction Control Subsystem Specification. Spec. D6A10118-1, rev. C, Boeing Company, Dec. 18, 1967.
54. Martin, A. W.: Propulsion System Dynamic Simulation Theory and Equations. Rept. no. NA-67-384 (NASA CR-928, Mar. 1968), North American Aviation, Inc., Apr. 1967.
55. Ames Research Staff: Equations, Tables, and Charts for Compressible Flow. NACA Rept. 1135, 1953.
56. Barry, F. W.: Determination of Mach Number from Pressure Measurements. Trans. ASME, vol. 78, no. 3, Apr. 1956, pp. 581-589.
57. Hartsell, C. W.: Derivation of an Analytical Expression for Supersonic Spillage of Single-Cone Inlets. J. Aerospace Sci., vol. 27, no. 10, Oct. 1960, pp. 788-789.
58. Sims, J. L.: Tables For Supersonic Flow Around Right Circular Cones at Zero Angle of Attack. NASA SP-3004, 1964.
59. Crabbe, R. S.; and Campbell, G. S.: Tables of Derivatives to Extend the Zero Incidence Cone Tables to Intermediate Mach Numbers and Cone Angles. Rept. LR-451, Canadian National Research Council, May 1966.
60. Barry, F. W.: Conical Flow Properties for Use in the Design of Supersonic Inlets. Rept. M-1266-1, Research Dept., United Aircraft Corp., Nov. 1958.
61. Mascitti, V. R.: Charts of Additive Drag Coefficient and Mass-Flow Ratio for Inlets Utilizing Right Circular Cones at Zero Angle of Attack. NASA TN D-3434, 1966.
62. Bowditch, D. N.; and Anderson, B. H.: Performance of an Isentropic, All-Internal-Contraction, Axisymmetric Inlet Designed for Mach 2.50. NACA RM E58E16, 1958.
63. Anderson, B. H.; and Bowditch, D. N.: Investigation of Inlet Control Parameters for an External-Internal-Compression Inlet From Mach 2.1 to 3.0. NACA RM E58G08, 1958.
64. Stitt, L. E.; and Salami, R. J.: Performance of a Mach 3.0 External-Internal-Compression Axisymmetric Inlet at Mach Numbers From 2.0 to 3.5. NASA TM X-145, 1960.
65. Anderson, B. H.; and Bowditch, D. N.: Performance of Three Isentropic All-Internal-Compression Axisymmetric Inlets Designed for Mach 2.5. NASA TM X-259, 1960.
66. Bowditch, D. N.; Anderson, B. H.; and Tabata, W. K.: Performance and Control of a Full-Scale, Axially Symmetric, External-Internal-Compression Inlet from Mach 2.0 to 3.0. NASA TM X-471, 1961.
67. Sorensen, N. E.; and Smeltzer, D. B.: Investigation of a Large-Scale Mixed-Compression Axisymmetric Inlet System Capable of High Performance at Mach Numbers 0.6 to 3.0. NASA TM X-1507, 1968.

68. Smeltzer, D. B.; and Sorensen, N. E.: Investigation of a Nearly Isentropic Mixed-Compression Axisymmetric Inlet System at Mach Numbers 0.6 to 3.2. NASA TN D-4557, 1968.

69. Barry, F. W.: An Analysis of Transient Shock Displacement in a Diffuser. HSIR 1303, Hamilton Standard, Nov. 1959.

70. Barry, F. W.: Transient Shock Motion in a Supersonic Diffuser Having a Variable Bypass. Rep. R-0925-4, Research Dept., United Aircraft Corp., May 1959.

71. Weber, R. J.; and Luidens, R. W.: A Simplified Method for Evaluating Jet-Propulsion-System Components in Terms of Airplane Performance. NACA RM E56J26, 1956.

72. Kepler, C. E.; and Barry, F. W.: Engine Air Inlet Compatibility for the Supersonic Transport. Trans. SAE, vol. 74, 1966, pp. 971-985. (Preprint 650225, SAE, Apr. 12-15, 1965).

73. Dutton, J. A.: Broadening Horizons in Prediction of the Effects of Atmospheric Turbulence on Aeronautical Systems. Paper No. 68-1065, AIAA, Oct. 1968.

74. Anon.: AEC-0 Programming Manual. M.I.T., 1964.

TABLE I

PROBABILITY OF ATMOSPHERIC TURBULENCE

Ref. No.	Earliest Date	Aircraft	Altitude, 1000 ft: 30-35	30-40	35-40	40-45	40-50	45-50	50-55	50-60	55-60	60-65	60-70	65-70	70-75	Sample Over 30 000 ft Altitude	Threshold
12	10/60	U-2		.079			.0164			.0189			.0035		.0013	303 183 mi.	U_{DE} 2 fps
13	1/65	U-2		.102			.025			.020			.006		.001	801 610 mi.	U_{DE} 2 fps
14	9/65	WU-2 (HICAT)								.14						43 hr	
15	12/66	Canberra				.114										2200 mi.	U_{DE} fps
16	4/67	B-52		.036		.033										11 279 hr	.05 g
17	10/67	B-70				.068		.072	.071		.074	.072		.036	.029	75 757 mi.	.06 g
18	11/67	WU-2 (HICAT)						.098	.100		.050	.027		.029		256 000 mi.	.05 g
19	2/68	Commercial	.068		.08	.036										1 083 488 mi.	U_{DE} 2 fps
20	5/68	Commercial	.059													232 000 mi.	.2 g
21	6/68	Commercial	.044		.03	.022											
*	7/68	WU-2 (HICAT)						.08	.088		.054	.03		.05		329 000 mi.	
		Altitude, Km	9.1-10.7	9.1-12.2	10.7-12.2	12.2-13.7	12.2-15.2	13.7-15.2	15.2-16.8	15.2-18.3	16.8-18.3	18.3-19.8	18.3-21.3	19.8-21.3	21.3-22.9		

* through end of program, unpublished

TABLE II

THEORETICAL POWER SPECTRAL DENSITY OF ATMOSPHERIC TURBULENCE

Family	Longitudinal spectra, $\phi_u(\Omega)$	Vertical spectra, $\phi_w(\Omega)$	Slope for large Ω
Taylor-Bullen (Ref. 18)	$\dfrac{2\sigma_u^2 L}{\pi\left[1+\dfrac{\Gamma^2(n)\Omega^2L^2}{\pi\Gamma^2(n+0.5)}\right]^{n+0.5}}$	$\dfrac{\sigma_w^2 L\left[1+2(n+1)\dfrac{\Gamma^2(n)\Omega^2L^2}{\pi\Gamma^2(n+0.5)}\right]}{\pi\left[1+\dfrac{\Gamma^2(n)\Omega^2L^2}{\pi\Gamma^2(n+0.5)}\right]^{n+1.5}}$	-1-2n
Von Karman (n = 1/3)	$\dfrac{2\sigma_u^2 L}{\pi\left[1+1.793\,\Omega^2L^2\right]^{5/6}}$	$\dfrac{\sigma_w^2 L\left[1+4.78\,\Omega^2L^2\right]}{\pi\left[1+1.793\Omega^2L^2\right]^{11/6}}$	- 5/3
Dryden (n = 1/2)	$\dfrac{2\sigma_u^2 L}{\pi\left[1+\Omega^2L^2\right]}$	$\dfrac{\sigma_w^2 L\left[1+3\Omega^2L^2\right]}{\pi\left[1+\Omega^2L^2\right]^2}$	-2
Case 6 (Ref. 30)	$\dfrac{2\sigma_u^2 L C^2}{\pi(1+C^2)}\left[\dfrac{1}{1+Y^2}+\dfrac{C^2-Y^2}{(C^2+Y^2)^2}\right]$ $Y=\dfrac{C^2\Omega L}{1+C^2}$	$\dfrac{\sigma_w^2 L C^2}{\pi(1+C^2)}\left[\dfrac{1+3Y^2}{(1+Y^2)^2}+\dfrac{C^4+6C^2Y^2-3Y^4}{(C^2+Y^2)^3}\right]$ $Y=\dfrac{C^2\Omega L}{1+C^2}$	-4
Case 2 (Ref. 30)	$\dfrac{2\sigma_u^2 L}{\pi}\left[1-\dfrac{\Omega L}{2}\,\mathrm{ATAN}\,\dfrac{2}{\Omega L}\right]$	$\dfrac{\sigma_w^2 L}{\pi\left[1+\dfrac{\Omega^2L^2}{4}\right]}$	-2

Notes:
1. Γ is gamma function
2. $\phi(\Omega) = V\phi(\omega) = V\phi(f)/2\pi = \phi(\lambda)/2\pi$
3. $\Omega = \omega/V = 2\pi f/V = 2\pi/\lambda$
4. $2\Phi_w(\Omega) = \phi_u(\Omega) - \Omega\, d\phi_u(\Omega)/d\Omega$ for isotropic turbulence
5. $\Phi_w/\sigma_w^2 = \phi_v/\sigma_v^2$ for isotropic turbulence
6. $\sigma_u = \sigma_v = \sigma_w$ for isotropic turbulence
7. $\phi(-\Omega) = \phi(\Omega)$

TABLE III

ATMOSPHERIC TURBULENCE MODELS

Ref. No.	Earliest Date	Power Spectral Density Family	Scale Length, L, ft	Data Source	Parameter *	Altitude, 1000 ft 30	30-40	40	40-50	50	50-60	60	60-70	70	80	100
32	9/58	Dryden	1000	Tables	P_1 P_2 b_1 b_2		.065 .000045 3.4 11.1		.023 .00001 3.1 11.7		.02 .000 2.8 12.5					
33	5/60	Dryden	1000	Table III	P_1 P_2 b_1 b_2		.065 .0006 3.4 11.1		.023 .0002 3.1 11.7		.02 .0001 2.8 12.5					
34	8/61	Dryden	1000	Tables I and V, Fig. 15	P_1 P_2 b_1 b_2		.017 .00020 2.62 8.78		.0070 .00025 3.07 8.13		.0031 .00016 3.75 6.77		.0014 .00012 2.95 4.51			
35	6/65	Von Karman	2500	Tables 5-1 and 5-2, Figs. 5-3 and 5-4	P_1 P_2 b_1 b_2	.017 .00009 3.03 11.45	.0108 .0000908 2.93 9.84	.007 .00011 3.0 9.35	.00446 .000114 3.28 8.81	.003 .000095 3.55 8.15	.00197 .0000727 3.82 7.04	.0012 .000062 3.70 5.75	.000892 .0000545 2.93** 4.33	.00055 .00005 3.07 3.07	.00025 .00004 2.45 0.50	
36	11/65	Dryden	2000	Tables 7 and 8, Figs. 21 and 22	P_1 P_2 b_1 b_2	.085 .0007 2.6 9.1		.06 .00035 2.5 9.0		.02 .00011 2.4 8.5		.008 .000027 2.35 7.8		.002 .00001 2.3 7.1	.0003 .000002 2.25 6.4	.00001 .0000006 2.2 5.0
37	4/66	Von Karman	2500	Fig. 2	P_1 b_1	.065 3.0		.05 3.0		.02 3.0		.008 3.0		.0035 3.0	.0013 3.0	
38	8/66	Dryden	1000	Appendix	P_1 P_2 P_3 b_1 b_2 b_3		.075 .013 .000039 1.36 2.65 7.1									
39	9/66	Dryden	1000	Table 1, Fig. 6	P_1 P_2 b_1 b_2	.085 .0007 2.6 9.1		.06 .00035 2.5 9.0		.02 .00011 2.4 8.5		.008 .000027 2.35 7.8		.002 .00001 2.3 7.1	.0003 .000002 2.25 6.4	.00001 .0000006 2.2 5.0

TABLE III - Concluded

ATMOSPHERIC TURBULENCE MODELS

Ref. No.	Earliest Date	Power Spectral Density Family	Scale Length, L, ft	Data Source	Para-meter *	Altitude, 1000 ft: 30	30-40	40	40-50	50	50-60	60	60-70	70	80	100
40	11-12/66	Dryden	1000	Table 1	P_1 P_2 b_1 b_2		.13 .01 1.8 4.8									
16	4/67	Dryden	1000	Table VII	P_1 P_2 P_3 b_1 b_2 b_3		.0457 .00153 .000178 2.01 3.85 5.40		.0398 .00035 .00000 2.36 4.65 0.00							
41	7/67	Von Karman	2500	Table 1	P_1 P_2 b_1 b_2		.011 .000095 2.93 9.84		.0046 .000115 3.28 8.81		.002 .000078 3.82 7.04		.00088 .000057 2.93 4.33			
42	8/67	Von Karman	Fig. 10	Fig. 8, eq. 30	P***	.0700	.0450	.0289	.0186	.0119	.00765	.00491	.00315	.00202		
43	11-12/67	Modified Lappe	Fig. 6	Figs. 4 and 5	P_1 P_2 b_1 b_2 L	.018 .000165 3.2 8.3 3350	.0143 .000133	.0113 .000113 3.2 7.75 4500	.009 .000096	.007 .000081 3.2 6.6 6300	.0054 .00007	.004 .000059 11 100	.003 .00005	.002 .000041		
					a_0	994.7	972.9	968.1	968.1	968.1	968.1	968.1	968.1	971.1	977.8	991.2
					Altitude, Km	9.7	9.1-12.2	12.2	12.2-15.2	15.2	15.2-18.3	18.3	18.3-21.3	21.3	24.4	30.5

* a_o, b_1, b_2 & b_3 in fps, true

** From Table 5-1, does not lie on curve in figure 5-4.

*** Day, multiply by 0.3 for night, by 0.6 for average; b depends on L.

TABLE IV

EQUATIONS FOR CHANGES IN FLOW PARAMETERS DOWNSTREAM OF NORMAL SHOCK

Change in Downstream Flow Parameter		Due to Change in Upstream P_{t1}	Upstream T_{t1}	Duct Area A_1	Upstream Mach Number M_1	Shock Position X_s	Shock Velocity U_s	i
$\frac{\Delta P_2}{P_2}$	=	$+\frac{\Delta P_{t1}}{P_{t1}}$	$+0.0\Delta T_{t1}$	$+0.0\Delta A_1$	$-\frac{7M_1(5M_1^2-11)}{(7M_1^2-1)(M_1^2+5)}\Delta M_1$	$-\frac{7(1+7.4M_1^2)}{6(7M_1^2-1)}\frac{dA}{AdX}\Delta X_s$	$-\frac{14M_1\sqrt{1+.2M_1^2}}{7M_1^2-1}\frac{U_s}{a_t}$	1
$\frac{\Delta P_{t2}}{P_{t2}}$	=	$+\frac{\Delta P_{t1}}{P_{t1}}$	$+0.0\Delta T_{t1}$	$+0.0\Delta A_1$	$-\frac{35(M_1^2-1)^2}{M_1(7M_1^2-1)(M_1^2+5)}\Delta M_1$	$-\frac{7(M_1^2-1)}{7M_1^2-1}\frac{dA}{AdX}\Delta X_s$	$-\frac{35(M_1^2-1)\sqrt{1+.2M_1^2}}{6M_1(7M_1^2-1)}\frac{U_s}{a_t}$	2
$\frac{\Delta T_{t2}}{T_{t2}}$	=	$+0.0\Delta P_{t1}$	$+\frac{\Delta T_{t1}}{T_{t1}}$	$+0.0\Delta A_1$	$+0.0\Delta M_1$	$+0.0\Delta X_s$	$-\frac{M_1^2-1}{3M_1\sqrt{1+.2M_1^2}}\frac{U_s}{a_t}$	3
$\frac{\Delta w_2}{w_2}$	=	$+\frac{\Delta P_{t1}}{P_{t1}}$	$-\frac{1}{2}\frac{\Delta T_{t1}}{T_{t1}}$	$+\frac{\Delta A_1}{A_1}$	$-\frac{5(M_1^2-1)}{M_1(M_1^2+5)}\Delta M_1$	$+0.0\Delta X_s$	$-\frac{M_1^2-1}{(7M_1^2-1)\sqrt{1+.2M_1^2}}\frac{U_s}{a_t}$	4
$\frac{\Delta w_{c2}}{w_{c2}}$	=	$+0.0\Delta P_{t1}$	$+0.0\ \Delta T_{t1}$	$+\frac{\Delta A_1}{A_1}$	$-\frac{30(M_1^2-1)}{M_1(7M_1^2-1)(M_1^2+5)}\Delta M_1$	$+\frac{7(M_1^2-1)}{7M_1^2-1}\frac{dA}{AdX}\Delta X_s$	$+\frac{(M_1^2-1)(7M_1^2+5)}{M_1(7M_1^2-1)\sqrt{1+.2M_1^2}}\frac{U_s}{a_t}$	5
ΔM_2	=	$+0.0\Delta P_{t1}$	$+0.0\ \Delta T_{t1}$	$+0.0\Delta A_1$	$-\frac{36M_1}{\sqrt{M_1^2+5}\ (7M_1^2-1)^{1.5}}\Delta M_1$	$+\frac{8.4M_1^2\sqrt{M_1^2+5}}{(7M_1^2-1)^{1.5}}\frac{dA}{AdX}\Delta X_s$	$+\frac{6M_1(7M_1^2+5)}{\sqrt{5}\ (7M_1^2-1)^{1.5}}\frac{U_s}{a_t}$	6
$\frac{\Delta s^*_2}{R}$	=	$-\frac{\Delta P_{t1}}{P_{t1}}$	$+3.5\frac{\Delta T_{t1}}{T_{t1}}$	$+0.0\Delta A_1$	$+\frac{35(M_1^2-1)^2}{M_1(7M_1^2-1)(M_1^2+5)}\Delta M_1$	$+\frac{7(M_1^2-1)}{7M_1^2-1}\frac{dA}{AdX}\Delta X_s$	$-\frac{7(M_1^2-1)^2}{M_1(7M_1^2-1)\sqrt{1+.2M_1^2}}\frac{U_s}{a_t}$	7
j		1	2	3	4	5	6	

*Entropy divided by gas constant, dimensionless

$$\frac{\Delta s_1}{R} = -\frac{\Delta P_{t1}}{P_{t1}} + 3.5\frac{\Delta T_{t1}}{T_{t1}}$$

TABLE V

EQUATIONS FOR STEADY-STATE NORMAL SHOCK DISPLACEMENT

Constant Parameters	Steady-State Shock Displacement, ΔX_s, =
M_1 , P_{t1}	$-\frac{6\,(7M_1^2-1)}{7\,(1+7.4M_1^2)} \quad \frac{AdX}{dA} \quad \frac{\Delta P_2}{P_2}$
M_1 , A_1	$\frac{(7M_1^2-1)^{1.5}}{8.4\,M_1^2\,\sqrt{M_1^2+5}} \quad \frac{AdX}{dA} \quad \Delta M_2$
M_1 , A_1	$\frac{7M_1^2-1}{7(M_1^2-1)} \quad \frac{AdX}{dA} \quad \frac{\Delta w_{c2}}{w_{c2}}$
A_1 , w_{c2}	$\frac{30}{7M_1\,(M_1^2+5)} \quad \frac{AdX}{dA} \quad \Delta M_1$
M_1 , w_{c2}	$-\frac{7M_1^2-1}{7(M_1^2-1)} \quad \frac{AdX}{dA} \quad \frac{\Delta A_1}{A_1}$
w_1 , w_{c2}	$-\frac{AdX}{dA} \quad \frac{\Delta A_1}{A_1}$

TABLE VI - EQUATIONS FOR SQUARE OF TRANSFER FUNCTION

Transfer Function, H (S)	Square of Transfer Function, $H(i\omega)H(-i\omega)$ $\lvert H(\omega)\rvert^2$
C_1	C_1^2
$C_1 e^{-\tau_d S}$	C_1^2
$C_1 + C_2 e^{-\tau_d S}$	$C_1^2 + C_2^2 + 2C_1C_2 \cos(\tau_d\omega)$
S^n	ω^{2n}
$\tau_1 S + C_1$	$\tau_1^2\omega^2 + C_1^2$
$(\tau_1 S + 1)(\tau_2 S + 1)S + C_1$	$(\tau_1^2\omega^2 + 1)(\tau_2^2\omega^2 + 1)\omega^2 - 2C_1(\tau_1 + \tau_2)\omega^2 + C_1^2 = \tau_1^2\tau_2^2\omega^6 + (\tau_1^2 + \tau_2^2)\omega^4 + (1 - 2C_1(\tau_1 + \tau_2))\omega^2 + C_1^2$
$(\tau_1 S + C_1)(\tau_2 S + 1)(\tau_3 S + 1)S + C_2(\tau_4 S + C_3)$	$(\tau_1^2\omega^2 + C_1^2)(\tau_2^2\omega^2 + 1)(\tau_3^2\omega^2 + 1)\omega^2 + C_2^2(\tau_4^2\omega^2 + C_3^2) + 2C_2\omega^2[\{\tau_1\tau_2(C_3\tau_3 - \tau_1) - \tau_1\tau_3(C_1\tau_2 + \tau_4)\}\omega^2$ $- C_3(C_1\tau_2 + \tau_1) + C_1(\tau_1 - C_3\tau_3)]$
$(\tau_1 S + C_1) + C_2 e^{-\tau_d S}$	$(\tau_1^2\omega^2 + C_1^2) + C_2^2 + 2C_2\{C_1\cos(\tau_d\omega) - \tau_1\omega\sin(\tau_d\omega)\}$
$(\tau_1 S + C_1)S + C_2 e^{-\tau_d S}$	$(\tau_1^2\omega^2 + C_1^2)\omega^2 + C_2^2 - 2C_2\{\tau_1\omega^2\cos(\tau_d\omega) + C_1\omega\sin(\tau_d\omega)\}$
$(\tau_1 S + 1)(\tau_2 S + 1)(\tau_3 S + 1)S + C_1 e^{-\tau_d S}$	$(\tau_1^2\omega^2 + 1)(\tau_2^2\omega^2 + 1)(\tau_3^2\omega^2 + 1)\omega^2 + C_1^2 + 2C_1[\{\tau_1\tau_2\tau_3\omega^2 - \tau_1 - \tau_2 - \tau_3\}\omega^2\cos(\tau_d\omega)$ $+ \{(\tau_1\tau_2 + \tau_2\tau_3 + \tau_1\tau_3)\omega^2 - 1\}\omega\sin(\tau_d\omega)]$
$\tau_1^2 S^2 + \tau_2 S + C_1$	$\tau_1^4\omega^4 + (\tau_2^2 - 2\tau_1^2 C_1)\omega^2 + C_1^2$
$(\tau_1 S + C_1)(\tau_2 S + 1)(\tau_3 S + 1)(C_2^2 S^2 + C_3 S + 1) + C_4$	$(\tau_1^2\omega^2 + C_1^2)(\tau_2^2\omega^2 + 1)(\tau_3^2\omega^2 + 1)(C_2^4\omega^4 + (C_3^2 - 2C_2^2)\omega^2 + 1) + C_4^2 + 2C_4[\{\tau_1\tau_2(\tau_3 C_3 + C_2^2) + \tau_3(C_1\tau_2 + \tau_1)C_2^2\}\omega^4$ $- \{\tau_1\tau_2 + (\tau_2 C_1 + \tau_1)(\tau_3 + C_3) + C_1C_3(\tau_1 + \tau_3) + C_1(\tau_2 C_3 + C_2^2)\}\omega^2 + C_1]$
$(\tau_1 S + 1)(\tau_2 S + 1)(\tau_3^2 S^2 + \tau_4 S + 1)S + C_1 e^{-\tau_d S}$	$(\tau_1^2\omega^2 + 1)(\tau_2^2\omega^2 + 1)\{\tau_3^4\omega^4 + (\tau_4^2 - 2\tau_3^2)\omega^2 + 1\}\omega^2 + C_1^2 - 2C_1[\{-(\tau_1\tau_2\tau_4 + (\tau_1 + \tau_2)\tau_3^2)\omega^2 + \tau_1 + \tau_2 + \tau_4\}\omega^2\cos(\tau_d\omega)$ $+ \{\tau_1\tau_2\tau_3^2\omega^4 - (\tau_1\tau_2 + \tau_4(\tau_1 + \tau_2) + \tau_3^2)\omega^2 + 1\}\omega\sin(\tau_d\omega)]$
$\tau_4 S^4 + \tau_3 S^3 + \tau_2 S^2 + \tau_1 S + C_1$	$\tau_4^2\omega^8 + (\tau_3^2 - 2\tau_2\tau_4)\omega^6 + (\tau_2^2 + 2\tau_4 C_1 - 2\tau_1\tau_3)\omega^4 + (\tau_1^2 - 2\tau_2 C_1)\omega^2 + C_1^2$
$\{\tau_1(\tau_2 S + 1)(\tau_3 S + 1)S^2 + C_1(\tau_1 S + C_2) + C_3\}$ $S(\tau_4 S + 1)(\tau_5 S + 1)$	$(\tau_1\tau_2\tau_3\tau_4\tau_5)^2\omega^{14} + \tau_1^2\{\tau_2^2\tau_3^2(\tau_4^2 + \tau_5^2) + \tau_4^2\tau_5^2(\tau_2^2 + \tau_3^2)\}\omega^{12} + [\tau_1^2\{\tau_2^2(\tau_3^2 + \tau_4^2 + \tau_5^2) + \tau_3^2(\tau_4^2 + \tau_5^2) + \tau_4^2\tau_5^2 - 2\tau_4^2\tau_5^2$ $(\tau_2 + \tau_3)C_1\} + 2\tau_1\tau_2\tau_3\tau_4^2\tau_5^2(C_1C_2 + C_3)]\omega^{10} + [\tau_1^2\{\tau_2^2 + \tau_3^2 + \tau_4^2 + \tau_5^2 + \tau_4^2\tau_5^2C_1^2 - 2(\tau_3\tau_4^2 + \tau_3\tau_5^2 + \tau_2\tau_4^2)C_1$ $- 2\tau_2\tau_5^2C_2\} + 2\tau_1\{\tau_2\tau_3(\tau_4^2 + \tau_5^2) - \tau_4^2\tau_5^2\}(C_1C_2 + C_3)]\omega^8 + \{\tau_4^2\tau_5^2(C_1C_2 + C_3)^2 - 2\tau_1(\tau_4^2 + \tau_5^2 - \tau_2\tau_3)$ $(C_1C_2 + C_3) + \tau_1^2\{(\tau_4^2 + \tau_5^2)C_1^2 - 2(\tau_2 + \tau_3)C_1 + 1\}]\omega^6 + \{(\tau_4^2 + \tau_5^2)(C_1C_2 + C_3)^2 - 2\tau_1(C_1C_2 + C_3) + \tau_1^2C_1^2\}\omega^4$ $+ (C_1C_2 + C_3)^2\omega^2$
$(\tau_1 S + C_1) + (\tau_2 S + 1)(\tau_3 S + 1)(\tau_4 S + C_2)S$	$(\tau_1\omega^2 + C_1^2) + (\tau_2^2\omega^2 + 1)(\tau_3^2\omega^2 + 1)(\tau_4^2\omega^2 + C_2^2)\omega^2 + 2(\tau_2\tau_3\tau_4C_1 - \tau_1\tau_2\tau_4 - \tau_1\tau_3\tau_4 - \tau_1\tau_2\tau_3C_2)\omega^4$ $+ 2(\tau_1C_2 - \tau_4C_1 - (\tau_2 + \tau_3)C_1C_2)\omega^2$
$T_1 S(C_1 + (\tau_2^2 S^2 + \tau_3 S + 1)(\tau_4 S + 1)(\tau_5 S + 1)S) +$ $C_2[C_3(\tau_2^2 S^2 + \tau_3 S + 1)(\tau_4 S + 1)(\tau_5 S + 1)S(\tau_6 S^2 +$ $\tau_7 S + 1) - C_4C_5(\tau_8 S + 1)]$	See figure 49.
$(\tau_1 S + 1)(\tau_2 S + 1)(C_1^2 S^2 + C_2 S + 1)(\tau_5 S^3 + \tau_4 S^2 + \tau_3 S + 1)$ $S + C_3(\tau_6 S + 1)e^{-\tau_7 S}$	See figure 49.

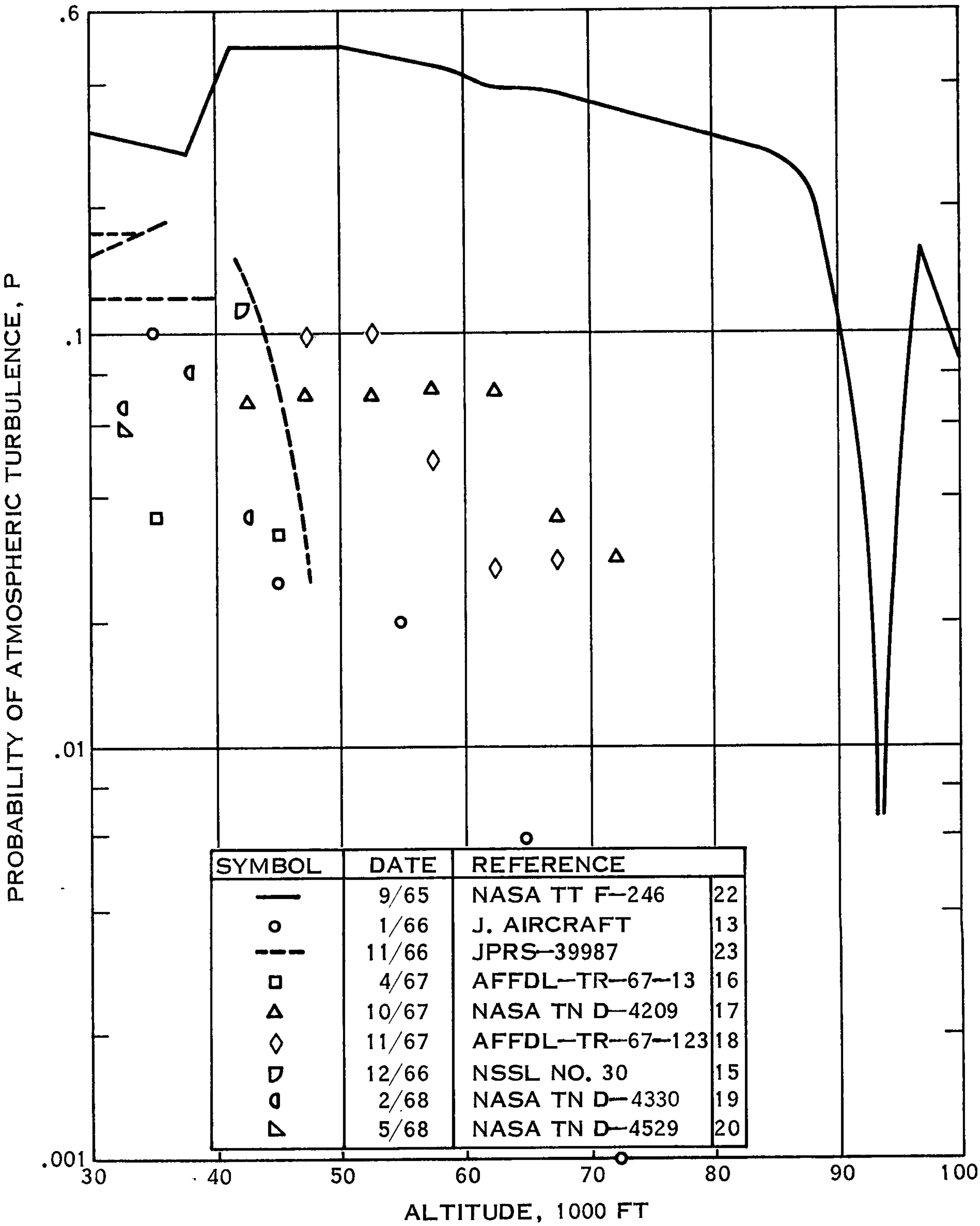

Figure 1. Probability of Atmospheric Turbulence

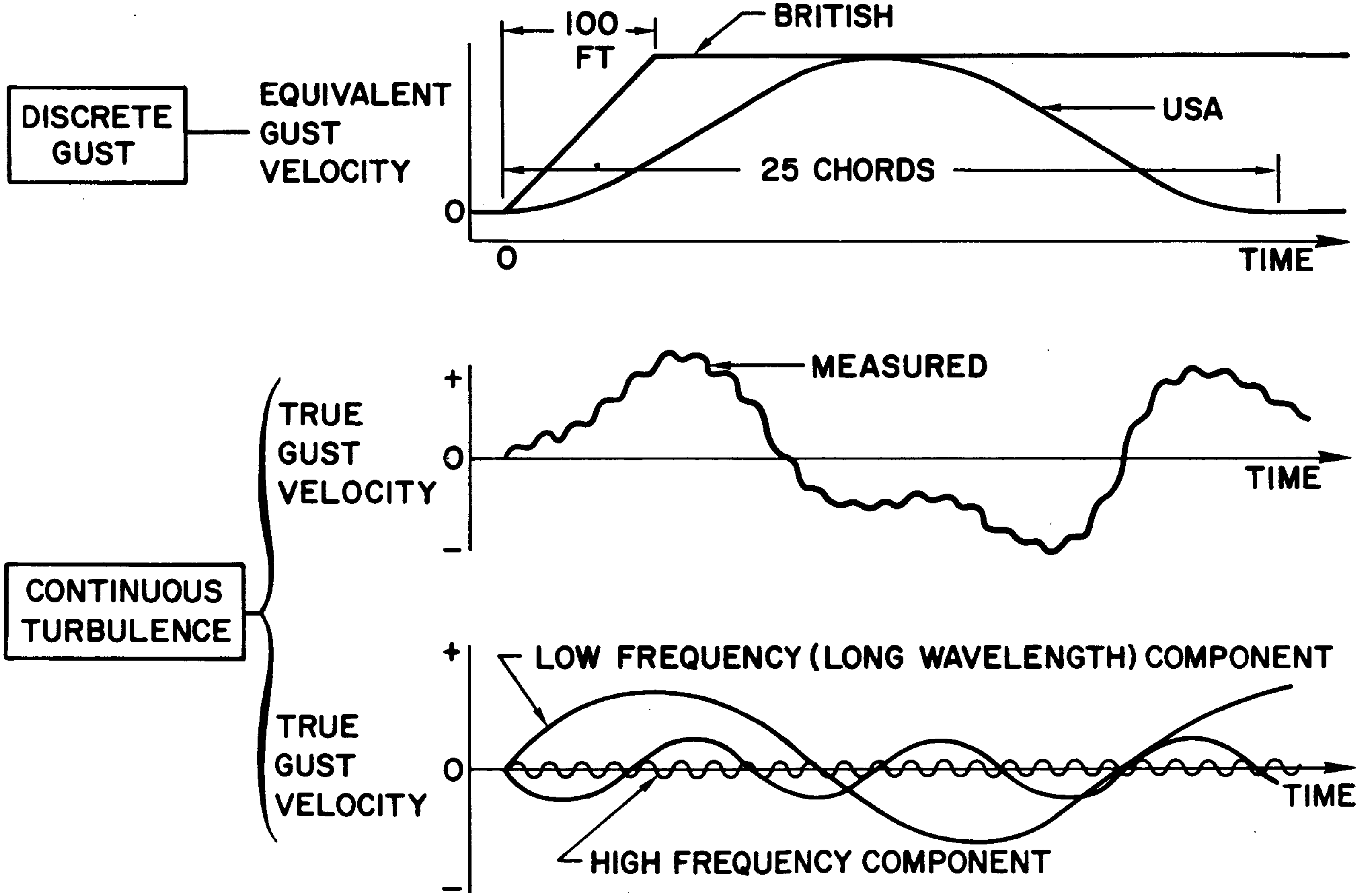

Figure 2. Representations of Atmospheric Turbulence

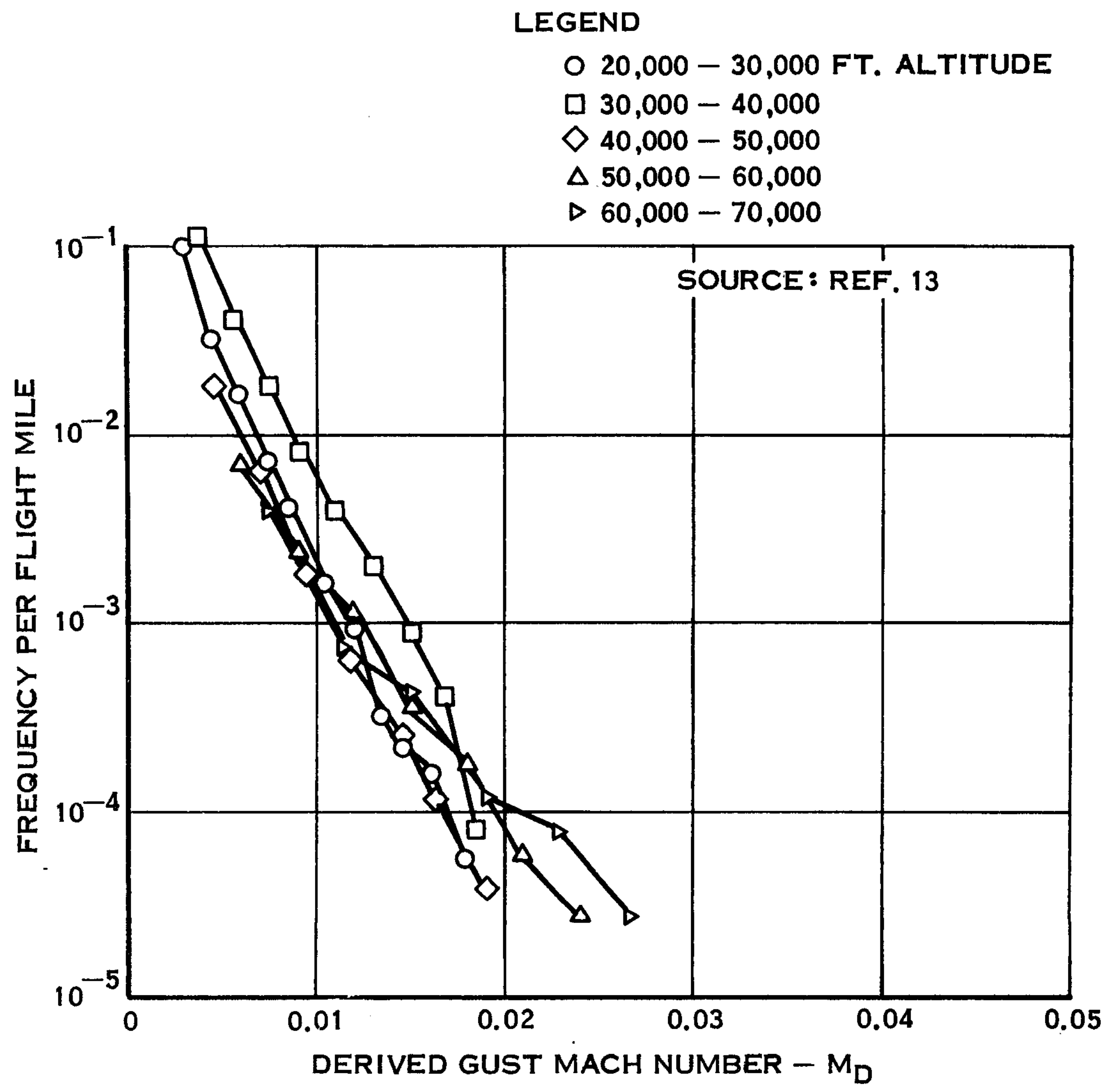

Figure 3. Cumulative Frequency of Exceeding Derived Gust Mach Number

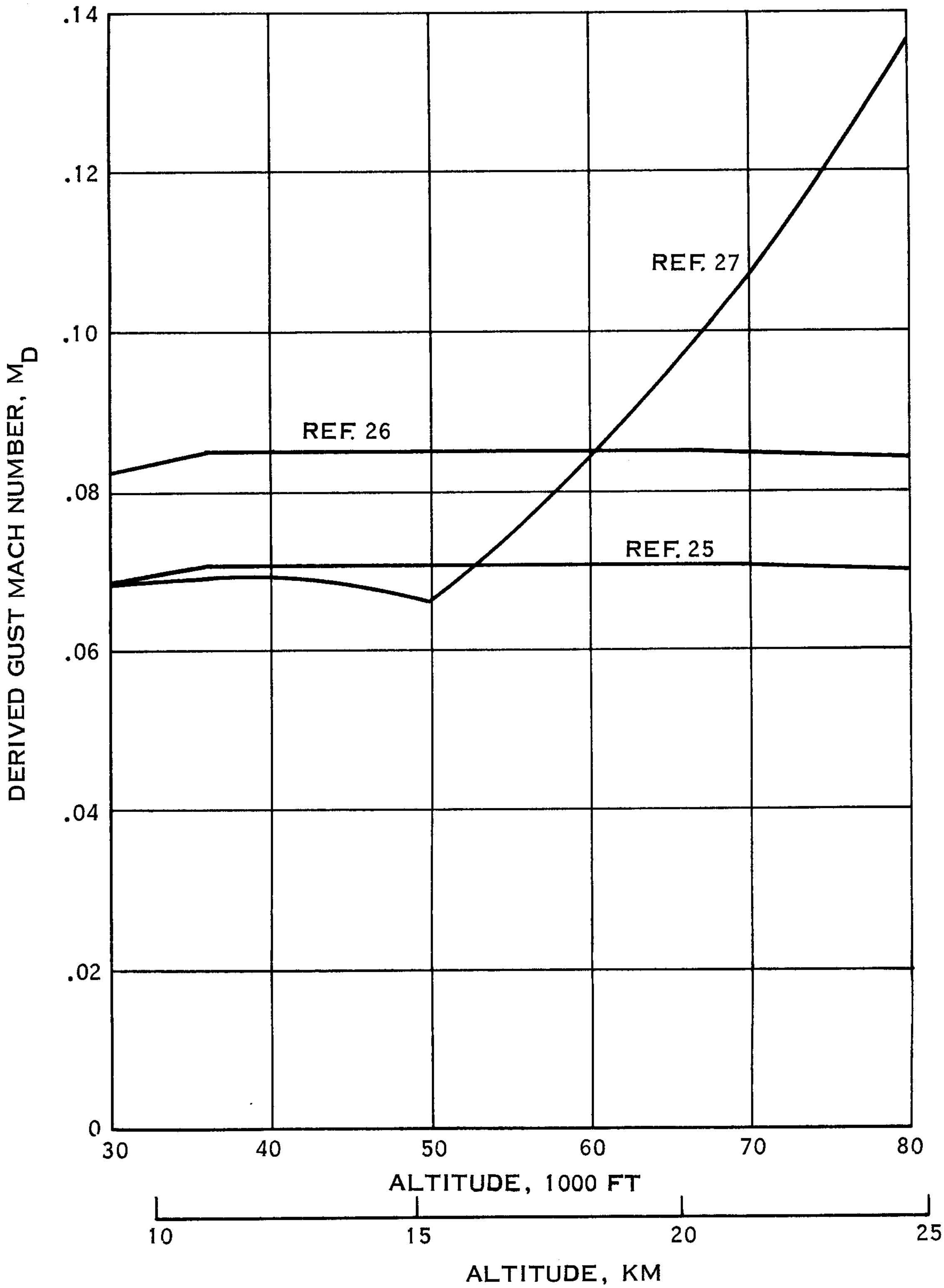

Figure 4. Derived Gust Mach Numbers in Specifications

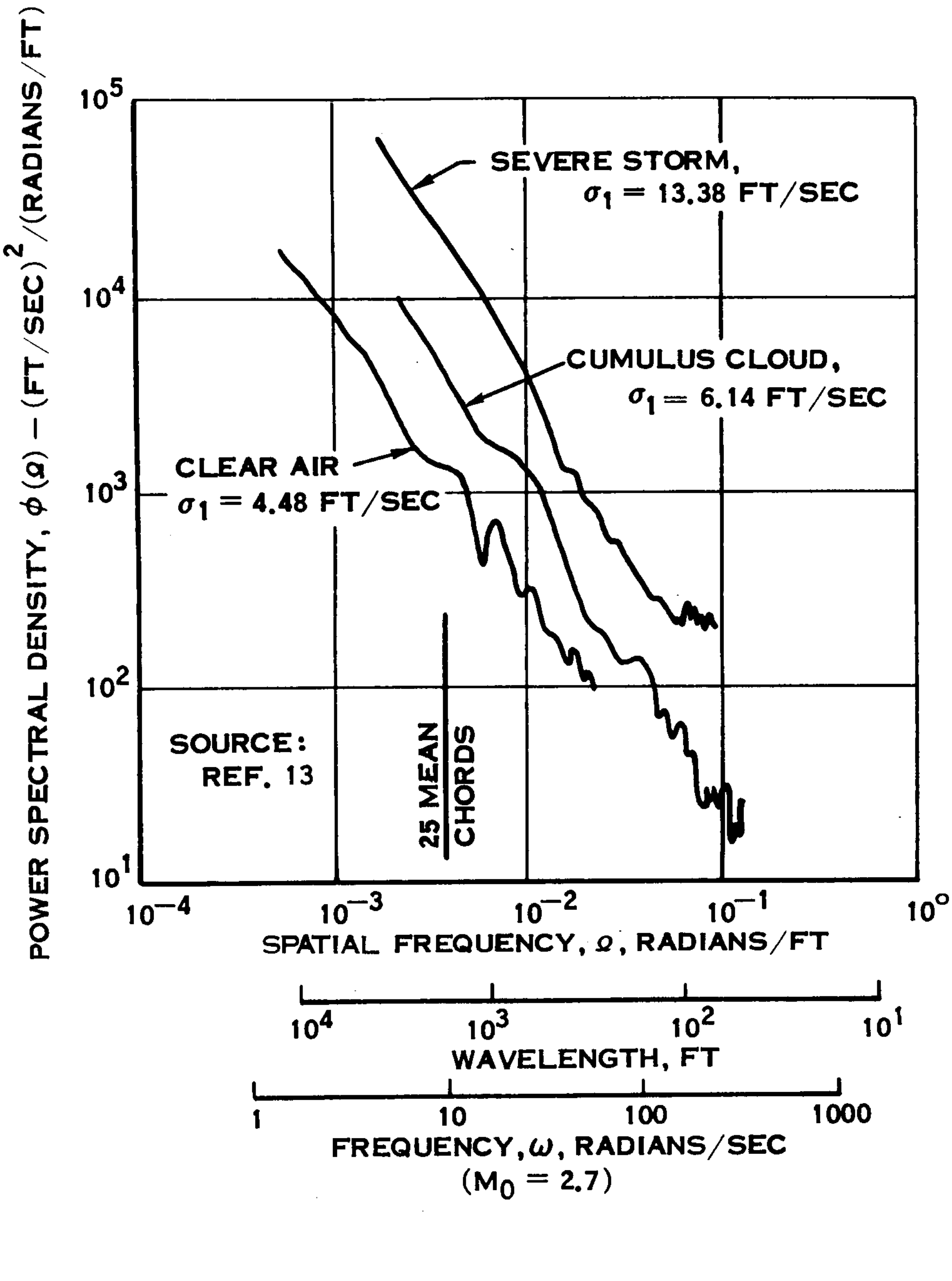

Figure 5. Typical Power Spectral Density Data for Vertical Gust Velocity

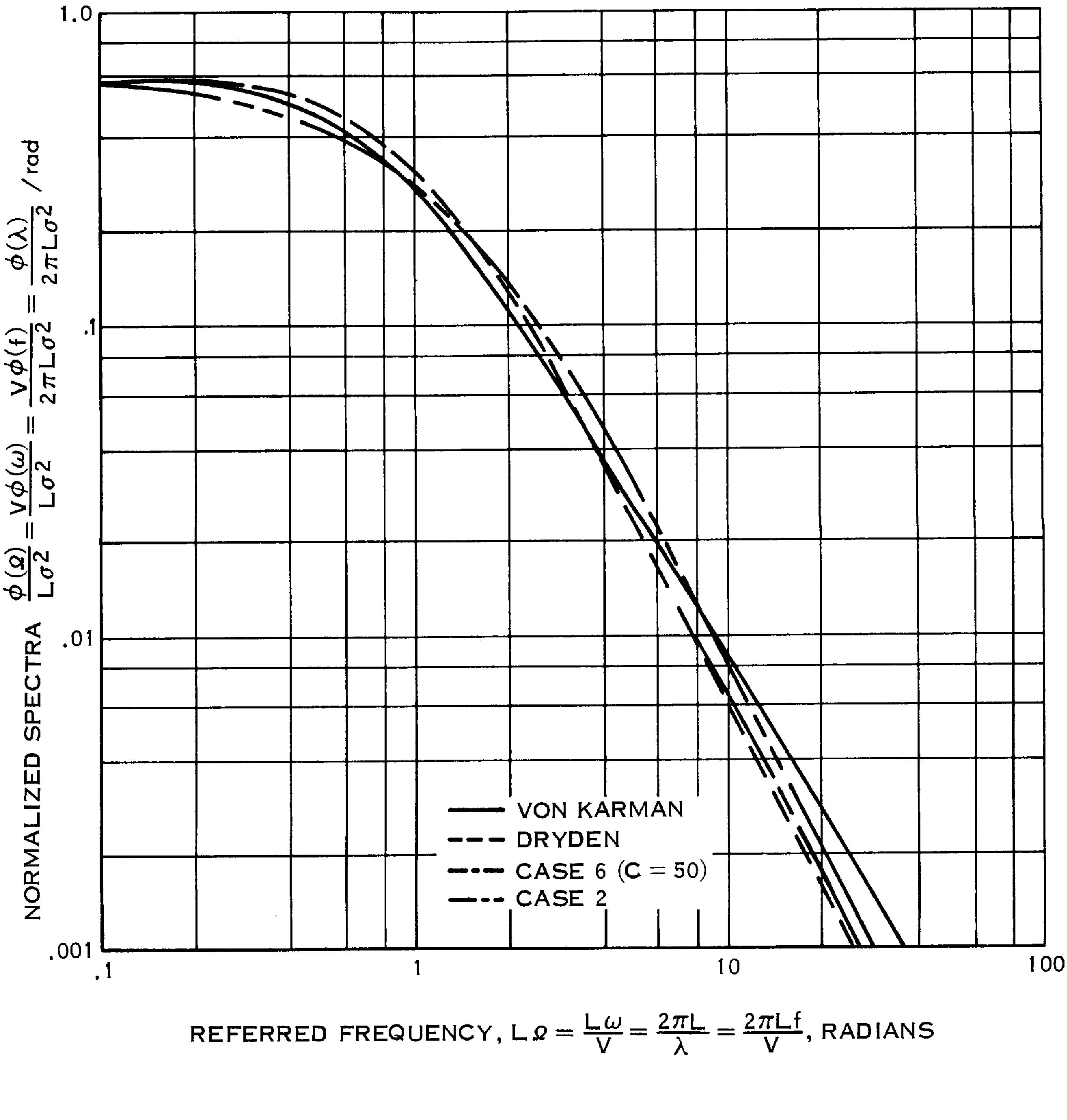

Figure 6. Normalized Longitudinal Spectra

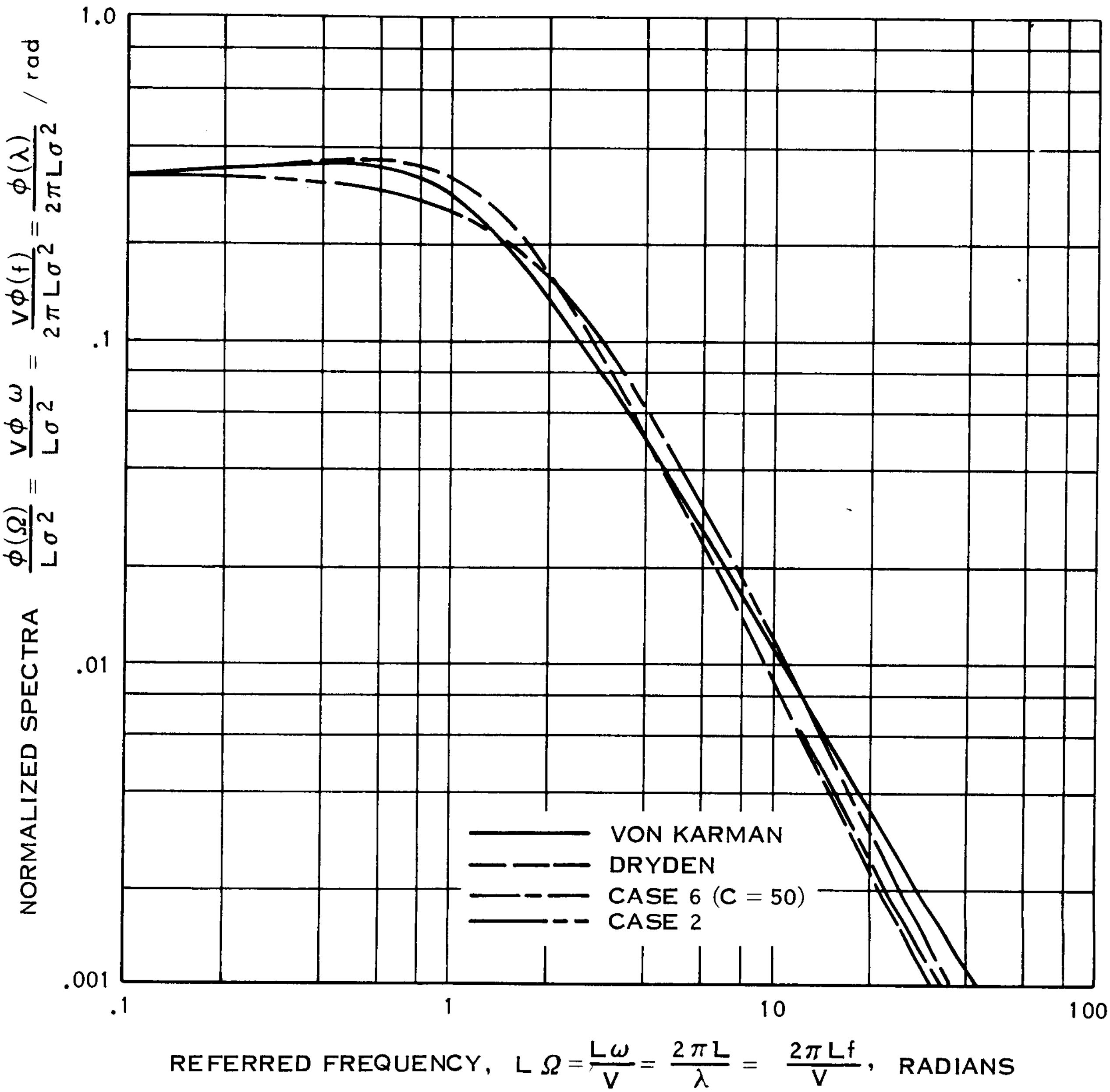

Figure 7. Normalized Vertical Spectra

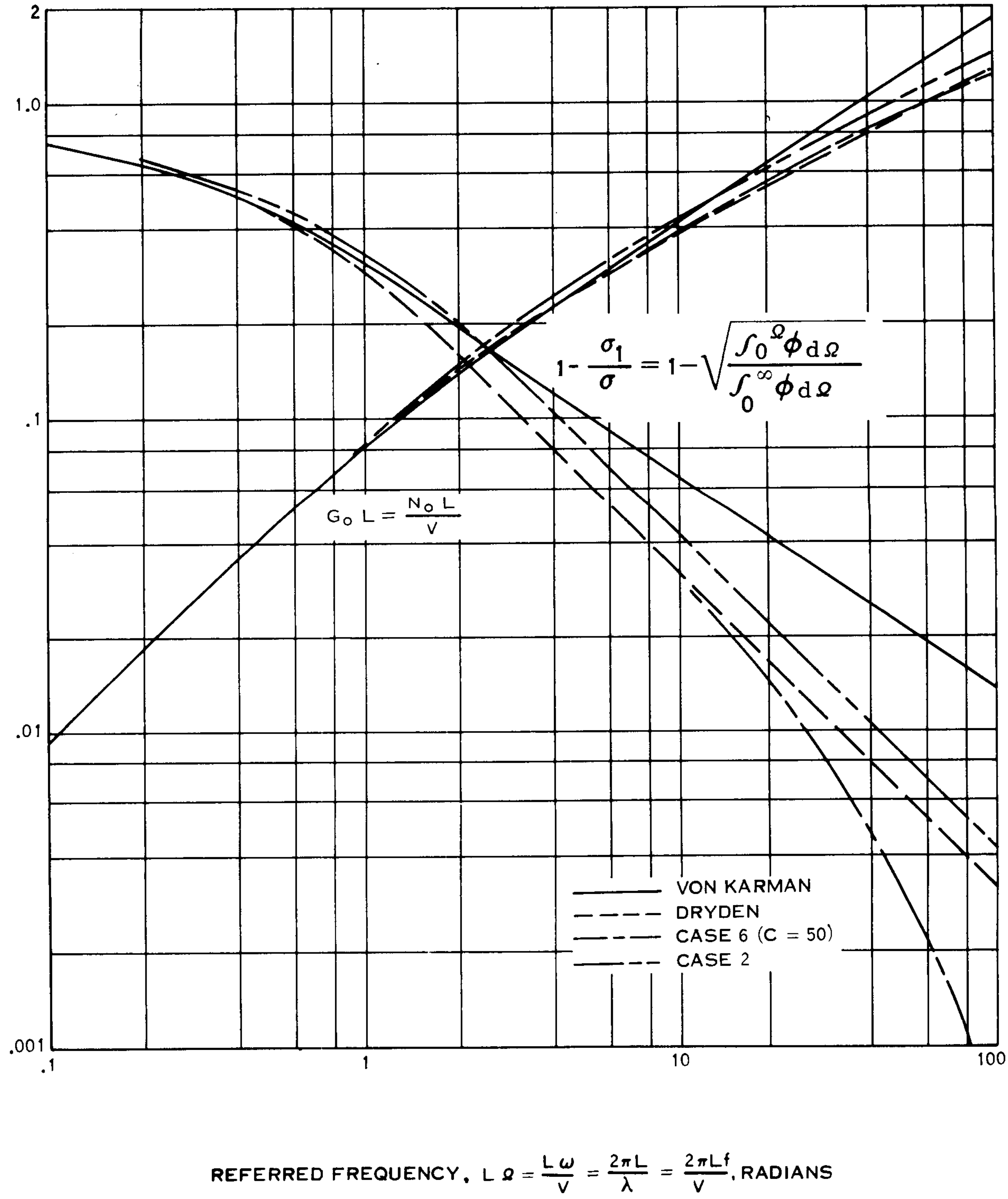

Figure 8. Integrals of Longitudinal Spectra

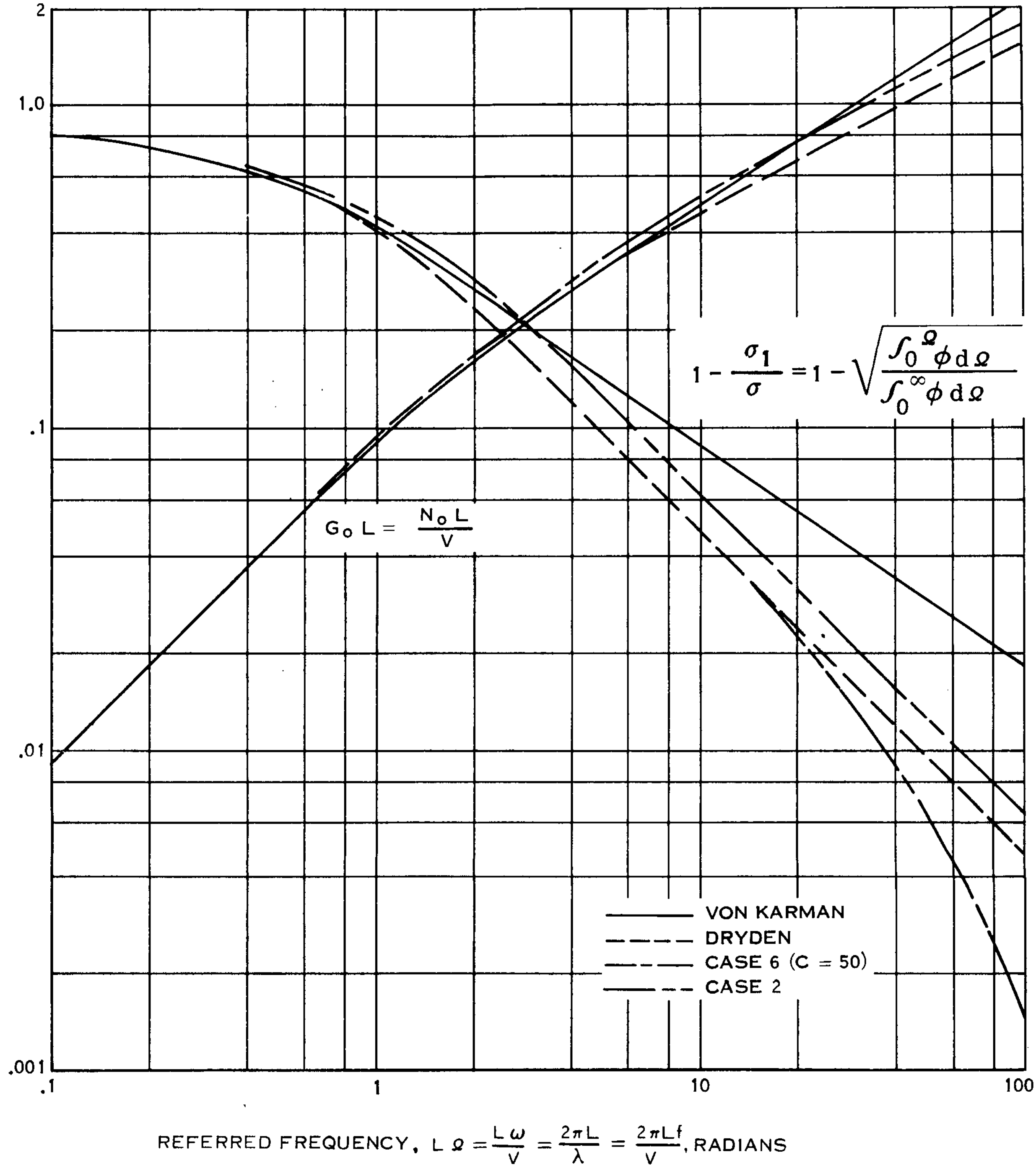

Figure 9. Integrals of Vertical Spectra

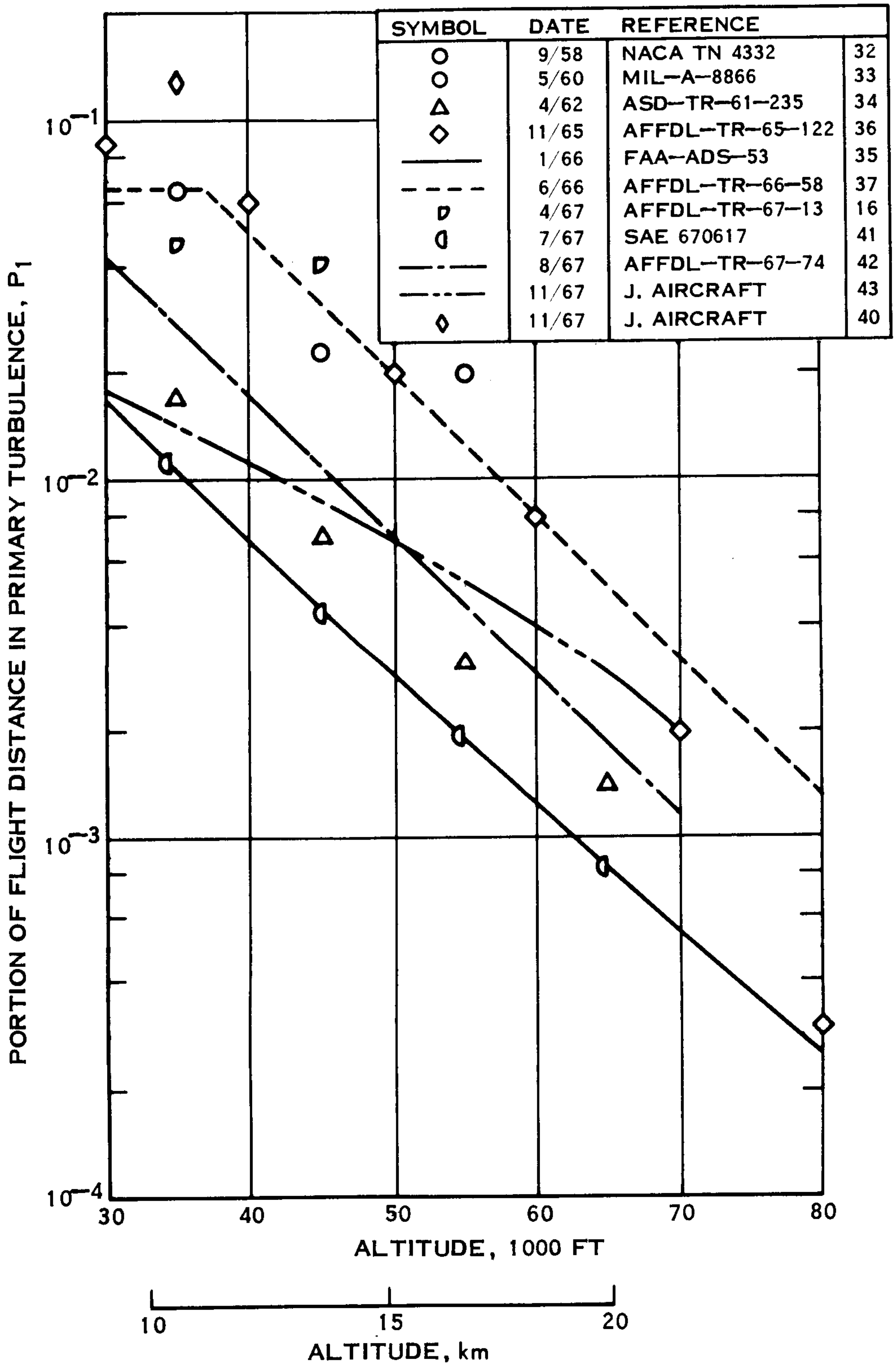

Figure 10. Probability of Primary Turbulence, P_1

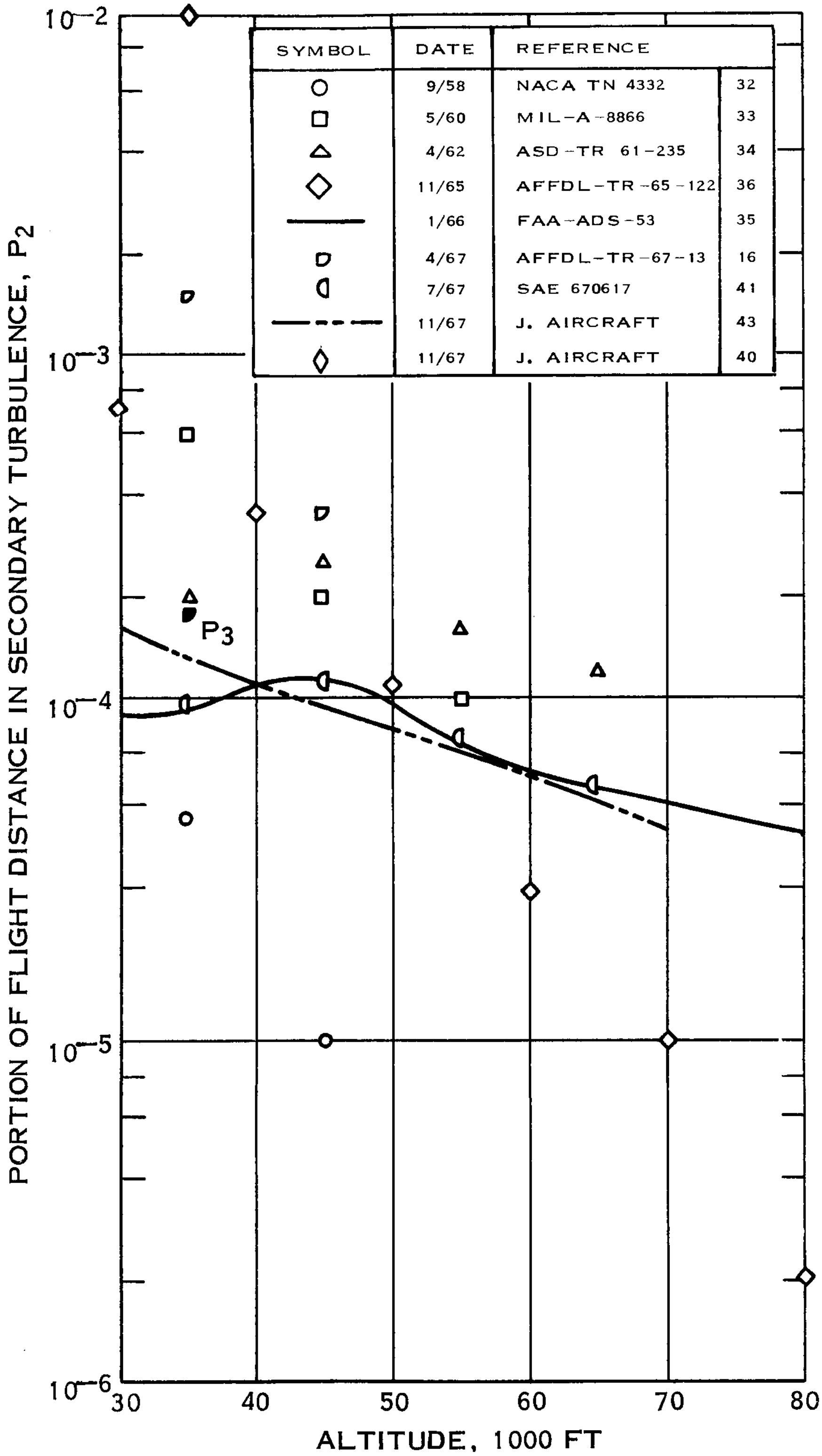

Figure 11. Probability of Secondary Turbulence, P_2

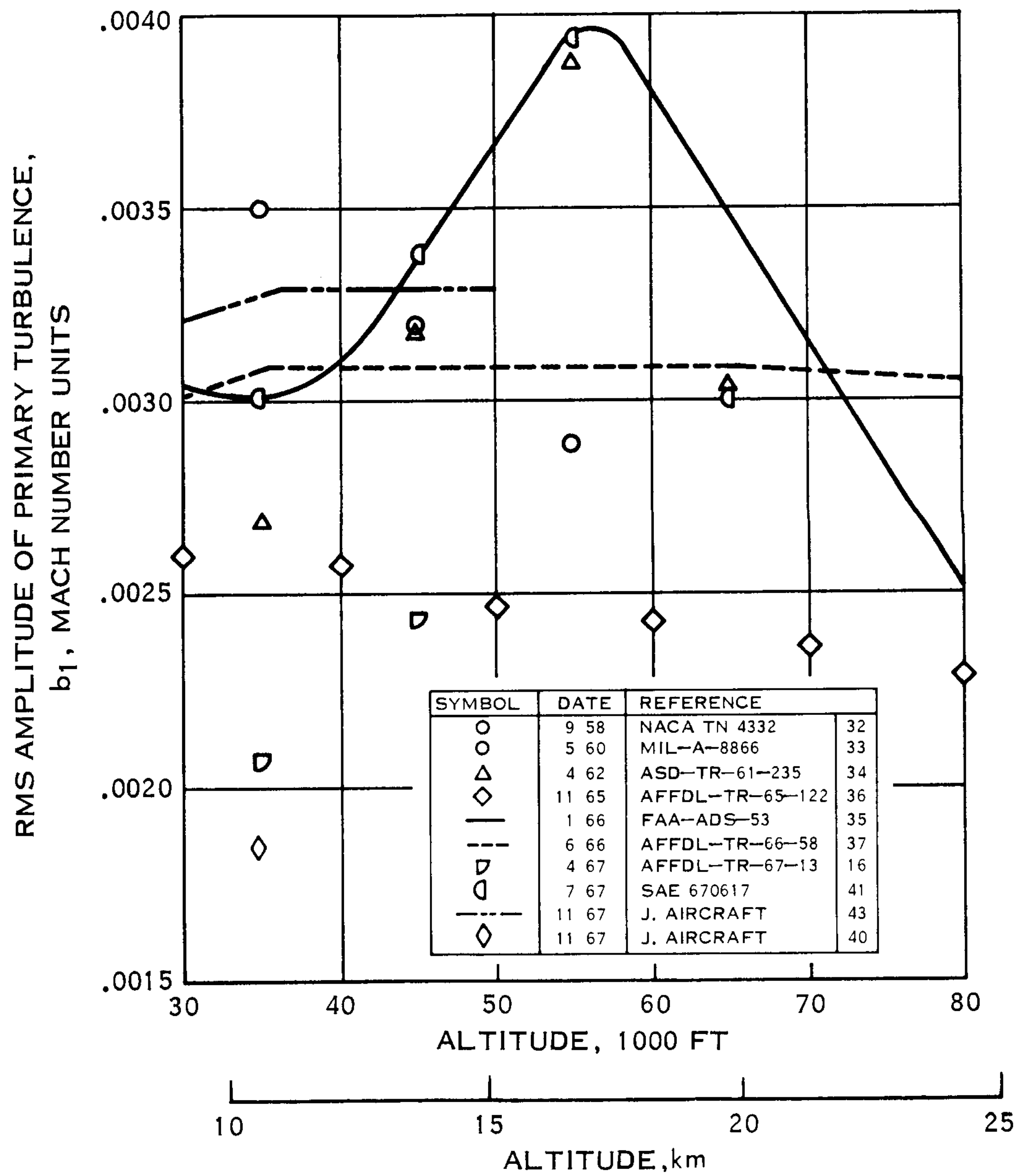

Figure 12. Amplitude of Primary Turbulence, b_1

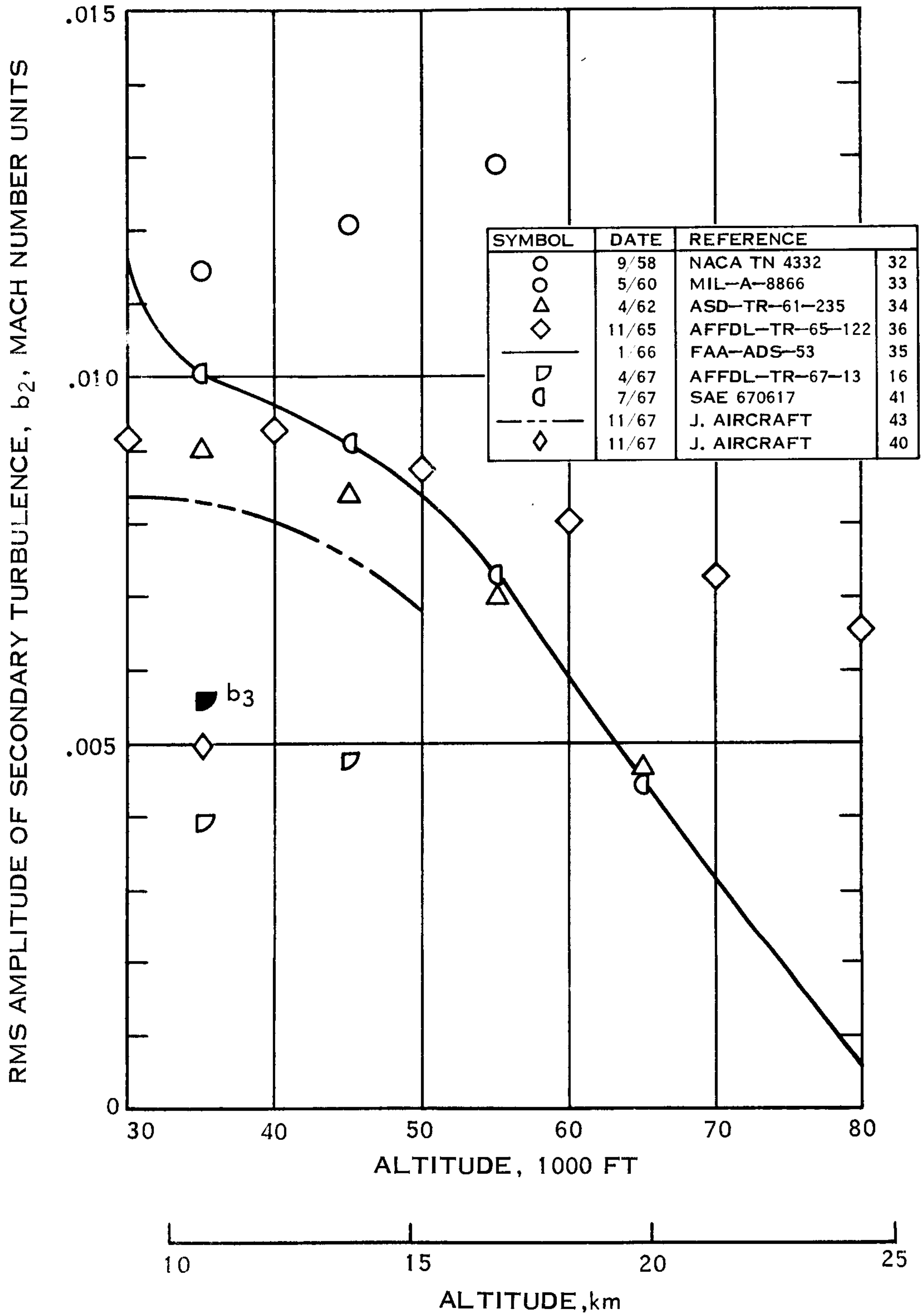

Figure 13. Amplitude of Secondary Turbulence, b_2

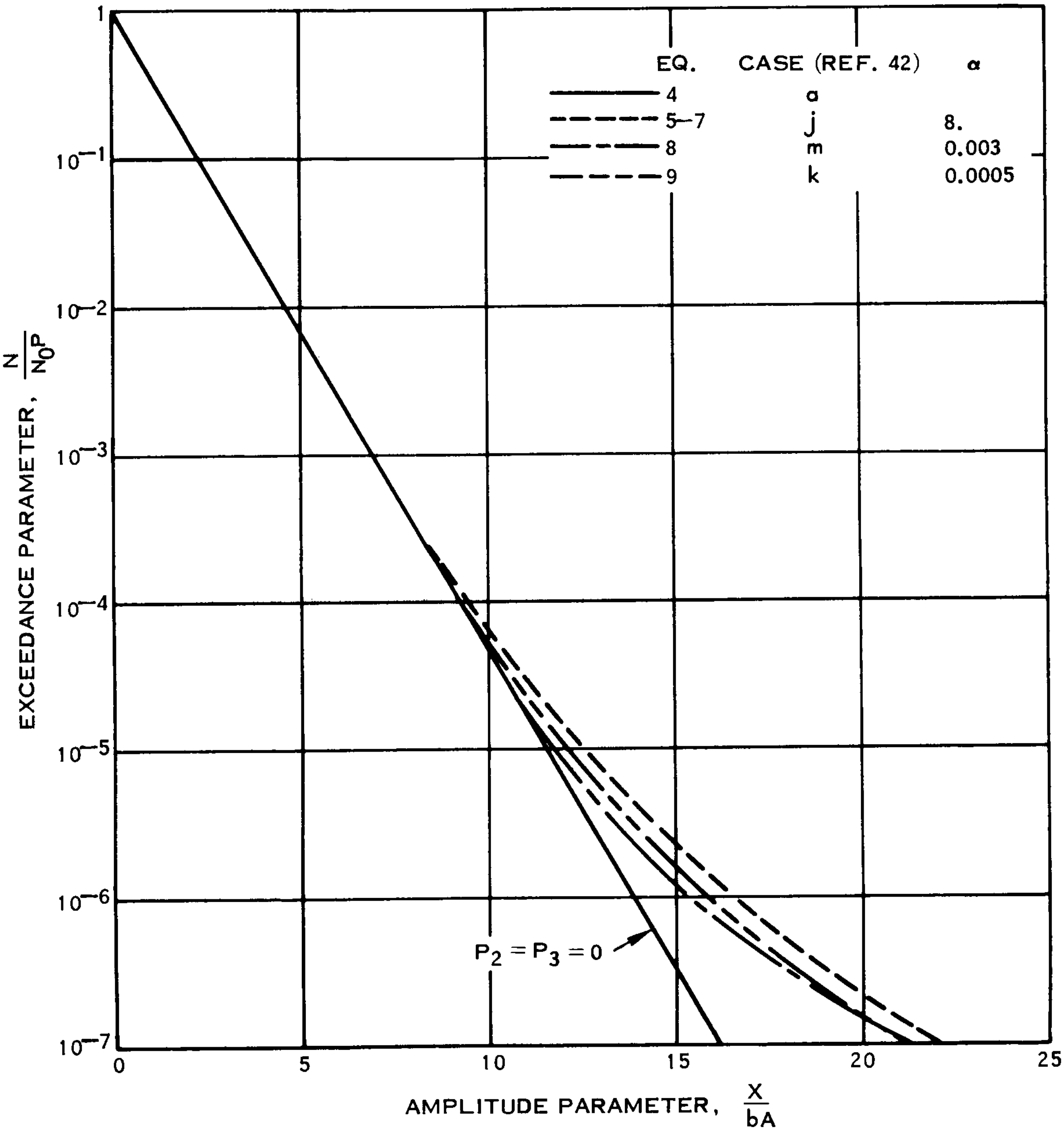

Figure 14. Exceedance Models

3$\not{0}$

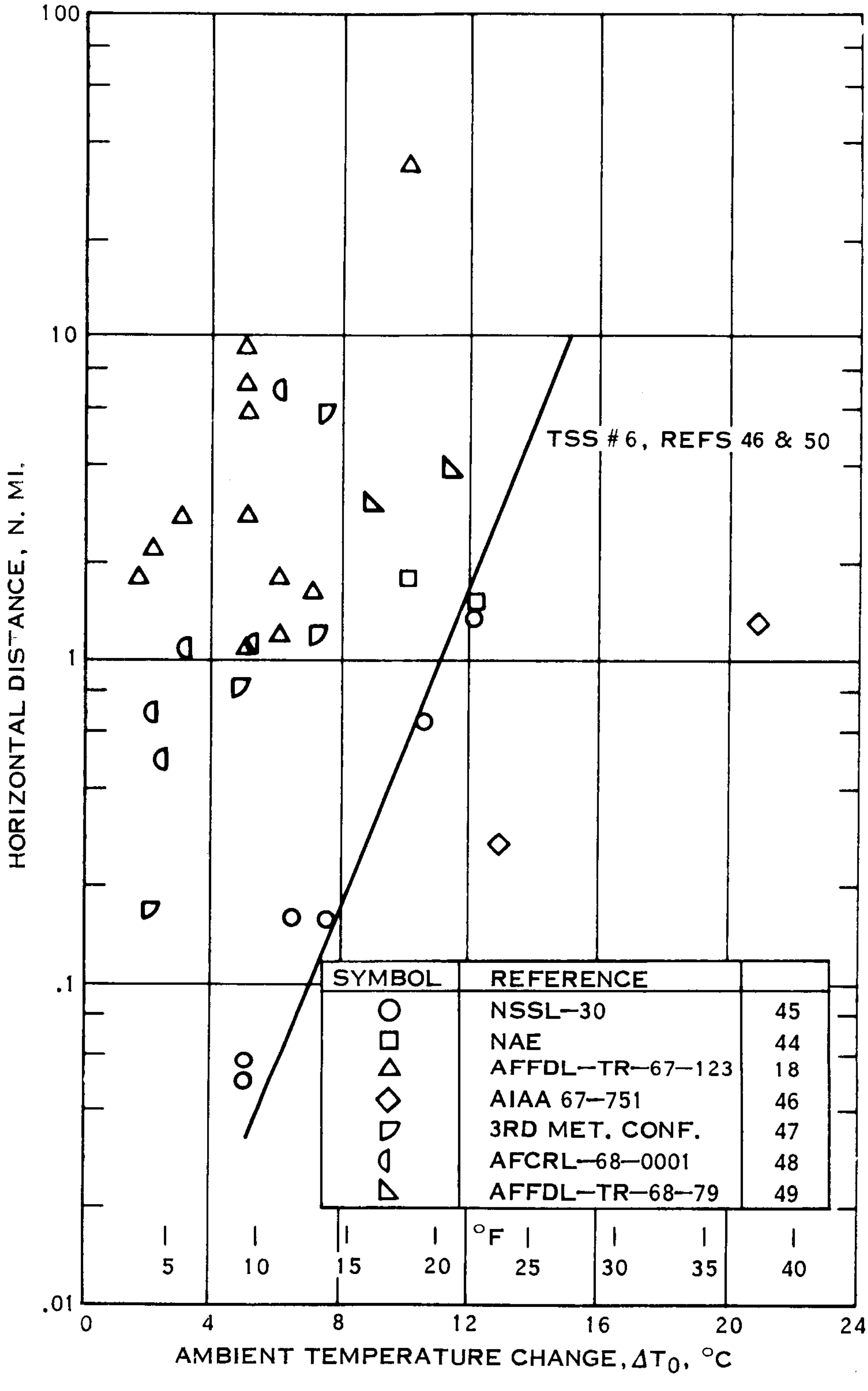

Figure 15. Horizontal Atmospheric Temperature Changes

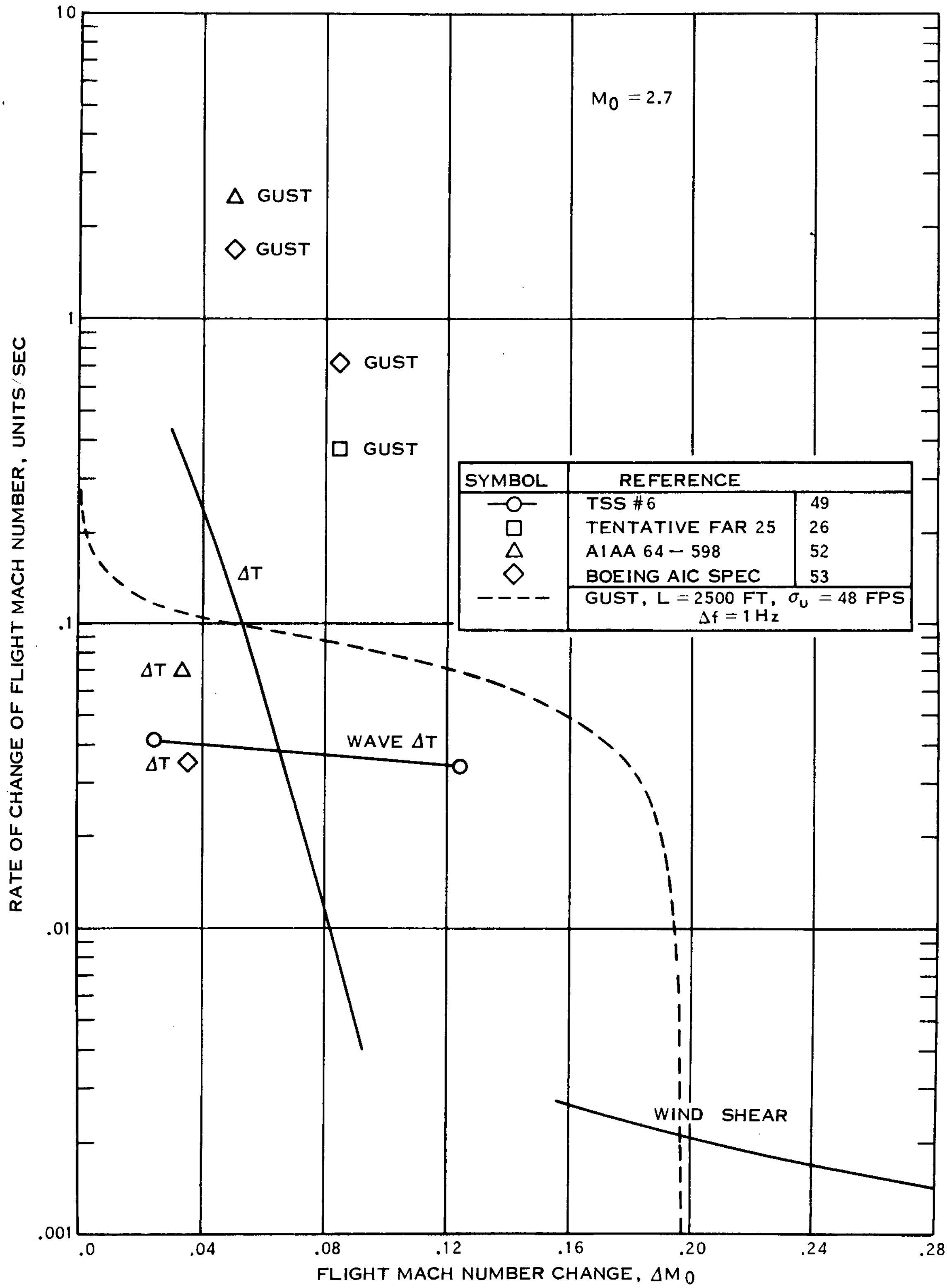

Figure 16. Rate of Change of Flight Mach Number Versus Amplitude

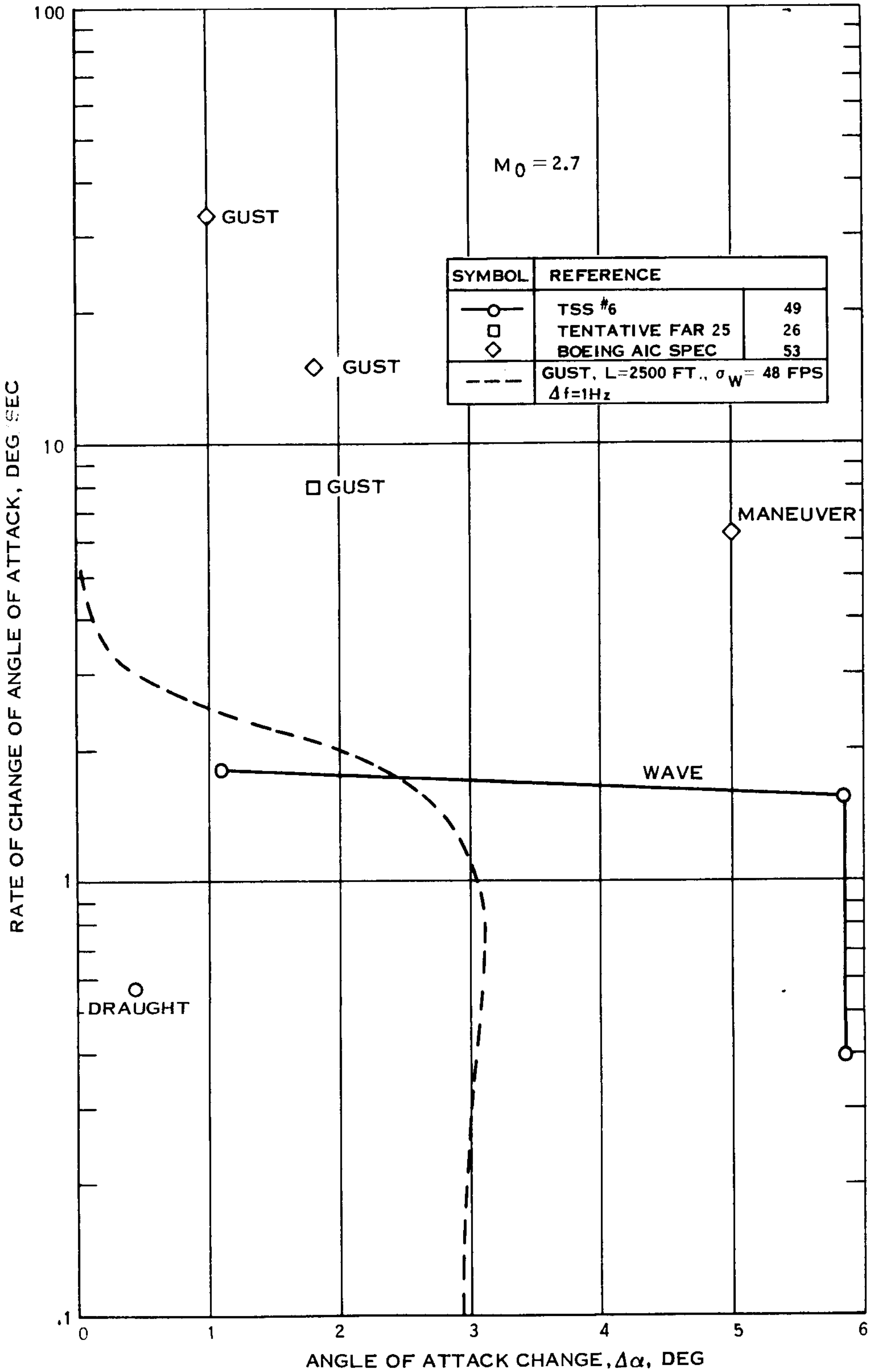

Figure 17. Rate of Change of Angle of Attack Versus Amplitude

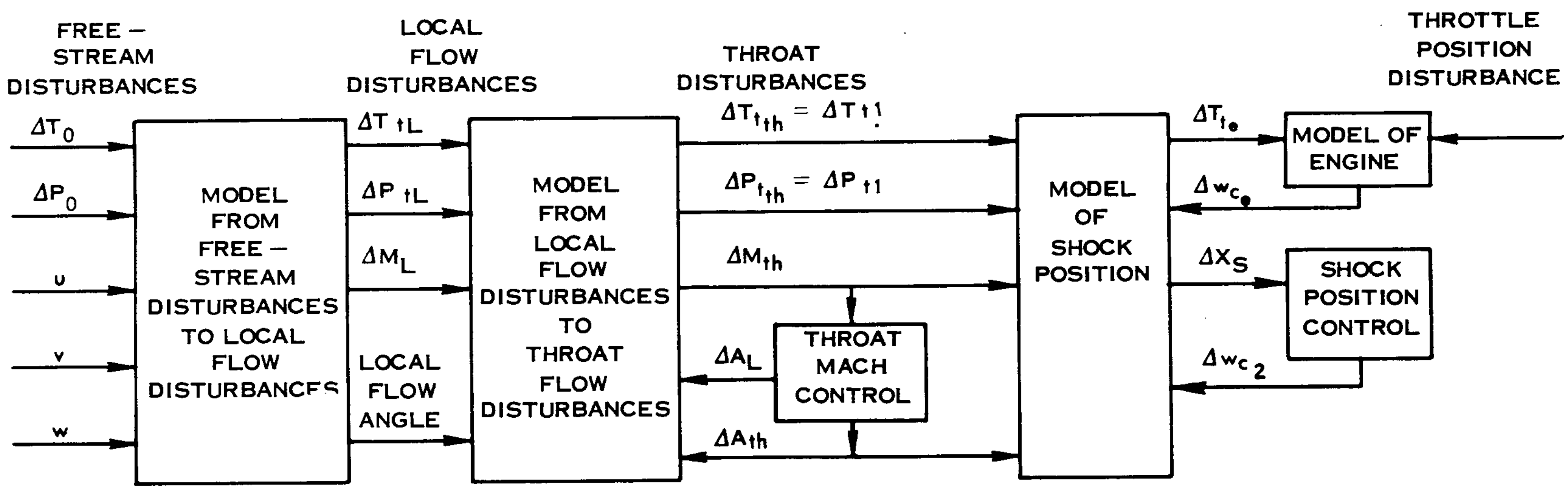

Figure 18. Schematic of Analytical Inlet Model

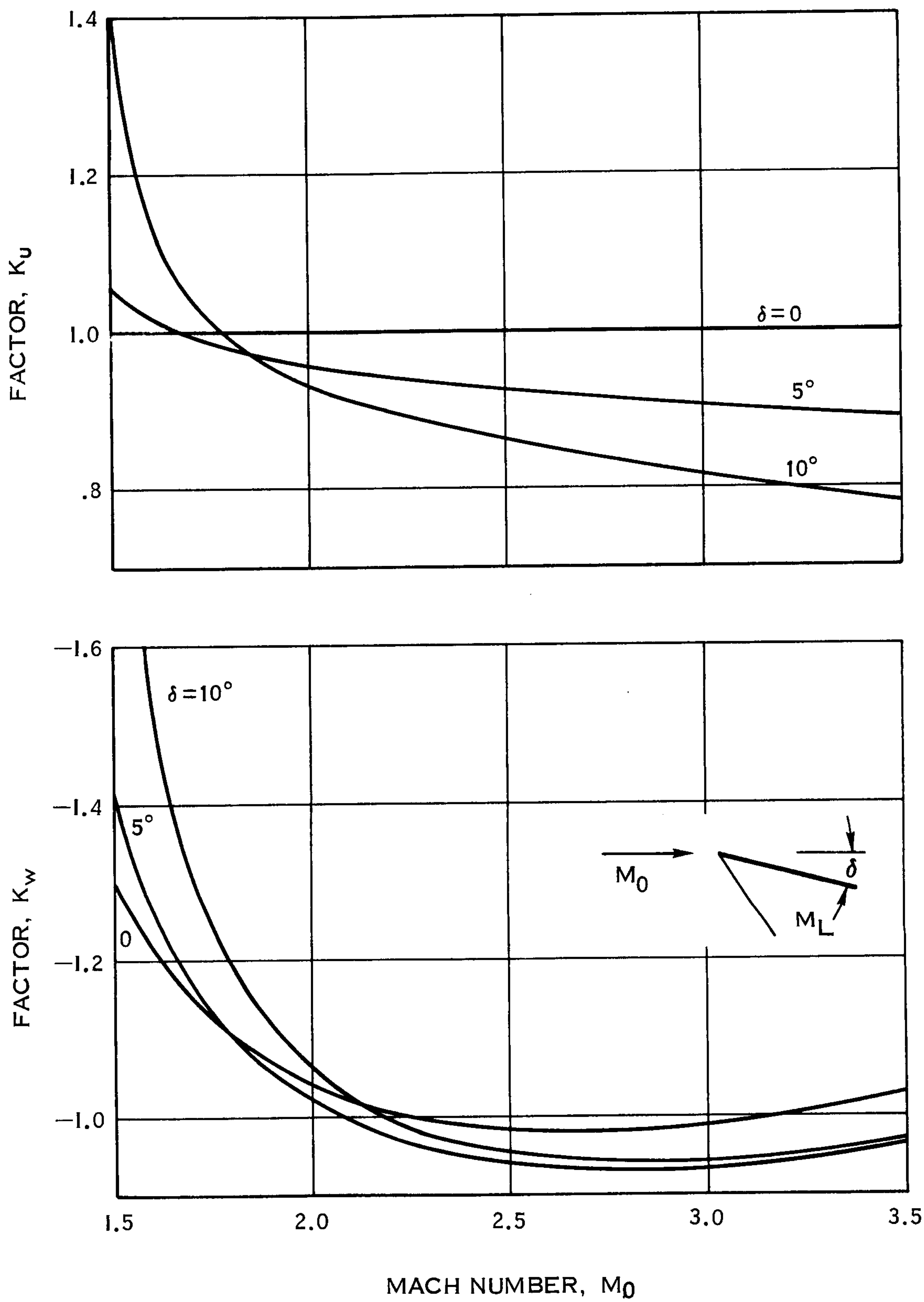

Figure 19. Factors K_u and K_w

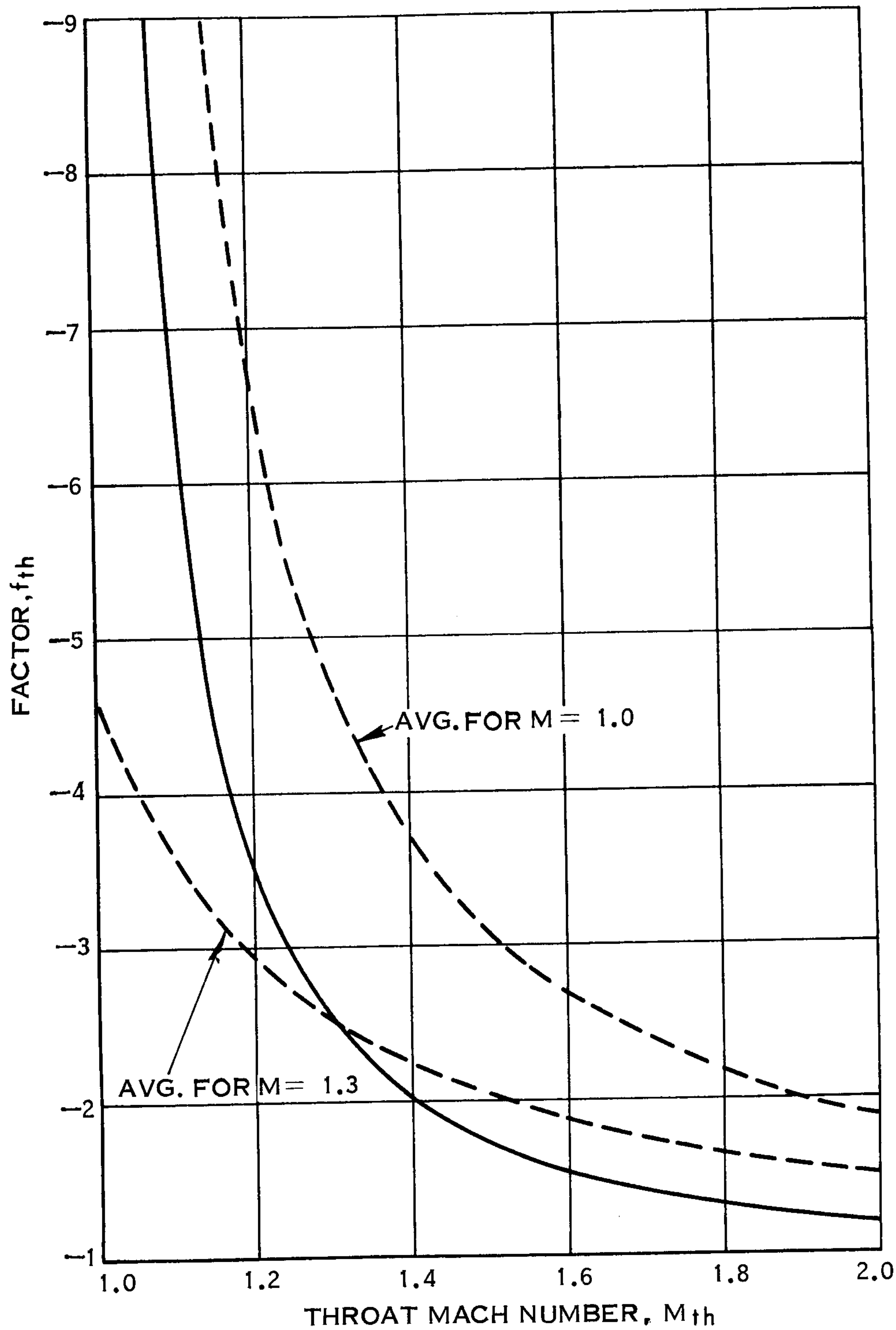

Figure 20. Factor f_{th} in Equation for ΔM_{th}

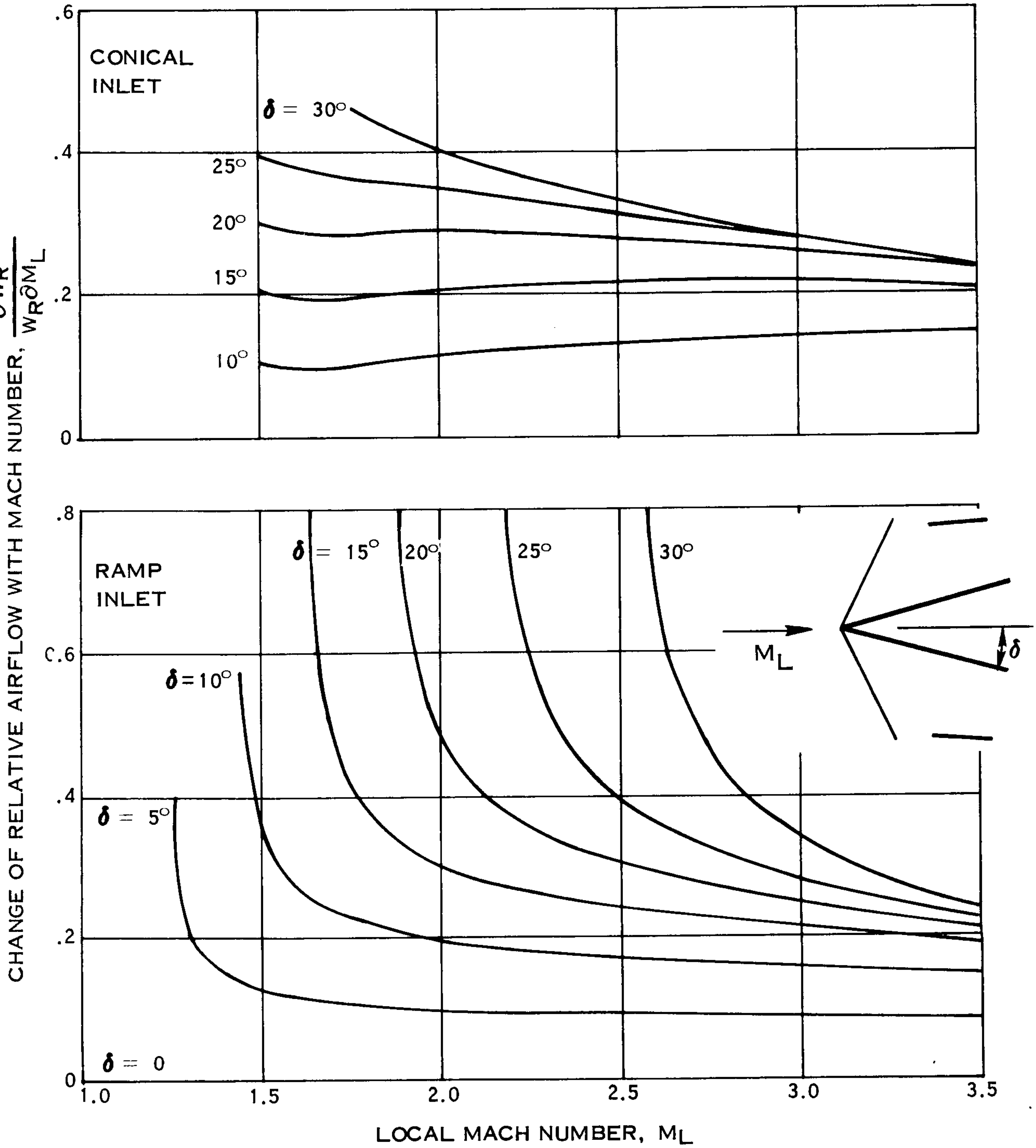

Figure 21. Change of Relative Airflow with Mach Number. Note, $\partial W_R / W_R \, \partial M_L = 0.0$ if initial shock intercepts lip, i.e., if $\theta_w < \theta_\ell$.

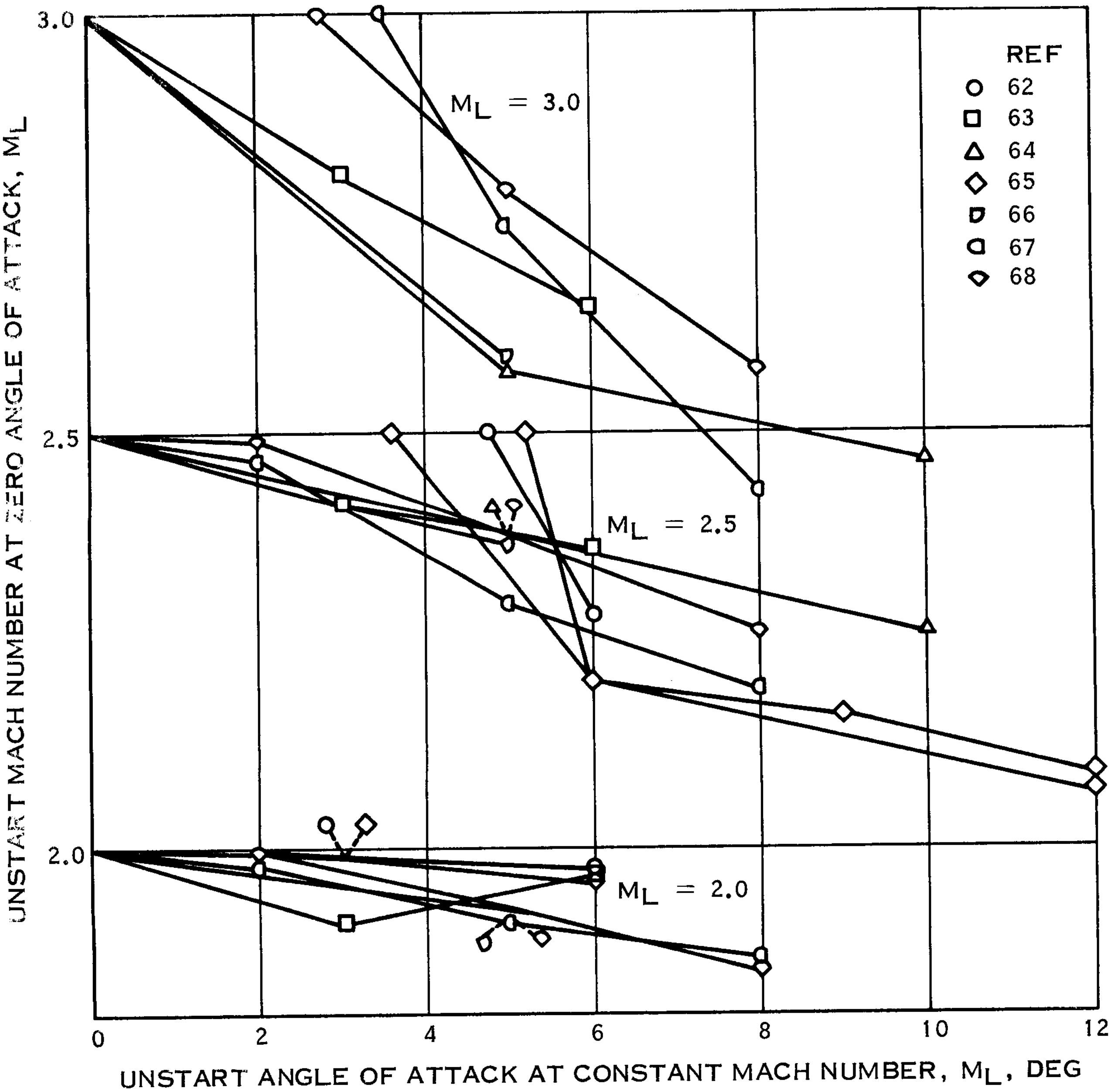

Figure 22. Effect of Inlet Angle of Attack on Inlet Unstart

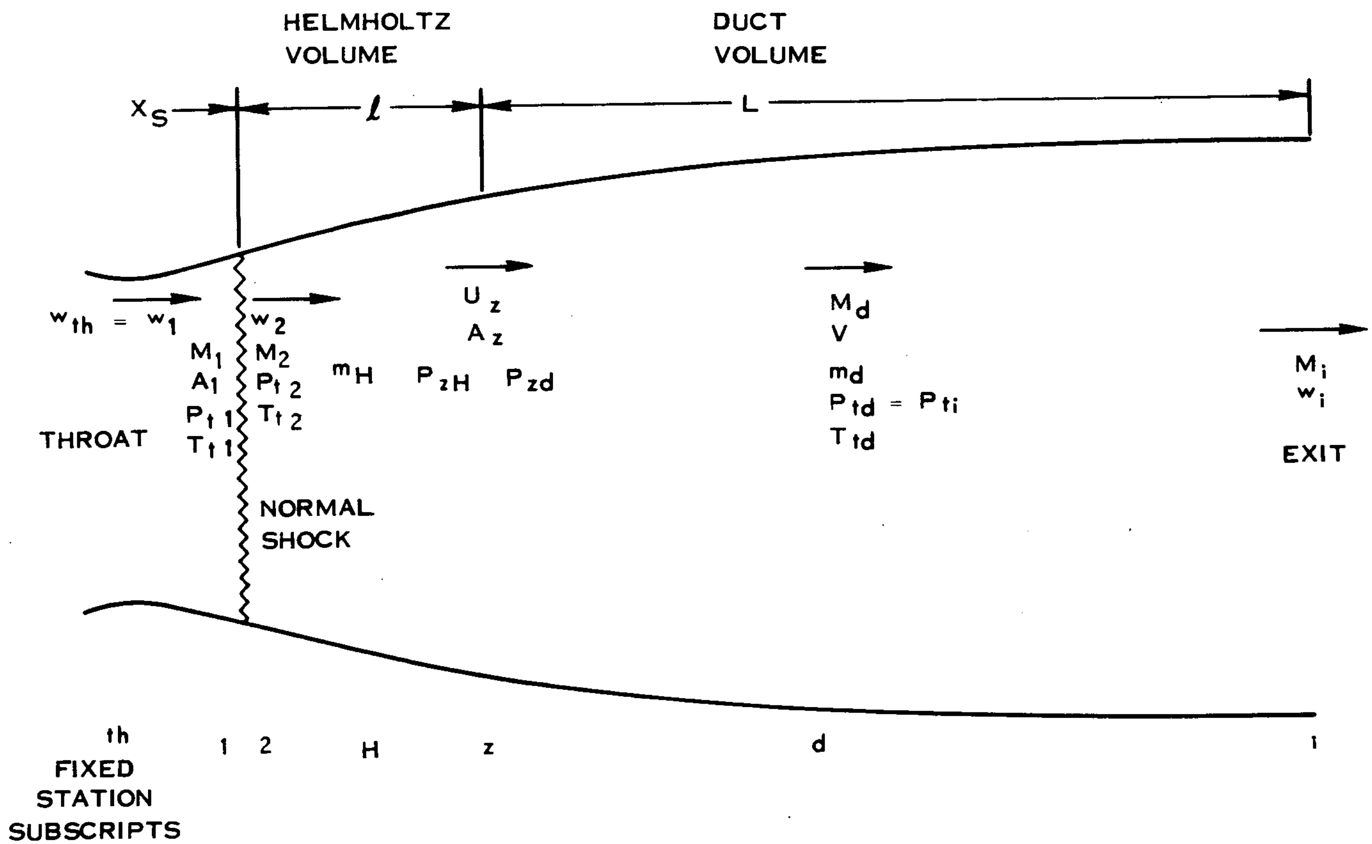

Figure 23. Sketch of Diffuser Illustrating Nomenclature for Analytical Model of Normal Shock Position

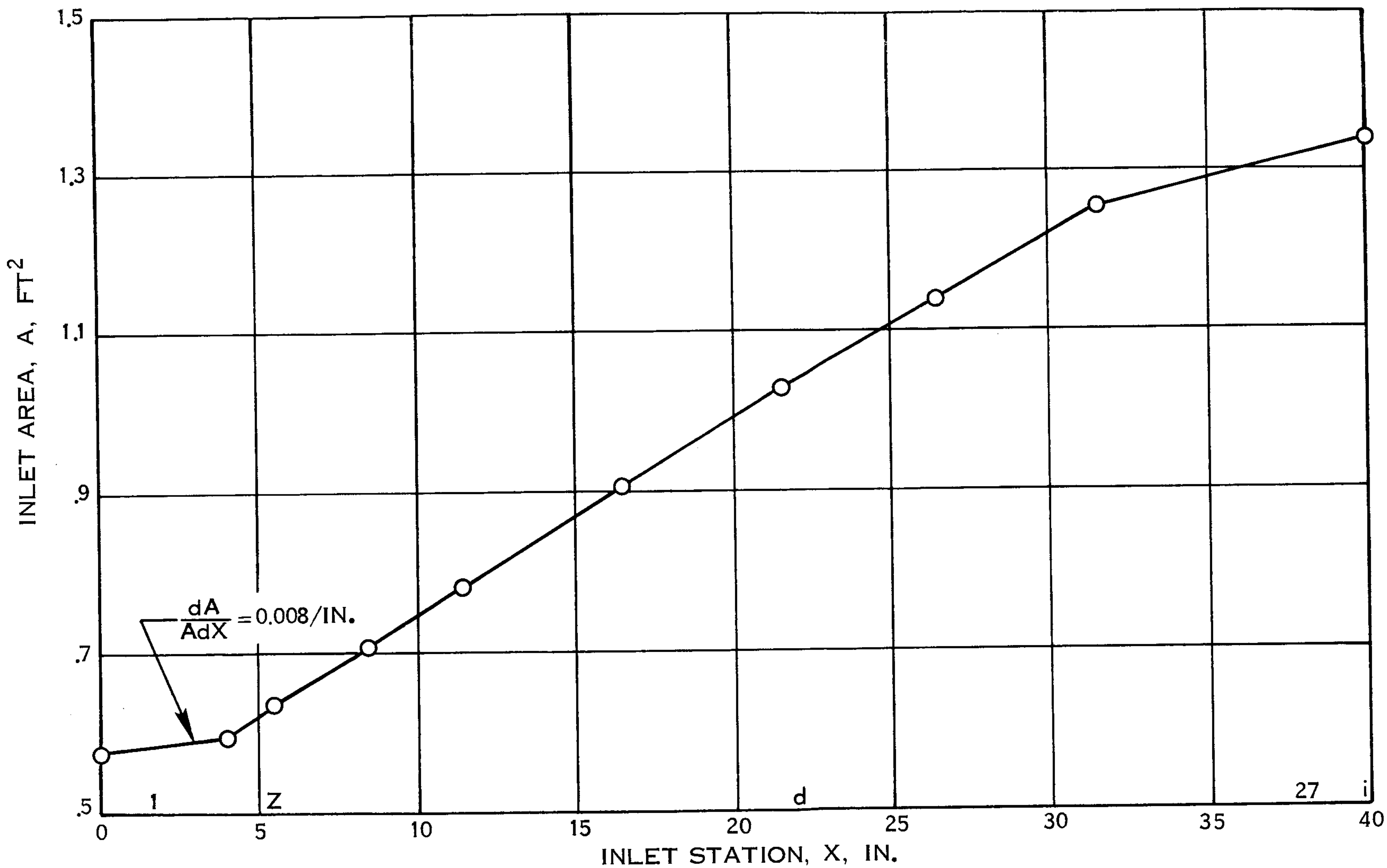

Figure 24. Representative Inlet Area Distribution

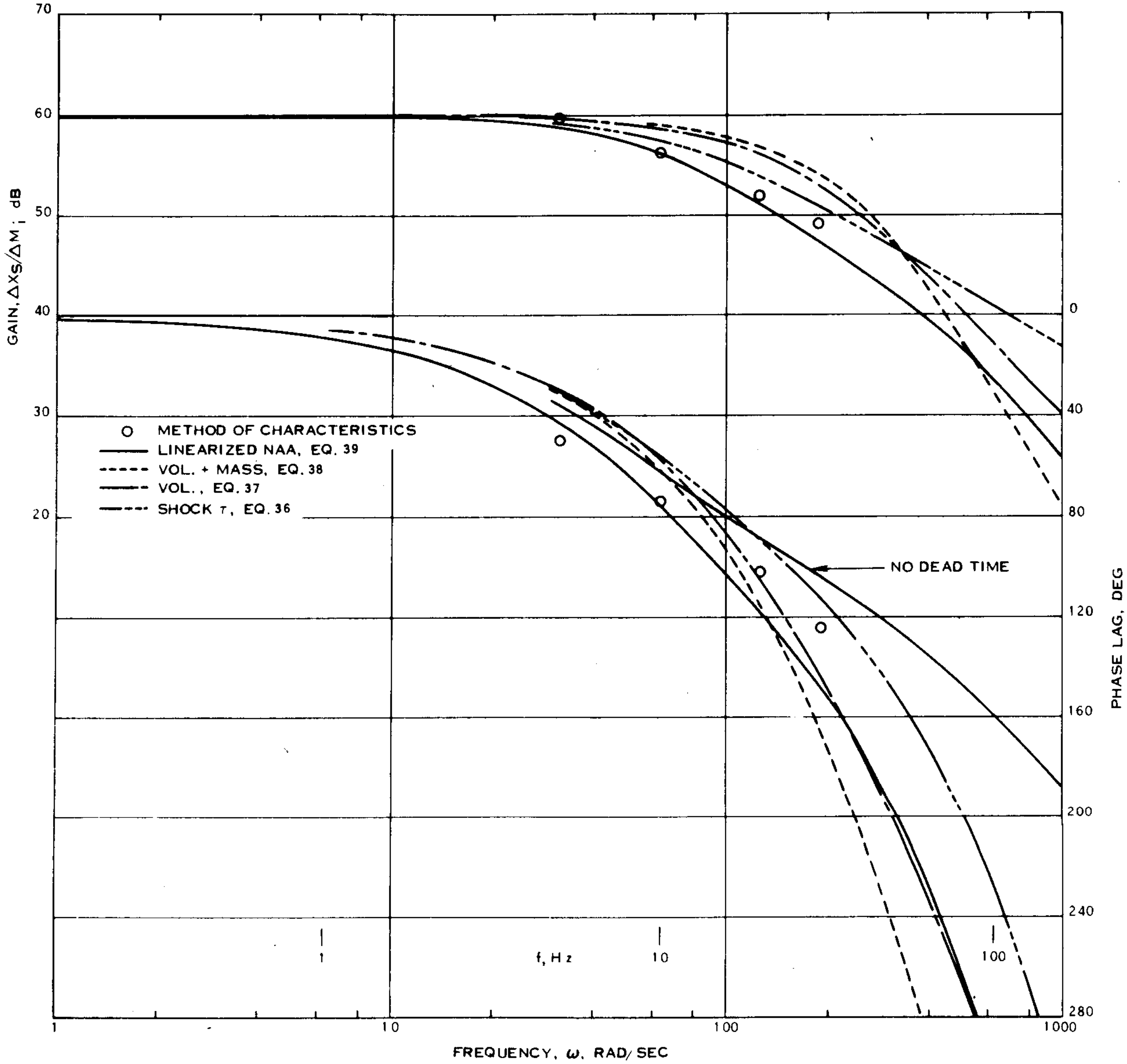

Figure 25. Frequency Response of Normal Shock to Diffuser Exit Mach Number

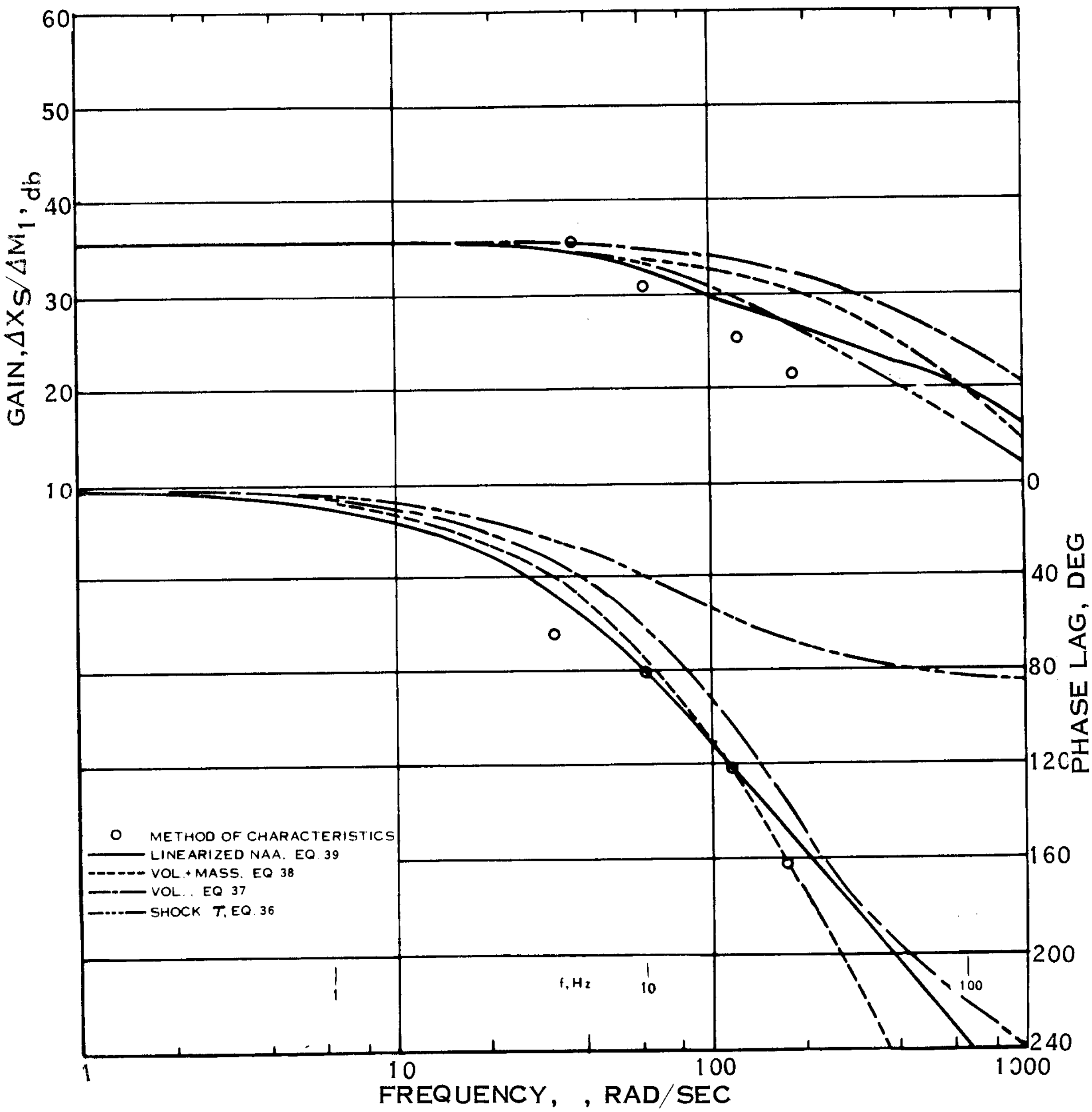

Figure 26. Frequency Response of Normal Shock to Mach Number Upstream of Shock

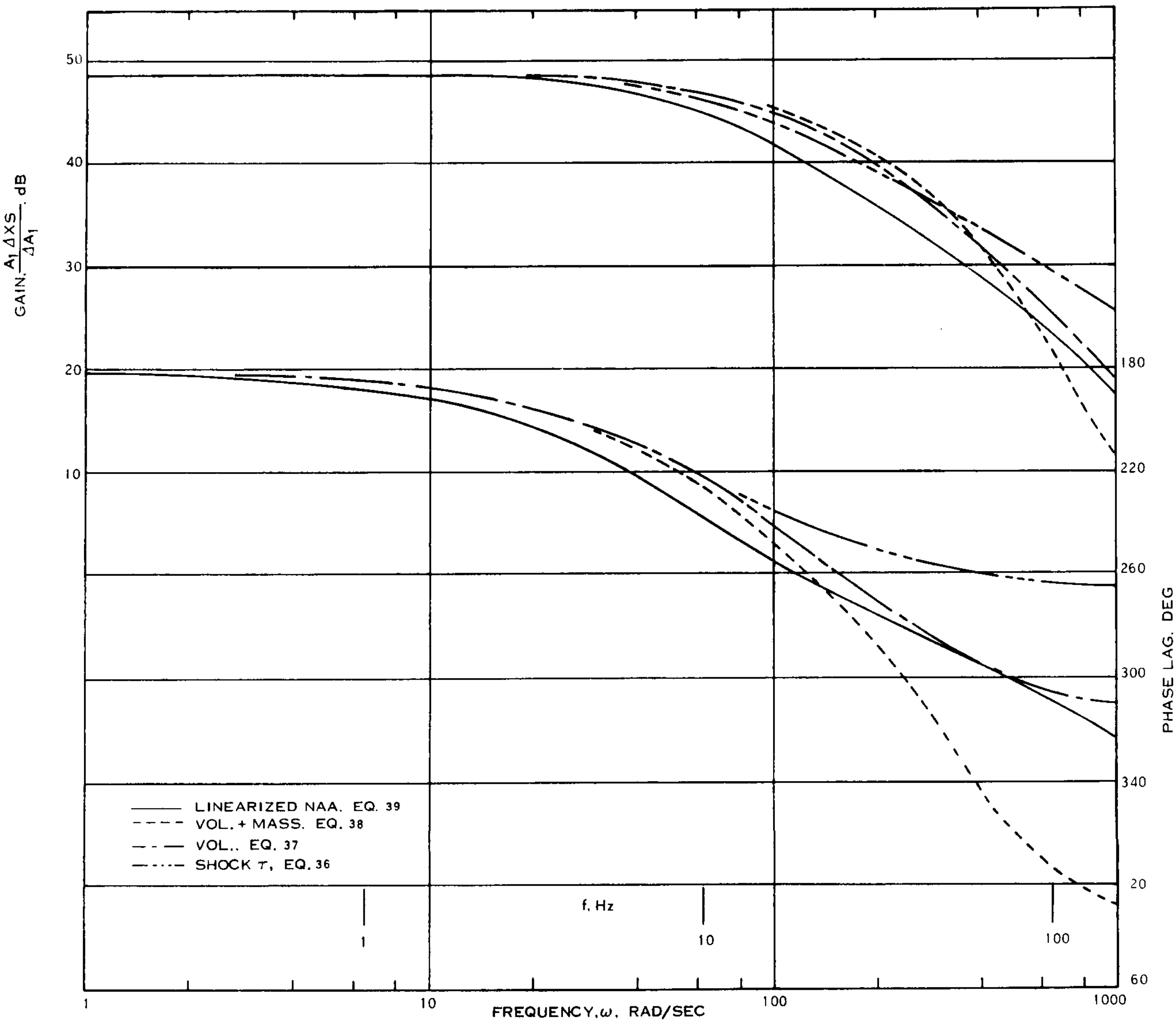

Figure 27. Frequency Response of Normal Shock to Area at Shock

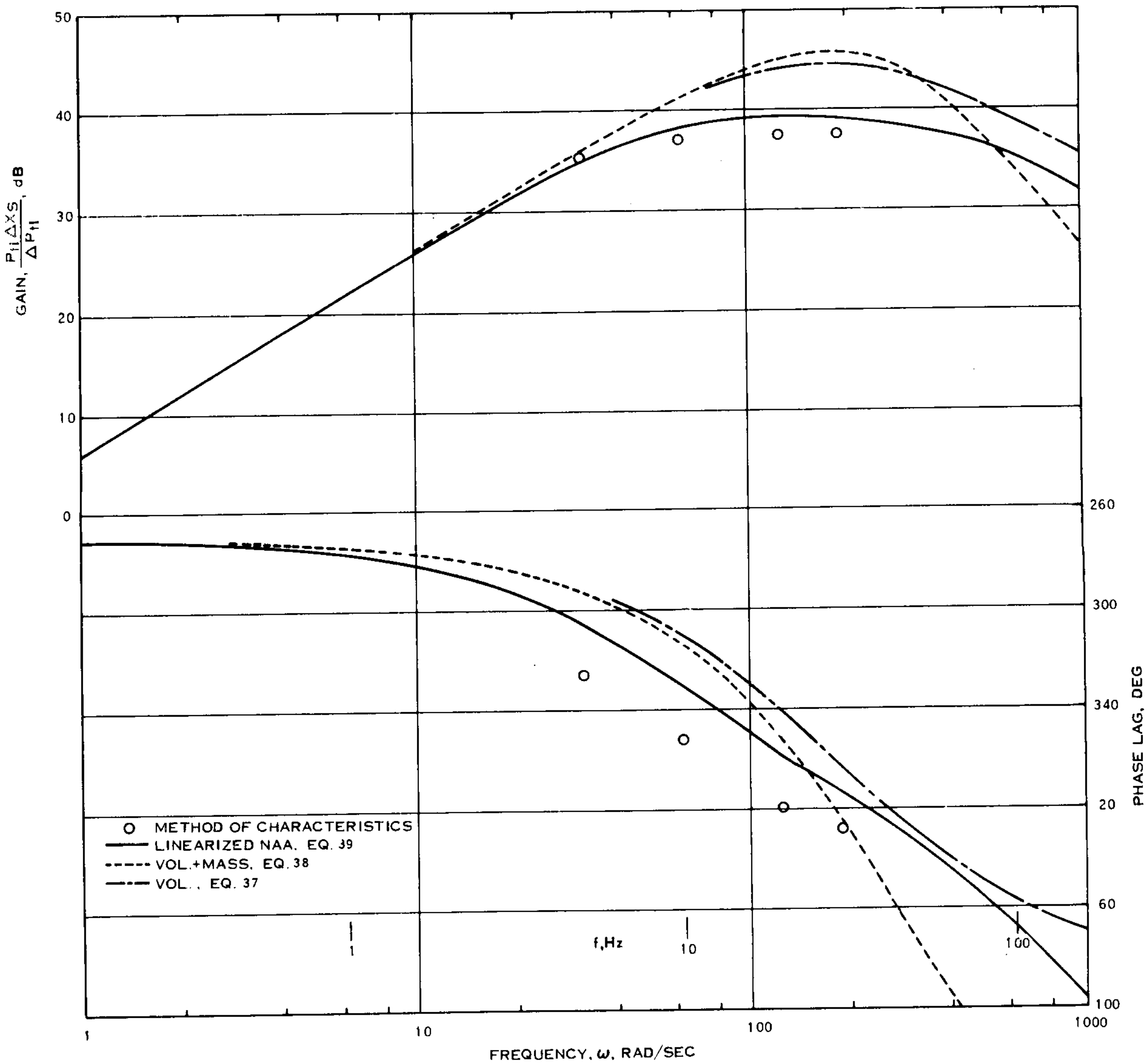

Figure 28. Frequency Response of Normal Shock to Upstream Total Pressure

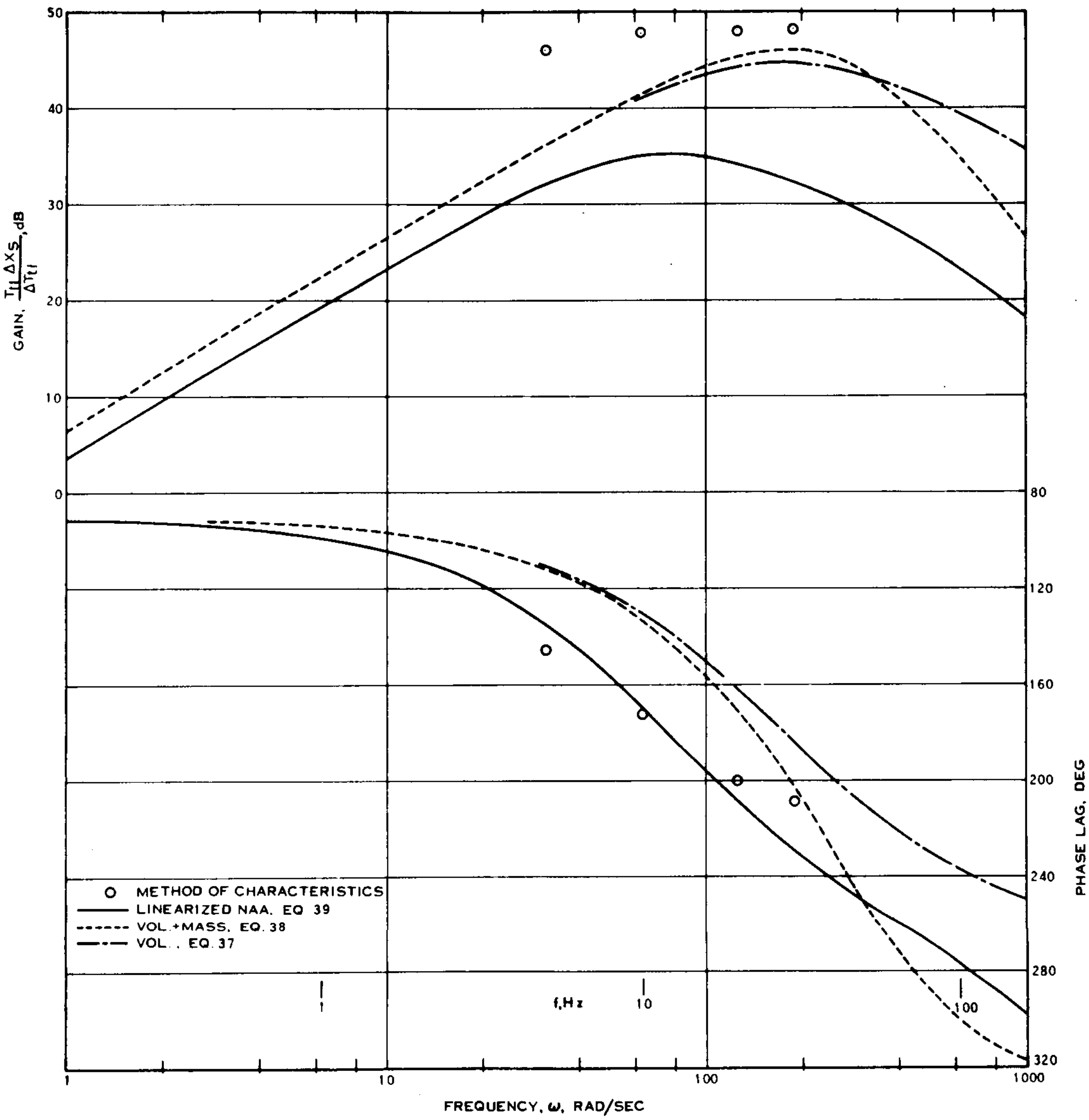

Figure 29. Frequency Response of Normal Shock to Upstream Total Temperature

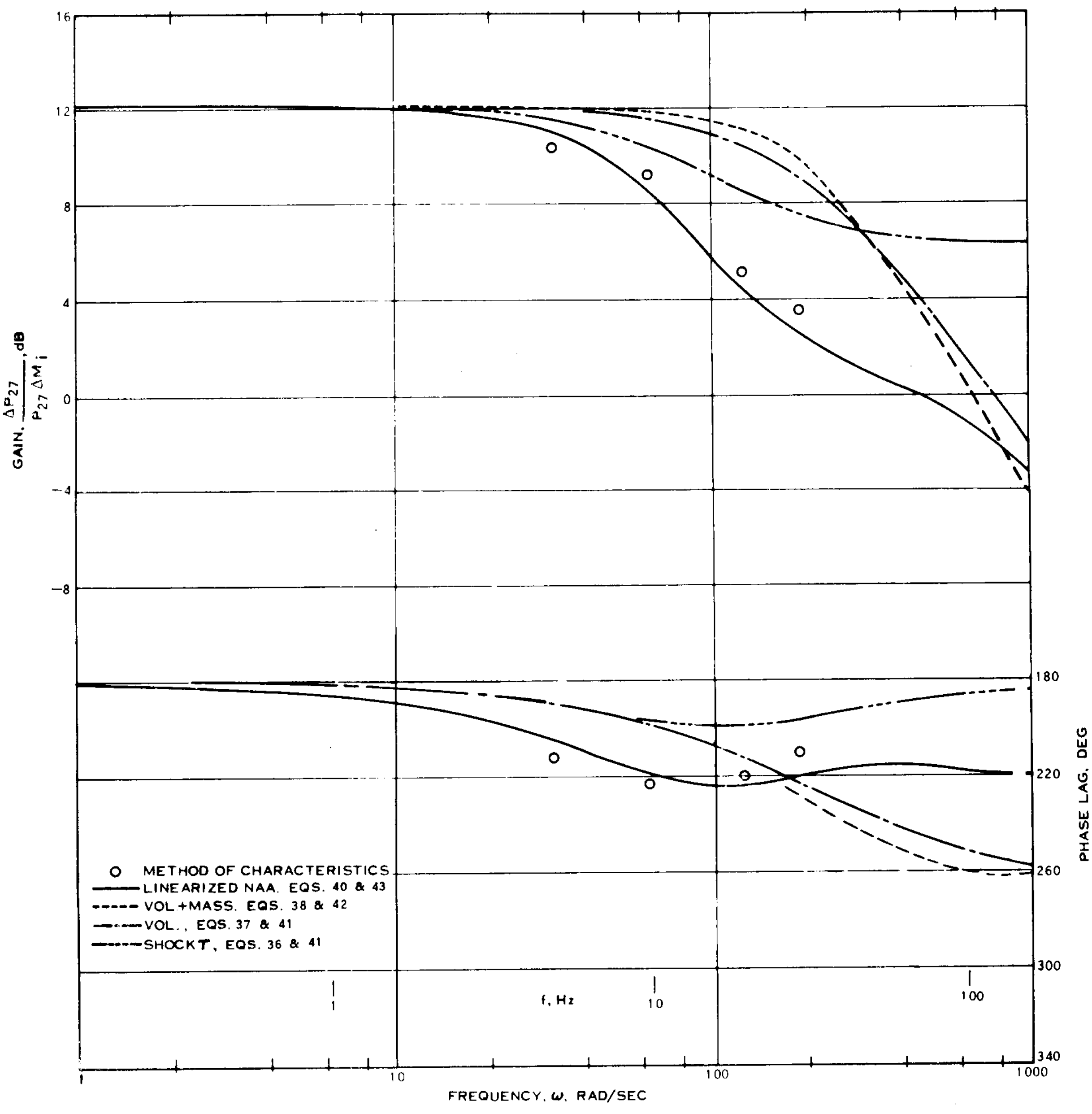

Figure 30. Frequency Response of Diffuser Exit Static Pressure to Diffuser Exit Mach Number

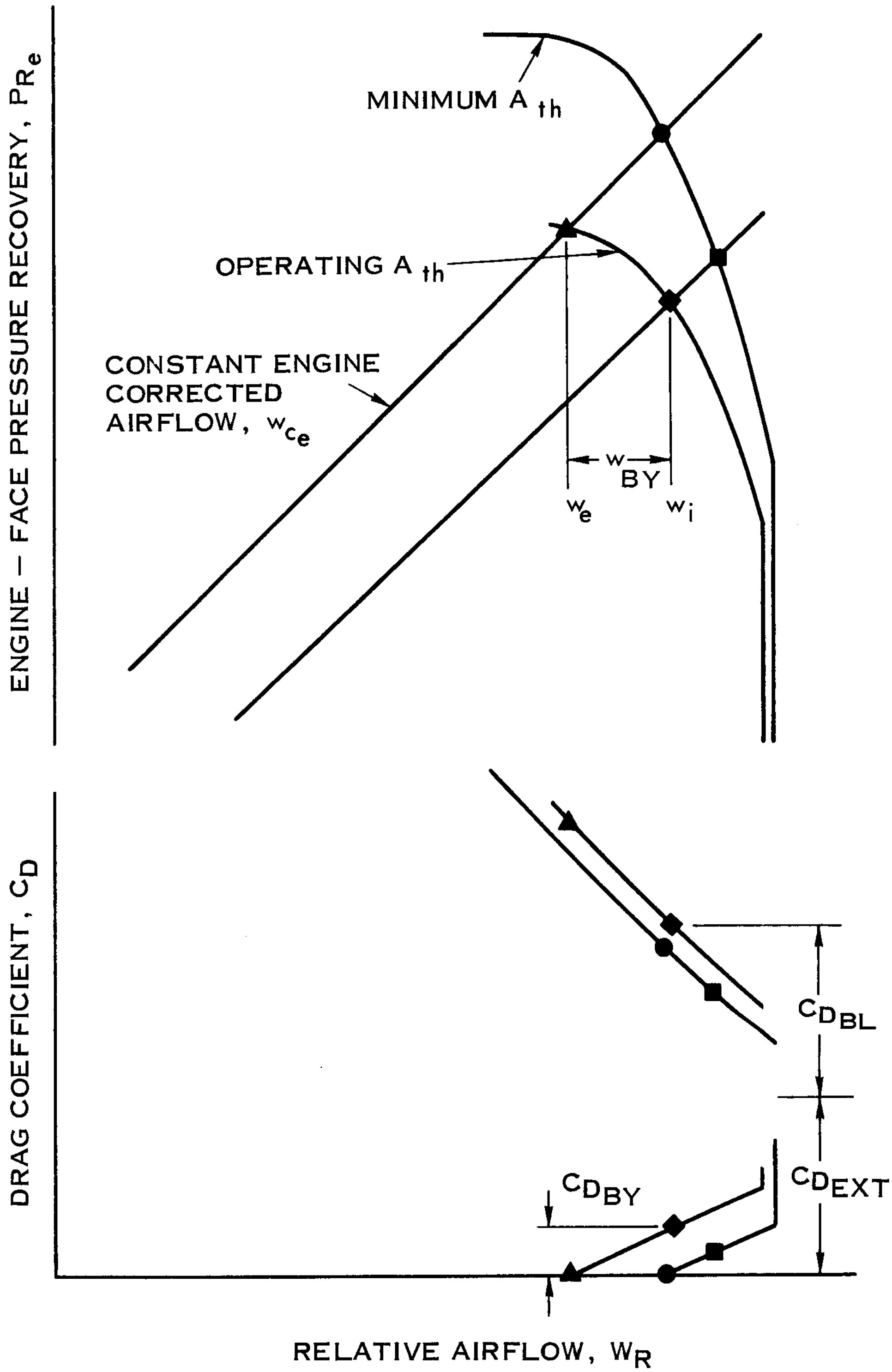

Figure 31. Inlet Performance Characteristics

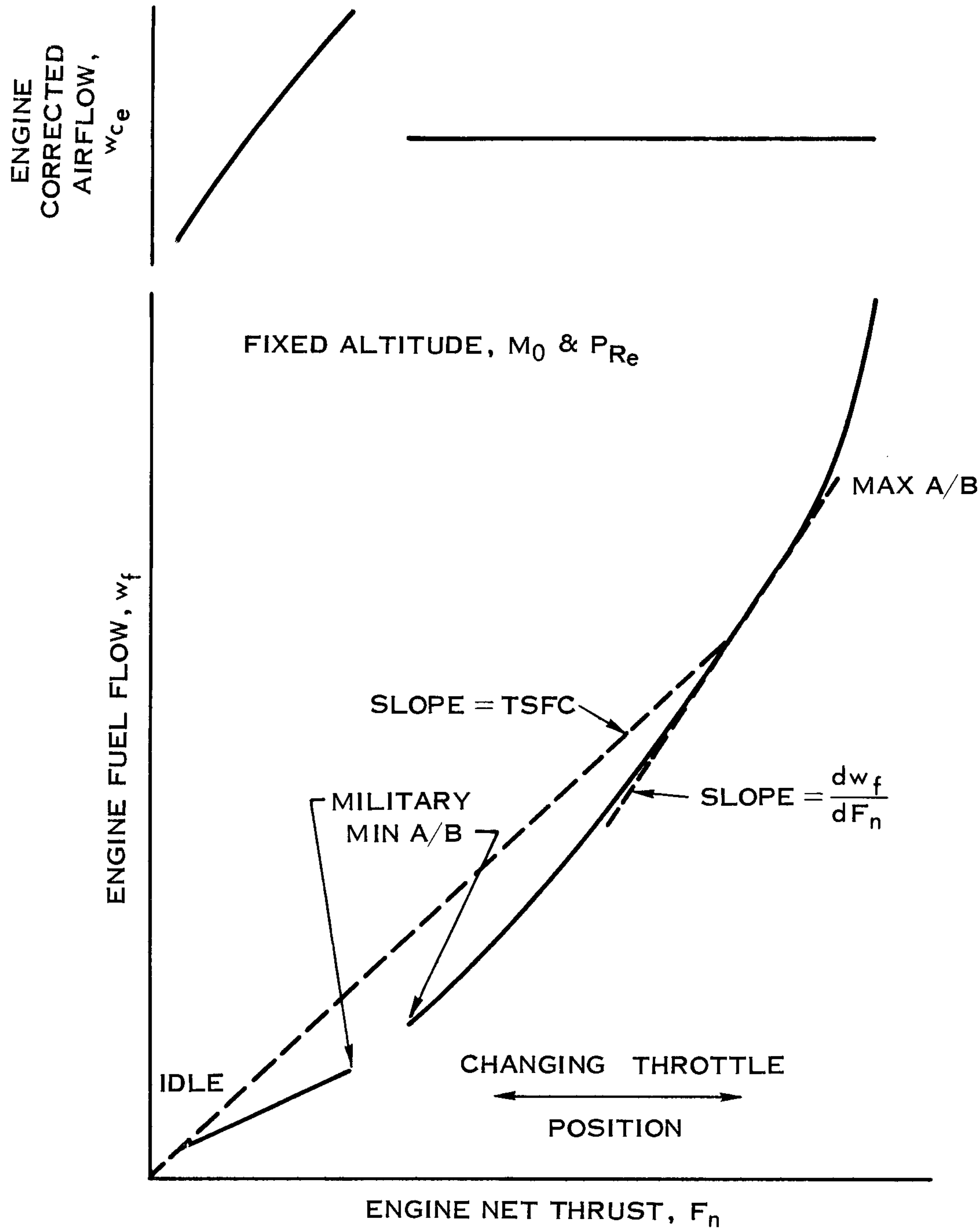

Figure 32. Engine Performance Characteristics

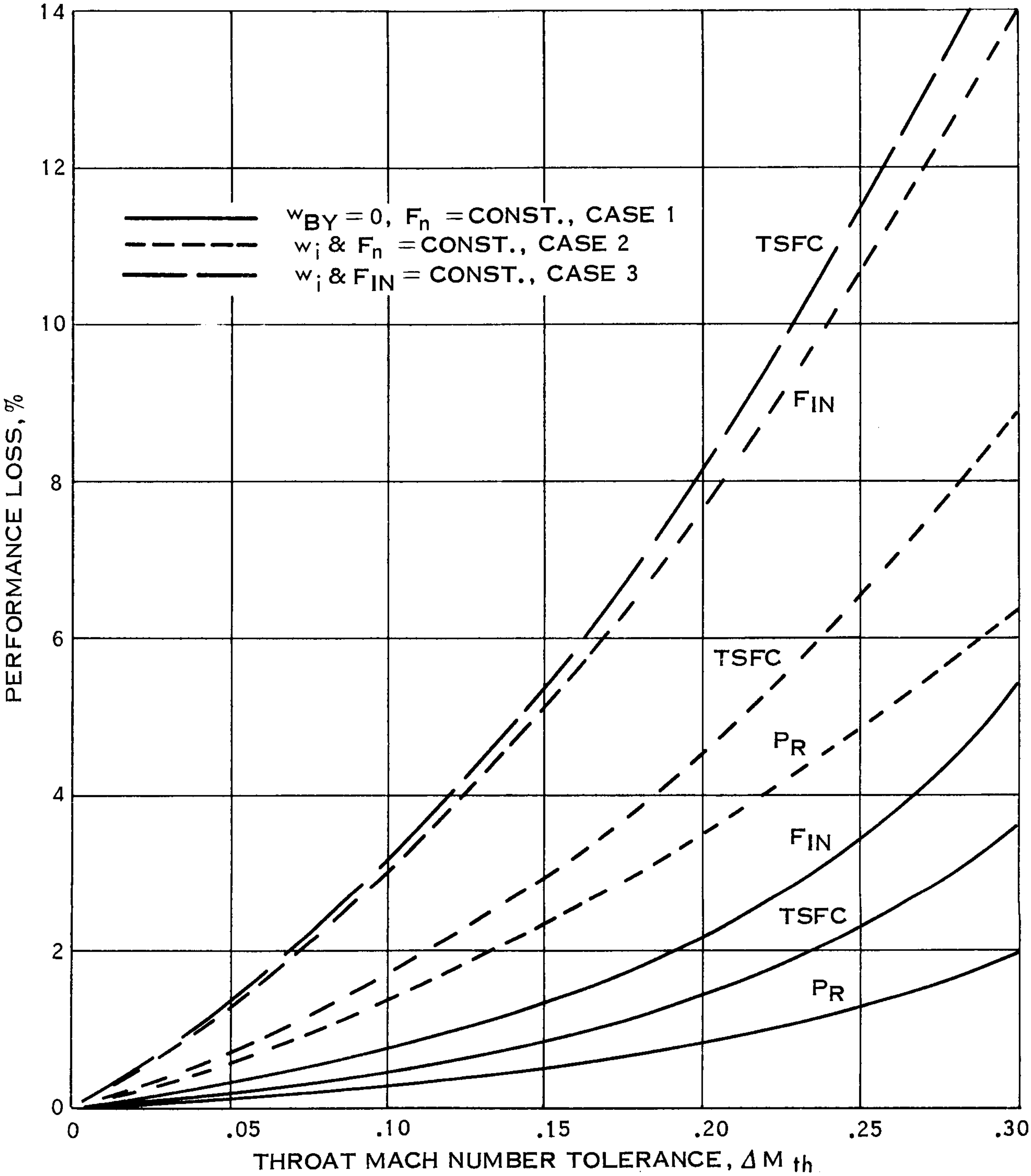

Figure 33. Performance Penalties Due to Throat Mach Number Tolerance

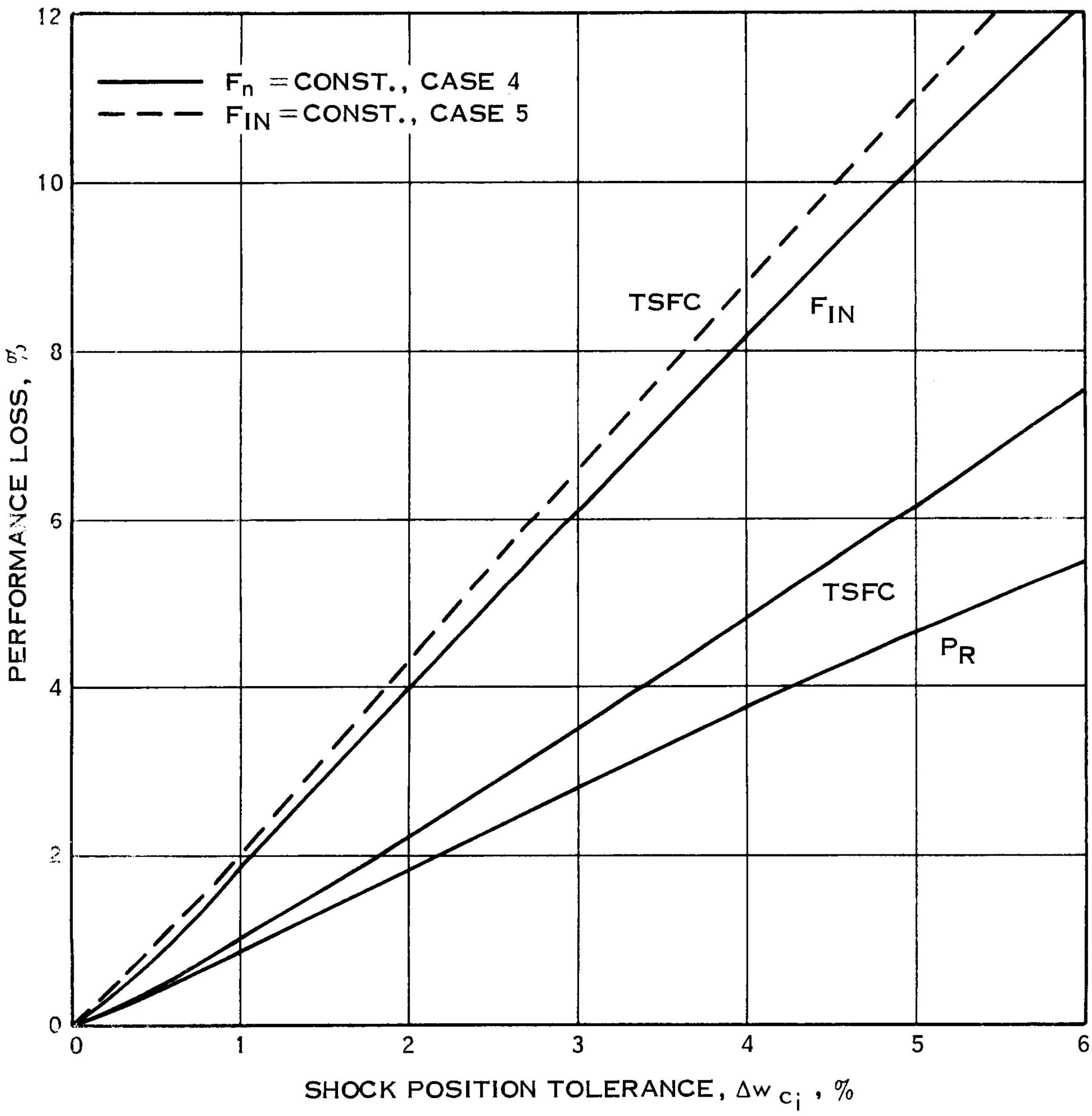

Figure 34. Performance Penalties Due to Shock Position Tolerance

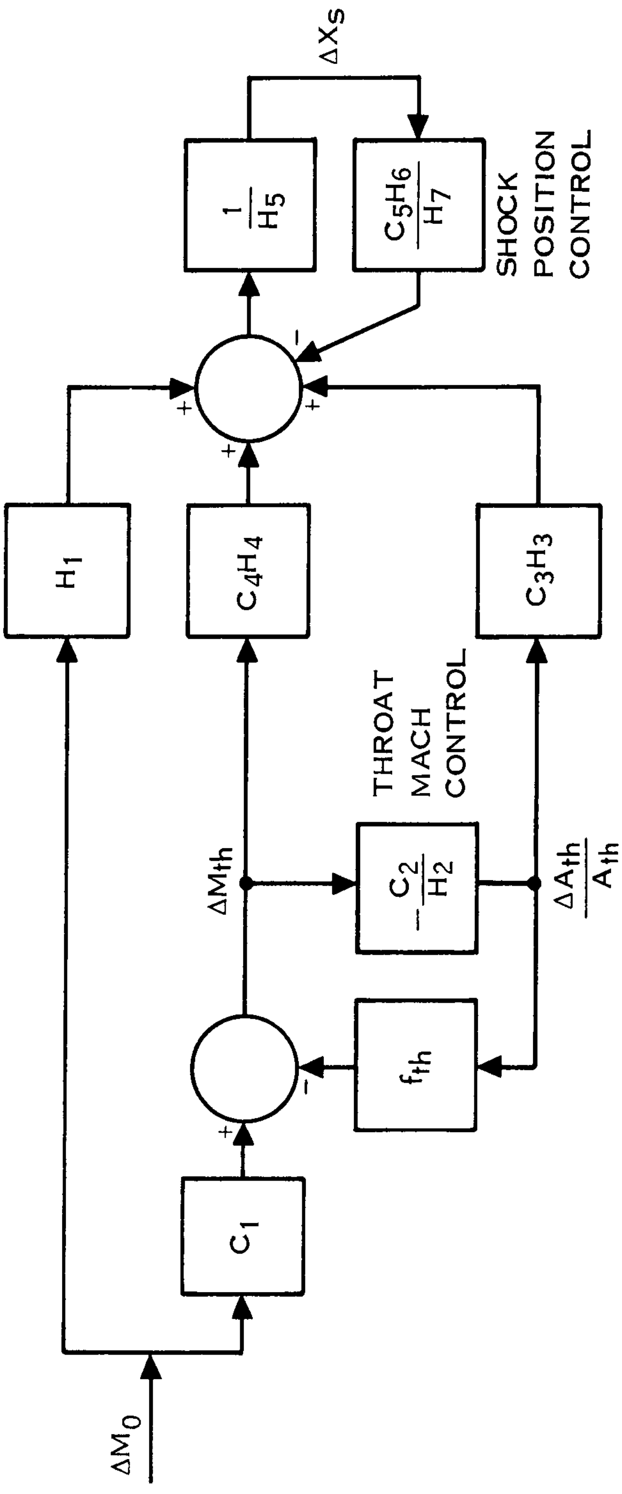

$$\Delta M_{th} = \frac{C_1 H_2}{-f_{th} C_2 + H_2} \Delta M_0$$

$$\Delta X_s = \frac{H_7 \left[H_1(-f_{th} C_2 + H_2) + C_1(C_4 H_2 H_4 - C_2 C_3 H_3) \right]}{(-f_{th} C_2 + H_2)(C_5 H_6 + H_5 H_7)} \Delta M_0$$

Figure 35. Block Diagram of Inlet and Control

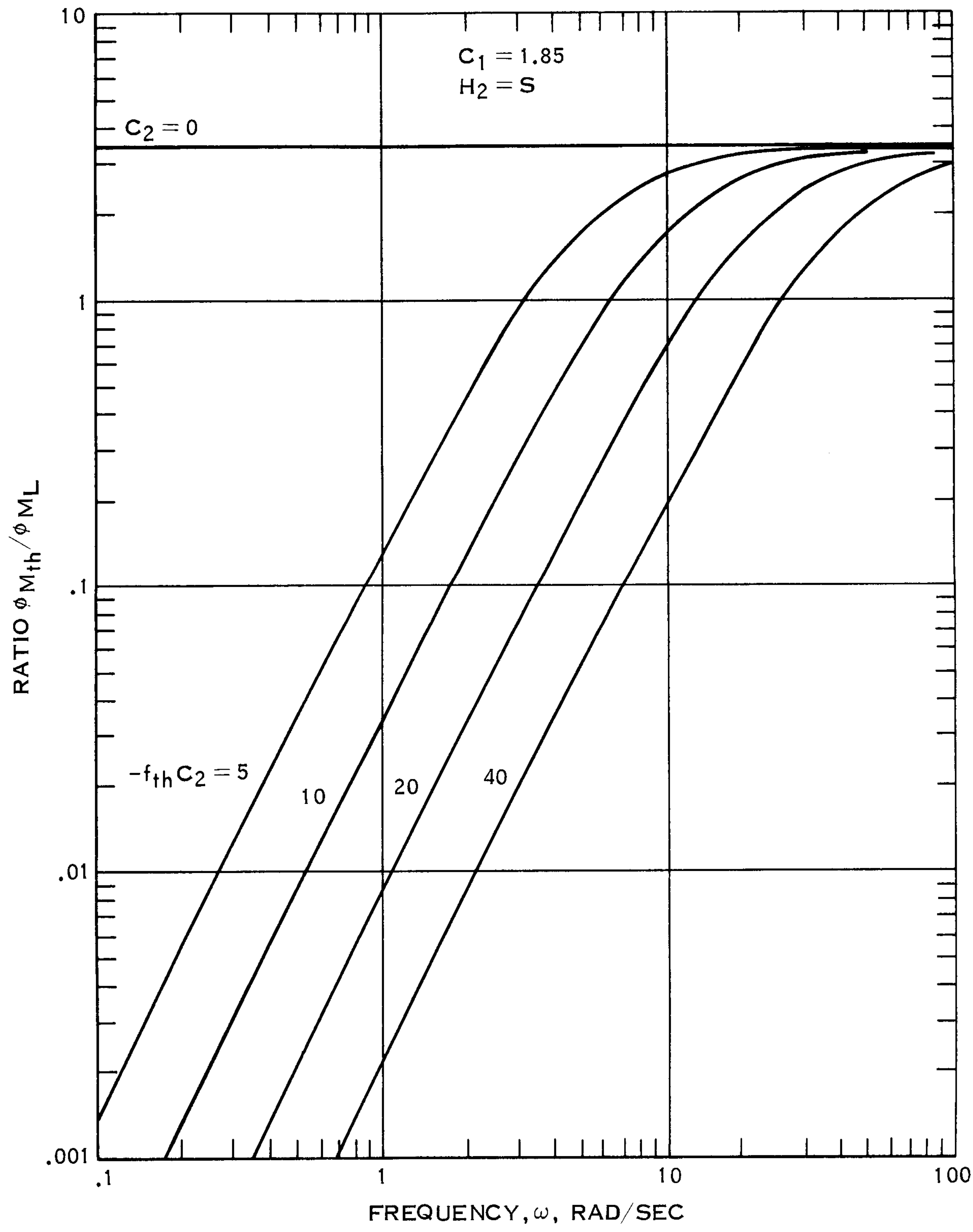

Figure 36. Ratio $\phi_{M_{th}}/\phi_{M_L}$ for Single Integral Throat Mach Control

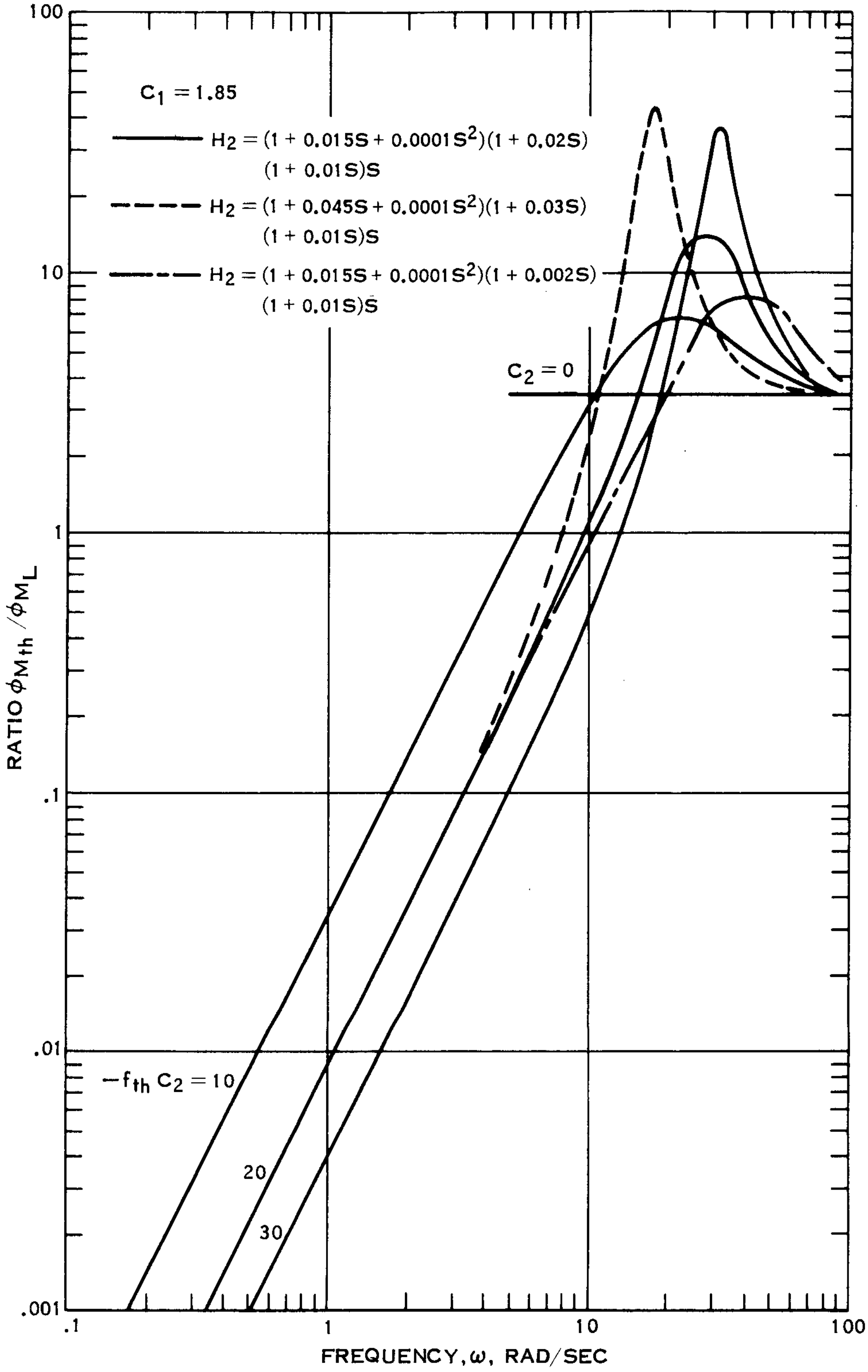

Figure 37. Ratio $\phi M_{th}/\phi M_L$ for Throat Mach Control

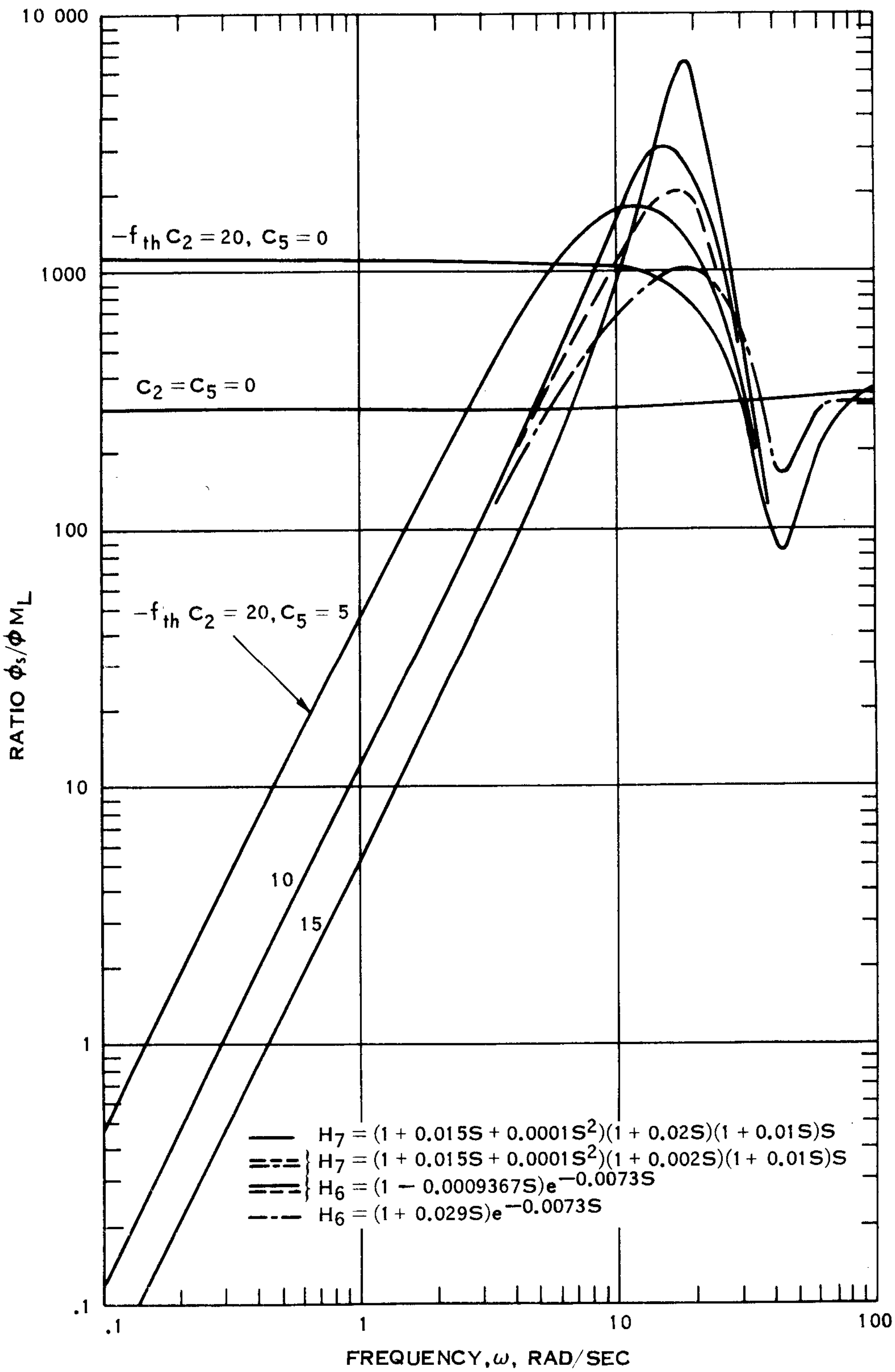

Figure 38. Ratio ϕ_s/ϕ_{M_L} for Shock Position

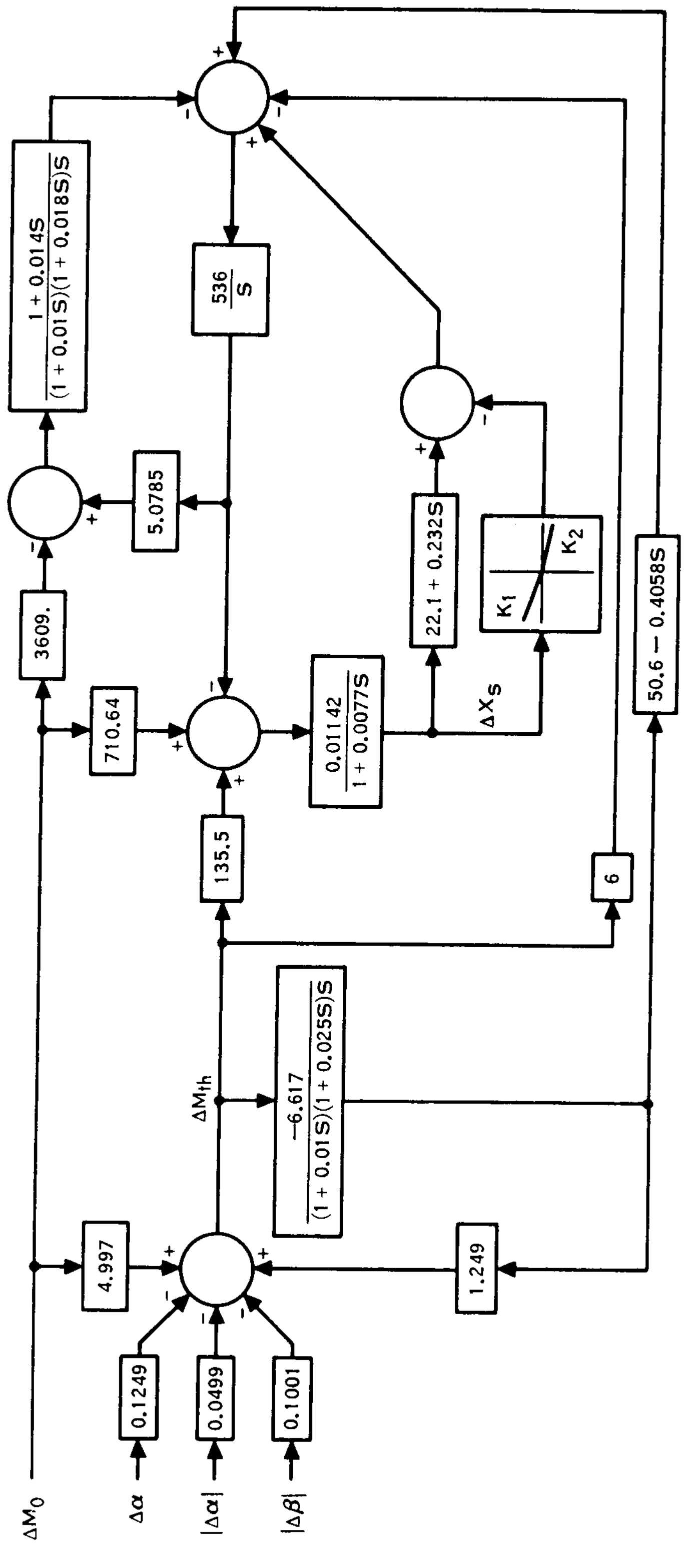

Figure 39. Block Diagram of Representative Inlet for $M_0 = 2.7$ at 60 000 ft Altitude

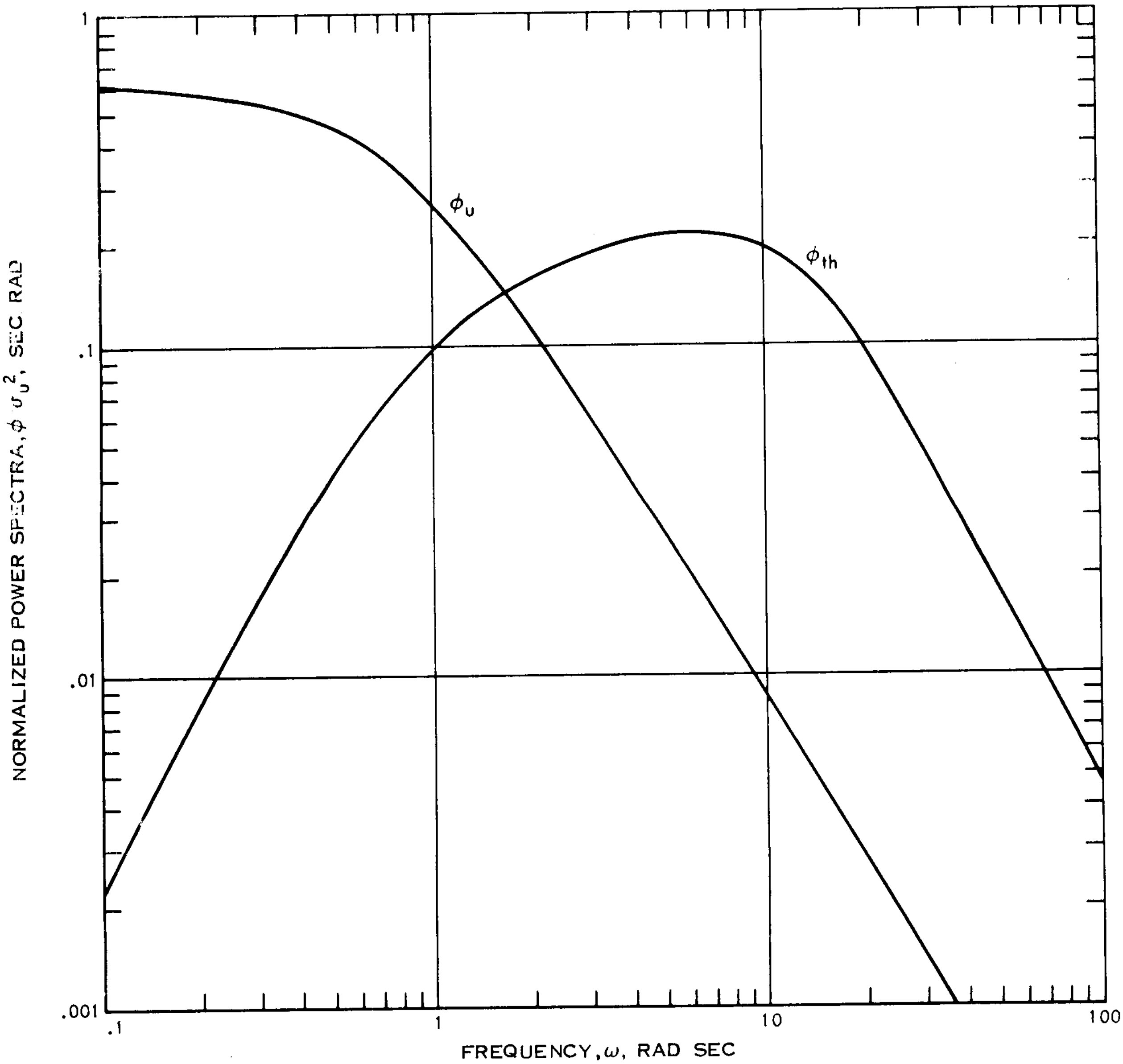

Figure 12 Normalized Power Spectra of Free-Stream Longitudinal Turbulence and of Throat Mach Number Change Due to Longitudinal Turbulence

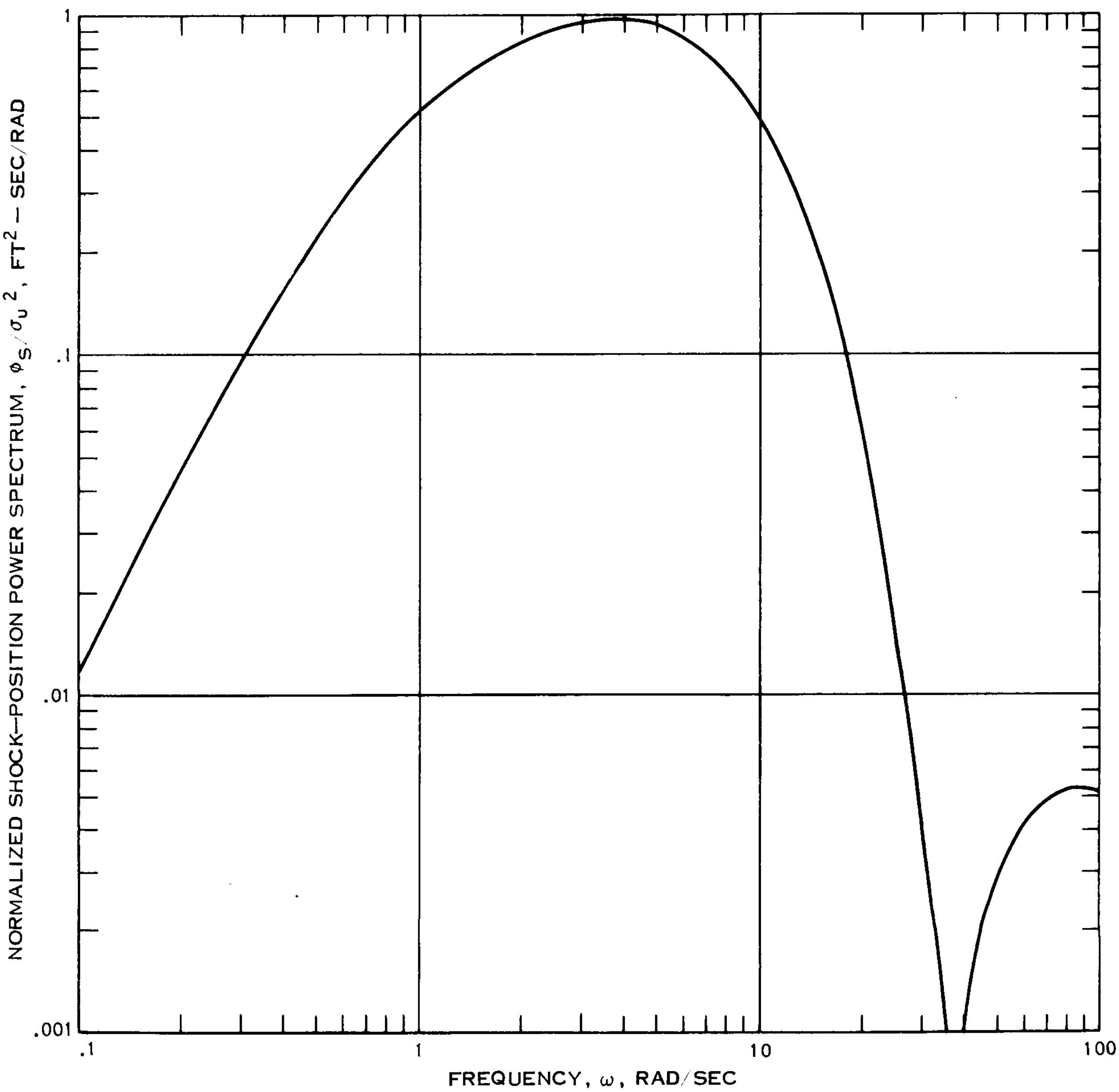

Figure 41. Normalized Shock-Position Power Spectrum Due to Longitudinal Turbulence

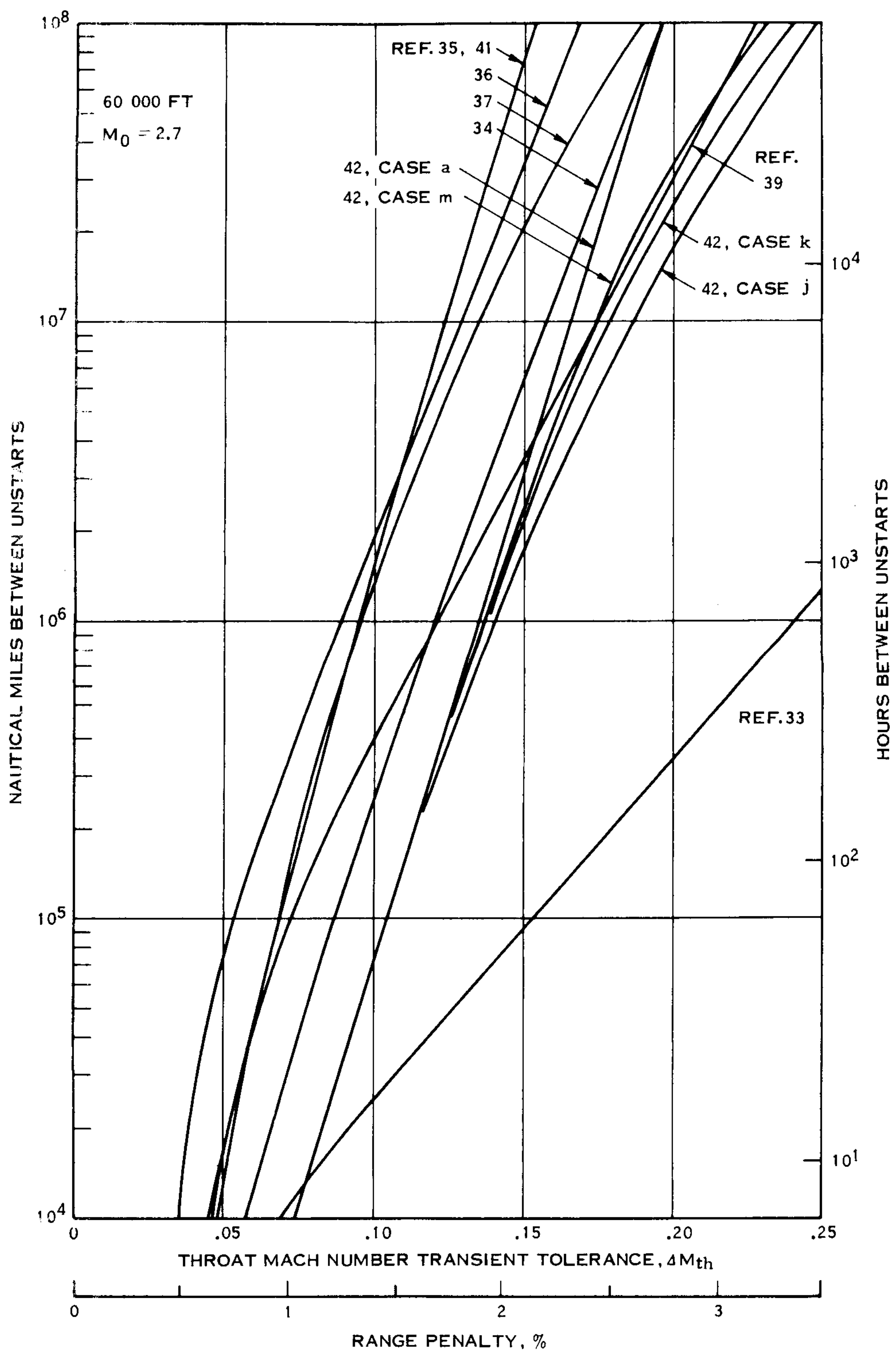

Figure 42. Effect of Throat Mach Number Transient Tolerance on Frequency of Inlet Unstarts Due to Longitudinal Turbulence

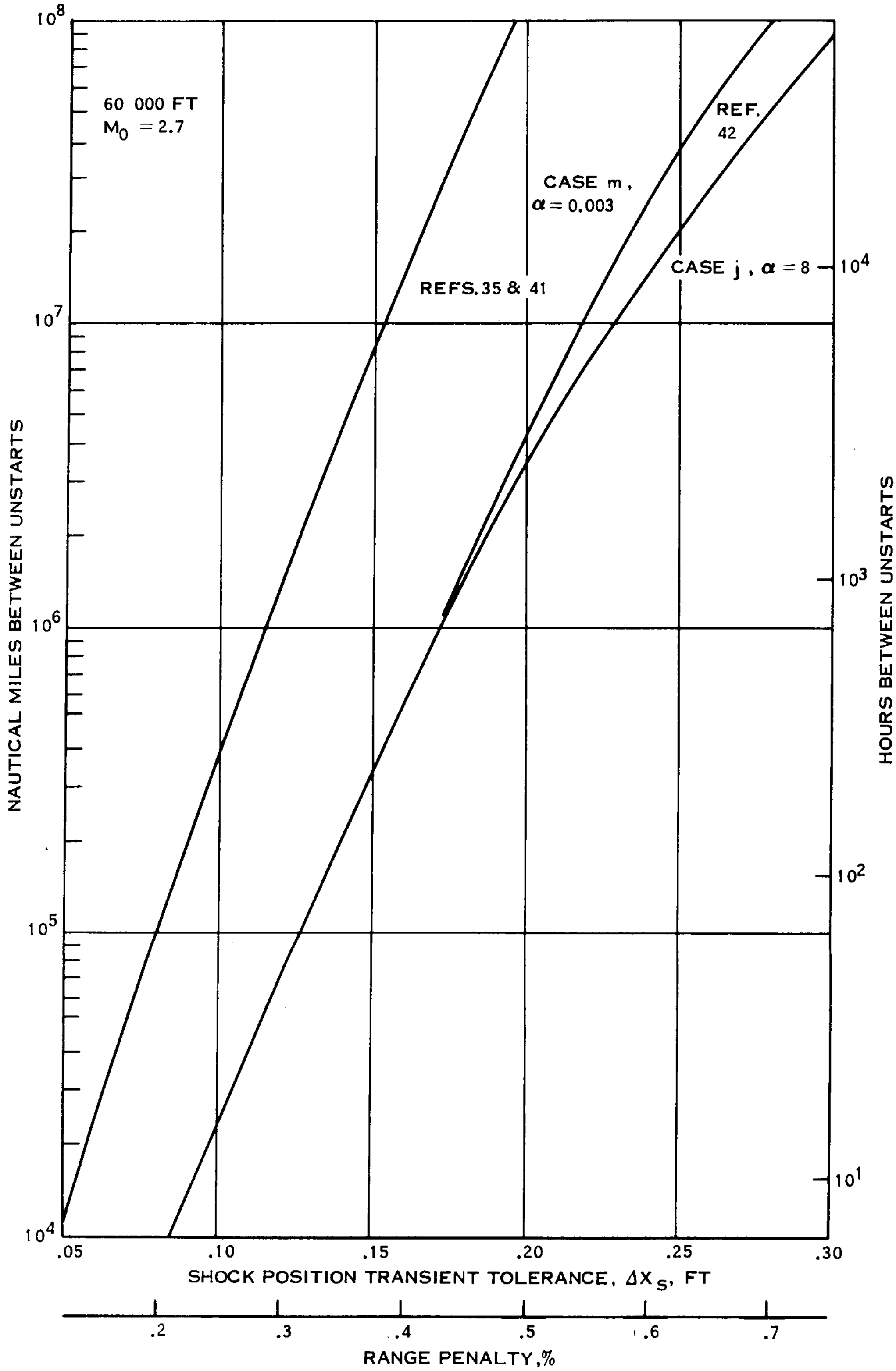

Figure 43. Effect of Shock Position Transient Tolerance on Frequency of Inlet Unstarts Due to Longitudinal Turbulence

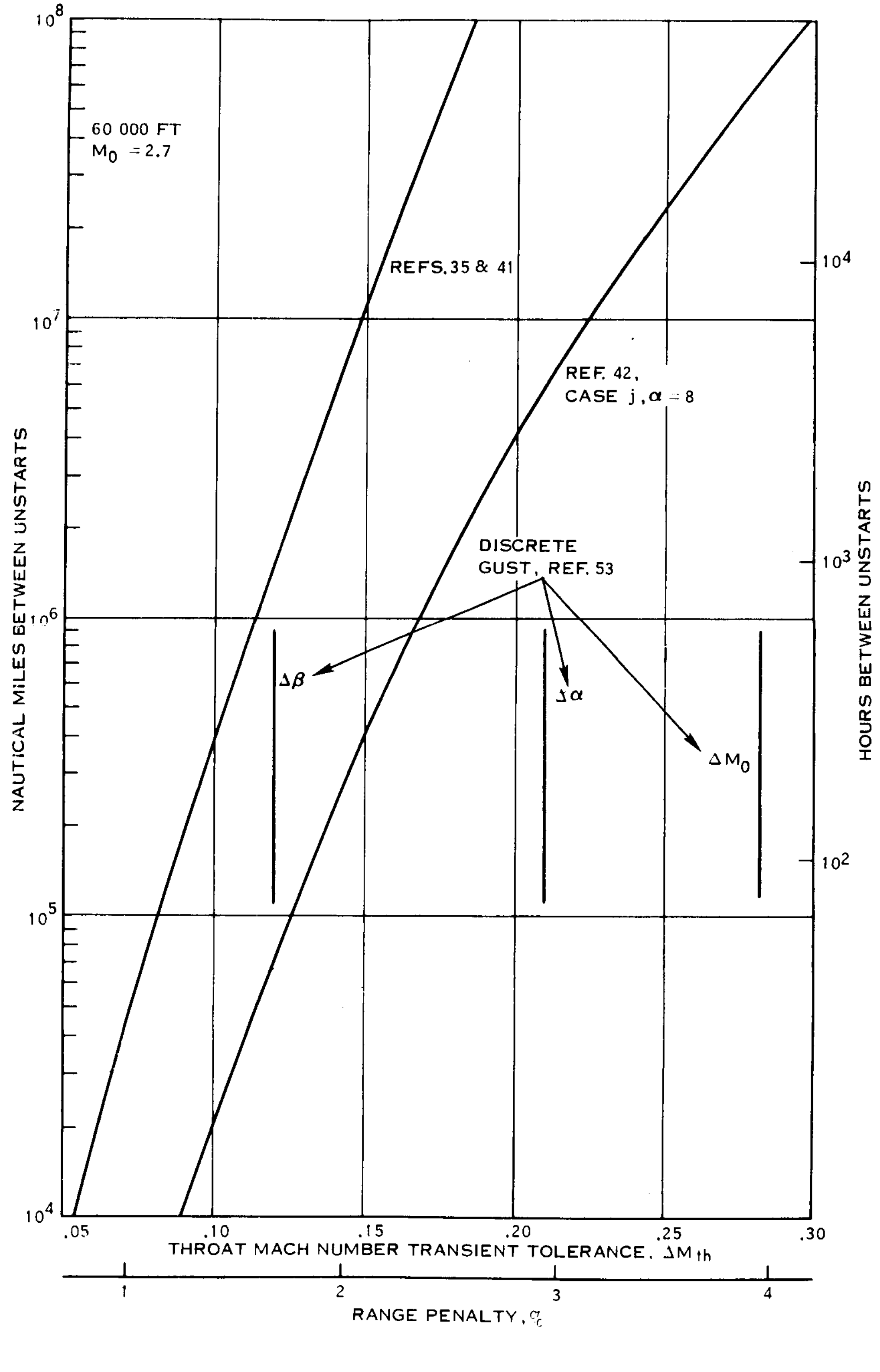

Figure 44. Effect of Throat Mach Number Transient Tolerance on Frequency of Inlet Unstarts

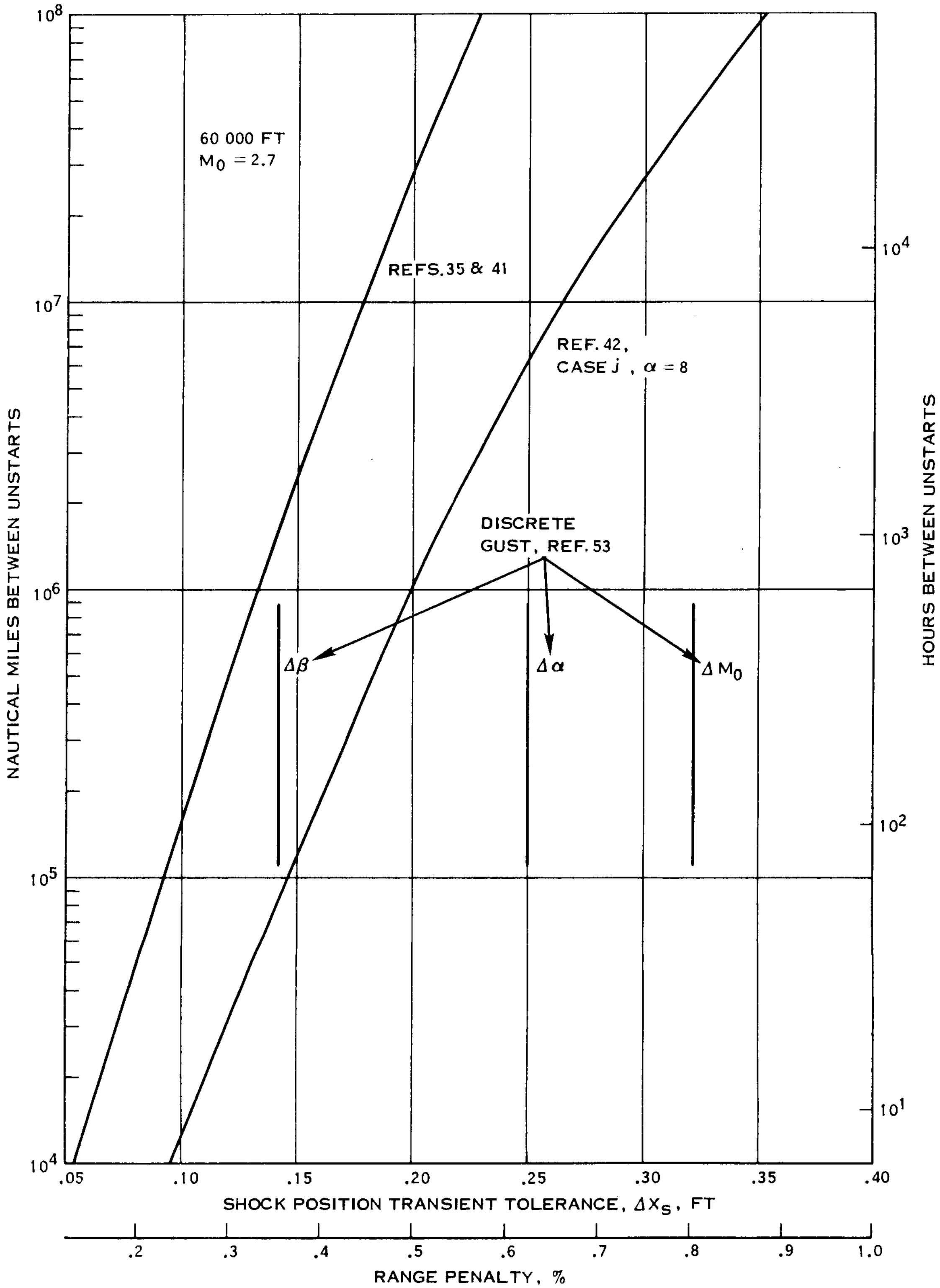

Figure 45. Effect of Shock Position Transient Tolerance on Frequency of Inlet Unstarts

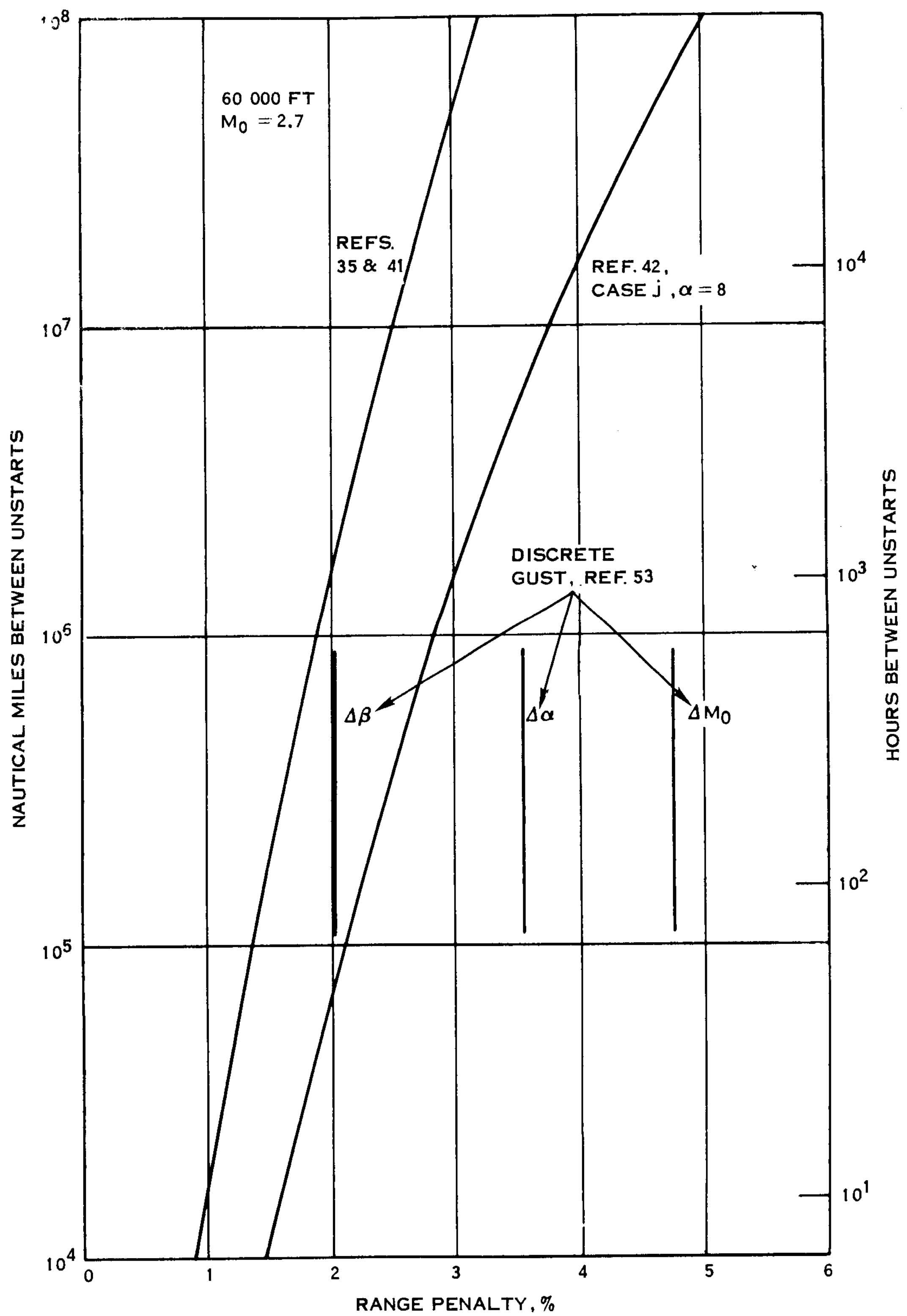

Figure 46. Effect of Combined Transient Range Penalty on Frequency of Inlet Unstarts

```
'P      AED MAIN
        BEGIN
COMMENT
  THIS PROGRAM WAS WRITTEN BY UNITED AIRCRAFT RESEARCH LABORATORIES FOR
  HAMILTON STANDARD, UNDER CONTRACT NAS2-4515 TASK 4, IN THE AED-0
  PROGRAMMING LANGUAGE.

$,
COMMENT
  THE MAIN PROGRAM CALLS THE VARIOUS SUBROUTINES, AND ESTIMATES THE FREE
      STORAGE USED BY THE FINAL ANSWER. IT ALSO PRINTS THE TIME TAKEN BY
      THE PROBLEM.
$,
      SYNONYMS INTEGER = POINTER $,
      POINTER  PZ  $,
      INTEGER M $,
      REAL X1,X2,X3,X4,X5,X6, XT $,
      PROCEDURE EXIT, DOITF, PARSE, ALGEB, PRNT,  COLECT, SUBST $,
      REAL PROCEDURE TMINS $,
      M = M $,
      FNEWBD (27777C,50000C, M2) $,
      PRINT F10 $,
  M1$ PRINT F11 $,
      DOITF(TMINS,X1) $,
      PARSE(PZ)  $,
      DOITF(TMINS,X2) $,
      ALGEB(PZ) $,
      DOITF(TMINS,X3) $,
      COLECT(PZ) $,
      DOITF(TMINS,X4) $,
      PRNT() $,
      DOITF(TMINS,X5) $,
      SUBST() $,
      DOITF(TMINS,X6) $,
      PRINT F2 $,
      PRINT F9 $,
      XT = (X2-X1) * 60.0 $,
      PRINT F3, XT $,
      XT = (X3-X2) * 60.0 $,
      PRINT F4, XT $,
      XT = (X4-X3) * 60.0 $,
      PRINT F5, XT $,
      XT = (X5-X4) * 60.0 $,
      PRINT F6, XT $,
      XT = (X6-X5) * 60.0 $,
      PRINT F7, XT $,
      XT = (X6-X1) * 60.0 $,
      PRINT F8, XT $,
      PRINT F2 $,
      GOTO M1 $,
  M2$ PRINT F12 $,
      EXIT () $,
  F2$ FORMAT (////////) $,
  F3$ FORMAT ('0 PARSE'    ' F6.1,' SECONDS') $,
  F4$ FORMAT ('0 ALGEB'    ' F6.1,' SECONDS') $,
  F5$ FORMAT ('0 COLECT'   ' F6.1,' SECONDS') $,
  F6$ FORMAT ('0 PRNT'     ' F6.1,' SECONDS') $,
  F7$ FORMAT ('0 SUBST'    ' F6.1,' SECONDS') $,
  F8$ FORMAT (//'0 TOTAL'    ' F6.1,' SECONDS') $,
  F9$ FORMAT ('0 THE TIMES TAKEN BY THE VARIOUS SUBROUTINES ARE''//) $,
```

Figure 47. Listing of Digital Program to Derive Equation for Square of Frequency Response Function (1 of 26)

```
F10$ FORMAT (1H1//////////1HO'THIS PROGRAM WAS WRITTEN BY UNITED AIRCRAFT RESEAR
CH LABORATORIES FOR HAMILTON STANDARD, UNDER CONTRACT NAS2-4515 TO PERFORM '/
   1H036X 'CERTAIN ALGEBRAIC MANIPULATIONS OF TRANSFER FUNCTIONS' ) $,
F11$ FORMAT (1H1) $,
F12$ FORMAT ('OTROUBLE IN FREE STORAGE. CALLED FROM FNEWBD. ') $,
     END FINI

'P   AED RDCARD
     BEGIN
COMMENT
  THIS PROGRAM WAS WRITTEN BY UNITED AIRCRAFT RESEARCH LABORATORIES FOR
  HAMILTON STANDARD, UNDER CONTRACT NAS2-4515 TASK 4, IN THE AED-0
  PROGRAMMING LANGUAGE.

$,
COMMENT
  THIS ROUTINE READS 72 HOLLERITH CHARACTERS. IT WAS MADE A PROCEDURE
  SOLELY TO SAVE STORAGE SPACE, AND TO AVOID HAVING TO WRITE IT OUT
  SEVERAL TIMES. THE ROUTINE ALSO SENSES COMMENT CARDS ('C' IN COLUMN 1)
  AND PRINTS THEM OUT.
$,
     DEFINE PROCEDURE RDCARD TOBE
     BEGIN
     INTEGER ARRAY J(72) $,
     COMMON J $,
     INTEGER I $,
     BOOLEAN K $,
     PROCEDURE  EXIT ,SETASM, CARET, ASMBCD $,
     K = FALSE $,
 RO$ READ F1, J(1), J(2), J(3), J(4), J(5), J(6), J(7), J(8), J(9),
      J(10), J(11), J(12), J(13), J(14), J(15), J(16), J(17), J(18),
      J(19), J(20), J(21), J(22), J(23), J(24), J(25), J(26), J(27),
      J(28), J(29), J(30), J(31), J(32), J(33), J(34), J(35), J(36),
      J(37), J(38), J(39), J(40), J(41), J(42), J(43), J(44), J(45),
      J(46), J(47), J(48), J(49), J(50), J(51), J(52), J(53), J(54),
      J(55), J(56), J(57), J(58), J(59), J(60), J(61), J(62), J(63),
      J(64), J(65), J(66), J(67), J(68), J(69), J(70), J(71), J(72) $,
     IF J(1) EQL .BCD. /$/ THEN EXIT() $,
     IF J(1) EQL .BCD. /C/ THEN
       BEGIN  IF NOT K THEN  BEGIN  PRINT F2 $,
                                    SETASM (3,110,-0,-0,-0,-0) $,
                                    K = TRUE $,
                             END $,
              FOR I=2 STEP 1 UNTIL 72 DO ASMBCD (1,J(I)) $,
              CARET () $,
              GOTO RO $,
       END $,
     GOTO RETURN $,
 F1$ FORMAT (72A1) $,
 F2$ FORMAT (1H1) $,
     END $,
     END FINI

'P   AED PARSE
     BEGIN
COMMENT
  THIS PROGRAM WAS WRITTEN BY UNITED AIRCRAFT RESEARCH LABORATORIES FOR
  HAMILTON STANDARD, UNDER CONTRACT NAS2-4515 TASK 4, IN THE AED-0
  PROGRAMMING LANGUAGE.
```

Figure 47. Listing of Digital Program to Derive Equation for Square of Frequency Response Function (2 of 26)

```
$.
COMMENT
  THE PARSING ROUTINE TAKES THE EXPRESSION FOR H(S) AND SETS UP THE
  INTERNAL BINARY TREE STRUCTURE. IT EXAMINES H(S) FOR OBVIOUS ERRORS
  SUCH AS PARENTHESES IMBALANCE,AND PRINTS ERROR MESSAGES.
$.
      DEFINE PROCEDURE PARSE(PTOP) WHERE POINTER PTOP TOBE
      BEGIN
      SYNONYMS INTEGER = POINTER $.
      POINTER PUSH $.
      POINTER COMPONENT RV.LV   $.
      INTEGER COMPONENT OP,    HOL    $.
      POINTER  P.TOP.Q.Z.Z3.Z4.P1.P2.Q1.ANGLE $.
      BOOLEAN COMPONENT ATOM.NUM.BSIGN $.
      BOOLEAN  DFLAG.ERROR. MINFLAG $.
      REAL COMPONENT CONS $.
      REAL NUMBER , DCT $.
      INTEGER  K.I.IST.M.MSK.L.PARCT. SYMST $.
      POINTER COMPONENT RVAR.LVAR $.
      INTEGER COMPONENT TYPE.ALPHA $.
      BOOLEAN COMPONENT AFLAG.NB $.
      REAL COMPONENT DEC $.
      PROCEDURE EXIT.MSEA , RDCARD , STKSX $.
      PROCEDURE SETASM.NEWPOS. ASM.C.. ASMBCD. CARET $.
      INTEGER PROCEDURE SETFR1.FREE1.FRET $.
      POINTER PROCEDURE STINIT. UNSTAK $.
      INTEGER PROCEDURE  FKILL $.
      PACK 777777C0.0. SPECIAL COMPONENTS RV $.
      PACK 777777C18.18. SPECIAL COMPONENTS LV $.
      PACK 77C24.24.SPECIAL COMPONENTS OP $.
      PACK 1C0.0. SPECIAL COMPONENTS ATOM $.
      PACK 77C30.30. SPECIAL COMPONENTS BSIGN $.
      PACK 777777C12.12.SPECIAL COMPONENTS HOL $.
      PACK 1C1.1.SPECIAL COMPONENTS NUM $.
      PACK 1C0.0.SPECIAL COMPONENTS ATOM $.
      RVAR $=$ 0$.
      LVAR $=$ 1 $.
      TYPE $=$ 2 $.
      ALPHA $=$ 0 $.
      AFLAG $=$ 1 $.
      NB $=$ 2 $.
      DEC $=$ 3 $.
      OP $=$ ATOM $=$ BSIGN $=$ 0 $.
      LV $=$ RV $=$ 1 $.
      HOL $=$ NUM $=$ ATOM $=$ BSIGN $=$ 0 $.
      CONS $=$ 1 $.
      REAL ARRAY  REALL(1500). NM(10)  $.
      INTEGER ARRAY J(72). DIG(10). IN(300). GOEDEL(1500)  $.
      INTEGER ARRAY SYM(35). PRIME(35) $.
      COMMON J.ERROR.ANGLE. GOEDEL. REALL. Z. SYM. PRIME. SYMST. DIG.
             NM $.
      MSEA() $.
      DIG(0) = .BCD. /0/ $.
      DIG(1) = .BCD. /1/ $.
      DIG(2) = .BCD. /2/ $.
      DIG(3) = .BCD. /3/ $.
      DIG(4) = .BCD. /4/ $.
      DIG(5) = .BCD. /5/ $.
      DIG(6) = .BCD. /6/ $.
      DIG(7) = .BCD. /7/ $.
```

Figure 47. Listing of Digital Program to Derive Equation for Square of Frequency Response Function (3 of 26)

```
      DIG(8) = .BCD. /8/ $,
      DIG(9) = .BCD. /9/ $,
      NM(0) = 0.0 $,
      NM(1) = 1.0 $,
      NM(2) = 2.0 $,
      NM(3) = 3.0 $,
      NM(4) = 4.0 $,
      NM(5) = 5.0 $,
      NM(6) = 6.0 $,
      NM(7) = 7.0 $,
      NM(8) = 8.0 $,
      NM(9) = 9.0 $,
      ANGLE = 0 $,
      ERROR = FALSE $,
      PARCT = 0 $,
      IST = 1 $,
      MSK = 770000000000C $,
  D1$ FOR I=0 STEP 1 UNTIL 4 DO
        BEGIN  RDCARD () $,
        FOR K=1 STEP 1 UNTIL 72 DO
         BEGIN  IF J(K) EQL .BCD. /$/ THEN BEGIN IN(0) = .BCD. /(/ $,
                                                 IN(IST) = .BCD. /)/ $,
                                                 IN(IST=IST+1) =
                                                   .BCD. /$/ $,
                                                 GOTO D2 $,
                                           END
                                           ELSE
                  IF J(K) NEQ .BCD. / / THEN
                       BEGIN  IF (IN(IST) = J(K)) EQL .BCD. /(/ THEN
                              PARCT = PARCT+1 ELSE IF IN(IST) EQL
                              .BCD. /)/ THEN PARCT = PARCT-1  $,
                              IST = IST+1 $,
                       END $,
         END $,
        END $,
 COMMENT
   H(S) READ IN COMPLETED. NOW PRINT IT OUT.
 $,
  D2$ SETASM (5,110,-0,-0,-0,-0) $,
      CARET () $,
      CARET () $,
      CARET () $,
      CARET () $,
      ASM.C. (.C. /H(S) = /) $,
      NEWPOS(12) $,
      FOR I=1 STEP 1 UNTIL IST-2 DO ASMBCD (0,IN(I))  $,
      CARET () $,
      CARET () $,
      CARET () $,
      CARET () $,
COMMENT
  IF PARENTHESES DO NOT BALANCE, INDICATE AND SET ERROR FLAG.
$,
      IF PARCT NEQ 0 THEN  BEGIN  ERROR = TRUE $,
                                  PRINT F0 $,
                           END $,
      IF Z   NEQ 0 THEN FKILL(Z ) $,
      IF Z3  NEQ 0 THEN FKILL(Z3) $,
      IF Z4  NEQ 0 THEN FKILL(Z4) $,
      Z = SETFR1 (5000,100,0,2,0) $,
```

Figure 47. Listing of Digital Program to Derive Equation for Square of Frequency Response Function (4 of 26)

```
        Z3 = SETFR1 (100,25,0,3,0) $,
        Z4 = SETFR1 (100,25,0,4,0) $,
        P = (TOP = FREE1(Z3)) $,
        FOR I=0 STEP 1 UNTIL IST DO
          BEGIN  IF IN(I) EQL .BCD. /-/ THEN
             BEGIN  FOR K=0 STEP 1 UNTIL 9 DO IF IN(I+1) EQL DIG(K) AND
                         IN(I-1) EQL .BCD. /(/ THEN GOTO D10 $,
                    ERROR = TRUE $,
                    PRINT F4,IN(I-1),IN(I),IN(I+1),IN(I+2),IN(I+3),IN(I+4),
                    IN(I+5) $,
             END $,
                   LVAR(P) = FREE1(Z4) $,
                   RVAR(P) = FREE1(Z3) $,
                         IF IN(I) EQL .BCD. /+/ OR IN(I) EQL .BCD. /$/ OR
                   IN(I) EQL .BCD. /*/ OR IN(I) EQL .BCD. /E/ THEN
             BEGIN    TYPE(P) = 1 $,
                      ALPHA(LVAR(P)) = IN(I) $,
                      AFLAG(LVAR(P)) = FALSE $,
                      NB(LVAR(P)) = FALSE $,
                      P = RVAR(P) $,
                      GOTO D10 $,
             END
             ELSE    IF IN(I) EQL .BCD. /(/ OR IN(I) EQL .BCD. /)/ THEN
             BEGIN    TYPE(P) = 3 $,
                      ALPHA(LVAR(P)) = IN(I) $,
                      AFLAG(LVAR(P)) = FALSE $,
                      NB(LVAR(P)) = FALSE $,
                      P = RVAR(P) $,
                      GOTO D10 $,
             END
             ELSE
                      FOR K=0 STEP 1 UNTIL 9 DO
             BEGIN    IF IN(I)    EQL DIG(K) THEN
                 BEGIN        NUMBER = 0 $,
                              DCT = 0.0  $,
                              DFLAG = FALSE $,
                              MINFLAG = IF IN(I-1) EQL .BCD. /-/ THEN
                              TRUE ELSE FALSE $,
                         D4$  NUMBER = 10*NUMBER + NM(K) $,
                              IF DFLAG THEN DCT = DCT+1.0 $,
                              IF IN(I+1) EQL .BCD. /./ THEN
                                BEGIN  DFLAG = TRUE $,
                                       I = I+1 $,
                                END $,
                              FOR K=0 STEP 1 UNTIL 9 DO
                              IF IN(I+1) EQL DIG(K) THEN BEGIN I=I+1 $,
                                                             GOTO D4 $,
                                                        END $,
COMMENT
  ADD 0.0 TO NORMALIZE NUMBER.
$,
                      NUMBER = 10.0**(-DCT)*NUMBER + 0.0 $,
                      TYPE(P) = 2 $,
                      AFLAG(LVAR(P)) = TRUE $,
                      NB(LVAR(P)) = TRUE $,
                      DEC(LVAR(P)) = IF MINFLAG THEN -NUMBER ELSE NUMBER $,
                      P = RVAR(P) $,
                      GOTO D10 $,
                 END
             END $,
```

Figure 47. Listing of Digital Program to Derive Equation for Square of Frequency Response Function (5 of 26)

```
COMMENT
           ANYTHING ELSE MUST BE S,T1,T2,....,C1,C2,....,W1,W2,....,Z1W,
           Z2W,...., ETC.
$,
           IF IN(I) EQL .BCD. /T/ OR IN(I) EQL .BCD. /C/ OR IN(I) EQL
           .BCD. /W/ OR IN(I) EQL .BCD. /Z/ OR IN(I) EQL  .BCD. /S/
           THEN
                BEGIN  TYPE(P) = 2 $,
                       AFLAG(LVAR(P)) = TRUE $,
                       NB(LVAR(P)) = FALSE $,
                       IF IN(I) EQL .BCD. /S/ THEN ALPHA(LVAR(P))
                       = IN(I) .A. MSK ELSE
                       IF IN(I) EQL .BCD. /Z/ THEN
                         BEGIN  ALPHA(LVAR(P)) = (IN(I).A. MSK)
                                + (IN(I+1).A. MSK) .RS. 6
                                + (IN(I+2).A. MSK) .RS. 12 $,
                                I = I+2 $,
                         END   ELSE
                                IF IN(I+1) EQL DIG(1) AND IN(I+2) EQL
                                DIG(0) THEN BEGIN  ALPHA(LVAR(P)) =
                                                    (IN(I).A. MSK) +
                                                   (DIG(1) .A. MSK)
                                                   .RS. 6 + (DIG(0)
                                                   .A. MSK) .RS. 12 $,
                                                   I = I+2 $,
                                            END ELSE
                                     BEGIN  ALPHA(LVAR(P)) = (IN(I).A.
                                            MSK)+ (IN(I+1).A. MSK) .RS.
                                            6 $,
                                            I = I+1 $,
                                     END $,
                       P = RVAR(P) $,
                END
                ELSE  BEGIN  PRINT F2, IN(I) $,
                             ERROR = TRUE $,
                      END $,
  D10$  END $,
COMMENT
  CHARACTERS CLASSIFIED.OPERATORS (EXPONENTIATION, MULTIPLICATION, AND
  ADDITION) ARE TYPE 1. AS IS $ (END OF EXPRESSION).  LEFT AND RIGHT
  PARENTHESES ARE TYPE 3. ATOMIC SYMBOLS AND CONSTANTS ARE TYPE 2.
  CHECK FOR OBVIOUS ERRORS BEFORE ATTEMPTING SIMPLIFICATION. THESE
  ERRORS ARE, USING EXAMPLES, THE FOLLOWING IMPOSSIBLE ADJACENT
  CHARACTERS.
           1.  * +  OR  + +  .
           2.  S  T1  OR  T1  Z1W  OR  6  7.3  .
           3.  ( )  OR  ) (  .
           4.  +, )  OR  * )  OR  E )
$,
     P = TOP $,
 D11$ IF TYPE(P) EQL 1  AND TYPE(RVAR(P)) EQL 1 AND ALPHA(LVAR(RVAR(P)))
     NEQ .BCD. /E/ OR TYPE (P) EQL 2 AND
     TYPE(RVAR(P)) EQL 2  OR TYPE(P) EQL 3 AND TYPE(RVAR(P)) EQL 3
     AND ALPHA(LVAR(P)) NEQ ALPHA(LVAR(RVAR(P))) OR TYPE(P) EQL 1 AND
     ALPHA(LVAR(RVAR(P))) EQL .BCD. /)/  THEN
           BEGIN  PRINT F1, ALPHA(LVAR(P)), ALPHA(LVAR(RVAR(P))) $,
                  ERROR = TRUE $,
           END $,
     IF ALPHA(LVAR(RVAR(P))) NEQ .BCD. /$/ THEN BEGIN P=RVAR(P) $,
                                                GOTO D11 $,
```

Figure 47. Listing of Digital Program to Derive Equation for Square of Frequency Response Function (6 of 26)

```
                                                      END $,
      IF ERROR THEN GOTO RETURN $,
      PUSH = STINIT () $,
      COMMENT
            STACK ALL POINTERS WHICH POINT TO '(' .
      $,
      P = TOP $,
  D3$ IF ALPHA(LVAR(P)) EQL .BCD. /$/ THEN GOTO D14 $,
      IF ALPHA(LVAR(P)) EQL .BCD. /(/ THEN
        BEGIN  STKSX(PUSH,P) $,
      COMMENT
            REMOVE '(' FROM STRING
      $,
                TYPE(P) = TYPE(RVAR(P)) $,
               LVAR(P) = LVAR(RVAR(P)) $,
               RVAR(P) = RVAR(RVAR(P)) $,
         END
        ELSE   P = RVAR(P) $,
      GOTO D3 $,
COMMENT
      CHANGE ATOMS TO PACKED FORMAT,
 $,
 D14$ P = TOP $,
 D13$ IF TYPE(P) EQL 2 OR ALPHA(LVAR(P)) EQL .BCD. /$/ THEN
        BEGIN  Q1 = FREE1(Z) $,
               IF NB(LVAR(P)) THEN CONS(Q1) = DEC(LVAR(P)) ELSE HOL(Q1)
               = ALPHA(LVAR(P)) .RS. 18 $,
               BSIGN(Q1) = TRUE $,
               ATOM(Q1) = TRUE $,
               NUM(Q1) = NB(LVAR(P)) $,
               IF ALPHA(LVAR(P)) EQL .BCD. /$/ THEN
                                                        BEGIN  LVAR(P) = Q1 $,
                                                               GOTO D5 $,
                                                        END
                                                        ELSE
                                                        BEGIN  LVAR(P) = Q1 $,
                                                               P = RVAR(P) $,
                                                               GOTO D13 $,
                                                        END $,
        END ELSE
           BEGIN  P = RVAR(P) $,
                  GOTO D13 $,
           END $,
      COMMENT
      STACKING OF '(' DONE. NOW START SIMPLIFICATION. DO E,*,+ IN ORDER.
      $,
  D5$ P1 = UNSTAK(PUSH,D8) $,
      P = P1 $,
      FOR K = .BCD. /E/, .BCD. /*/ , .BCD. /+/ DO
  D6$   BEGIN IF TYPE(     RVAR(P))  EQL 3 THEN BEGIN  P2 = P $,
                                                       P = P1 $,
                                                       GOTO D7 $,
                                                END $,
               IF TYPE(P) EQL 1 AND TYPE(RVAR(P)) EQL 2 AND
               ALPHA(LVAR(P)) EQL .BCD. /E/ THEN
                 BEGIN  Q = FREE1(Z) $,
                        OP(Q) = .BCD. /     E/    $,
                        BSIGN(Q) = TRUE $,
                        ATOM(Q) = FALSE $,
                        ANGLE = LVAR(RVAR(P)) $,
```

Figure 47. Listing of Digital Program to Derive Equation for Square of Frequency Response Function (7 of 26)

```
                    BSIGN(ANGLE) = FALSE $,
                    LVAR(P) = Q $,
                    RVAR(P) = RVAR(RVAR(P)) $,
                    TYPE(P) = 2 $,
              END
              ELSE
            IF TYPE(P) EQL 2 AND TYPE(RVAR(P)) EQL 1 AND
            ALPHA(LVAR(RVAR(P))) EQL K THEN
              BEGIN  Q = FREE1(Z) $,
                    OP(Q) = K .RS. 30 $,
                    LV(Q) = LVAR(P) $,
                    RV(Q) = LVAR(RVAR(RVAR(P))) $,
                    BSIGN(Q) = TRUE $,
                    ATOM(Q) = FALSE $,
                    LVAR(P) = Q $,
                    RVAR(P) = RVAR(RVAR(RVAR(P))) $,
                    TYPE(P) = 2 $,
             END  ELSE P = RVAR(P) $,
                      GOTO D6 $,
 D7$   END $,
COMMENT
     REMOVE ')' FROM END OF SUBEXPRESSION
$,
     RVAR(P2) = RVAR(RVAR(P2)) $,
       GOTO D5 $,
 D8$ PTOP = LVAR(TOP) $,
     GOTO RETURN $,
 F0$ FORMAT ('0PARENTHESES IN H(S) DO NOT BALANCE. H(S) WILL NOT BE PROCESSED B
UT ERROR SCAN WILL CONTINUE.') $,
 F1$ FORMAT ('0THE ADJACENT CHARACTERS  ' A6,' AND  ' A6,' ARE ILLEGAL IN THIS
CONTEXT. H(S) WILL NOT BE PROCESSED BUT ERROR SCAN WILL CONTINUE.') $,
 F2$ FORMAT ('0 THE CHARACTER  'A6, 'IS ILLEGAL. H(S) WILL NOT BE PROCESSED BUT
 ERROR SCAN WILL CONTINUE.' ) $,
  F3$ FORMAT (1H1)  $,
 F4$ FORMAT('0THE SEQUENCE ' 7A1, ' .... IS NOT PERMITTED. REMEMBER THAT A MINU
S SIGN MUST BE'/'0PRECEDED BY A '('' AND FOLLOWED BY A NUMERIC. H(S) WILL NOT B
E PROCESSED BUT ERROR SCAN WILL CONTINUE. ') $,
     END $,
     END FINI

'P    AED ALGEB
      BEGIN
COMMENT
  THIS PROGRAM WAS WRITTEN BY UNITED AIRCRAFT RESEARCH LABORATORIES FOR
  HAMILTON STANDARD, UNDER CONTRACT NAS2-4515 TASK 4, IN THE AED-0
  PROGRAMMING LANGUAGE.

$,
COMMENT
  THE ALGEBRAIC ROUTINE CONSTRUCTS H(-S) FROM H(S). IT THEN SETS UP THE
  TREE STRUCTURE FOR H(S)*H(-S). NEXT IT LOOKS FOR EXPRESSIONS OF THE
  FORM EXP( T*S ) AND SUBSTITUTES I*W FOR S (I=SQRT(-1)) GIVING THE
  FORM COS( T*W ) + I*SIN( T*W ). THE SUBSTITUTION OF I*W FOR S IN THE
  REST OF H(S)*H(-S) IS DEFERRED UNTIL THE PRINT ROUTINE WHERE IT IS
  MORE EASILY PERFORMED. NEXT H(S)*H(-S) IS SIMPLIFIED FROM PRODUCTS OF
  SUMS TO SUMS OF PRODUCTS, BY REPEATED APPLICATIONS OF THE DISTRIBUTIVE
  LAW OF MULTIPLICATION AND ADDITION, I.E. A*(B+C) = A*B+A*C.
$,
     DEFINE PROCEDURE ALGEB(TOP) WHERE POINTER TOP TOBE
     BEGIN
```

Figure 47. Listing of Digital Program to Derive Equation for Square of Frequency Response Function (8 of 26)

```
SYNONYMS INTEGER = POINTER $,
POINTER COMPONENT  RV, LV, HOL   $,
POINTER P,     Y,TMP,Q1,Q2,Q3,Z,    Q,PTOP,QTOP, ANGLE $,
BOOLEAN     ERROR $,
INTEGER  SYMST , I $,
INTEGER COMPONENT OP $,
BOOLEAN COMPONENT ATOM,NUM,BSIGN $,
BOOLEAN COMPONENT    SEALER $,
POINTER TM1, TM2, TM3, TM4, TM5, TM6, TM7, TM8, TM9, TM10 $,
REAL COMPONENT CONS $,
POINTER PROCEDURE STINIT, UNSTAK $,
PROCEDURE STKSX  $,
PROCEDURE EXIT , MSEA $,
INTEGER PROCEDURE SETFR1, FREE1, CRSTK, POP, STACK, FRET1 $,
COMMON J,ERROR,ANGLE, GOEDEL, REALL, Z, SYM, PRIME, SYMST, DIG,
       NM , I $,
INTEGER ARRAY GOEDEL(1500), DIG(10),J(72),SYM(35),PRIME(35) $,
REAL ARRAY  REALL(1500), NM(10) $,
DEFINE BOOLEAN PROCEDURE EQUIV(BL1,BL2) WHERE BOOLEAN BL1,BL2
TOBE   EQUIV = IF (BL1 AND BL2) OR (NOT BL1 AND NOT BL2)
                THEN TRUE ELSE FALSE $,
PACK 777777C0,0, SPECIAL COMPONENTS RV $,
PACK 777777C18,18,SPECIAL COMPONENTS LV $,
PACK 77C24,24, SPECIAL COMPONENTS OP $,
PACK 1C0,0, SPECIAL COMPONENTS ATOM $,
PACK 77C30,30,  SPECIAL COMPONENTS BSIGN $,
PACK 777777C12,12, SPECIAL COMPONENTS HOL $,
PACK 1C1,1,    SPECIAL COMPONENTS NUM $,
PACK 1C0,0, SPECIAL COMPONENTS ATOM $,
PACK 1C2,2, SPECIAL COMPONENTS SEALER $,
OP $=$ ATOM $=$ BSIGN $=$ SEALER $=$ 0  $,
LV $=$ RV $=$ 1 $,
HOL $=$ NUM $=$ ATOM $=$ BSIGN $=$ SEALER $=$ 0  $,
CONS $=$ 1 $,
POINTER PUSH, QUSH $,
IF ERROR THEN GOTO RETURN $,
PTOP = TOP $,
PUSH = STINIT () $,
QUSH = STINIT () $,
QTOP = FREE1(Z) $,
P = PTOP$,
Q = QTOP $,
A1$  IF ATOM(P) THEN
      BEGIN   ATOM(Q) = TRUE $,
              NUM(Q) = NUM(P) $,
              IF NUM(P) THEN
                        BEGIN  CONS(Q) = CONS(P) $,
                               BSIGN(Q) = BSIGN(P) $,
                        END
          ELSE BEGIN
                  HOL(Q) = HOL(P) $,
                  BSIGN(Q) = EQUIV(NOT(HOL(P) EQL
                   0    300000C ), BSIGN(P)) $,
               END $,
COMMENT
  THE SEALER BOOLEAN COMPONENT IS USED TO SEAL OFF BRANCHES OF THE TREE
  WHICH HAVE BEEN SIMPLIFIED. SINCE THE ALGEBRAIC SIMPLIFICATION
  ROUTINE BUILDS A TREE WHICH SHARES STORAGE, THIS PREVENTS REDUNDANT
  TRIPS THROUGH THE TREE.
$,
```

Figure 47. Listing of Digital Program to Derive Equation for Square of Frequency Response Function (9 of 26)

```
                  SEALER(P) = TRUE $,
                  SEALER(Q) = TRUE $,
                  P = UNSTAK (PUSH,A2) $,
                  Q = UNSTAK(QUSH,A2) $,
                  GOTO A1 $,
         END
                  ELSE
         BEGIN    LV(Q) = FREE1(Z) $,
                  RV(Q) = FREE1(Z) $,
                  ATOM(Q) = FALSE $,
                  OP(Q) = OP(P) $,
                  BSIGN(Q) = BSIGN(P) $,
                  IF OP(P) NEQ OP(.C. / E     /) THEN
                     BEGIN  STKSX(QUSH,RV(Q)) $,
                            STKSX(PUSH,RV(P)) $,
                     END ELSE
                       BEGIN  OP(Q) = .BCD. /      M/   $,
                              P = UNSTAK(PUSH,A2) $,
                              Q = UNSTAK(QUSH,A2) $,
                              GOTO A1 $,
                       END $,
                  SEALER(P) = FALSE $,
                  SEALER(Q) = FALSE $,
                  Q = LV(Q) $,
                  P = LV(P) $,
                  GOTO A1 $,
         END $,
   COMMENT
                NOW JOIN H(S) AND H(-S) WITH * OPERATOR
    $,
   A2$  TOP = FREE1(Z) $,
        LV( TOP) = PTOP $,
        RV( TOP) = QTOP $,
        OP( TOP) = OP(.C. / *     /) $,
        ATOM( TOP) = FALSE $,
        BSIGN( TOP) = TRUE $,
        SEALER(TOP) = FALSE $,
   A6$ P = TOP $,
   COMMENT
             SUBSTITUTE I*W FOR S WHERE I = SQRT(-1) . EXP**IW BECOMES
   COS(W)+I*SIN(W) . LEAVE OTHER TERMS INVOLVING S TO OUTPUT ROUTINE.
             $,
   PUSH = STINIT () $,
B1$ IF NOT ATOM(P) AND (OP(P) EQL OP(.C. / E     /) OR OP(P) EQL
   OP(.C. / M     /)) THEN
         BEGIN    Q1 = FREE1(Z) $,
                  LV(Q1) = FREE1(Z) $,
                  RV(Q1) = FREE1(Z) $,
                  TM1 = LV(Q1) $,
                  ATOM(TM1) = FALSE $,
                  OP(TM1) = .BCD. /      C/ $,
                  BSIGN(TM1) = BSIGN(P) $,
                  SEALER(TM1) = TRUE $,
         TM5 = RV(Q1) $,
         ATOM(TM5) = FALSE $,
         OP(TM5) = .BCD. /      */ $,
         LV(TM5) = FREE1(Z) $,
         RV(TM5) = FREE1(Z) $,
         BSIGN(TM5) = EQUIV(EQUIV(BSIGN(P),BSIGN(LV(P))),
                      EQUIV(BSIGN(LV(LV(P))),BSIGN(RV(LV(P))))) $,
```

Figure 47. Listing of Digital Program to Derive Equation for Square of Frequency Response Function (10 of 26)

```
                SEALER(TM5) = TRUE $,
                TM6 = LV(TM5) $,
                ATOM(TM6) = TRUE $,
                        BSIGN(TM6) = IF OP(P) EQL OP(.C. / E     /) THEN
                        FALSE ELSE TRUE $,
                NUM(TM6) = FALSE $,
                HOL(TM6) = .BCD. /      I/ $,
                TM7 = RV(TM5) $,
                ATOM(TM7) = FALSE $,
                BSIGN(TM7) = TRUE $,
                OP(TM7) = .BCD. /      S/ $,
                        OP(P) = .BCD. /      +/ $,
                        LV(P) = LV(Q1) $,
                        RV(P) = RV(Q1) $,
                        BSIGN(P) = TRUE $,
                        ATOM(P) = FALSE $,
                        SEALER(P) = FALSE $,
                        FRET1 (Q1,Z) $,
                        P = UNSTAK(PUSH,A8) $,
                        GOTO B1 $,
                END ELSE IF ATOM(P) OR OP(P) EQL OP(.C. / C     /)
                         OR OP(P) EQL OP(.C. / S     /) THEN P=UNSTAK(PUSH,A8
                      ) ELSE
                BEGIN
                        STKSX(PUSH,RV(P)) $,
                        P = LV(P) $,
                END $,
                        GOTO B1 $,
A8$ P = TOP $,
    PUSH = STINIT () $,
A3$ IF NOT ATOM(P) AND OP(P) EQL OP(.C. / *      /) AND SEALER(LV(P))
    AND SEALER (RV(P)) THEN  BEGIN  SEALER(P) = TRUE $,
                                    GOTO A7 $,
                             END $,
    IF NOT ATOM(P) AND OP(P) EQL OP(.C. / *      /) AND NOT ATOM(RV(P))
    AND OP(RV(P)) EQL OP(.C. / +     /) THEN
    A5$    BEGIN    Q1 = FREE1(Z) $,
                    Q2 = FREE1(Z) $,
                    Q3 = FREE1(Z) $,
                    TM2 = RV(P) $,
                    LV(Q1) = Q2 $,
                    RV(Q1) = Q3 $,
                    LV(Q2) = LV(P) $,
                    RV(Q2) = LV(TM2) $,
                    OP(Q2) = .BCD. /      */ $,
                    ATOM(Q2) = FALSE $,
                    BSIGN(Q2) = EQUIV(BSIGN(P), BSIGN(TM2)) $,
                    SEALER(Q2) =    SEALER(LV(P)) AND SEALER(LV(TM2)) $,
                    LV(Q3) = LV(P) $,
                    RV(Q3) = RV(TM2) $,
                    OP(Q3) = .BCD. /      */ $,
                    ATOM(Q3) = FALSE $,
                    BSIGN(Q3) = BSIGN(Q2) $,
                    SEALER(Q3) =    SEALER(LV(P)) AND SEALER(RV(TM2)) $,
                    BSIGN(P) = TRUE $,
                    LV(P) = LV(Q1) $,
                    RV(P) = RV(Q1) $,
                    OP(P) =.BCD. /      +/ $,
                    SEALER(P) = FALSE $,
                    FRET1 (Q1,Z)   $,
```

Figure 47. Listing of Digital Program to Derive Equation for Square of Frequency Response Function (11 of 26)

```
                    P = UNSTAK(PUSH,A8) $,
                    GOTO A3 $,
                END $,
      IF NOT ATOM(P) AND OP(P) EQL OP(.C. / *      /) AND NOT ATOM(LV(P))
      AND OP(LV(P)) EQL OP(.C. / +     /) THEN
                    BEGIN
                        TMP = LV(P) $,
                        LV(P) = RV(P) $,
                        RV(P) = TMP $,
                        GOTO A5 $,
                    END $,
      IF ATOM(P) OR OP(P) EQL OP(.C. / S     /) OR OP(P) EQL
      OP(.C. / C     /) OR OP(P) EQL OP(.C. / E     /) THEN
   A7$  BEGIN  P = RV(UNSTAK(PUSH,RETURN)) $,
                    GOTO A3      $,
             END    ELSE
             BEGIN  STKSX(PUSH,P) $,
                    P = LV(P) $,
                    GOTO A3      $,
             END $,
      END $,
      END FINI

*P    AED COLECT
      BEGIN
COMMENT
  THIS PROGRAM WAS WRITTEN BY UNITED AIRCRAFT RESEARCH LABORATORIES FOR
  HAMILTON STANDARD, UNDER CONTRACT NAS2-4515 TASK 4, IN THE AED-0
  PROGRAMMING LANGUAGE.

$,
COMMENT
  THIS ROUTINE COLLECTS LIKE TERMS IN THE SIMPLIFIED EXPRESSION. FIRST,
  EACH SYMBOL USED IN H(S) IS ASSIGNED A UNIQUE PRIME. THEN FOR EACH
  TERM A GOEDEL NUMBER IS COMPUTED WHICH IS THE PRODUCT OF ALL THE
  PRIMES CORRESPONDING TO THE SYMBOLS IN THE TERM. NOW BY THE UNIQUE
  FACTORIZATION THEOREM, ANY TERMS WITH THE SAME GOEDEL NUMBER CONTAIN
  THE SAME SYMBOLS AND ASSOCIATED EXPONENTS, AND TERMS WITH DIFFERENT
  GOEDEL NUMBERS ARE DIFFERENT. COLLECTING LIKE TERMS THEN IS SIMPLY A
  MATTER OF SELECTING THE TERMS WITH LIKE GOEDEL NUMBERS AND ADDING
  THEIR NUMERICAL COEFFICIENTS.  SIN AND COS ARE ARBITRARILY ASSIGNED
  THE PRIMES 3 AND 5, RESPECTIVELY.  SIMPLIFICATION INVOLVING THE
  IDENTITY SIN(A)**2 + COS(A)**2 = 1 ARE THEN EASILY HANDLED BY TESTING
  THE GOEDEL NUMBER FOR DIVISIBILITY BY 9 AND 25.
  IF A TERM HAS A GOEDEL NUMBER GREATER THAN (2**35)-1, TWO OR MORE
  LOCATIONS ARE USED. IN THIS CASE, A NEGATIVE GOEDEL NUMBER INDICATES
  THAT THE NEXT GOEDEL NUMBER IN THE TABLE IS THE NEXT FACTOR. THE
  GOEDEL NUMBER HERE WILL BE TRANSFORMED INTO A0+A1*2**35 + A2*2**70
  + ...  WHEN COLLECTING TERMS. IN ORDER TO KEEP THE GOEDEL NUMBER IN
  ONE LOCATION, IT IS BEST TO LIST THE SYMBOLS USED IN ORDER OF THEIR
  FREQUENCY OF USE, SINCE THE PRIMES ARE ASSIGNED SMALLEST FIRST.
  AS AN EXAMPLE, CONSIDER THE EXPRESSION'
      S*T1*T1*S*S + 2*T2*S*S + 3.0*T1*S*S*S*T1
  THE PRIMES ASSIGNED TO THE SYMBOLS ARE S=2,  T1=7, T2=11. THE GOEDEL
  NUMBERS FOR THE TERMS ARE THEN 2*7*7*2*2, 11*2*2, AND 7*2*2*2*7 OR
  392, 44, AND 392. THUS THE 1ST AND 3RD TERMS ARE THE SAME DESPITE THE
  DIFFERENCE IN THE ORDER OF THE SYMBOLS, AND CAN BE COMBINED BY ADDING
  THEIR NUMERICAL COEFFICIENTS.
 $,
      DEFINE PROCEDURE COLECT (TOP) WHERE POINTER TOP TOBE
```

Figure 47. Listing of Digital Program to Derive Equation for Square of Frequency Response Function (12 of 26)

```
BEGIN
SYNONYMS INTEGER = POINTER $,
POINTER  PUSH $,
DEFINE PROCEDURE GMUL(FAC) WHERE INTEGER FAC TOBE
 BEGIN  IF (GT(KL)*FAC)/FAC NEQ GT(KL) THEN
           BEGIN  GT(KL) = -GT(KL)$,
                  GT(KL=KL+1) = FAC $,
           END
           ELSE   GT(KL) = GT(KL)*FAC $,
 END $,
DEFINE PROCEDURE SIG TOBE  IF NOT BSIGN(P) THEN RL = -RL $,
POINTER COMPONENT RV,LV   $,
INTEGER COMPONENT OP,   HOL , RHALF $,
BOOLEAN COMPONENT ATOM,NUM,BSIGN $,
REAL COMPONENT CONS $,
PROCEDURE EXIT,MSEA , PDUMPN  $,
PROCEDURE RDCARD, ASM.C., ASMDEC, ASMBCD, CARET $,
PROCEDURE  ASMFLO, SETASM, NEWPOS, STKSX $,
POINTER PROCEDURE  STINIT, UNSTAK $,
INTEGER PROCEDURE GPOL $,
REAL  RL $,
INTEGER PROCEDURE SETFR1,FREE1,FRET $,
PACK 777777C0,0, SPECIAL COMPONENTS RV $,
PACK 1C0,0, SPECIAL COMPONENTS ATOM $,
PACK 777777C18,18, SPECIAL COMPONENTS LV $,
PACK 77C24,24,SPECIAL COMPONENTS OP $,
PACK 77C30,30, SPECIAL COMPONENTS BSIGN $,
PACK 777777C12,12,SPECIAL COMPONENTS HOL $,
PACK 1C1,1,SPECIAL COMPONENTS NUM $,
PACK 1C0,0,SPECIAL COMPONENTS ATOM $,
OP $=$ ATOM $=$ BSIGN $=$ 0 $,
LV $=$ RV $=$ 1 $,
HOL $=$ NUM $=$ ATOM $=$ BSIGN $=$ 0 $,
CONS $=$ 1 $,
COMMON J,ERROR,ANGLE, GOEDEL, REALL, Z, SYM, PRIME, SYMST, DIG,
       NM , I $,
INTEGER ARRAY  GOEDEL(1500), PRIME(35),SYM(35),J(72),GT(10) $,
INTEGER ARRAY DIG(10) $,
REAL ARRAY REALL(1500), NM(10) $,
INTEGER ARRAY T1(10), T2(10) $,
BOOLEAN  B1,B2,Y, FLIP, SW, SW1, ISIG, ERROR  $,
INTEGER I,T,K,L,M,EX,R,SYMST , MSK , N,SINDEX $,
INTEGER  KK,KL,II, KN,GD  ,GDT , JJ, KM $,
INTEGER J1, J2, J3, J4  $,
POINTER P, ANGLE , LL , Z $,
MSEA() $,
MSK = 770000000000C  $,
FLIP = FALSE $,
FOR N=0 STEP 1 UNTIL 1499 DO GOEDEL(N) = (REALL(N) = 0.0) $,
PRIME (0) =  2 $,
PRIME (1) =  7 $,
PRIME (2) = 11 $,
PRIME (3) = 13 $,
PRIME (4) = 17 $,
PRIME (5) = 19 $,
PRIME (6) = 23 $,
PRIME (7) = 29 $,
PRIME (8) = 31 $,
PRIME (9) = 37 $,
PRIME(10) = 41 $,
```

Figure 47. Listing of Digital Program to Derive Equation for Square of Frequency Response Function (13 of 26)

```
        PRIME(11) = 43 $,
        PRIME(12) = 47 $,
        PRIME(13) = 53 $,
        PRIME(14) = 59 $,
        PRIME(15) = 61 $,
        PRIME(16) = 67 $,
        PRIME(17) = 71 $,
        PRIME(18) = 73 $,
        PRIME(19) = 79 $,
        PRIME(20) = 83 $,
        PRIME(21) = 89 $,
        PRIME(22) = 97 $,
        PRIME(23) = 101 $,
        PRIME(24) = 103 $,
        PRIME(25) = 107 $,
        PRIME(26) = 109 $,
        PRIME(27) = 113 $,
        PRIME(28) = 127 $,
        PRIME(29) = 131 $,
        PRIME(30) = 137 $,
        PRIME(31) = 139 $,
        PRIME(32) = 149 $,
        PRIME(33) = 151 $,
        PRIME(34) = 157 $,
        L = -1 $,
  C12$  FOR M=0 STEP 1 UNTIL 4 DO
           BEGIN  RDCARD () $,
                FOR K=1 STEP 1 UNTIL 72 DO
                   IF J(K) EQL .BCD. /$/ THEN GOTO CO
                   ELSE IF J(K) NEQ .BCD. / / THEN IF J(K) NEQ .BCD. /T/ AND
                   J(K) NEQ .BCD. /C/ AND J(K) NEQ .BCD. /W/ AND J(K) NEQ
                   .BCD. /Z/ AND J(K) NEQ .BCD. /S/ THEN  BEGIN
                                                           ERROR = TRUE $,
                                                           PRINT FO $,
                                                          END ELSE
                      IF J(K) EQL .BCD. /S/ THEN
                   BEGIN     SYM(L=L+1) = (J(K) .A. MSK)   $,
                             SINDEX = L $,
                   END
                      ELSE IF J(K) EQL .BCD. /Z/ THEN
                      BEGIN  SYM(L=L+1) = (J(K) .A. MSK)
                                        +(J(K+1) .A. MSK) .RS. 6
                                        + (J(K+2) .A. MSK) .RS. 12 $,
                             K = K+2 $,
                      END
                      ELSE IF J(K+1) EQL .BCD. /1/ AND J(K+2) EQL .BCD. /0/
                      THEN BEGIN SYM(L=L+1) = (J(K) .A. MSK)
                                +( (.BCD. /1/) .A. MSK) .RS. 6
                                +( (.BCD. /0/) .A. MSK) .RS. 12  $,
                                   K = K+2 $,
                           END
                           ELSE BEGIN  SYM(L=L+1) = (J(K) .A. MSK)
                                                  + (J(K+1) .A. MSK) .RS.
                                                   6 $,
                                                  K = K+1 $,
                                  END $,
           END $,
  CO$  F = TOP $,
       IF ERROR THEN GOTO RETURN $,
       SYMST = L $,
```

Figure 47. Listing of Digital Program to Derive Equation for Square of Frequency Response Function (14 of 26)

```
        PUSH = STINIT() $,
        I = 0 $,
   C3$  RL = 1.0  $,
        ISIG = FALSE $,
        GT(KL=0) = 1 $,
   C1$  IF ATOM(P) THEN GOTO C2 ELSE
                 IF OP(P) EQL OP(.C. / +     /) OR OP(P) EQL
                 OP(.C. / *     /) THEN
              BEGIN  STKSX(PUSH,P) $,
                     SIG () $,
                     P = LV(P) $,
                     GOTO C1 $,
              END
              ELSE
COMMENT
  CHECK FOR SIN OR COS OPERATOR
$,
           IF OP(P) EQL OP(.C. / S     /) THEN
              BEGIN  GMUL(3) $,
                     SIG ()$,
                     GOTO C4 $,
              END
              ELSE
           IF OP(P) EQL OP(.C. / C     /) THEN
              BEGIN  GMUL(5) $,
                     SIG () $,
                     GOTO C4 $,
              END
              ELSE
COMMENT
  P IS AN ATOM
$,
  C2$         IF NUM(P) THEN
                BEGIN  SIG () $,
                       RL = RL*CONS(P) $,
                       GOTO C4 $,
                END
                ELSE
COMMENT
  CHECK FOR SQRT(-1)
$,
              IF HOL(P) EQL HOL(.C. /    I   /) THEN
 C15$           BEGIN  SIG () $,
                       IF NOT (ISIG=NOT ISIG) THEN RL = -RL $,
                       GOTO C4 $,
                END
                ELSE
              IF HOL(P) EQL 000000300000C  THEN
                  BEGIN  GMUL(PRIME(SINDEX)) $,
                         GOTO C15 $,
                  END  ELSE
                FOR K=0 STEP 1 UNTIL SYMST DO
                  IF HOL(P) EQL (SYM(K) .RS. 18) THEN
                   BEGIN  GMUL(PRIME(K)) $,
                    SIG () $,
                    GOTO C4 $,
                   END $,
                    PRINT F3 $,
                    ERROR = TRUE $,
                    GOTO RETURN $,
```

Figure 47. Listing of Digital Program to Derive Equation for Square of Frequency Response Function (15 of 26)

```
  C4$ P = UNSTAK(PUSH,C13) $,
COMMENT
  IF TERM IS IMAGINARY DO NOT CONSIDER IT.
$,
      IF OP(P) EQL OP(.C. / +     /) THEN
       BEGIN  IF ISIG THEN BEGIN  P = RV(P) $,
                                  GOTO C3 $,
                          END ELSE IF I EQL 0 THEN GOTO C5 ELSE
                          GOTO IF KL EQL 0 THEN C6 ELSE C10 $,
       END
        ELSE
        BEGIN  SIG () $,
               P = RV(P) $,
               GOTO C1 $,
        END $,
COMMENT
  LAST TERM IN EXPRESSION NEEDS SPECIAL HANDLING
$,
 C13$ FLIP = TRUE $,
      IF ISIG THEN GOTO C8$,
      IF KL EQL 0 THEN GOTO C6 ELSE GOTO C10 $,
COMMENT
  TRY COLLECTING TERMS. FIRST TEST FOR SIN**2 + COS**2 REDUCTION, THEN
  FOR COMBINING OF LIKE TERMS.
$,
  C6$ GD = GT(0)  $,
      B1 =  (GD/9) * 9 EQL GD $,
      B2 =  (GD/25) * 25 EQL GD $,
      FOR K=0 STEP 1 UNTIL I DO
             IF (K EQL 0 AND GOEDEL(0) GRT 0 OR K NEQ 0 AND GOEDEL
             (K-1) GRT 0) AND REALL(K) NEQ 0  THEN
             BEGIN  GDT = GOEDEL(K) $,
                    IF B1 AND (GDT/25)*25 EQL GDT AND GDT/25 EQL GD/9
                    OR   B2 AND (GDT/9)*9 EQL GDT AND GDT/9 EQL GD/25
                    THEN  BEGIN    REALL(K) = REALL(K)-RL $,
                                   GD = GD/IF GDT/9 EQL GD/25 THEN 25
                                   ELSE 9  $,
                          END $,
             END $,
      GT(0) = GD $,
COMMENT
  NOW TRY TO COLLECT LIKE TERMS
$,
 C10$ GPOL(GT,T1,0,J1) $,
      J2 = 0 $,
  C9$ GPOL(GOEDEL,T2,J2,J3) $,
      FOR J4=0 STEP 1 UNTIL 9 DO
        BEGIN  IF T1(J4) LEQ 0 AND T2(J4) LEQ 0 AND T1(J4+1) LES 0 AND
               T2(J4+1) LES 0 THEN GOTO C7 $,
               IF T1(J4) NEQ T2(J4) THEN IF J3 GEQ I-1 THEN GOTO C5 ELSE
                 BEGIN  J2 = J3+1 $,
                        GOTO C9 $,
                 END $,
        END $,
COMMENT
  TERMS CAN BE COMBINED.
$,
  C7$ FOR KK=J2 STEP 1 UNTIL J3 DO REALL(KK) = REALL(KK) + RL $,
      GOTO C14 $,
COMMENT
```

Figure 47. Listing of Digital Program to Derive Equation for Square of Frequency Response Function (16 of 26)

```
   CAN'T COMBINE LIKE TERMS. ADD GOEDEL NUMBER(S) TO LIST.
$,
   C5$ FOR KK=0 STEP 1 UNTIL KL DO
         BEGIN  GOEDEL(I) = GT(KK) $,
                REALL(I) = RL $,
                I = I+1 $,
                IF I GRT 1500 THEN BEGIN PRINT F1 $,
                                         PDUMPN () $,
                                         ERROR = TRUE $,
                                         GOTO RETURN $,
                                   END $,
         END $,
 C14$                          IF FLIP THEN GOTO C8 $,
                               P = RV(P) $,
                               GOTO C3 $,
COMMENT
   REPLACE 00 IN SYMBOL TABLE BY BLANK. CHANGE S SYMBOL TO W.
$,
   C8$ FOR N=0 STEP 1 UNTIL SYMST DO
         IF SYM(N) .A. MSK EQL 370000000000C THEN SYM(N) =
         SYM(N) + 000000050505C
         ELSE IF SYM(N) .A. 007777000000C EQL 006160000000C
         THEN SYM(N) = SYM(N) + 000000050505C
         ELSE SYM(N) = SYM(N) + 000005050505C  $,
         SYM(SINDEX) = 340505050505C $,
      I = I-1 $,
      GOTO RETURN $,
  F0$ FORMAT ('0 ILLEGAL CHARACTER IN ADMISSIBLE SYMBOL SET.' ) $,
  F1$ FORMAT ('0 GOEDEL NUMBER TABLE OVERFLOWS.') $,
  F3$ FORMAT ('0 SYMBOL MISSING FROM ADMISSIBLE SYMBOL SET.') $,
      END $,
      END FINI


'P    AED GPOL
      BEGIN
COMMENT
  THIS PROGRAM WAS WRITTEN BY UNITED AIRCRAFT RESEARCH LABORATORIES FOR
  HAMILTON STANDARD, UNDER CONTRACT NAS2-4515 TASK 4, IN THE AED-0
  PROGRAMMING LANGUAGE.

$,
COMMENT
  THIS ROUTINE TAKES ALL GOEDEL NUMBERS INCLUDING THOSE OCCUPYING MORE THAN ONE
  LOCATION AND TRANSFORMS THE GOEDEL NUMBER INTO THE COEFFICIENTS OF A POLY-
  NOMIAL IN POWERS OF 2**35. SINCE THE POLYNOMIAL IS UNIQUE, THIS LETS US TEST
  ALL GOEDEL NUMERS FOR EQUALITY.
$,
      DEFINE PROCEDURE GPOL(IN,T,ISTART,IEND) WHERE INTEGER ARRAY
      IN(300), T(10) $, INTEGER ISTART, IEND TOBE
      BEGIN  INTEGER ARRAY TLO(10), TUP(10) $,
             BOOLEAN ARRAY   OFLO(10) $,
             INTEGER  K1,K2,K3,K4 $,
      FOR K1=0 STEP 1 UNTIL 9 DO T(K1) = TLO(K1) = TUP(K1) = -1 $,
      IF IN(ISTART) GRT 0 THEN
        BEGIN  T(0) = IN(ISTART) $,
               IEND = ISTART  $,
               GOTO RETURN $,
        END $,
      DOUBML(ABS(IN(ISTART)), ABS(IN(ISTART+1)), T(1),T(0)) $,
```

Figure 47. Listing of Digital Program to Derive Equation for Square of Frequency Response Function (17 of 26)

```
IF IN(ISTART+1) GRT 0 THEN
  BEGIN  IEND = ISTART+1 $,
         GOTO RETURN $,
  END $,
FOR K2=2 STEP 1 UNTIL 9 DO
  BEGIN  FOR K3=0 STEP 1 UNTIL K2-1 DO DOUBML(ABS(IN(ISTART+K2)),
         T(K3),TUP(K3+1),TLO(K3)) $,
         T(K2) = TUP(K2) $,
         T(0) = TLO(0) $,
         FOR K4=1 STEP 1 UNTIL K2-1 DO
           BEGIN  T(K4) = TLO(K4) + TUP(K4) $,
                  OFLO(K4)=TLO(K4) + TUP(K4) LES 0 $,
           END $,
         FOR K4=1 STEP 1 UNTIL K2-1 DO IF OFLO(K4) THEN
           BEGIN  T(K4) = T(K4) .A. 377777777777C $,
                  T(K4+1) = T(K4+1) + 1 $,
           END $,
         IF IN(ISTART+K2) GRT 0 THEN BEGIN  IEND = ISTART+K2  $,
                                            GOTO RETURN $,
                                     END $,
  END $,
END $,
END FINI
```

```
•P     AED PRNT
       BEGIN
COMMENT
  THIS PROGRAM WAS WRITTEN BY UNITED AIRCRAFT RESEARCH LABORATORIES FOR
  HAMILTON STANDARD, UNDER CONTRACT NAS2-4515 TASK 4, IN THE AED-O
  PROGRAMMING LANGUAGE.

$,
COMMENT
  THIS ROUTINE PRINTS THE EXPRESSION H(I*W)*H(-I*W) AFTER ALL LIKE TERMS
  HAVE BEEN COLLECTED. EACH GOEDEL NUMBER IN TURN IS DECOMPOSED INTO
  PRIMES, AND THE SYMBOL CORRESPONDING TO EACH PRIME IS PRINTED.
$,
       DEFINE PROCEDURE PRNT TOBE
       BEGIN
       SYNONYMS INTEGER = POINTER $,
       DEFINE PROCEDURE NUMPRT(Q) WHERE REAL Q TOBE
       BEGIN  REAL U $,
              U = Q $,
               U = U+0.0 $,
                IF U EQL (K=U) THEN
           BEGIN  KSP = IF U LES 10.0 THEN 2 ELSE (2.001+ALOG10(U)) $,
COMMENT
  IF NUMERICAL COEFFICIENT IS AN INTEGER, USE LOG BASE 10 TO COMPUTE PROPER
  SPACING. NORMALIZE NUMBER FIRST .
$,
                  ASMDEC(KSP,K) $,
                  ASM.C. (.C. /.0/) $,
           END ELSE ASMFLO (12,U) $,
         END $,
       POINTER COMPONENT RV,LV   $,
       INTEGER COMPONENT OP,    HOL , RHALF $,
       BOOLEAN COMPONENT ATOM,NUM,BSIGN $,
       REAL COMPONENT CONS $,
       PROCEDURE EXIT,MSEA , PDUMPN  , RWT, RTD, WTD $,
       PROCEDURE RDCARD, ASM.C., ASMDEC, ASMBCD, CARET $,
```

Figure 47. Listing of Digital Program to Derive Equation for Square of Frequency Response Function (18 of 26)

```
        PROCEDURE ASMFLO, SETASM, NEWPOS $,
        REAL PROCEDURE ALOG10 $,
        REAL  RL, V $,
        PACK 777777C0,0, SPECIAL COMPONENTS RV $,
        PACK 1C0,0, SPECIAL COMPONENTS ATOM $,
        PACK 777777C18,18, SPECIAL COMPONENTS LV $,
        PACK 77C24,24,SPECIAL COMPONENTS OP $,
        PACK 77C30,30, SPECIAL COMPONENTS BSIGN $,
        PACK 777777C12,12,SPECIAL COMPONENTS HOL $,
        PACK 1C1,1,SPECIAL COMPONENTS NUM $,
        PACK 1C0,0,SPECIAL COMPONENTS ATOM $,
        PACK 777777C0,0, SPECIAL COMPONENTS RHALF $,
        OP $=$ ATOM $=$ BSIGN $=$ 0 $,
        LV $=$ RV $=$ 1 $,
        HOL $=$ NUM $=$ ATOM $=$ BSIGN $=$ 0 $,
        CONS $=$ 1 $,
        RHALF $=$ 0 $,
        INTEGER ARRAY  GOEDEL(1500),PRIME(35),SYM(35),J(72),GT(10) $,
        INTEGER ARRAY  DIG(10) $,
        INTEGER ARRAY SV,ARRAY(6) $,
        COMMON J,ERROR,ANGLE, GOEDEL, REALL, Z, SYM, PRIME, SYMST, DIG,
               NM , I $,
        REAL ARRAY  REALL(1500), NM(10) $,
        BOOLEAN  B1,B2,Y, FLIP, SW, SW1, ISIG, ERROR  $,
        INTEGER I,T,K,L,M,EX,R,SYMST , MSK , N,SINDEX $,
        INTEGER  KK,KL,II, KN,GD  ,GDT , JJ, KM $,
        INTEGER  KSP , LK, LJ, LI , JZ $,
        POINTER P, ANGLE , LL, Z $,
        MSEA() $,
        IF ERROR THEN GOTO RETURN $,
        T = .BCD. /       / $,
        PRINT F2 $,
        SW1 = FALSE $,
        SETASM (5,-0,-0,-0,-0,-0 ) $,
        ASM.C.  (.C. /H(W)*H(W)  =  /)  $,
        NEWPOS(19) $,
COMMENT
  FIRST REPLACE S IN ANGLE BY W AND REPLACE O BY BLANK IN OTHER SYMBOLS.
$,
        IF ANGLE NEQ 0 THEN
        FOR LL = LV(ANGLE), RV(ANGLE) DO
        IF HOL(LL) EQL 300000C THEN HOL(LL)  =  HOL(.C. /   W  /)
        ELSE IF HOL(LL) .A. 77C EQL 0C THEN HOL(LL) = HOL(LL) + 5C $,
COMMENT
  SAVE GOEDEL NUMBERS AND COEFFICIENTS ON TAPE
$,
        JZ = 8 $,
        RWT(JZ) $,
        FOR N=0 STEP 1 UNTIL I DO WTD(JZ,F3,GOEDEL(N),REALL(N)) $,
        FOR M=0 STEP 1 UNTIL I DO
          BEGIN IF REALL(M) EQL 0.0 THEN GOTO C11 $,
COMMENT
  BEFORE PRINTING CHECK ANGLE FOR SIGN. THEN APPLY SIN(-X) = -SIN(X) AND
  COS(-X) = COS(X). LOOP TWICE IN CASE OF SIN**2 OR COS**2.
$,
        IF ANGLE EQL 0 THEN GOTO C5 $,
        FOR LI=LV(ANGLE), RV(ANGLE) DO
         BEGIN  IF NOT NUM(LI) THEN GOTO C9 $,
                FOR LJ=0 STEP 1 UNTIL I DO
                 BEGIN  FOR LK=0 STEP 1 UNTIL 1 DO
```

Figure 47. Listing of Digital Program to Derive Equation for Square of Frequency Response Function (19 of 26)

```
                BEGIN IF (GOEDEL(M+LJ)/3)*3 EQL GOEDEL(M+LJ) THEN
                      BEGIN  IF CONS(LI) LES 0.0 THEN
                             BEGIN  REALL(M) = -REALL(M) $,
                                    CONS(LI) = -CONS(LI) $,
                             END $,
                      END $,
                     IF (GOEDEL(M+LJ)/5)*5 EQL GOEDEL(M+LJ) THEN IF
                     CONS(LI) LES 0 THEN CONS(LI) = -CONS(LI) $,
                END $,
                IF GOEDEL(M+LJ) GRT 0 THEN GOTO C5 $,
               END $,
C9$   END $,
C5$            IF REALL(M) LES 0.0 THEN ASM.C. (.C. /    -   /) ELSE
               IF SW1 THEN ASM.C. (.C. /   +   /) $,
               SW1 = TRUE $,
               IF Y = (V=ABS(REALL(M))) NEQ 1.0 OR GOEDEL(M) EQL 1
               THEN NUMPRT(V) $,
               SW = FALSE $,
               FOR L=0 STEP 1 UNTIL SYMST DO
                 BEGIN  EX = 0 $,
                        FOR KN=0 STEP 1 UNTIL I  DO
C10$                    BEGIN  IF (R=GOEDEL(M+KN)/PRIME(L))*PRIME(L)
                               EQL GOEDEL(M+KN) THEN
                                 BEGIN  EX = EX+1 $,
                                        GOEDEL(M+KN) = R $,
                                        GOTO C10 $,
                                 END $,
                               IF GOEDEL(M+KN) GRT 0 THEN GOTO C17 $,
                        END $,
C17$                IF EX EQL 0 THEN GOTO C16 ELSE
                    BEGIN  IF Y OR SW THEN ASM.C. (.C. /*/) $,
                           ASMBCD (0,SYM(L)) $,
                           SW = TRUE $,
                              IF EX GRT 1 THEN
                              BEGIN ASM.C. (.C. /**/) $,
                                    IF EX GRT 9 THEN ASMDEC(3,EX)
                                    ELSE ASMDEC(2,EX) $,
                                    ASM.C. (.C. / /) $,
                              END $,
                    END $,
C16$             END $,
COMMENT
  CHECK FOR PRESENCE OF SIN AND COS TERMS.
$,
      IF ANGLE EQL 0 THEN GOTO C19 $,
      $,
      FOR JJ=3 STEP 2 UNTIL 5 DO
        BEGIN  EX = 0 $,
               FOR KM=0 STEP 1 UNTIL I  DO
C20$    BEGIN  IF (R=GOEDEL(M+KM)/JJ)*JJ EQL GOEDEL(M+KM) THEN
                 BEGIN  EX = EX+1 $,
                        GOEDEL(M+KM) = R $,
                        GOTO C20 $,
                 END $,
               IF GOEDEL(M+KM) GRT 0 THEN GOTO C18 $,
        END $,
C18$           IF EX EQL 0 THEN GOTO C19 ELSE
               BEGIN  IF Y OR SW THEN ASM.C. (.C. /*/) $,
                     IF JJ EQL 3 THEN ASM.C. (.C. /SIN(/) ELSE
                      ASM.C. (.C. /COS(/)   $,
```

Figure 47. Listing of Digital Program to Derive Equation for Square of Frequency Response Function (20 of 26)

```
THE QUOTIENT IS TAKEN AS THE NEW GOEDEL NUMBER, AND THE NUMERICAL
NUMERICAL VALUE OF THE SUBSTITUTED VARIABLE. AFTER ALL SUCH
SUBSTITUTIONS ARE MADE, ALL GOEDEL NUMBERS WHICH WERE LARGER THEN
(2**35)-1 AND CONSEQUENTLY OCCUPY MORE THAN ONE LOCATION ARE TESTED
TO SEE WHETHER THEY ARE NOW LESS THAN (2**35)-1. AN ATTEMPT IS THEN
MADE TO COLLECT LIKE TERMS IN THE NEW EXPRESSION FOR H(I*W) * H(-I*W).
$,
      DEFINE PROCEDURE SUBST TOBE
      BEGIN
      SYNONYMS INTEGER = POINTER $,
      PROCEDURE MSEA, RDCARD, RWT,RTD,WTD, PRNT  $,
      INTEGER  SYMST $,
      INTEGER ARRAY GOEDEL(1500),PRIME(35),SYM(35),P(35),SB(35) $,
      INTEGER ARRAY T1(10), T2(10) $,
      POINTER  ANGLE ,Z, LL $,
      REAL ARRAY  REALL(1500),NMB(35) $,
      REAL  ARRAY  NM(10) $,
      REAL  DCT, NUMBER $,
      BOOLEAN DFLAG,MFLAG,ERROR, CFLAG $,
      COMMON J,ERROR,ANGLE,GOEDEL,REALL,Z,SYM,PRIME,SYMST,   DIG, NM ,
      I $,
      INTEGER   R,  NA,MSK,IA,GTEST,L,JZ,IJ,IK,IL,IM,IN,IO,IP,I,JA,JB $,
      INTEGER  JC,JD,JE ,JF ,JG, IH $,
      INTEGER SCT, VCT, MM, MN , N $,
      INTEGER IQ $,
      INTEGER ARRAY  J(72), DIG(10) $,
      POINTER COMPONENT   RV,LV $,
      INTEGER COMPONENT OP, HOL $,
      BOOLEAN COMPONENT ATOM, NUM, BSIGN  $,
      REAL COMPONENT CONS $,
      PACK 777777C0,0, SPECIAL COMPONENTS RV $,
      PACK 1C0,0, SPECIAL COMPONENTS ATOM $,
      PACK 777777C18,18, SPECIAL COMPONENTS LV $,
      PACK 77C24,24,SPECIAL COMPONENTS OP $,
      PACK 77C30,30, SPECIAL COMPONENTS BSIGN $,
      PACK 777777C12,12,SPECIAL COMPONENTS HOL $,
      PACK 1C1,1,SPECIAL COMPONENTS NUM $,
      PACK 1C0,0,SPECIAL COMPONENTS ATOM $,
      OP $=$ ATOM $=$ BSIGN $=$ 0 $,
      LV $=$ RV $=$ 1 $,
      HOL $=$ NUM $=$ ATOM $=$ BSIGN $=$ 0 $,
      CONS $=$ 1 $,
      MSEA() $,
      MSK = 770000000000C $,
  E0$ READ F2, SCT  $,
      IF SCT EQL 0 THEN GOTO RETURN $,
      FOR MM=1 STEP 1 UNTIL SCT DO
      BEGIN  READ F2, VCT $,
      IA = -1 $,
       FOR MN=1 STEP 1 UNTIL VCT DO
        BEGIN  RDCARD()  $,
               MFLAG = FALSE $,
               IA = IA+1 $,
               FOR NA=1 STEP 1 UNTIL 72 DO
                 BEGIN  IF J(NA) EQL .BCD. / / THEN GOTO E8  $,
                                 IF J(NA) EQL .BCD. /Z/ THEN
                         BEGIN  SB(IA) = (J(NA) .A. MSK) + (J(NA+1)
                                .A. MSK) .RS. 6 + (J(NA+2) .A. MSK)
                                .RS. 12 + 050505C $,
                                NA = NA+2 $,
```

Figure 47. Listing of Digital Program to Derive Equation for Square of Frequency Response Function (22 of 26)

```
                    SW = TRUE $,
COMMENT
  NOW PRINT ANGLE. CHECK FOR 2 CASES, NAMELY ONE NUMERIC,ONE SYMBOLIC
  AND BOTH SYMBOLIC.
$,
                    IF NUM(RV(ANGLE)) THEN
               BEGIN  NUMPRT(CONS(RV(ANGLE))) $,
                         ASM.C. (.C. /*/) $,
                         RHALF(LOC T) = RHALF(LOC HOL(LV(ANGLE))) $,
                         ASMBCD (0,T)  $,
                 END ELSE
                    IF NUM(LV(ANGLE)) THEN
               BEGIN  NUMPRT(CONS(LV(ANGLE))) $,
                         ASM.C. (.C. /*/) $,
                         RHALF(LOC T) = RHALF(LOC HOL(RV(ANGLE))) $,
                         ASMBCD (0,T)  $,
                 END ELSE
                 BEGIN   RHALF(LOC T) = RHALF(LOC HOL(LV(ANGLE))) $,
                         ASMBCD (0,T)  $,
                         ASM.C. (.C. /*/) $,
                         RHALF(LOC T) = RHALF(LOC HOL(RV(ANGLE))) $,
                         ASMBCD (0,T) $,
                 END $,
                    ASM.C. (.C. /)/) $,
                             IF EX GRT 1 THEN
                              BEGIN  ASM.C. (.C. /**/) $,
                                     IF EX GRT 9 THEN ASMDEC(3,EX)
                                     ELSE ASMDEC(2,EX) $,
                                     ASM.C. (.C. / /) $,
                              END $,
               END $,
 C19$    END $,
               IF SV.ARRAY(0) GRT 90 THEN CARET () $,
     M = M+KN $,
 C11$    END $,
     CARET () $,
COMMENT
  RESTORE GOEDEL NUMBERS AND COEFFICIENTS
$,
     RWT(JZ) $,
     FOR N=0 STEP 1 UNTIL I DO RTD(JZ,F3,GOEDEL(N),REALL(N)) $,
     GOTO RETURN  $,
  F2$ FORMAT (//////) $,
  F3$ FORMAT (O12) $,
     END $,
     END FINI

'P   AED SUBST
     BEGIN
COMMENT
  THIS PROGRAM WAS WRITTEN BY UNITED AIRCRAFT RESEARCH LABORATORIES FOR
  HAMILTON STANDARD, UNDER CONTRACT NAS2-4515 TASK 4, IN THE AED-O
  PROGRAMMING LANGUAGE.

$,
COMMENT
  THIS ROUTINE SUBSTITUTES NUMERICAL VALUES FOR ANY OF THE VARIABLES IN
  H(S). THE PRIME CORRESPONDING TO EACH SUCH VARIABLE IS FOUND AND
  DIVIDED INTO EACH GOEDEL NUMBER. IF THE DIVISION LEAVES NO REMAINDER,
  COEFFICIENT CORRESPONDING TO THE GOEDEL NUMBER IS MULTIPLIED BY THE
```

Figure 47. Listing of Digital Program to Derive Equation for Square of Frequency Response Function (21 of 26)

```
                THEN PRINT F1, SB(IJ), NMB(IJ) ELSE PRINT F4,
                SB(IJ), NMB(IJ) $,
                FOR IK=0 STEP 1 UNTIL SYMST DO
                  IF SB(IJ) EQL SYM(IK) THEN
                  BEGIN  P(IJ) = PRIME(IK) $,
                         GOTO E3 $,
                  END $,
                  PRINT F0, SB(IJ) $,
  E3$    END $,
COMMENT
  NOW SUBSTITUTE THE GIVEN NUMERICAL VALUE OF EACH VARIABLE INTO THE
  LIST OF GOEDEL NUMBERS.
$,
      FOR IL=0 STEP 1 UNTIL I DO
      BEGIN  IF REALL(IL) EQL 0.0 THEN GOTO E9 $,
      FOR IM=0 STEP 1 UNTIL IA DO
  E4$ IF (R=GOEDEL(IL)/P(IM))*P(IM) EQL GOEDEL(IL) THEN
        BEGIN  IH = IL $,
  E6$           IF IH-1 GEQ 0 AND GOEDEL(IH-1) LES 0 THEN
                  BEGIN  IH = IH-1 $,
                         GOTO E6 $,
                  END $,
  E5$           REALL(IH) = REALL(IH) * NMB(IM) $,
                IF GOEDEL(IH) LES 0 THEN BEGIN  IH = IH+1 $,
                                                GOTO E5 $,
                                         END $,
                GOEDEL(IL) = R $,
                GOTO E4 $,
        END $,
  E9$ END  $,
COMMENT
  NOW ATTEMPT TO COLLECT TERMS IN THE MODIFIED GOEDEL TABLE.
$,    FOR JA=0 STEP 1 UNTIL I-1 DO
        BEGIN  IF REALL(JA) EQL 0.0 THEN GOTO E12 ELSE
          BEGIN  GPOL(GOEDEL,T1,JA,JB) $,
                 IF JB GEQ I THEN GOTO E14 $,
                 FOR JC=JB+1 STEP 1 UNTIL I DO
                   BEGIN  IF REALL(JC) NEQ 0.0 THEN
                     BEGIN  GPOL(GOEDEL,T2,JC,JD) $,
                            FOR JE=0 STEP 1 UNTIL 9 DO
                            IF T1(JE) LEQ 0 AND T2(JE) LEQ 0 AND
                            T1(JE+1) LES 0 AND T2(JE+1) LES 0 THEN GOTO
                            E10 ELSE IF T1(JE) NEQ T2(JE) THEN IF JD
                            GEQ I THEN GOTO E11 ELSE BEGIN JC = JD $,
                                                        GOTO E13 $,
                                                 END $,
                     END $,
 E13$              END $,
          END $,
          GOTO E11 $,
 E10$                FOR JF=JC STEP 1 UNTIL JD DO
                     REALL(JF) = REALL(JF) + REALL(JA) $,
                     FOR JG=JA STEP 1 UNTIL JB DO REALL(JG) = 0.0 $,
 E11$                JA = JB $,
 E12$    END $,
COMMENT
  CHECK IF ANGLE IS INVOLVED IN SUBSTITUTION.
$,
 E14$ IF ANGLE NEQ 0 THEN FOR IQ=0 STEP 1 UNTIL IA DO
      FOR LL=LV(ANGLE), RV(ANGLE) DO
```

Figure 47. Listing of Digital Program to Derive Equation for Square of Frequency Response Function (24 of 26)

```
                                        GOTO E1 $,
                                  END ELSE IF J(NA+1) EQL DIG(1) AND J(NA+2)
                                        EQL DIG(0) THEN
                                        BEGIN  SB(IA) = (J(NA) .A. MSK) +
                                               (DIG(1) .A. MSK) .RS. 6
                                               + (DIG(0) .A. MSK) .RS. 12
                                               + 050505C  $,
                                               NA = NA+2 $,
                                               GOTO E1 $,
                                        END ELSE
                                        BEGIN  SB(IA) = (J(NA) .A. MSK) +
                                               (J(NA+1) .A. MSK) .RS. 6
                                               + 05050505C $,
                                               NA = NA+1 $,
                                               GOTO E1 $,
                                        END $,
  E1$                           NA = NA+1 $,
                                IF J(NA) EQL .BCD. / / OR J(NA) EQL .BCD. /+/
                                OR J(NA) EQL .BCD. /=/ THEN GOTO E1 $,
                                IF J(NA) EQL .BCD. /-/ THEN BEGIN MFLAG =TRUE $,
                                                                GOTO E1 $,
                                                           END $,
                                FOR L=0 STEP 1 UNTIL 9 DO
              BEGIN             IF J(NA) EQL DIG(L) THEN
                BEGIN           NUMBER  = 0.0  $,
                                DCT = 0.0 $,
                                DFLAG = FALSE $,
  E2$                           NUMBER = 10*NUMBER + NM(L) $,
                                IF DFLAG THEN DCT = DCT+1.0 $,
                                IF J(NA+1) EQL .BCD. /./ THEN
                                  BEGIN  DFLAG = TRUE $,
                                         NA = NA+1 $,
                                  END $,
                                FOR L=0 STEP 1 UNTIL 9 DO
                                IF J(NA+1) EQL DIG(L) THEN BEGIN  NA = NA+1 $,
                                                                  GOTO E2 $,
                                                           END $,
                                NMB(IA) = 10.0**(-DCT)*NUMBER *(IF MFLAG THEN
                                -1.0 ELSE 1.0)  $,
                                GOTO E7  $,
                END  $,
              END $,
                PRINT F5, J(NA) $,
  E8$                END $,
  E7$    END $,
COMMENT
  AT THIS POINT, SB AND NMB ARE ARRAYS CONTAINING RESPECTIVELY, THE
  NAMES OF THE VARIABLES TO BE SUBSTITUTED FOR, AND THEIR NUMERICAL
  VALUES. NOW SAVE GOEDEL NUMBERS AND COEFFICIENTS ON TAPE.
$,
      IF ERROR THEN GOTO RETURN $,
      PRINT F3 $,
      JZ = 9 $,
      RWT(JZ) $,
      FOR N=0 STEP 1 UNTIL I DO  WTD(JZ,F6 ,GOEDEL(N),REALL(N)) $,
COMMENT
  NOW FIND THE PRIMES ASSOCIATED WITH THE VARIABLES.
$,
      FOR IJ=0 STEP 1 UNTIL IA DO
        BEGIN  IF ABS(NMB(IJ)) GEQ 10000.0 OR ABS(NMB(IJ)) LES 0.0001
```

Figure 47. Listing of Digital Program to Derive Equation for Square of Frequency Response Function (23 of 26)

```
        IF NOT NUM(LL) AND SB(IQ) .RS. 18 EQL HOL(LL) THEN
          BEGIN  NUM(LL) = TRUE $,
                 CONS(LL) = NMB(IQ) $,
          END $,
        PRNT () $,
COMMENT
  NOW RESTORE GOEDEL TABLE TO ORIGINAL CONDITION.
$,
        RWT(JZ) $,
        FOR N=0 STEP 1 UNTIL I DO  RTD(JZ,F6 ,GOEDEL(N),REALL(N)) $,
        END $,
        GOTO RETURN $,
  F0$ FORMAT ('0THE SYMBOL 'A6, ' DOES NOT APPEAR IN H(S). ') $,
  F1$ FORMAT ('0    ' A6, ' = ' E15.5) $,
  F2$ FORMAT (I3) $,
  F3$ FORMAT (///////'0 THE FOLLOWING NUMERICAL SUBSTITUTIONS WILL NOW BE MADE.'
 //) $,
  F4$ FORMAT ('0    ' A6, ' = ' F15.5) $,
  F5$ FORMAT('0 THE ILLEGAL CHARACTER 'A6, ' APPEARED ON THE RIGHT HAND SIDE OF
THE EQUAL SIGN DURING THE SUBSTITUTION. ' ) $,
  F6$ FORMAT (O12) $,
        END $,
        END FINI

'ILP   ASM    DOUBML/ASM,DOUBML
                 REGNAM
DOUBML*   J        $+1           .
          LMJ        13,SETUP$   .
          +        4,CSBD        .
                L      A0,*AA    .
                MI     A0,*BB    .
                LDSC   A0,1      .
                SSL    A1,1      .
                S      A0,*CC    .
                S      A1,*DD    .
          LMJ      B11,*CSBD     .
CSBD      +        0700000000    .
          +        0             .
          +        0             .
AA        +        0             .
BB        +        0             .
CC        +        0             .
DD        +        0             .
                END
```

Figure 47. Listing of Digital Program to Derive Equation for Square of Frequency Response Function (25 of 26)

```
.P AND STAKS
      BEGIN
COMMENT
  THIS PROGRAM WAS WRITTEN BY UNITED AIRCRAFT RESEARCH LABORATORIES FOR
  HAMILTON STANDARD, UNDER CONTRACT NAS2-4515 TASK 4, IN THE AED-0
  PROGRAMMING LANGUAGE.

$,
      POINTER PROCEDURE STINIT, UNSTAK $,
      PROCEDURE STKSX $,
      POINTER PROCEDURE FREZ1 $,
      PROCEDURE FRET1 $,
       BEGIN   POINTER TEMP, STAKZON $,
               POINTER COMPONENT  NEXT, STACKED $,
               SYNONYMS  777777C = ENDSTR $,




            PACK 777777C,0,SPECIAL COMPONENTS NEXT $,
            PACK 777777C18,18,SPECIAL COMPONENTS STACKED $,
            NEXT $=$ STACKED $=$ 0 $,
      DEFINE POINTER PROCEDURE STINIT TOBE
        BEGIN   STAKZON = SETFR1(100,50,0,1,0,0) $,
                NEXT(STINIT=FREZ1(STAKZON)) = ENDSTR $,
        END $,
      DEFINE PROCEDURE STKSX(STAK,P) WHERE POINTER P,STAK TOBE
        BEGIN   NEXT(TEMP=FREZ1(STAKZON)) = NEXT(STAK) $,
                NEXT(STAK) = TEMP $,
                STACKED(TEMP) = P $,
        END $.
      DEFINE POINTER PROCEDURE UNSTAK(STAK,EMPTY) WHERE POINTER STAK $,
      POINTER PROCEDURE EMPTY TOBE
        IF NEXT(STAK) EQL ENDSTR THEN UNSTAK = EMPTY(STAK)
        ELSE BEGIN  UNSTAK = STACKED(TEMP=NEXT(STAK)) $,
                    NEXT(STAK) = NEXT(TEMP) $,
                    FRET1(TEMP,STAKZON) $,
             END $,
       END $,
      END FINI
```

Figure 47. Listing of Digital Program to Derive Equation for Square of Frequency Response Function (26 of 26)

```
C H1*(-FTH*C2+H2) + C1*(C4*H2*H4 - C2*C3*H3) OF SHOCK POSITION TR. FCN.
C IN FORM H2(H1+C1*C4*H4) + H1*(-FTH)*C2 + C1*(-C2)*C3*H3
C H1 =W3*S     H2 =(1+Z1W*S+W1**2*S**2)(1+T1*S)(1+T2*S)S     H3 =1+T4*S
C H4 =1+T5*S+T6*S**2     C6 =C1*C4     T3 =W3+C1*C4*T5     W2 =C1*C4*T6
C C5 =-FTH*C2     C6 =C1*C4     C7 =-C1*C2*C3
(1+S*Z1W+S*S*W1*W1)*(1+T1*S)*(1+T2*S)*S*(C6+T3*S+W2*S*S) + W3*C5*S +
 C7*(1+T4*S) $
S Z1W W1 T1 T2 C6 T3 W2 W3 C5 T4 C7 $
  1
 11
    Z1W= 0.015
    W1  = 0.01
    T1  = 0.002
    T2  = 0.01
    C6  = 17.21647
    T3  = 0.26239676
    W2  = 0.0002286519
    W3  = 0.34
    C5  = 20
    T4  = 0.0009367
    C7  = 677.646788
CTEST CASE OF ALGEBRAIC PROGRAM FOR REPRESENTATIVE INLET
C H5*H7 + C5*H6 OF SHOCK POSITION TRANSFER FUNCTION
(T1*S+1)*(T2*S+1)*(C1*C1*S*S+C2*S+1)*(T5*S*S*S+T4*S*S+T3*S+1)*S +
  C3*(T6*S+1)*E(-T7*S) $
S T1 T2 C1 C2 T5 T4 T3 C3 T6 T7 $
  5
 10
  C3  = 5.
  T1  = 0.02
  T2  = 0.01
  C1  = 0.01
  C2  = 0.015
  T5  = 0.00000026830
  T4  = 0.00010504
  T3  = 0.018987
  T6  = -0.0009367
  T7  = 0.0073
 10
  C3  = 10.
  T1  = 0.02
  T2  = 0.01
  C1  = 0.01
  C2  = 0.015
  T5  = 0.00000026830
  T4  = 0.00010504
  T3  = 0.018987
  T6  = -0.0009367
  T7  = 0.0073
 10
  C3  = 10.
  T1  = 0.002
  T2  = 0.01
  C1  = 0.01
  C2  = 0.015
  T5  = 0.00000026830
  T4  = 0.00010504
  T3  = 0.018987
  T6  = -0.0009367
  T7  = 0.0073
```

Figure 48. Listing of Input Cards for Four Sample Cases (Page 1 of 2)

4 9

```
 10
  C3  =  10.
  T1  =  0.002
  T2  =  0.01
  C1  =  0.01
  C2  =  0.015
  T5  =  0.00000026830
  T4  =  0.00010504
  T3  =  0.018987
  T6  =  0.029
  T7  =  0.0073
 10
  C3  =  15.
  T1  =  0.02
  T2  =  0.01
  C1  =  0.01
  C2  =  0.015
  T5  =  0.00000026830
  T4  =  0.00010504
  T3  =  0.018987
  T6  =  -0.0009367
  T7  =  0.0073
CTEST CASE OF ALGEBRAIC PROGRAM FOR REPRESENTATIVE INLET
C   REPRESENTS (H2 - FTH*C2) OF TRANSFER FUNCTION
C   FIRST 2 SETS OF SUBSTITUTIONS SHOW EFFECT OF VARYING VELOCITY
C      CONSTANT OF THROAT MACH CONTROL , THIRD SET SHOWS EFFECT OF
C      DECREASING PRESSURE LEVEL . LAST OF ADDING LEAD
   (S*S*W1*W1 + S*Z1W + 1) * (S*T1 + 1) * (S*T2 + 1) * S + C2   $
   S W1 Z1W T1 T2 C2   $
   4
   5
   W1  =0.01
   Z1W  =0.015
   T1  =0.02
   T2  =0.01
   C2  =  10
   5
   W1  =0.01
   Z1W  =0.015
   T1  =0.02
   T2  =0.01
   C2  =  30
   5
   W1  =0.01
   Z1W  =0.045
   T1  =0.03
   T2  =0.01
   C2  =  20
   5
   W1  =0.01
   Z1W  =0.015
   T1  =0.002
   T2  =0.01
   C2  =  20
CTEST CASE OF ALGEBRAIC PROGRAM FOR REPRESENTATIVE INLET
C   REPRESENTS (H2 - FTH*C2) OF TRANSFER FUNCTION
   (S*S*0.0001 + S*0.015 + 1) * (S*0.02 + 1) * (S*0.01 + 1) * S + 20.   $
   S $
   0
$
```

Figure 48. Listing of Input Cards for Four Sample Cases (Page 2 of 2)

THIS PROGRAM WAS WRITTEN BY UNITED AIRCRAFT RESEARCH LABORATORIES FOR HAMILTON STANDARD, UNDER CONTRACT NAS2-4515 TO PERFORM CERTAIN ALGEBRAIC MANIPULATIONS OF TRANSFER FUNCTIONS

Figure 49. Output of Program to Derive Equation for Square of Frequency Response Function for Four Sample Cases (Page 1 of 12)

```
H1*(-FTH*C2+H2) + C1*(C4*H2*H4 - C2*C3*H3) OF SHOCK POSITION TR. FCN.
IN FORM H2(H1+C1*C4*H4) + H1*(-FTH)*C2 + C1*(-C2)*C3*H3
H1 =W3*S     H2 =(1+Z1W*S+W1**2*S**2)(1+T1*S)(1+T2*S)S     H3 =1+T4*S
H4 =1+T5*S+T6*S**2     C6 =C1*C4     T3 =W3+C1*C4*T5     W2 =C1*C4*T6
C5 =-FTH*C2     C6 =C1*C4     C7 =-C1*C2*C3


 H(S) = (1+S*Z1W+S*S*W1*W1)*(1+T1*S)*(1+T2*S)*S*(C6+T3*S+W2*S*S)+W3*C5*S+C7*(1+T4*S)
```

```
H(W)*H(W)  =  W** 2 *C6** 2   +  W** 4 *Z1W** 2 *C6** 2   -  2.0*W** 4 *W1** 2 *C6** 2   +  W** 6 *W1** 4
              *C6** 2   +  W** 4 *T1** 2 *C6** 2   -  2.0*W** 6 *W1** 2 *T1** 2 *C6** 2   +  W** 6 *Z1W**
               2 *T1** 2 *C6** 2   +  W** 8 *W1** 4 *T1** 2 *C6** 2   +  W** 4 *T2** 2 *C6** 2   -  2.0*W
              ** 6 *W1** 2 *T2** 2 *C6** 2   +  W** 6 *Z1W** 2 *T2** 2 *C6** 2   +  W** 8 *W1** 4 *T2** 2
              *C6** 2   +  W** 6 *T1** 2 *T2** 2 *C6** 2   -  2.0*W** 8 *W1** 2 *T1** 2 *T2** 2 *C6** 2
                +  W** 8 *Z1W** 2 *T1** 2 *T2** 2 *C6** 2   +  W** 10 *W1** 4 *T1** 2 *T2** 2 *C6** 2
                +  W** 4 *T3** 2   -  2.0*W** 6 *W1** 2 *T3** 2   +  W** 6 *Z1W** 2 *T3** 2   +  W** 8 *W1
              ** 4 *T3** 2   +  W** 6 *T1** 2 *T3** 2   -  2.0*W** 8 *W1** 2 *T1** 2 *T3** 2   +  W** 8 *
              Z1W** 2 *T1** 2 *T3** 2   +  W** 10 *W1** 4 *T1** 2 *T3** 2   +  W** 6 *T2** 2 *T3** 2   -
              2.0*W** 8 *W1** 2 *T2** 2 *T3** 2   +  W** 8 *Z1W** 2 *T2** 2 *T3** 2   +  W** 10 *W1** 4 *
              T2** 2 *T3** 2   +  W** 8 *T1** 2 *T2** 2 *T3** 2   -  2.0*W** 10 *W1** 2 *T1** 2 *T2** 2 *
              T3** 2   +  W** 10 *Z1W** 2 *T1** 2 *T2** 2 *T3** 2   +  W** 12 *W1** 4 *T1** 2 *T2** 2 *T3
              ** 2   -  2.0*W** 4 *C6*W2  +  4.0*W** 6 *W1** 2 *C6*W2  -  2.0*W** 6 *Z1W** 2 *C6*W2  -  2
              .0*W** 8 *W1** 4 *C6*W2  -  2.0*W** 6 *T1** 2 *C6*W2  +  4.0*W** 8 *W1** 2 *T1** 2 *C6*W2
                -  2.0*W** 8 *Z1W** 2 *T1** 2 *C6*W2  -  2.0*W** 10 *W1** 4 *T1** 2 *C6*W2  -  2.0*W** 6 *
              T2** 2 *C6*W2  +  4.0*W** 8 *W1** 2 *T2** 2 *C6*W2  -  2.0*W** 8 *Z1W** 2 *T2** 2 *C6*W2
                -  2.0*W** 10 *W1** 4 *T2** 2 *C6*W2  -  2.0*W** 8 *T1** 2 *T2** 2 *C6*W2  +  4.0*W** 10 *
              W1** 2 *T1** 2 *T2** 2 *C6*W2  -  2.0*W** 10 *Z1W** 2 *T1** 2 *T2** 2 *C6*W2  -  2.0*W** 12
              *W1** 4 *T1** 2 *T2** 2 *C6*W2  +  W** 6 *W2** 2   -  2.0*W** 8 *W1** 2 *W2** 2   +  W** 8 *
              Z1W** 2 *W2** 2   +  W** 10 *W1** 4 *W2** 2   +  W** 8 *T1** 2 *W2** 2   -  2.0*W** 10 *W1**
               2 *T1** 2 *W2** 2   +  W** 10 *Z1W** 2 *T1** 2 *W2** 2   +  W** 12 *W1** 4 *T1** 2 *W2** 2
                +  W** 8 *T2** 2 *W2** 2   -  2.0*W** 10 *W1** 2 *T2** 2 *W2** 2   +  W** 10 *Z1W** 2 *T2
              ** 2 *W2** 2   +  W** 12 *W1** 4 *T2** 2 *W2** 2   +  W** 10 *T1** 2 *T2** 2 *W2** 2   -  2
              .0*W** 12 *W1** 2 *T1** 2 *T2** 2 *W2** 2   +  W** 12 *Z1W** 2 *T1** 2 *T2** 2 *W2** 2   +
              W** 14 *W1** 4 *T1** 2 *T2** 2 *W2** 2   +  2.0*W** 2 *C6*W3*C5  -  2.0*W** 4 *W1** 2 *C6*W3
              *C5  -  2.0*W** 4 *Z1W*T1*C6*W3*C5  -  2.0*W** 4 *Z1W*T2*C6*W3*C5  -  2.0*W** 4 *T1*T2*C6*W3
              *C5  +  2.0*W** 6 *W1** 2 *T1*T2*C6*W3*C5  -  2.0*W** 4 *Z1W*T3*W3*C5  -  2.0*W** 4 *T1*T3*
              W3*C5  +  2.0*W** 6 *W1** 2 *T1*T3*W3*C5  -  2.0*W** 4 *T2*T3*W3*C5  +  2.0*W** 6 *W1** 2 *
              T2*T3*W3*C5  +  2.0*W** 6 *Z1W*T1*T2*T3*W3*C5  -  2.0*W** 4 *W2*W3*C5  +  2.0*W** 6 *W1** 2
              *W2*W3*C5  +  2.0*W** 6 *Z1W*T1*W2*W3*C5  +  2.0*W** 6 *Z1W*T2*W2*W3*C5  +  2.0*W** 6 *T1*T2
              *W2*W3*C5  -  2.0*W** 8 *W1** 2 *T1*T2*W2*W3*C5  +  2.0*W** 2 *C6*T4*C7  -  2.0*W** 2 *Z1W*
              C6*C7  -  2.0*W** 4 *W1** 2 *C6*T4*C7  -  2.0*W** 2 *T1*C6*C7  -  2.0*W** 4 *Z1W*T1*C6*T4*C7
                +  2.0*W** 4 *W1** 2 *T1*C6*C7  -  2.0*W** 2 *T2*C6*C7  -  2.0*W** 4 *Z1W*T2*C6*T4*C7  +
              2.0*W** 4 *W1** 2 *T2*C6*C7  -  2.0*W** 4 *T1*T2*C6*T4*C7  +  2.0*W** 4 *Z1W*T1*T2*C6*C7
                +  2.0*W** 6 *W1** 2 *T1*T2*C6*T4*C7  -  2.0*W** 2 *T3*C7  -  2.0*W** 4 *Z1W*T3*T4*C7  +
              2.0*W** 4 *W1** 2 *T3*C7  -  2.0*W** 4 *T1*T3*T4*C7  +  2.0*W** 4 *Z1W*T1*T3*C7  +  2.0*W**
               6 *W1** 2 *T1*T3*T4*C7  -  2.0*W** 4 *T2*T3*T4*C7  +  2.0*W** 4 *Z1W*T2*T3*C7  +  2.0*W** 6
               *W1** 2 *T2*T3*T4*C7  +  2.0*W** 4 *T1*T2*T3*C7  +  2.0*W** 6 *Z1W*T1*T2*T3*T4*C7  -  2.0*W
              ** 6 *W1** 2 *T1*T2*T3*C7  -  2.0*W** 4 *W2*T4*C7  +  2.0*W** 4 *Z1W*W2*C7  +  2.0*W** 6 *W1
              ** 2 *W2*T4*C7  +  2.0*W** 4 *T1*W2*C7  +  2.0*W** 6 *Z1W*T1*W2*T4*C7  -  2.0*W** 6 *W1** 2
              *T1*W2*C7  +  2.0*W** 4 *T2*W2*C7  +  2.0*W** 6 *Z1W*T2*W2*T4*C7  -  2.0*W** 6 *W1** 2 *T2*
              W2*C7  +  2.0*W** 6 *T1*T2*W2*T4*C7  -  2.0*W** 6 *Z1W*T1*T2*W2*C7  -  2.0*W** 8 *W1** 2 *T1
```

Figure 49. Output of Program to Derive Equation for Square of Frequency Response Function for Four Sample Cases (Page 2 of 12)

```
*T2*W2*T4*C7  +  W** 2 *W3** 2 *C5** 2   +  2.0*W** 2 *W3*C5*T4*C7  +  C7** 2   +  W** 2 *T4
** 2 *C7** 2
```

THE FOLLOWING NUMERICAL SUBSTITUTIONS WILL NOW BE MADE.

```
Z1W    =        .01500
W1     =        .01000
T1     =        .00200
T2     =        .01000
C6     =      17.21647
T3     =        .26240
W2     =        .00023
W3     =        .34000
C5     =      20.00000
T4     =        .00094
C7     =     677.64678
```

```
H(W)*H(W)  =   6.58931E-14*W** 10   +   2.98811E-19*W** 12   +   2.09126E-25*W** 14   +   6.37236E-02*W**
               4  +   1.79803E-05*W** 6   +   1.10389E-09*W** 8   +   4.59205E 05  -   3.77942E 02*W** 2
```

THE TIMES TAKEN BY THE VARIOUS SUBROUTINES ARE:

```
PARSE:      1.0 SECONDS
ALGEB:     31.0 SECONDS
COLECT:    35.0 SECONDS
PRNT:      12.0 SECONDS

SUBST:     20.0 SECONDS

TOTAL:     99.0 SECONDS
```

Figure 49. Output of Program to Derive Equation for Square of Frequency Response Function for Four Sample Cases (Page 3 of 12)

```
TEST CASE OF ALGEBRAIC PROGRAM FOR REPRESENTATIVE INLET
H5*H7 + C5*H6 OF SHOCK POSITION TRANSFER FUNCTION


H(S) = (T1*S+1)*(T2*S+1)*(C1*C1*S*S+C2*S+1)*(T5*S*S*S+T4*S*S+T3*S+1)*S+C3*(T6*S+1)*E(-T7*S)


H(W)*H(W)  =  W** 16 *T1** 2 *T2** 2 *C1** 4 *T5** 2   +  W** 14 *T2** 2 *C1** 4 *T5** 2   +  W** 14 *T1**
               2 *C1** 4 *T5** 2   +  W** 12 *C1** 4 *T5** 2   +  W** 14 *T1** 2 *T2** 2 *C2** 2 *T5** 2
                +  W** 12 *T2** 2 *C2** 2 *T5** 2   +  W** 12 *T1** 2 *C2** 2 *T5** 2   +  W** 10 *C2** 2
              *T5** 2   -  2.0*W** 14 *T1** 2 *T2** 2 *C1** 2 *T5** 2   -  2.0*W** 12 *T2** 2 *C1** 2 *T5
              ** 2   -  2.0*W** 12 *T1** 2 *C1** 2 *T5** 2   -  2.0*W** 10 *C1** 2 *T5** 2   +  W** 12 *T1
              ** 2 *T2** 2 *T5** 2   +  W** 10 *T2** 2 *T5** 2   +  W** 10 *T1** 2 *T5** 2   +  W** 8 *T5
              ** 2   +  W** 14 *T1** 2 *T2** 2 *C1** 4 *T4** 2   -  2.0*W** 12 *T1** 2 *T2** 2 *C1** 2 *T4
              ** 2   +  W** 12 *T2** 2 *C1** 4 *T4** 2   -  2.0*W** 10 *T2** 2 *C1** 2 *T4** 2   +  W** 12
               *T1** 2 *C1** 4 *T4** 2   -  2.0*W** 10 *T1** 2 *C1** 2 *T4** 2   +  W** 10 *C1** 4 *T4** 2
                 -  2.0*W** 8 *C1** 2 *T4** 2   +  W** 12 *T1** 2 *T2** 2 *C2** 2 *T4** 2   +  W** 10 *T2
              ** 2 *C2** 2 *T4** 2   +  W** 10 *T1** 2 *C2** 2 *T4** 2   +  W** 8 *C2** 2 *T4** 2   +  W**
               10 *T1** 2 *T2** 2 *T4** 2   +  W** 8 *T2** 2 *T4** 2   +  W** 8 *T1** 2 *T4** 2   +  W** 6
               *T4** 2   -  2.0*W** 14 *T1** 2 *T2** 2 *C1** 4 *T5*T3  +  4.0*W** 12 *T1** 2 *T2** 2 *C1**
               2 *T5*T3  -  2.0*W** 12 *T2** 2 *C1** 4 *T5*T3  +  4.0*W** 10 *T2** 2 *C1** 2 *T5*T3  -  2
              .0*W** 12 *T1** 2 *C1** 4 *T5*T3  +  4.0*W** 10 *T1** 2 *C1** 2 *T5*T3  -  2.0*W** 10 *C1**
               4 *T5*T3  +  4.0*W** 8 *C1** 2 *T5*T3  -  2.0*W** 12 *T1** 2 *T2** 2 *C2** 2 *T5*T3  -  2.0
              *W** 10 *T2** 2 *C2** 2 *T5*T3  -  2.0*W** 10 *T1** 2 *C2** 2 *T5*T3  -  2.0*W** 8 *C2** 2 *
              T5*T3  -  2.0*W** 10 *T1** 2 *T2** 2 *T5*T3  -  2.0*W** 8 *T2** 2 *T5*T3  -  2.0*W** 8 *T1**
               2 *T5*T3  -  2.0*W** 6 *T5*T3  +  W** 12 *T1** 2 *T2** 2 *C1** 4 *T3** 2   -  2.0*W** 10 *
              T1** 2 *T2** 2 *C1** 2 *T3** 2   +  W** 10 *T2** 2 *C1** 4 *T3** 2   -  2.0*W** 8 *T2** 2 *
              C1** 2 *T3** 2   +  W** 10 *T1** 2 *C1** 4 *T3** 2   -  2.0*W** 8 *T1** 2 *C1** 2 *T3** 2
                +  W** 8 *C1** 4 *T3** 2   -  2.0*W** 6 *C1** 2 *T3** 2   +  W** 10 *T1** 2 *T2** 2 *C2**
               2 *T3** 2   +  W** 8 *T2** 2 *C2** 2 *T3** 2   +  W** 8 *T1** 2 *C2** 2 *T3** 2   +  W** 6
              *C2** 2 *T3** 2   +  W** 8 *T1** 2 *T2** 2 *T3** 2   +  W** 6 *T2** 2 *T3** 2   +  W** 6 *T1
              ** 2 *T3** 2   +  W** 4 *T3** 2   -  2.0*W** 12 *T1** 2 *T2** 2 *C1** 4 *T4  +  4.0*W** 10 *
              T1** 2 *T2** 2 *C1** 2 *T4  -  2.0*W** 10 *T2** 2 *C1** 4 *T4  +  4.0*W** 8 *T2** 2 *C1** 2
              *T4  -  2.0*W** 10 *T1** 2 *C1** 4 *T4  +  4.0*W** 8 *T1** 2 *C1** 2 *T4  -  2.0*W** 8 *C1**
               4 *T4  +  4.0*W** 6 *C1** 2 *T4  -  2.0*W** 10 *T1** 2 *T2** 2 *C2** 2 *T4  -  2.0*W** 8 *
              T2** 2 *C2** 2 *T4  -  2.0*W** 8 *T1** 2 *C2** 2 *T4  -  2.0*W** 6 *C2** 2 *T4  -  2.0*W** 8
               *T1** 2 *T2** 2 *T4  -  2.0*W** 6 *T2** 2 *T4  -  2.0*W** 6 *T1** 2 *T4  -  2.0*W** 4 *T4
                +  W** 10 *T1** 2 *T2** 2 *C1** 4   -  2.0*W** 8 *T1** 2 *T2** 2 *C1** 2   +  W** 8 *T2**
               2 *C1** 4   -  2.0*W** 6 *T2** 2 *C1** 2   +  W** 8 *T1** 2 *C1** 4   -  2.0*W** 6 *T1** 2
              *C1** 2   +  W** 6 *C1** 4   -  2.0*W** 4 *C1** 2   +  W** 8 *T1** 2 *T2** 2 *C2** 2   +  W
              ** 6 *T2** 2 *C2** 2   +  W** 6 *T1** 2 *C2** 2   +  W** 4 *C2** 2   +  W** 6 *T1** 2 *T2**
               2   +  W** 4 *T2** 2   +  W** 4 *T1** 2   +  W** 2   +  2.0*W** 8 *T1*T2*C1** 2 *T5*C3*COS(
              T7*W)  +  2.0*W** 9 *T1*T2*C1** 2 *T5*C3*T6*SIN(T7*W)  -  2.0*W** 8 *T2*C1** 2 *T5*C3*T6*
              COS(T7*W)  +  2.0*W** 7 *T2*C1** 2 *T5*C3*SIN(T7*W)  -  2.0*W** 8 *T1*C1** 2 *T5*C3*T6*COS(
              T7*W)  +  2.0*W** 7 *T1*C1** 2 *T5*C3*SIN(T7*W)  -  2.0*W** 6 *C1** 2 *T5*C3*COS(T7*W)  -  2
              .0*W** 7 *C1** 2 *T5*C3*T6*SIN(T7*W)  -  2.0*W** 8 *T1*T2*C2*T5*C3*T6*COS(T7*W)  +  2.0*W**
               7 *T1*T2*C2*T5*C3*SIN(T7*W)  -  2.0*W** 6 *T2*C2*T5*C3*COS(T7*W)  -  2.0*W** 7 *T2*C2*T5*C3
              *T6*SIN(T7*W)  -  2.0*W** 6 *T1*C2*T5*C3*COS(T7*W)  -  2.0*W** 7 *T1*C2*T5*C3*T6*SIN(T7*W)
                +  2.0*W** 6 *C2*T5*C3*T6*COS(T7*W)  -  2.0*W** 5 *C2*T5*C3*SIN(T7*W)  -  2.0*W** 6 *T1*T2
              *T5*C3*COS(T7*W)  -  2.0*W** 7 *T1*T2*T5*C3*T6*SIN(T7*W)  +  2.0*W** 6 *T2*T5*C3*T6*COS(T7*W
              )  -  2.0*W** 5 *T2*T5*C3*SIN(T7*W)  +  2.0*W** 6 *T1*T5*C3*T6*COS(T7*W)  -  2.0*W** 5 *T1*
              T5*C3*SIN(T7*W)  +  2.0*W** 4 *T5*C3*COS(T7*W)  +  2.0*W** 5 *T5*C3*T6*SIN(T7*W)  -  2.0*W**
```

Figure 49. Output of Program to Derive Equation for Square of Frequency Response Function for Four Sample Cases (Page 4 of 12)

```
 8 *T1*T2*C1** 2 *T4*C3*T6*COS(T7*W)  +  2.0*W** 7 *T1*T2*C1** 2 *T4*C3*SIN(T7*W)  -  2.0*W
** 6 *T2*C1** 2 *T4*C3*COS(T7*W)  -  2.0*W** 7 *T2*C1** 2 *T4*C3*T6*SIN(T7*W)  -  2.0*W** 6
*T1*C1** 2 *T4*C3*COS(T7*W)  -  2.0*W** 7 *T1*C1** 2 *T4*C3*T6*SIN(T7*W)  +  2.0*W** 6 *C1**
 2 *T4*C3*T6*COS(T7*W)  -  2.0*W** 5 *C1** 2 *T4*C3*SIN(T7*W)  -  2.0*W** 6 *T1*T2*C2*T4*C3*
COS(T7*W)  -  2.0*W** 7 *T1*T2*C2*T4*C3*T6*SIN(T7*W)  +  2.0*W** 6 *T2*C2*T4*C3*T6*COS(T7*W)
  -  2.0*W** 5 *T2*C2*T4*C3*SIN(T7*W)  +  2.0*W** 6 *T1*C2*T4*C3*T6*COS(T7*W)  -  2.0*W** 5
*T1*C2*T4*C3*SIN(T7*W)  +  2.0*W** 4 *C2*T4*C3*COS(T7*W)  +  2.0*W** 5 *C2*T4*C3*T6*SIN(T7*W
)  +  2.0*W** 6 *T1*T2*T4*C3*T6*COS(T7*W)  -  2.0*W** 5 *T1*T2*T4*C3*SIN(T7*W)  +  2.0*W** 4
 *T2*T4*C3*COS(T7*W)  +  2.0*W** 5 *T2*T4*C3*T6*SIN(T7*W)  +  2.0*W** 4 *T1*T4*C3*COS(T7*W)
  +  2.0*W** 5 *T1*T4*C3*T6*SIN(T7*W)  -  2.0*W** 4 *T4*C3*T6*COS(T7*W)  +  2.0*W** 3 *T4*C3
*SIN(T7*W)  -  2.0*W** 6 *T1*T2*C1** 2 *T3*C3*COS(T7*W)  -  2.0*W** 7 *T1*T2*C1** 2 *T3*C3*
T6*SIN(T7*W)  +  2.0*W** 6 *T2*C1** 2 *T3*C3*T6*COS(T7*W)  -  2.0*W** 5 *T2*C1** 2 *T3*C3*
SIN(T7*W)  +  2.0*W** 6 *T1*C1** 2 *T3*C3*T6*COS(T7*W)  -  2.0*W** 5 *T1*C1** 2 *T3*C3*SIN(
T7*W)  +  2.0*W** 4 *C1** 2 *T3*C3*COS(T7*W)  +  2.0*W** 5 *C1** 2 *T3*C3*T6*SIN(T7*W)  +  2
.0*W** 6 *T1*T2*C2*T3*C3*T6*COS(T7*W)  -  2.0*W** 5 *T1*T2*C2*T3*C3*SIN(T7*W)  +  2.0*W** 4
*T2*C2*T3*C3*COS(T7*W)  +  2.0*W** 5 *T2*C2*T3*C3*T6*SIN(T7*W)  +  2.0*W** 4 *T1*C2*T3*C3*
COS(T7*W)  +  2.0*W** 5 *T1*C2*T3*C3*T6*SIN(T7*W)  -  2.0*W** 4 *C2*T3*C3*T6*COS(T7*W)  +  2
.0*W** 3 *C2*T3*C3*SIN(T7*W)  +  2.0*W** 4 *T1*T2*T3*C3*COS(T7*W)  +  2.0*W** 5 *T1*T2*T3*C3
*T6*SIN(T7*W)  -  2.0*W** 4 *T2*T3*C3*T6*COS(T7*W)  +  2.0*W** 3 *T2*T3*C3*SIN(T7*W)  -  2.0
*W** 4 *T1*T3*C3*T6*COS(T7*W)  +  2.0*W** 3 *T1*T3*C3*SIN(T7*W)  -  2.0*W** 2 *T3*C3*COS(T7*
W)  -  2.0*W** 3 *T3*C3*T6*SIN(T7*W)  +  2.0*W** 6 *T1*T2*C1** 2 *C3*T6*COS(T7*W)  -  2.0*W
** 5 *T1*T2*C1** 2 *C3*SIN(T7*W)  +  2.0*W** 4 *T2*C1** 2 *C3*COS(T7*W)  +  2.0*W** 5 *T2*C1
** 2 *C3*T6*SIN(T7*W)  +  2.0*W** 4 *T1*C1** 2 *C3*COS(T7*W)  +  2.0*W** 5 *T1*C1** 2 *C3*T6
*SIN(T7*W)  -  2.0*W** 4 *C1** 2 *C3*T6*COS(T7*W)  +  2.0*W** 3 *C1** 2 *C3*SIN(T7*W)  +  2
.0*W** 4 *T1*T2*C2*C3*COS(T7*W)  +  2.0*W** 5 *T1*T2*C2*C3*T6*SIN(T7*W)  -  2.0*W** 4 *T2*C2
*C3*T6*COS(T7*W)  +  2.0*W** 3 *T2*C2*C3*SIN(T7*W)  -  2.0*W** 4 *T1*C2*C3*T6*COS(T7*W)  +
2.0*W** 3 *T1*C2*C3*SIN(T7*W)  -  2.0*W** 2 *C2*C3*COS(T7*W)  -  2.0*W** 3 *C2*C3*T6*SIN(T7*
W)  -  2.0*W** 4 *T1*T2*C3*T6*COS(T7*W)  +  2.0*W** 3 *T1*T2*C3*SIN(T7*W)  -  2.0*W** 2 *T2*
C3*COS(T7*W)  -  2.0*W** 3 *T2*C3*T6*SIN(T7*W)  -  2.0*W** 2 *T1*C3*COS(T7*W)  -  2.0*W** 3
*T1*C3*T6*SIN(T7*W)  +  2.0*W** 2 *C3*T6*COS(T7*W)  -  2.0*W*C3*SIN(T7*W)  +  W** 2 *C3** 2
*T6** 2   +  C3** 2
```

THE FOLLOWING NUMERICAL SUBSTITUTIONS WILL NOW BE MADE.

C3	=	5.00000
T1	=	.02000
T2	=	.01000
C1	=	.01000
C2	=	.01500
T5	=	.26830-06
T4	=	.00011
T3	=	.01899
T6	=	-.00094
T7	=	.00730

Figure 49. Output of Program to Derive Equation for Square of Frequency Response Function for Four Sample Cases (Page 5 of 12)

```
H(W)*H(W)  =   2.87939E-29*W** 16   +   7.69900E-25*W** 14   +   6.97393E-20*W** 12   +   1.39316E-15*W**
               10   +   1.59172E-11*W** 8   +   1.42318E-07*W** 6   +   6.75426E-04*W** 4   -
               5.02633E-17*W** 9 *SIN( 7.29999E-03*W)  +   8.84171E-14*W** 8 *COS( 7.29999E-03*W)  +
               4.84513E-11*W** 7 *SIN( 7.29999E-03*W)  -   1.42175E-08*W** 6 *COS( 7.29999E-03*W)  -
               2.48413E-06*W** 5 *SIN( 7.29999E-03*W)  +   2.68365E-04*W** 4 *COS( 7.29999E-03*W)  +
               1.76939E-02*W** 3 *SIN( 7.29999E-03*W)  -   6.49236E-01*W** 2 *COS( 7.29999E-03*W)  -   10
              .0*W*SIN( 7.29999E-03*W)  +   1.00002E 00*W** 2   +   25.0
```

```
THE FOLLOWING NUMERICAL SUBSTITUTIONS WILL NOW BE MADE.

C3     =       10.00000

T1     =         .02000

T2     =         .01000

C1     =         .01000

C2     =         .01500

T5     =      .26830-06

T4     =         .00011

T3     =         .01899

T6     =        -.00094

T7     =         .00730
```

```
H(W)*H(W)  =   2.87939E-29*W** 16   +   7.69900E-25*W** 14   +   6.97393E-20*W** 12   +   1.39316E-15*W**
               10   +   1.59172E-11*W** 8   +   1.42318E-07*W** 6   +   6.75426E-04*W** 4   -
               1.00526E-16*W** 9 *SIN( 7.29999E-03*W)  +   1.76834E-13*W** 8 *COS( 7.29999E-03*W)  +
               9.69027E-11*W** 7 *SIN( 7.29999E-03*W)  -   2.84350E-08*W** 6 *COS( 7.29999E-03*W)  -
               4.96826E-06*W** 5 *SIN( 7.29999E-03*W)  +   5.36731E-04*W** 4 *COS( 7.29999E-03*W)  +
               3.53878E-02*W** 3 *SIN( 7.29999E-03*W)  -   1.29847E 00*W** 2 *COS( 7.29999E-03*W)  -   20
              .0*W*SIN( 7.29999F-03*W)  +   1.00008E 00*W** 2   +   100.0
```

Figure 49. Output of Program to Derive Equation for Square of Frequency Response Function for Four Sample Cases (Page 6 of 12)

```
THE FOLLOWING NUMERICAL SUBSTITUTIONS WILL NOW BE MADE.

  C3     =        10.00000

  T1     =          .00200

  T2     =          .01000

  C1     =          .01000

  C2     =          .01500

  T5     =       .26830-06

  T4     =          .00011

  T3     =          .01899

  T6     =        -.00094

  T7     =          .00730


  H(W)*H(W)  =   2.87939E-31*W** 16   +   7.89640E-26*W** 14   +   2.42473E-21*W** 12   +   1.82218E-16*W**
                 10   +   3.18652E-12*W** 8   +   3.32499E-08*W** 6   +   2.79426E-04*W** 4   -
                 1.00526E-17*W** 9 *SIN( 7.29999E-03*W)  +   2.22071E-14*W** 8 *COS( 7.29999E-03*W)  +
                 1.74216E-11*W** 7 *SIN( 7.29999E-03*W)  -   6.81755E-09*W** 6 *COS( 7.29999E-03*W)  -
                 1.57770E-06*W** 5 *SIN( 7.29999E-03*W)  +   2.23201E-04*W** 4 *COS( 7.29999E-03*W)  +
                 1.92152E-02*W** 3 *SIN( 7.29999E-03*W)  -   9.38473E-01*W** 2 *COS( 7.29999E-03*W)  -   20
                .0*W*SIN( 7.29999E-03*W)  +   1.00008E 00*W** 2   +   100.0


THE FOLLOWING NUMERICAL SUBSTITUTIONS WILL NOW BE MADE.

  C3     =        10.00000

  T1     =          .00200

  T2     =          .01000

  C1     =          .01000

  C2     =          .01500

  T5     =       .26830-06

  T4     =          .00011

  T3     =          .01899
```

Figure 49. Output of Program to Derive Equation for Square of Frequency Response Function for Four Sample Cases (Page 7 of 12)

```
[illegible]    =         .02900

[illegible]    =         .00730


H(W)*H(W)  =   2.87939E-31*W** 16   +   7.89640E-26*W** 14   +   2.42473E-21*W** 12   +   1.82218E-16*W**
               10   +   3.18652E-12*W** 8   +   3.32499E-08*W** 6   +   2.79426E-04*W** 4   +
               3.11227E-16*W** 9 *SIN( 7.29999E-03*W)  -   3.44535E-13*W** 8 *COS( 7.29999E-03*W)  -
               1.47843E-10*W** 7 *SIN( 7.29999E-03*W)  +   3.46367E-08*W** 6 *COS( 7.29999E-03*W)  +
               4.58954E-06*W** 5 *SIN( 7.29999E-03*W)  -   3.26249E-04*W** 4 *COS( 7.29999E-03*W)  -
               8.31867E-03*W** 3 *SIN( 7.29999E-03*W)  -   3.39739E-01*W** 2 *COS( 7.29999E-03*W)  -   20
              .0*W*SIN( 7.29999E-03*W)  +   1.08409E 00*W** 2   +   100.0


THE FOLLOWING NUMERICAL SUBSTITUTIONS WILL NOW BE MADE.


C3     =         15.00000

T1     =           .02000

T2     =           .01000

C1     =           .01000

C2     =           .01500

T5     =         .26830-06

T4     =           .00011

T3     =           .01899

T6     =          -.00094

T7     =           .00730


H(W)*H(W)  =   2.87939E-29*W** 16   +   7.69900E-25*W** 14   +   6.97393E-20*W** 12   +   1.39316E-15*W**
               10   +   1.59172E-11*W** 8   +   1.42318E-07*W** 6   +   6.75426E-04*W** 4   -
               1.50789E-16*W** 9 *SIN( 7.29999E-03*W)  +   2.65251E-13*W** 8 *COS( 7.29999E-03*W)  +
               1.45354E-10*W** 7 *SIN( 7.29999E-03*W)  -   4.26525E-08*W** 6 *COS( 7.29999E-03*W)  -
               7.45240E-06*W** 5 *SIN( 7.29999E-03*W)  +   8.05097E-04*W** 4 *COS( 7.29999E-03*W)  +
               5.30817E-02*W** 3 *SIN( 7.29999E-03*W)  -   1.94771E 00*W** 2 *COS( 7.29999E-03*W)  -   30
              .0*W*SIN( 7.29999E-03*W)  +   1.00019E 00*W** 2   +   225.0


THE TIMES TAKEN BY THE VARIOUS SUBROUTINES ARE:


PARSE:      1.0 SECONDS

ALGEB:     62.0 SECONDS

COLECT:    64.0 SECONDS

PRNT:      20.0 SECONDS

BOOST:    161.0 SECONDS


TOTAL.    326.0 SECONDS
```

Figure 49. Output of Program to Derive Equation for Square of Frequency Response Function for Four Sample Cases (Page 8 of 12)

```
TEST CASE OF ALGEBRAIC PROGRAM FOR REPRESENTATIVE INLET
  REPRESENTS (H2 - FTH*C2) OF TRANSFER FUNCTION
  FIRST 2 SETS OF SUBSTITUTIONS SHOW EFFECT OF VARYING VELOCITY
    CONSTANT OF THROAT MACH CONTROL , THIRD SET SHOWS EFFECT OF
    DECREASING PRESSURE LEVEL , LAST OF ADDING LEAD


 H(S) = (S*S*W1*W1+S*Z1W+1)*(S*T1+1)*(S*T2+1)*S+C2


 H(W)*H(W)  =  W** 10 *W1** 4 *T1** 2 *T2** 2   +  W** 8 *Z1W** 2 *T1** 2 *T2** 2   -  2.0*W** 8 *W1** 2 *
               T1** 2 *T2** 2   +  W** 6 *T1** 2 *T2** 2   +  W** 8 *W1** 4 *T2** 2   -  2.0*W** 6 *W1** 2
               *T2** 2   +  W** 6 *Z1W** 2 *T2** 2   +  W** 4 *T2** 2   +  W** 8 *W1** 4 *T1** 2   -  2.0*W
               ** 6 *W1** 2 *T1** 2   +  W** 6 *Z1W** 2 *T1** 2   +  W** 4 *T1** 2   +  W** 6 *W1** 4   -
               2.0*W** 4 *W1** 2   +  W** 4 *Z1W** 2   +  W** 2   +  2.0*W** 4 *Z1W*T1*T2*C2  +  2.0*W** 4
               *W1** 2 *T2*C2  -  2.0*W** 2 *T2*C2  +  2.0*W** 4 *W1** 2 *T1*C2  -  2.0*W** 2 *T1*C2  -  2
               .0*W** 2 *Z1W*C2  +  C2** 2


THE FOLLOWING NUMERICAL SUBSTITUTIONS WILL NOW BE MADE.

 W1      =          .01000

 Z1W     =          .01500

 T1      =          .02000

 T2      =          .01000

 C2      =        10.00000


 H(W)*H(W)  =   3.99999E-16*W** 10   +   5.99999E-12*W** 8   +   6.24999E-08*W** 6   +   6.44999E-04*W** 4
                  +   1.00000E-01*W** 2   +   100.0
```

Figure 49. Output of Program to Derive Equation for Square of Frequency Response Function for Four Sample Cases (Page 9 of 12)

```
THE FOLLOWING NUMERICAL SUBSTITUTIONS WILL NOW BE MADE.

 W1    =         .01000
 Z1W   =         .01500
 T1    =         .02000
 T2    =         .01000
 C2    =       30.00000


H(W)*H(W)  =  3.99999E-16*W** 10   +   5.99999E-12*W** 8   +   6.24999E-08*W** 6   +   8.84999E-04*W** 4
           -   1.69999E 00*W** 2   +    900.0


THE FOLLOWING NUMERICAL SUBSTITUTIONS WILL NOW BE MADE.

 W1    =         .01000
 Z1W   =         .04500
 T1    =         .03000
 T2    =         .01000
 C2    =       20.00000


H(W)*H(W)  =  8.99999E-16*W** 10   +   1.74249E-10*W** 8   +   1.92499E-06*W** 6   +   3.52499E-03*W** 4
           -   2.39999E 00*W** 2   +    400.0


THE FOLLOWING NUMERICAL SUBSTITUTIONS WILL NOW BE MADE.

 W1    =         .01000
```

Figure 49. Output of Program to Derive Equation for Square of Frequency Response Function for Four Sample Cases (Page 10 of 12)

```
Z1W     =        .01500

T1      =        .00200

T2      =        .01000

C2      =      20.00000


H(W)*H(W)  =   3.99999E-18*W** 10   +   1.04999E-12*W** 8   +   1.29999E-08*W** 6   +   1.88999E-04*W** 4
                -    7.99999E-02*W** 2   +    400.0


THE TIMES TAKEN BY THE VARIOUS SUBROUTINES ARE:

PARSE:      1.0 SECONDS

ALGEB:      1.0 SECONDS

COLECT:     2.0 SECONDS

PRNT:       2.0 SECONDS

SUBST:     10.0 SECONDS


TOTAL:     16.0 SECONDS
```

Figure 49. Output of Program to Derive Equation for Square of Frequency Response Function for Four Sample Cases (Page 11 of 12)

```
TEST CASE OF ALGEBRAIC PROGRAM FOR REPRESENTATIVE INLET
 REPRESENTS (H2 - FTH*C2) OF TRANSFER FUNCTION


 H(S) = (S*S*0.0001+S*0.015+1)*(S*0.02+1)*(S*0.01+1)*S+20.



 H(W)*H(W)  =    3.99999E-16*W** 10   +   5.99999E-12*W** 8   +   6.24999E-08*W** 6   +   7.64999E-04*W** 4
               -   7.99999E-01*W** 2   +   400.0



THE TIMES TAKEN BY THE VARIOUS SUBROUTINES ARE:

PARSE:      1.0 SECONDS
ALGEB:      1.0 SECONDS
COLECT:     2.0 SECONDS
PRNT:        .0 SECONDS
SUBST:       .0 SECONDS

TOTAL:      4.0 SECONDS
```

Figure 49. Output of Program to Derive Equation for Square of Frequency Response Function for Four Sample Cases (Page 12 of 12)

```
C       PROGRAM WRITTEN BY HAMILTON STANDARD , A DIVISION OF UAC , UNDER CONTRACT
C         NAS2-4515 TASK 4 , IN FORTAN V
C       EVALUATES POWER SPECTRAL DENSITY PARAMETERS
C       REQUIRES FUNCTION PSD TO COMPUTE POWER SPECTRAL DENSITY AS FUNCTION OF
C       WR (FREQUENCY IN RADIANS/SEC)
C       DW         INITIAL WR , PROGRAM DOUBLES WR EACH STEP , RADIANS/SEC
C       I          NUMBER OF CARDS LOADED AND PRINTED TO SHOW FORMULA FOR POWER
C                  SPECTRAL DENSITY USED IN SUBROUTINE PSD(WR,J)
C       J          INDEX FOR CASE , USED IN SUBROUTINE PSD(WR,J)
C       PS         SQUARE ROOT OF (PWO*WO) = (PWR*WR) , UNITS
C       PWO        POWER SPECTRAL DENSITY (WO) , UNITS**2/RAD/FT
C       PWR        POWER SPECTRAL DENSITY (WR) , UNITS**2/RAD/SEC
C       QLF        WAVELENGTH , FEET
C       QLM        WAVELENGTH , METERS
C       QG         NUMBER OF ZERO CROSSINGS PER NAUTICAL MILE
C       QN         NUMBER OF ZERO CROSSINGS PER HOUR
C       S          INTEGRAL OF PSD FROM ZERO FREQUENCY , SIGMA , UNITS
C       VF         VELOCITY , FEET/SEC
C       VK         VELOCITY , KNOTS
C       VM         VELOCITY , METERS/SEC
C       WC         FREQUENCY , CYCLES/SEC , HZ
C       WM         MAXIMUM WR REQUIRED , RADIANS/SEC
C       WO         REDUCED REQUENCY , RADIANS/FOOT
C       WR         FREQUENCY , RADIANS/SEC
C       FOLLOWING 2 CARDS MAY NEED TO BE CHANGED TO FIT INSTALLATION , THEY DEFINE
C         UNITS USED IN READ AND WRITE STATEMENTS RESPECTIVELY
        IR         = 2
        IP         = 3
        WRITE(IP,1)
      1 FORMAT(108H1PROGRAM WRITTEN BY HAMILTON STANDARD UNDER CONTRACT NA
       1S2-4515 TO EVALUATE POWER SPECTRAL DENSITY PARAMETERS)
        J          = 0
C       READ COMMENT CARD , IF BLANK RETURN TO MONITOR , IF NOT BLANK PRINT WITH
C         1 EJECT AND RETURN TO PROGRAM
      2 CALL START
        J          = J+1
C       READ EITHER VF OR VK , VF USED IF NOT ZERO
        READ(IR,3)VF,VK,DW,WM,I
      3 FORMAT(4F10.5,I10)
        IF (VF)    4,6,5
C       ERROR IN INPUT , TERMINATE JOB
      4 CALL EXIT
C       USE INPUT VELOCITY IN FEET/SEC
      5 VK         = VF*.5924838
        GO TO 8
      6 IF (VK)    4,4,7
C       USE INPUT VELOCITY IN KNOTS
      7 VF         = VK/.5924838
      8 VM         = VF*.3048
        WRITE(IP,9)VF,VK,VM
      9 FORMAT(11H VELOCITY =F10.2,9H FT/SEC =F10.2,8H KNOTS =F10.2,32H ME
       1TERS/SEC , W=RAD/SEC , WS=W*W)
C       READ AND PRINT I CARDS SHOWING FORMULA FOR POWER SPECTRAL DENSITY ,
C         COLUMN 1 SHOULD BE BLANK AND IS NOT PRINTED
        DO 11 K=1,I
        READ(IR,10)
     10 FORMAT(80H
       1
     11 WRITE(IP,10)
        WRITE(IP,12)
```

Figure 50. Listing of Digital Program to Evaluate Power Spectral Density Parameters (Page 1 of 2)

```
   12 FORMAT(120H0      WAVELENGTH       REDUCED FREQ      PSD             FR
     1EQUENCY          PSD        SQRT(PSD*W)     SIGMA   NO OF  0 CROSSINGS/
     2119H        FEET      METERS      RAD/FT    UNITS**2/R/F      CPS, HZ   RAD/
     3SEC UNITS**2/R/S        UNITS          UNITS     /NAUT MI     /HOUR)
C       INTEGRATES FOR S, QG AND QN BY 5-PT GAUSS
      S1         = 0.
      S2         = 0.
      WR         = 0.
   13 X1         = WR+DW*.046910077
      X2         = WR+DW*.230765345
      X3         = WR+DW*.5
      X4         = WR+DW*.769234655
      X5         = WR+DW*.953089923
      P1         = PSD(X1,J)
      P2         = PSD(X2,J)
      P3         = PSD(X3,J)
      P4         = PSD(X4,J)
      P5         = PSD(X5,J)
      S1         = S1+DW*(.11846344*(P1+P5)+.23931434*(P2+P4)+.28444444*P3
     1             )
      S2         = S2+DW*(.11846344*(P1*X1*X1+P5*X5*X5)+.23931434*(P2*X2*
     1             X2+P4*X4*X4)+.28444444*P3*X3*X3)
      S          = SQRT(S1)
      QN         = 572.9578*SQRT(S2/S1)
      QG         = QN/VK
      WO         = X3/VF
      WC         = X3/6.2831853
      QLF        = 6.2831853/WO
      QLM        = QLF*.3048
      PWO        = P3*VF
      PS         = SQRT(X3*P3)
      WRITE(IP,14)QLF,QLM,WO,PWO,WC,X3,P3,PS
   14 FORMAT(1H 2F10.1,2E12.4,F11.3,F10.3,E12.4,E13.4,F10.5,F10.3,F10.0)
      WR         = WR+DW
      WO         = WR/VF
      WC         = WR/6.2831853
      QLF        = 6.2831853/WO
      QLM        = QLF*.3048
      PWR        = PSD(WR,J)
      PWO        = PWR*VF
      PS         = SQRT(WR*PWR)
      WRITE(IP,14)QLF,QLM,WO,PWO,WC,WR,PWR,PS,S,QG,QN
      DW         = WR
      IF (WR-WM)    13,2,2
      END
```

Figure 50. Listing of Digital Program to Evaluate Power Spectral Density Parameters. (Page 2 of 2)

```
      FUNCTION PSD(W,J)
      WS=W**2
      GO TO (1,2,3),J
C     SAMPLE CASE 1
    1 PSD=.6089/(1.+1.6401*WS)**.8333333
      RETURN
C     SAMPLE CASE 2
    2 PSD=.6089/(1.+1.6401*WS)**.8333333*3.4225*(1.E-8*WS*WS+.25E-4*WS+
     11.)*(.0004*WS+1.)*(.0001*WS+1.)*WS/(((((4.E-16*WS+6.E-12)*WS+
     26.25E-8)*WS+7.65E-4)*WS-.8)*WS+400.)
      RETURN
C     ERROR IF J=3
    3 CALL EXIT
      END
```

```
SAMPLE CASE 1   VON KARMAN LONGITUDINAL SPECTRUM  L=2500 FT   M=2.7   LOAD VF
 2613.82          .0           .05      400.                1
 PSD=.6089/(1.+1.6401*WS)**.8333333
SAMPLE CASE 2   WITH THROAT MACH CONTROL   M=2.7   LOAD VK
     .0     1548.64            .05      400.                3
 PSD=.6089/(1.+1.6401*WS)**.8333333 * 1.85**2 * ((1.+.25E-4*WS+1.E-8*WS**2) *
  (1.+.0004*WS) * (1.+.0001*WS) * WS ) / (400. - .8*WS + .000765*WS**2 +
  6.25E-8*WS**3 + 6.E-12*WS**4 + 4.E-16*WS**5)
```

Figure 51. Listing of Function PSD(W,J,) and Input Cards for Two Sample Cases

PROGRAM WRITTEN BY HAMILTON STANDARD UNDER CONTRACT NAS2-4515 TO EVALUATE POWER SPECTRAL DENSITY PARAMETERS

Figure 52. Output of Program to Evaluate Power Spectral Density Parameters for Two Sample Cases (Page 1 of 3)

SAMPLE CASE 1 VON KARMAN LONGITUDINAL SPECTRUM L=2500 FT M=2.7 LOAD VF
VELOCITY = 2613.82 FT/SEC = 1548.64 KNOTS = 796.69 METERS/SEC , W=RAD/SEC , WS=W*W
PSD=.6089/(1.+1.6401*WS)**.8333333

WAVELENGTH FEET	WAVELENGTH METERS	REDUCED FREQ RAD/FT	PSD UNITS**2/R/F	FREQUENCY CPS, HZ	FREQUENCY RAD/SEC	PSD UNITS**2/R/S	SQRT(PSD*W) UNITS	SIGMA UNITS	NO OF 0 CROSSINGS /NAUT MI	NO OF 0 CROSSINGS /HOUR
656924.7	200230.6	0.9564E-05	0.1590E 04	0.003	0.025	0.6083E 00	0.1233E 00			
328462.3	100115.3	0.1912E-04	0.1586E 04	0.007	0.050	0.6068E 00	0.1741E 00	0.17438	0.010	16.
218974.9	66743.5	0.2869E-04	0.1579E 04	0.011	0.075	0.6042E 00	0.2126E 00			
164231.1	50057.6	0.3825E-04	0.1570E 04	0.015	0.100	0.6007E 00	0.2450E 00	0.24620	0.021	33.
109487.4	33371.7	0.5738E-04	0.1544E 04	0.023	0.150	0.5907E 00	0.2976E 00			
82115.5	25028.8	0.7651E-04	0.1509E 04	0.031	0.200	0.5774E 00	0.3398E 00	0.34588	0.042	65.
54743.7	16685.8	0.1147E-03	0.1419E 04	0.047	0.300	0.5428E 00	0.4035E 00			
41057.7	12514.4	0.1530E-03	0.1310E 04	0.063	0.400	0.5014E 00	0.4478E 00	0.47748	0.083	128.
27371.8	8342.9	0.2295E-03	0.1081E 04	0.095	0.600	0.4136E 00	0.4981E 00			
20528.8	6257.2	0.3060E-03	0.8751E 03	0.127	0.800	0.3348E 00	0.5175E 00	0.62775	0.156	242.
13685.9	4171.4	0.4590E-03	0.5794E 03	0.190	1.200	0.2216E 00	0.5157E 00			
10264.4	3128.6	0.6121E-03	0.4029E 03	0.254	1.600	0.1541E 00	0.4966E 00	0.75993	0.276	428.
6842.9	2085.7	0.9181E-03	0.2252E 03	0.381	2.400	0.8617E-01	0.4547E 00			
5132.2	1564.3	0.1224E-02	0.1445E 03	0.509	3.200	0.5528E-01	0.4206E 00	0.85139	0.457	708.
3421.4	1042.8	0.1836E-02	0.7549E 02	0.763	4.800	0.2888E-01	0.3723E 00			
2566.1	782.1	0.2448E-02	0.4718E 02	1.018	6.400	0.1805E-01	0.3398E 00	0.90835	0.731	1132.
1710.7	521.4	0.3672E-02	0.2416E 02	1.527	9.600	0.9246E-02	0.2979E 00			
1283.0	391.0	0.4897E-02	0.1499E 02	2.037	12.800	0.5738E-02	0.2710E 00	0.94317	1.153	1786.
855.3	260.7	0.7345E-02	0.7644E 01	3.055	19.200	0.2924E-02	0.2369E 00			
641.5	195.5	0.9794E-02	0.4735E 01	4.074	25.600	0.1811E-02	0.2153E 00	0.96457	1.815	2810.
427.6	130.3	0.1469E-01	0.2410E 01	6.111	38.400	0.9221E-03	0.1881E 00			
320.7	97.7	0.1958E-01	0.1492E 01	8.148	51.200	0.5709E-03	0.1709E 00	0.97783	2.857	4425.
213.8	65.1	0.2938E-01	0.7593E 00	12.223	76.800	0.2905E-03	0.1493E 00			
160.3	48.8	0.3917E-01	0.4701E 00	16.297	102.400	0.1798E-03	0.1357E 00	0.98609	4.508	6982.
106.9	32.5	0.5876E-01	0.2392E 00	24.446	153.600	0.9151E-04	0.1185E 00			
80.1	24.4	0.7835E-01	0.1480E 00	32.594	204.800	0.5665E-04	0.1077E 00	0.99126	7.126	11036.
53.4	16.2	0.1175E 00	0.7534E-01	48.892	307.200	0.2882E-04	0.9410E-01			
40.0	12.2	0.1567E 00	0.4664E-01	65.189	409.600	0.1784E-04	0.8549E-01	0.99450	11.279	17468.

Figure 52. Output of Program to Evaluate Power Spectral Density Parameters for Two Sample Cases (Page 2 of 3)

```
SAMPLE CASE 2  WITH THROAT MACH CONTROL  M=2.7   LOAD VK
VELOCITY =   2613.81 FT/SEC =   1548.64 KNOTS =    796.68 METERS/SEC , W=RAD/SEC , WS=W*W
PSD=.6089/(1.+1.6401*WS)**.8333333 * 1.85**2 * ((1.+.25E-4*WS+1.E-8*WS**2) *
 (1.+.0004*WS) * (1.+.0001*WS) * WS ) / (400. - .8*WS + .000765*WS**2 +
 6.25E-5*WS**3 + 6.E-12*WS**4 + 4.E-16*WS**5)
```

WAVELENGTH FEET	METERS	REDUCED FREQ RAD/FT	PSD UNITS**2/R/F	FREQUENCY CPS, HZ	RAD/SEC	PSD UNITS**2/R/S	SQRT(PSD*W) UNITS	SIGMA UNITS	NO OF 0 CROSSINGS /NAUT MI	/HOUR
656922.1	200229.8	0.9564E-05	0.8503E-02	0.003	0.025	0.3253E-05	0.2851E-03			
328461.0	100114.9	0.1912E-04	0.3392E-01	0.007	0.050	0.1298E-04	0.8056E-03	0.00046	0.014	22.
218974.0	66743.2	0.2869E-04	0.7601E-01	0.011	0.075	0.2908E-04	0.1476E-02			
[illegible]	50057.4	0.3825E-04	0.1343E 00	0.015	0.100	0.5139E-04	0.2267E-02	0.00131	0.028	[illegible]
109487.0	33371.6	0.5738E-04	0.2973E 00	0.023	0.150	0.1137E-03	0.4130E-02			
82115.2	25028.7	0.7651E-04	0.5166E 00	0.031	0.200	0.1976E-03	0.6287E-02	0.00366	0.057	88.
54743.5	16685.8	0.1147E-03	0.1092E 01	0.047	0.300	0.4181E-03	0.1120E-01			
41057.6	12514.3	0.1530E-03	0.1794E 01	0.063	0.400	0.6867E-03	0.1657E-01	0.00993	0.113	175.
27371.7	8342.9	0.2295E-03	0.3333E 01	0.095	0.600	0.1275E-02	0.2766E-01			
20528.8	6257.1	0.3060E-03	0.4800E 01	0.127	0.800	0.1836E-02	0.3832E-01	0.02463	0.221	343.
13685.8	4171.4	0.4590E-03	0.7165E 01	0.190	1.200	0.2741E-02	0.5735E-01			
10264.4	3128.5	0.6121E-03	0.8883E 01	0.254	1.600	0.3398E-02	0.7374E-01	0.05259	0.424	657.
6842.9	2085.7	0.9181E-03	0.1126E 02	0.381	2.400	0.4309E-02	0.1016E 00			
5132.2	1564.2	0.1224E-02	0.1299E 02	0.509	3.200	0.4971E-02	0.1261E 00	0.09796	0.810	1254.
3421.4	1042.8	0.1836E-02	0.1577E 02	0.763	4.800	0.6034E-02	0.1701E 00			
2566.1	782.1	0.2448E-02	0.1833E 02	1.018	6.400	0.7015E-02	0.2118E 00	0.16990	1.574	2438.
1710.7	521.4	0.3672E-02	0.2402E 02	1.527	9.600	0.9191E-02	0.2970E 00			
1283.0	391.0	0.4897E-02	0.3157E 02	2.037	12.800	0.1207E-01	0.3932E 00	0.29741	3.183	4929.
855.3	260.7	0.7345E-02	0.5462E 02	3.055	19.200	0.2089E-01	0.6334E 00			
641.5	195.5	0.9794E-02	0.6537E 02	4.074	25.600	0.2501E-01	0.8001E 00	0.58935	6.688	10357.
427.6	130.3	0.1469E-01	0.2106E 02	6.111	38.400	0.8058E-02	0.5562E 00			
320.7	97.7	0.1958E-01	0.7824E 01	8.148	51.200	0.2993E-02	0.3914E 00	0.78397	9.797	15173.
213.8	65.1	0.2938E-01	0.2706E 01	12.223	76.800	0.1035E-02	0.2819E 00			
160.3	48.8	0.3917E-01	0.1562E 01	16.297	102.400	0.5976E-03	0.2473E 00	0.82379	12.368	19153.
106.9	32.5	0.5876E-01	0.8062E 00	24.446	153.600	0.3084E-03	0.2176E 00			
80.1	24.4	0.7835E-01	0.5045E 00	32.594	204.800	0.1930E-03	0.1988E 00	0.84435	16.968	26278.
53.4	16.2	0.1175E 00	0.2577E 00	48.892	307.200	0.9860E-04	0.1740E 00			
40.0	12.2	0.1567E 00	0.1596E 00	65.189	409.600	0.6107E-04	0.1581E 00	0.85728	25.151	38950.

Figure 52. Output of Program to Evaluate Power Spectral Density Parameters for Two Sample Cases (Page 3 of 3)

```
C      PROGRAM WRITTEN BY HAMILTON STANDARD , A DIVISION OF UAC , UNDER CONTRACT
C        NAS2-4515 TASK 4 , IN FORTAN V
C      A           RMS AMPLITUDE OUTPUT / RMS AMPLITUDE INPUT
C      B1          RMS AMPLITUDE OF INPUT PRIMARY TURBULENCE
C      B2          RMS AMPLITUDE OF INPUT SECONDARY TURBULENCE
C      B2          ALPHA FOR CASE M IF L IS LESS THAN 0
C      B2          ALPHA FOR CASE J IF L IS GREATER THAN 0
C      B3          RMS AMPLITUDE OF INPUT TERTIARY TURBULENCE
C      DI          INITIAL OUTPUT DISTURBANCE AMPLITUDE SUPPLIED
C      DM          MAXIMUM OUTPUT DISTURBANCE AMPLITUDE REQUIRED
C      DX          STEP CHANGE IN OUTPUT DISTURBANCE AMPLITUDE
C      H( )        HOURS PER EXCEEDANCE OF OUTPUT
C      L           DETERMINES EQUATION USED FOR EXCEEDANCES
C      L           =0  N=QN*(P1*EXP(-X/(A*B1))+P2*EXP(-X/(A*B2))+P3*EXP(-X/(A*B3)))
C      L           =+  CASE J OF AFFDL-TR-67-74 ,B2 IS ALPHA
C      L           =-  CASE M OF AFFDL-TR-67-74 ,B2 IS ALPHA
C      P1          FRACTION OF FLIGHT DISTANCE IN PRIMARY TURBULENCE
C      P2          FRACTION OF FLIGHT DISTANCE IN SECONDARY TURBULENCE
C      P3          FRACTION OF FLIGHT DISTANCE IN TERTIARY TURBULENCE
C      QG          NO OF ZERO CROSSINGS OF OUTPUT IN + DIRECTION / NAUTICAL MILE
C      QNI         MINIMUM MILES / EXCEEDANCE REQUIRED
C      QNM         MAXIMUM MILES / EXCEEDANCE REQUIRED
C      QM( )       NAUTICAL MILES PER EXCEEDANCE OF OUTPUT
C      VF          VELOCITY , FEET/SEC
C      VK          VELOCITY , KNOTS
C      VM          VELOCITY , METERS/SEC
C      X( )        OUTPUT DISTURBANCE AMPLITUDE
       DIMENSION H(4),QM(4),X(4)
C      FOLLOWING 2 CARDS MAY NEED TO BE CHANGED TO FIT INSTALLATION , THEY DEFINE
C        UNITS USED IN READ AND WRITE STATEMENTS RESPECTIVELY
       IR          = 2
       IP          = 3
       WRITE(IP,1)
     1 FORMAT( 95H1PROGRAM WRITTEN BY HAMILTON STANDARD UNDER CONTRACT NA
      1S2-4515 TO COMPUTE EXCEEDANCE PARAMETERS)
C      READ COMMENT CARD , IF BLANK RETURN TO MONITOR , IF NOT BLANK PRINT WITH
C        1 EJECT AND RETURN TO PROGRAM
     2 CALL START
C      READ EITHER VF OR VK , VF USED IF NOT ZERO
       READ(IR,3)L,QG,A,VF,VK,DI,DX,DM,QNI,QNM,P1,P2,P3,B1,B2,B3
     3 FORMAT(I10,7F10.5/8F10.5)
       IF (VF)    4,6,5
C      ERROR IN INPUT , TERMINATE JOB
     4 CALL EXIT
C      USE INPUT VELOCITY IN FEET/SEC
     5 VK          = VF*.5924838
       GO TO 8
     6 IF (VK)    4,4,7
C      USE INPUT VELOCITY IN KNOTS
     7 VF          = VK/.5924838
     8 VM          = VF*.3048
       I           = 1
       J           = 1
       X(1)        = DI
       IF(L)   200,100,300
C      L = 0     SUM OF 3 CASE A
   100 WRITE(IP,101)P1,B1,QG,A,P2,B2,VF,VK,VM,P3,B3
   101 FORMAT( 91HON=GO*(P1*EXP(-X/A/B1)+P2*EXP(-X/A/B2)+P3*EXP*(-X/A/B3)
      1)   SUM OF 3 CASE A OF AFFDL-TR-67-74/ 4H P1=F11.7,5H  B1= F9.5,5H
      2 GO=F9.4,4H   A=F9.4/4H P2=F11.7,5H   B2=F9.5,11H   VELOCITY=F10.2,9H
```

Figure 53. Listing of Digital Program to Compute Exceedance Parameters (Page 1 of 3)

```
    3 FT/SEC =F10.2,8H KNOTS =F10.2,11H METERS/SEC/4H P3=F11.7,5H  B3=F
    49.5)
      WRITE(IP,25)
      B1          = B1*A
      B2          = B2*A
      B3          = B3*A
      P1          = QG*P1
      P2          = QG*P2
      P3          = QG*P3
      A           = 1.01/(P1+P2+P3)
      IF (A-QNI)   103,103,102
  102 QNI         = A
  103 IF (B3)   4,104,108
  104 K           = 2
      IF (B2)   4,106,105
  105 QM(J)       = 1./(P1/EXP(X(J)/B1)+P2/EXP(X(J)/B2))
      GO TO 9
  106 K           = 1
  107 QM(J)       = EXP(X(J)/B1)/P1
      GO TO 9
  108 K           = 3
  109 QM(J)       = 1./(P1/EXP(X(J)/B1)+P2/EXP(X(J)/B2)+P3/EXP(X(J)/B3))
    9 H(J)        = QM(J)/VK
      GO TO (10,17),I
   10 IF (QM(1)-QNI) 15,15,11
   11 IF (X(1)-1.4*DX)  12,12,14
   12 X(1)        = X(1)/2.
   13 IF (L)  203,110,303
  110 GO TO (107,105,109),K
   14 X(1)        = X(1)-DX
      GO TO 13
   15 I           = 2
   16 X(J+1)      = X(J)+DX
      J           = J+1
      GO TO 13
   17 IF (J-4)   20,18,4
   18 WRITE(IP,19)(X(M),QM(M),H(M),M=1,J)
   19 FORMAT(1H F7.4,F12.0,F9.1,3(F9.4,F12.0,F9.1))
      GO TO (4,20,2),I
   20 IF (X(J)-DM) 21,23,23
   21 IF (QM(J)-QNM)  22,23,23
   22 IF (J-4)        16,24,4
   23 I           = 3
      IF (J-4)   18,2,4
   24 X(1)        = X(4)+DX
      J           = 1
      GO TO 13
   25 FORMAT(118H0    AMPL     X EXCEEDED EVERY  *    AMPL     X EXCEEDED EV
     1ERY  *    AMPL     X EXCEEDED EVERY  *    AMPL     X EXCEEDED EVERY/11
     28H       X      N MILES     HOURS          X      N MILES     HOURS
     3  X       N MILES     HOURS          X      N MILES     HOURS)
C     L = -     CASE M
  200 P2          = 1.-B2
      P3          = B2/3.17
      WRITE(IP,201)P2,P3,B2,P1,B1,QG,A,VF,VK,VM
  201 FORMAT(9H0N=G0*P*(F8.5,15H *EXP(-X/A/B) +F9.6,50H *A*B/X*(EXP(-.28
     19X/A/B)-EXP(-3.46X/A/B))), ALPHA=F8.5/25H CASE M OF AFFDL-TR-67-74
     2/3H P=F11.7,4H  B=F9.5,5H  G0=F9.4,4H  A=F9.4,11H  VELOCITY=F10.2,
     39H FT/SEC =F10.2,8H KNOTS =F10.2,6H M/SEC)
      WRITE(IP,25)
```

Figure 53. Listing of Digital Program to Compute Exceedance Parameters (Page 2 of 3)

```
      B1          = B1*A
      P1          = 1./(QG*P1)
      A           = 1.01*P1
      IF (A-QNI)  203,203,202
  202 QNI         = A
  203 B3          = X(J)/B1
      QM(J)       = P1/(P2/EXP(B3)+P3/B3*(EXP(-.289*B3)-EXP(-3.46*B3)))
      GO TO 9
C     L = +    CASE J
  300 P2          = (B2+2.)/(B2-2.)/EXP(B2)
      P3          = SQRT(1.+P2)
      B3          = B2/P3
      X(2)        = B3/2.7182818
      X(3)        = B3*B1*A
      WRITE(IP,301)P3,X(3),B3,X(2),B2,X(3),B2,P1,B1,QG,A,VF,VK,VM
  301 FORMAT(12H0N=G0*P/EXP(F9.6,23H X/A/B)  IF X LESS THANF10.7,4H  ORF
     110.6,31H*A*B , CASE J OF AFFDL-TR-67-14/ 9H N=G0*P*(F9.6,9H*A*B/X)
     2**F7.4,19H  IF X GREATER THANF10.7,9H , ALPHA=F7.4/3H P=F11.7,4H
     3B=F9.5,5H  G0=F9.4,4H  A=F9.4,11H  VELOCITY=F10.2,9H FT/SEC =F10.2
     4,8H KNOTS =F10.2,6H M/SEC)
      WRITE(IP,25)
      B1          = B1*A
      P1          = 1./(QG*P1)
      B3          = X(3)
      P3          = P3/B1
      P2          = X(2)*B1
      A           = 1.01*P1
      IF (A-QNI)  303,303,302
  302 QNI         = A
  303 IF (X(J)-B3)  304,304,305
  304 QM(J)       = P1*EXP(P3*X(J))
      GO TO 9
  305 QM(J)       = P1/(P2/X(J))**B2
      GO TO 9
      END
```

Figure 53. Listing of Digital Program to Compute Exceedance Parameters (Page 3 of 3)

```
SAMPLE CASE A  WITH THROAT MACH CONTROL  55000FT  FAA-ADS-53  M=2.7  X=DMTH
         012.368     .82379     2613.82                .01       .002      .06
1000.      10000000. .00197     .0000727   .0          .00395    .00727    .0
SAMPLE CASE K  WITH THROAT MACH CONTROL  55000FT  AFFDL-TR-67-74  ALPHA=.0005
         012.368     .82379     2613.82   1234.56      .01       .002      .06
1000.      10000000. .0045877   .000002295.0           .0051831  .0129577  .0
SAMPLE CASE J  WITH THROAT MACH CONTROL  55000FT  AFFDL-TR-67-74  ALPHA=8.
         112.366     .8237                1548.64      .01       .002      .08
1000.      10000000. .00459                            .00519    8.
SAMPLE CASE M  WITH THROAT MACH CONTROL  55000FT  AFFDL-TR-67-74  ALPHA=.003
        -112.368     .8237                1548.64      .016      .002      .08
1000.      10000000. .00459                            .00519    .003
```

Figure 54. Listing of Input Cards for Sample Cases

PROGRAM WRITTEN BY HAMILTON STANDARD UNDER CONTRACT NAS2-4515 TO COMPUTE EXCEEDANCE PARAMETERS

Figure 55. Output of Program to Compute Exceedance Parameters for Four Sample Cases (Page 1 of 5)

```
SAMPLE CASE A  WITH THROAT MACH CONTROL  55000FT  FAA-ADS-53  M=2.7  X=DMTH

N=GO*(P1*EXP(-X/A/B1)+P2*EXP(-X/A/B2)+P3*EXP*(-X/A/B3))  SUM OF 3 CASE A OF AFFDL-TR-67-74
P1=  0.0019700  B1=  0.00395  GO=  12.3680  A=   0.8237
P2=  0.0000727  B2=  0.00727  VELOCITY=   2613.82 FT/SEC =   1548.64 KNOTS =    796.69 METERS/SEC
P3=  0.0000000  B3=  0.00000
```

AMPL X	X EXCEEDED EVERY N MILES	HOURS	*	AMPL X	X EXCEEDED EVERY N MILES	HOURS	*	AMPL X	X EXCEEDED EVERY N MILES	HOURS	*	AMPL X	X EXCEEDED EVERY N MILES	HOURS
0.0100	771.	0.4		0.0120	1367.	0.8		0.0139	2400.	1.5		0.0159	4157.	2.6
0.0179	7092.	4.5		0.0199	11897.	7.6		0.0219	19590.	12.6		0.0239	31636.	20.4
0.0259	50099.	32.3		0.0279	77840.	50.2		0.0299	118805.	76.7		0.0319	178433.	115.2
0.0339	264244.	170.6		0.0359	386667.	249.6		0.0379	560218.	361.7		0.0399	805129.	519.8
0.0419	1149646.	742.3		0.0439	1633213.	1054.6		0.0459	2310917.	1492.2		0.0479	3259708.	2104.8
0.0499	4587066.	2961.9		0.0519	6443097.	4160.4		0.0539	9037424.	5835.6		0.0559	12662850.	8176.7

Figure 55. Output of Program to Compute Exceedance Parameters for Four Sample Cases (Page 2 of 5)

```
SAMPLE CASE K  WITH THROAT MACH CONTROL  55000FT  AFFDL-TR-67-74  ALPHA=.0005

N=GO*(P1*EXP(-X/A/B1)+P2*EXP(-X/A/B2)+P3*EXP*(-X/A/B3))  SUM OF 3 CASE A OF AFFDL-TR-67-74
P1=  0.0045877  B1=  0.00518  GO=  12.3680  A=   0.8237
P2=  0.0000022  B2=  0.01295  VELOCITY=   2613.82 FT/SEC =   1548.64 KNOTS =    796.69 METERS/SEC
P3=  0.0000000  B3=  0.00000
```

AMPL X	X EXCEEDED EVERY N MILES	HOURS	*	AMPL X	X EXCEEDED EVERY N MILES	HOURS	*	AMPL X	X EXCEEDED EVERY N MILES	HOURS	*	AMPL X	X EXCEEDED EVERY N MILES	HOURS
0.0100	182.	0.1		0.0120	292.	0.1		0.0139	466.	0.3		0.0159	743.	0.4
0.0179	1186.	0.7		0.0199	1891.	1.2		0.0219	3013.	1.9		0.0239	4796.	3.0
0.0259	7626.	4.9		0.0279	12108.	7.8		0.0299	19188.	12.3		0.0319	30329.	19.5
0.0339	47783.	30.8		0.0359	74966.	48.4		0.0379	116984.	75.5		0.0399	181319.	117.0
0.0419	278672.	179.9		0.0439	423889.	273.7		0.0459	636829.	411.2		0.0479	942950.	608.8
0.0499	1373364.	886.8		0.0519	1964250.	1268.3		0.0539	2755754.	1779.4		0.0559	3790843.	2447.8
0.0579	5114875.	3302.8		0.0599	6776349.	4375.6		0.0619	8829148.	5701.2				

Figure 55. Output of Program to Compute Exceedance Parameters for Four Sample Cases (Page 3 of 5)

SAMPLE CASE J WITH THROAT MACH CONTROL 55000FT AFFDL-TR-67-74 ALPHA=8.

N=GO*P/EXP(1.000279 X/A/B) IF X LESS THAN 0.0341904 OR 7.997765*A*B , CASE J OF AFFDL-TR-67-14
N=GO*P*(2.942213*A*B/X)** 8.0000 IF X GREATER THAN 0.0341904 , ALPHA= 8.0000
P= 0.0045900 B= 0.00519 GO= 12.3680 A= 0.8237 VELOCITY= 2613.81 FT/SEC = 1548.64 KNOTS = 796.68 M/SEC

AMPL	X EXCEEDED	EVERY	*	AMPL	X EXCEEDED	EVERY	*	AMPL	X EXCEEDED	EVERY	*	AMPL	X EXCEEDED	EVERY
X	N MILES	HOURS		X	N MILES	HOURS		X	N MILES	HOURS		X	N MILES	HOURS
0.0100	182.	0.1		0.0120	291.	0.1		0.0139	466.	0.3		0.0159	744.	0.4
0.0179	1188.	0.7		0.0199	1897.	1.2		0.0219	3030.	1.9		0.0239	4838.	3.1
0.0259	7725.	4.9		0.0279	12336.	7.9		0.0299	19697.	12.7		0.0319	31452.	20.3
0.0339	50220.	32.4		0.0359	79326.	51.2		0.0379	122255.	78.9		0.0399	184280.	118.9
0.0419	272266.	175.8		0.0439	395021.	255.0		0.0459	563718.	364.0		0.0479	792371.	511.6
0.0499	1098396.	709.2		0.0519	1503231.	970.6		0.0539	2033054.	1312.7		0.0559	2719587.	1756.1
0.0579	3600996.	2325.2		0.0599	4722901.	3049.7		0.0619	6139488.	3964.4		0.0639	7914765.	5110.7
0.0659	10123934.	6537.3												

Figure 55. Output of Program to Compute Exceedance Parameters for Four Sample Cases (Page 4 of 5)

SAMPLE CASE M WITH THROAT MACH CONTROL 55000FT AFFDL-TR-67-74 ALPHA=.003

N=GO*P*(0.99700 *EXP(-X/A/B) + 0.000946 *A*B/X*(EXP(-.289X/A/B)-EXP(-3.46X/A/B))), ALPHA= 0.00300
CASE M OF AFFDL-TR-67-74
P= 0.0045900 B= 0.00519 GO= 12.3680 A= 0.8237 VELOCITY= 2613.81 FT/SEC = 1548.64 KNOTS = 796.68 M/SEC

AMPL	X EXCEEDED EVERY		*	AMPL	X EXCEEDED EVERY		*	AMPL	X EXCEEDED EVERY		*	AMPL	X EXCEEDED EVERY	
X	N MILES	HOURS		X	N MILES	HOURS		X	N MILES	HOURS		X	N MILES	HOURS
0.0160	743.	0.4		0.0179	1185.	0.7		0.0199	1890.	1.2		0.0219	3013.	1.9
0.0239	4801.	3.1		0.0259	7645.	4.9		0.0279	12165.	7.8		0.0299	19334.	12.4
0.0319	30683.	19.8		0.0339	48603.	31.3		0.0359	76793.	49.5		0.0379	120934.	78.0
0.0399	189626.	122.4		0.0419	295672.	190.9		0.0439	457717.	295.5		0.0459	702146.	453.3
0.0479	1064947.	687.6		0.0499	1593030.	1028.6		0.0519	2344193.	1513.7		0.0539	3385098.	2185.8
0.0559	4787049.	3091.1		0.0579	6620522.	4275.0		0.0599	8950516.	5779.5		0.0619	11834868.	7642.1

Figure 55. Output of Program to Compute Exceedance Parameters for Four Sample Cases (Page 5 of 5)